AD 740212

FOREIGN TECHNOLOGY DIVISION

TURBULENT BOUNDARY LAYER IN SUPERSONIC GAS FLOW

Yu. V. Lapin
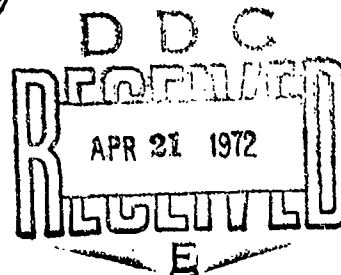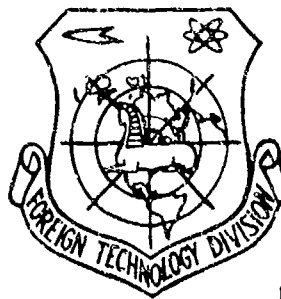
D D C

APR 21 1972

E

EDITED TRANSLATION

TURBULENT BOUNDARY LAYER IN SUPERSONIC FLOW

By: Yu. V. Lapin

English pages: 331

Source: Turbulentnyy Pogranichnyy Sloy v
Sverkhzvukovykh Potokakh Gaza 1970,
pp. 1-343

Translated under: F33657-71-D-0057

Approved for public release;
distribution unlimited.

UR/0000-70-000-000

THIS TRANSLATION IS A RENDITION OF THE ORIGI-NAL FOREIGN TEXT WITHOUT ANY ANALYTICAL OR EDITORIAL COMMENT. STATEMENTS OR THEORIES ADVOCATED OR IMPLIED ARE THOSE OF THE SOURCE AND DO NOT NECESSARILY REFLECT THE POSITION OR OPINION OF THE FOREIGN TECHNOLOGY DI-VISION.	PREPARED BY: TRANSLATION DIVISION FOREIGN TECHNOLOGY DIVISION WP-AFB, OHIO.

DOCUMENT CONTROL DATA - R & D

(Security classification of title, body of abstract and indexing annotation must be entered when the overall report is classified)

1. ORIGINATING ACTIVITY *(Corporate author)*	2a. REPORT SECURITY CLASSIFICATION
Foreign Technology Division	UNCLASSIFIED
Air Force Systems Command	2b. GROUP
U. S. Air Force	

3. REPORT TITLE

TURBULENT BOUNDARY LAYER IN SUPERSONIC GAS GLOW

4. DESCRIPTIVE NOTES *(Type of report and inclusive dates)*

Translation

5. AUTHOR(S) *(First name, middle initial, last name)*

Lapin, Yu. V.

6. REPORT DATE	7a. TOTAL NO. OF PAGES	7b. NO. OF REFS
1970	331	146

8a. CONTRACT OR GRANT NO.	9a. ORIGINATOR'S REPORT NUMBER(S)
F33657-71-D-0057	
b. PROJECT NO.	
	FTD-HC-23-723-71
c.	9b. OTHER REPORT NO(S) *(Any other numbers that may be assigned this report)*
d. DIA Task No. T70-01-12	

10. DISTRIBUTION STATEMENT

Approved for public release; distribution unlimited.

11. SUPPLEMENTARY NOTES	12. SPONSORING MILITARY ACTIVITY
	Foreign Technology Division
	Wright-Patterson AFB, Ohio

13. ABSTRACT

The book discusses the results of theoretical and experimental studies of skin friction, heat transfer, and mass transfer in a turbulent boundary layer at supersonic gas velocities. At the same time the book presents the fundamentals of the molecular theory of gas flow. It gives derivations of the equations of turbulent flow and of boundary layer equations, in particular, for a multicomponent reacting gas. Information on the kinetics of chemical reactions in air is discussed. Problems of heat and mass transfer through permeable surfaces are also discussed. Orig. article has: 101 illustrations.

DD FORM 1473 (1 NOV 65)

14. KEY WORDS	LINK A		LINK B		LINK C	
	ROLE	WT	ROLE	WT	ROLE	WT
Boundary Layer Equation						
Supersonic Aerodynamics						
Gas Flow						
Heat Transfer						
Turbulent Flow						

TABLE OF CONTENTS

PAGE

PREFACE

The problem of turbulence in general, and of turbulent boundary layers in particular, has recently become very important in view of its increasing practical significance.

Due to the intensive development of aerospace technology, power plant technology, and other branches of technology, scientists and engineers have become particularly interested in problems related to supersonic flow of homogeneous and inhomogeneous gases in a turbulent boundary layer. A flow at supersonic velocities in many cases results in such an extreme increase of the temperature of the gas that thermochemical processes begin to take place in it which lead to a disintegration of molecules into atoms, atoms into ions and electrons, and the formation of oxides and other compounds. In certain cases, a discussion of supersonic flow must take into account processes occurring on the surface around which the flow takes place such as fusion, sublimation, evaporation, chemical reactions, etc. Many of these phenomena were and still remain an object of detailed experimental and theoretical studies. The present book attempts to give a systematic exposition of some of the results of these studies. As far as theory is concerned, priority is usually given to results obtained on the basis of the semi-empirical theory of turbulence.

The semi-empirical theory of turbulence, being part of the statistical theory of turbulence, has until now remained an important, and in many cases the only instrument in solving a majority of practical problems. Created initially as a result of investigations of the flow of an incompressible fluid in tubes, channels, boundary layers, filaments, wakes, and used primarily to predict the properties of a flow of an incompressible fluid, the semi-empirical theory of turbulence has great potential for analyzing much more complicated flows, such as the flow of a compressible and heat-conducting gas, the flow of multicomponent reacting gas mixtures, etc. This is convincingly demonstrated by the results of numerous experimental and theoretical studies done during the past few years.

The book does not pretend to treat exhaustively all the problems arising in connection with studies of gas flows in a turbulent boundary layer at supersonic velocities. Partially this is due to an insufficient solution of these problems; this is especially the case for the problem of a turbulent boundary layer on loosened surfaces, and also in the case of ionized and radiating gas, etc. Partially, the personal interests of the author have also played their role. In particular, certain chapters of the book (III-V) include only those divisions of turbulent boundary layer theory to which the author contributed to a lesser or greater extent.

Chapter I presents the fundamentals of the molecular theory of gas flow and gives a derivation of the dynamic equations for a multicomponent reacting gas on the basis of the fundamental equation of the kinetic theory of gases, i.e., the Boltzmann equation.

Chapter II gives a derivation of a system of equations for a turbulent flow of a multicomponent reacting gas. This system of equations is used to obtain the equations of a turbulent boundary layer. The integral momentum and energy relations that play an important role in the semi-empirical theory of turbulent boundary layers are also derived therein.

Chapter III discusses the theoretical and experimental results obtained when studying the characteristics of a turbulent boundary layer on a nonpermeable surface in a supersonic gas flow which is homogeneous in composition. The semi-empirical and empirical methods for analyzing the boundary layer on a flat plate are presented. The effect of compressibility and heat transfer on the laminar sublayer is investigated. Experimental and theoretical data on the parameters characterizing the heat transfer between the gas and the wall (Reynolds similarity parameter connecting skin friction and heat transfer; recovery factor) are given. A generalization of the semi-empirical method to cases involving a flow over a cone at a zero angle of attack, over a sphere, as well as to bodies of arbitrary shape in a non-separated flow is also given.

Chapter IV discusses the flow of a dissociated gas in a turbulent boundary layer. A detailed treatment is given of the kinetics of chemical reactions occurring in a gas and on the surface of bodies, and in particular, data are presented on the kinetics of reactions of dissociation for oxygen and nitrogen. Various models of a dissociated, ideally dissociated and partially excited dissociated gas are described. The semi-empirical methods of computing skin friction and heat transfer on a flat plate for equilibrium, frozen, and nonequilibrium states of the gas are presented.

Chapter V gives the results of experimental and theoretical studies of a turbulent boundary layer in the presence of mass transfer between the gas and the surface around which the flow takes place. Methods of computing skin friction and heat transfer on a porous plate with various gases injected into the boundary layer are discussed.

CHAPTER I

EQUATIONS OF GAS DYNAMICS

§1. Introduction

The development of aerospace technology during the past few decades has aroused great interest in the problems of gas flow at supersonic and hypersonic velocities. A study of these problems has shown that these flows cannot be described using only classical gas dynamics, which is concerned with a flow at relatively low velocities. In this case, in addition to gas dynamics, one must turn to many areas of physics and chemistry.

Any flow of a viscous gas is accompanied by dissipation of mechanical energy, its conversion into heat. However, at low velocities viscous dissipation does not lead to the appearance of any noticeable temperature inhomogeneities (temperature gradients). Under these conditions, the density and viscosity of a gas may be considered to be constant physical parameters which are independent of the character of the flow.

An increase of the velocities of gases from low subsonic to moderately supersonic velocities, and as a result, the appearance of

substantial temperature gradients when a gas passes through shock waves and through boundary layers has made it necessary to consider the dependence of the density, viscosity, and heat capacity of a gas on the temperature. Here the flowing gas may be considered to be homogeneous.

A transition to hypersonic velocities causes such an enormous increase of the gas temperature in shock waves and boundary layers that thermochemical processes begin to take place in the gas that result in a dissociation of gas molecules into atoms, a dissociation of the atoms into ions and electrons (ionization), and the formation of oxides and other chemical compounds. In addition, in certain cases it is necessary to consider processes occurring on the surfaces of the bodies around which the flow takes place, such as fusion and sublimation of the surface layer of a body, chemical reactions, etc. Under these conditions, the moving medium must be regarded as a mixture of a number of components differing in their physical and chemical properties. A study of these complex processes using the usual methods of classical (phenomenological) gas dynamics in many cases turns out to be very difficult, especially if the thermochemical processes occur in a nonequilibrium fashion.

We must recall that the phenomenological approach to a study of various gas dynamic phenomena involves postulating certain relationships between the velocity gradient and the friction stress (Newton's law), heat flux and temperature gradient (Fourier's law), mass diffusion and concentration gradient (Fick's law), and using equations that can be obtained from the fundamental laws of classical mechanics and thermodynamics. The transport coefficients, i.e., the coefficients of proportionality in Newton's, Fourier's, and Fick's laws, reflecting certain properties of gas molecules and thus determined by its microstructure, are included in the phenomenological theory as constants or functions of the state that are known beforehand and cannot be calculated theoretically, but instead must be found experimentally. It is quite natural that the phenomenological

theory, based on an approximate macroscopic model of a gas, is
inadequate for describing the many complicated processes, whose
study must take into account various microscopic phenomena (excita-
tion of the internal degrees of freedom of molecules, dissociation,
ionization, etc.). The kinetic theory of gases is a tool that can
be used to describe such processes.

The kinetic theory enables us to determine the transport
coefficients as functions of the temperature of a gas mixture, of
molecular weights of the mixture components, and certain parameters
describing the field of intermolecular forces. It also makes it
possible to set up the macroscopic equations of motion for a gas
in question. The kinetic theory is valid only at sufficiently low
gas densities, when it is possible to neglect collisions of more
than two molecules. If the mean free path of a molecule in a gas is
small compared to the characteristic macroscopic dimensions of a body,
then the gas behaves like a continuous medium. In this case, the
basic equation of the kinetic theory, i.e., the Boltzmann equation,
can be used to obtain the gas-dynamic transport equations and
expressions for the transport coefficients. Since our intention is
to follow this path, we shall briefly present here some of the
elements of the kinetic theory of gases. A knowledge of the
fundamentals of the kinetic theory is necessary if one wishes to
understand the relationship between the micro- and macro-processes
occurring in a gas, and it is also practically useful when studying
the flow of multicomponent, chemically-reacting gas mixtures. Below
we shall present only those aspects of the kinetic gas theory that
will be found necessary later. A detailed and extensive presentation
of the theory is given in the monographs by Hirschfelder, Curtiss,
Bird [1], and by Chapman and Cowling [2].

§2.   Elements of the Molecular Theory of Gas Flows

The dynamic state of a system of particles can be completely
described by specifying the coordinates and velocities (momenta) of

all particles. The laws of classical mechanics enable us to pre-
dict the state of a system at any point in time from its initial
dynamic state.

At a certain time instant, each of the particles has a certain
velocity. Therefore to each particle we can assign a certain point
in velocity space, characterized by the vector v_1. The position of
a particle in the physical space is given by the vector r.

To fully describe the dynamic state of a system of particles,
the kinetic theory makes use of the concept of the distribution
function. If a mixture of (strictly speaking, monoatomic) gases in
a nonequilibrium state is considered, then the properties of each
component of the mixture can be described in terms of the distribu-
tion function $f_1(r, v_1, t)$, defined as the number of particles of
the species i which at time t are in an elementary unit volume of
the physical space containing the point r, whose velocities lie
inside the elementary unit volume in the velocity space containing
the point v_1.

The space $(x, y, z, v_{1x}, v_{1y}, v_{1z})$ is a phase space, and for
this reason the position and velocity coordinates are independent
variables.

The total number of particles in an elementary unit volume of
the physical space at time t can be obtained by integrating the
distribution function over all possible values of the velocities
v_{1x}, v_{1y} and v_{1z}:

$$n_i(r, t) = \int_{-\infty}^{+\infty} \int_{-\infty}^{+\infty} \int_{-\infty}^{+\infty} f_1 \, dv_{1x} \, dv_{1y} \, dv_{1z}. \tag{1.1}$$

By definition, n_1 is the numerical density of the particles of
species i. For convenience, the triple integral

$$\int_{-\infty}^{+\infty} \int_{-\infty}^{+\infty} \int_{-\infty}^{+\infty} (\ldots) \, dv_{1x} \, dv_{1y} \, dv_{1z}$$

will be denoted below by

$$\int (\dots) dv_i.$$

Knowing the distribution function, we can calculate the average value of any quantity ψ_i, associated with the particles of species i, and being a function of the velocity components alone. The formula for the average value of ψ_i can obviously be written as

$$\bar{\psi}_i(r, t) = \frac{1}{n_i} \int f_i(r, v_i, t) \psi_i(v_i) dv_i = \frac{\int f_i \psi_i dv_i}{\int f_i dv_i}. \qquad (1.2)$$

The line over ψ_i symbolizes averaging. Thus the average velocity $\bar{v}_i$ of the particles of the ith component whose numerical density is n_i is given by

$$\bar{v}_i(r, t) = \frac{1}{n_i} \int v_i f_i(r, v_i, t) dv_i. \qquad (1.3)$$

The average mass velocity, which is a weighted average since each particle makes a contribution to it which is proportional to its mass m_i, is defined by the formula

$$v(r, t) = \frac{\sum_i m_i n_i \bar{v}_i}{\sum_i m_i n_i}, \qquad (1.4)$$

where $\sum_i m_i n_i = \rho(r, t)$ is the density of the medium at the point in question.

The average mass velocity is usually termed the flow velocity, and possesses the property that the momentum of a unit volume of the gas is equal to the momentum that would result if all particles of this volume were moving at the velocity under consideration.

The thermal velocity of particles of species i is defined as the velocity of the particles relative to a coordinate system moving at the average mass velocity v:

$$\Gamma_i(r_i, r, t) = r_i - v. \tag{1.5}$$

The diffusive velocity of the ith component is defined as the flow velocity of particles of this component relative to a coordinate system moving at the average mass velocity of the gas. In other words, the diffusive velocity is defined as the average thermal velocity:

$$\overline{V}_i(r, t) = \frac{1}{n_i} \int (r_i - r) f_i(r, v_i, t) dv_i = \overline{v}_i - v. \tag{1.6}$$

The temperature in the kinetic theory is defined in terms of the kinetic energy of thermal motion averaged over all particles

$$\frac{3}{2} kT = \frac{1}{n} \sum_i \frac{1}{2} m_i n_i \overline{V_i^2}, \tag{1.7}$$

where $n = \sum_i n_i$, and k is the Boltzmann constant.

Listing the expressions for all the macroscopic quantities given in terms of the distribution function, we shall have

$$\left. \begin{array}{l} \rho(r, t) = \sum_i m_i n_i = \sum_i m_i \int f_i dv_i, \\[2mm] T(r, t) = \frac{1}{3nk} \sum_i m_i \int V_i^2 f_i dv_i, \\[2mm] v(r, t) = \frac{1}{\rho} \sum_i m_i \int r_i f_i dv_i, \\[2mm] p_i = \rho_i \frac{k}{m_i} T, \quad \rho_i = n_i m_i, \quad p = \sum_i p_i. \end{array} \right\} \tag{1.8}$$

In a gas in a state of nonequilibrium, the field of one or several quantities characterizing the macroscopic properties of a system may be inhomogeneous. The inhomogeneity of the fields — i.e., the existence of the gradients of macroscopic quantities (of the average mass velocity v, temperature T, mass concentration $c_i = \rho_i/\rho$, and others) — causes the molecular transport of the momentum $m_i V_i$, kinetic energy $\frac{1}{2} m_i V_i^2$, and mass m_i through the gas.

In order to characterize the molecular transport of some substance, in the kinetic theory one introduces the concept of the

flux density vector of ψ_1[1]:

$$\Psi_i = \int \psi_i J_i V_i \, dV_i. \tag{1.9}$$

The physical interpretation of the flux density is that its component in any direction is the density of the flow of the corresponding physical quantity through a surface normal to this direction.

If $\psi_1 = m_1$, then from Equation (1.9) we obtain the flux density for the mass

$$j_i = m_i \int f_i V_i \, dV_i = m_i n_i \overline{V}_i. \tag{1.10}$$

If $\psi_1 = m_1 V_1$, then

$$P_i = m_i \int f_i V_i V_i \, dV_i = m_i n_i \overline{V_i V_i} \tag{1.11}$$

is a symmetric tensor of second rank characterizing the partial pressure of the ith component of the gas[2]. The sum of the tensor partial pressures over all gas components forms the tensor of the pressures of the mixture

$$P = \sum_i P_i = \sum_i m_i n_i \overline{V_i V_i}. \tag{1.12}$$

The diagonal elements of the pressure tensor P_{xx}, P_{yy}, and P_{zz} are equal to the normal stresses, and the off-diagonal elements represent the shear stresses. For example, P_{yx} is equal to the force per unit area of a surface perpendicular to the y direction in the x direction.

If $\psi_i = \frac{1}{2} m_i V_i^2$, then

$$q_i = \frac{1}{2} m_i \int f_i V_i^2 V_i \, dV_i = \frac{1}{2} m_i n_i \overline{V_i^2 V_i} \tag{1.13}$$

Footnotes (1) and (2) appear on page 38.

is a flow vector characterizing the transport of the kinetic energy
by the particles of species 1. The sum of such vectors over all
components of the gas mixture gives the heat flux density vector

$$q = \sum_i q_i = \sum_i \frac{1}{2} m_i n_i \overline{V_i^2 V_i}. \tag{1.14}$$

The components q_x, q_y, q_z of the heat flux vector represent the
fluxes of th kinetic energy in the x, y, and z directions, respec-
tively.

Equations (1.8) and (1.10) - (1.14) indicate that, if the
distribution function f_1 is known, then the problem of determining
the field of flow and the transport characteristics can be completely
solved.

The variation of the distribution function f_1 is described by
the integro-differential Boltzmann equation which, assuming the
absence of an external force, becomes

$$\frac{\partial f_i}{\partial t} + v_i \cdot \frac{\partial f_i}{\partial r} = \sum_j I_{ij}. \tag{1.15}$$

Here

$$I_{ij} = 2\pi \iint (f_i' f_j' - f_i f_j) g_{ij} b\, db\, dv_j \tag{1.16}$$

is the collision integral accounting for the change in the number of
particles of a given group due to collisions; $g_{ij} = |v_i - v_j|$ is the
absolute value of the relative velocity of the particles of species
i and j before a collision; b is the minimum distance between the
colliding particles if there were no interaction (impact parameter);
f'_i and f'_j are the distribution functions of the colliding particles
of species i and j after the collision; f_i and f_j are the distribution
functions of the colliding particles before the collision.

Equations similar to Equation (1.15) can be written for all
components of the gas mixture. In each of these equations, the

integrand on the right-hand side will contain the distribution
functions of all components of the mixture. These integrals depend
implicitly on the intermolecular interaction. The distribution
functions f'_i and f'_j are functions of the velocities v'_i and v'_j
which can be found from the laws of mechanics assuming v_i, v_j, b,
and the potential of the intermolecular interaction are known.

§3. Gas Dynamic Transport Equations Expressed in Terms of the Flux Density Vectors

The basic gas dynamic transport equations — i.e., conservation
equations for mass, momentum, and energy — can be obtained directly
from the Boltzmann equation without specifying the form of the
distribution functions. Multiplying the Boltzmann Equation (1.15)
by ψ_i and integrating the result over all values of the velocity v_i,
we obtain

$$\int \psi_i \left(\frac{\partial f_i}{\partial t} + v_i \cdot \frac{\partial f_i}{\partial r} - \sum_j I_{ij} \right) dv_{ij} = 0. \tag{1.17}$$

The first two terms on the left-hand side of the equation can be put
in the form

$$\int \psi_i \frac{\partial f_i}{\partial t} dv_i = \frac{\partial}{\partial t} \int \psi_i f_i \, dv_i - \int f_i \frac{\partial \psi_i}{\partial t} dv_i =$$
$$= \frac{\partial}{\partial t} (n_i \overline{\psi_i}) - n_i \overline{\frac{\partial \psi_i}{\partial t}},$$
$$\int \psi_i v_i \cdot \frac{\partial f_i}{\partial r} dv_i = \frac{\partial}{\partial r} \cdot \int f_i \psi_i v_i dv_i - \int f_i \left(v_i \cdot \frac{\partial \psi_i}{\partial r} \right) dv_i =$$
$$= \frac{\partial}{\partial r} \cdot (n_i \overline{\psi_i v_i}) - n_i \overline{\left(v_i \cdot \frac{\partial \psi_i}{\partial r} \right)}.$$

Substituting these equations in the left-hand side of Equation
(1.17), we have

$$\frac{\partial}{\partial t} (n_i \overline{\psi_i}) + \frac{\partial}{\partial r} \cdot (n_i \overline{\psi_i v_i}) - n_i \left(\overline{\frac{\partial \psi_i}{\partial t}} + \overline{v_i \cdot \frac{\partial \psi_i}{\partial r}} \right) = \tag{1.18}$$
$$= \sum_j \int \psi_i I_{ij} dv_i.$$

This equation is known as Enskog's generalized transport equation for
ψ_i associated with particles of species i.

Summing Equation (1.18) over all components, we can obtain the transport equation for the mixture:

$$\frac{\partial}{\partial t} \sum_i n_i \overline{\psi_i} + \frac{\partial}{\partial r} \cdot \sum_i n_i \overline{\psi_i v_i} - \sum_i n_i \left(\overline{\frac{\partial \psi_i}{\partial t}} + \overline{v_i \cdot \frac{\partial \psi_i}{\partial r}} \right) =$$
$$= \sum_{j,i} \int \psi_i I_{ij} dv_i. \qquad (1.19)$$

It is very difficult to use Equation (1.19) for arbitrary quantities ψ_i due to the presence of very complicated integrals on the right-hand side of the equation. However, if ψ_i is identified as the mass m_i, momentum $m_i V_i$, or the kinetic energy of the molecules $\frac{1}{2} m_i V_i^2$ (in the case of the multi-atomic molecules, in addition to the kinetic energy, one must also consider the internal energy), then, as one can verify, the right-hand side of Equation (1.19) is equal to zero and the equation becomes considerably simplified. In fact, let us assume that the interacting system consists of two types of particles: one of type i with mass m_i, and the other of type j with mass m_j. Let us assume that the velocities of particles before collisions are V_i and V_j, respectively, and that the corresponding velocities after the collision are V'_i and V'_j. Then, assuming that the system of colliding particles as a whole is not subject to any external forces, and the collisions are adiabatic, on the basis of the conservation laws for mass, momentum, and energy we can write

$$\left. \begin{array}{l} m_i + m_j = m'_i + m'_j, \\ m_i V_i + m_j V_j = m'_i V'_i + m'_j V'_j, \\ \frac{1}{2} m_i V_i^2 + \frac{1}{2} m_j V_j^2 = \frac{1}{2} m'_i V'^2_i + \frac{1}{2} m'_j V'^2_j. \end{array} \right\} \qquad (1.20)$$

In the absence of chemical reactions $m_i = m'_i$, $m_j = m'_j$.

The above expressions for the conservation laws (1.20) for a system of colliding particles can be written in the following generalized form:

$$\psi_i + \psi_j = \psi'_i + \psi'_j. \qquad (1.21)$$

where ψ_i is any of the quantities m_i, $m_i V_i$ and $\frac{1}{2} m_i V_i^2$. It can be shown that any function of velocities, satisfying the relation (1.21),

is a linear combination of these quantities. The quantities ψ_1, satisfying Equation (1.21), came to be called summation invariants.

Now let us consider the integral under the summation sign on the right-hand side of Equation (1.19). This integral

$$\frac{1}{2!}\int\psi_i I_{ij}\,dv_i = \iiint\psi_i(f_if_j - ff_j)g_{ij}\,b\,db\,dv_j\,dv_i \qquad (1.22)$$

is equal to the integral

$$\iiint\psi_i(ff_j - f_if_j)g_{ij}'\,b'\,db'\,dv_j'\,dv_i. \qquad (1.23)$$

written for reverse collisions.

It can be shown[3] that $g_{ij} = g'_{ij}$, $b = b'$ and $dv_j \cdot dv_1 = dv'_j \cdot dv'_1$. Therefore, the integral (1.23) can be written as

$$-\iiint\psi_i(f_if_j - ff_j)g_{ij}\,b\,db\,dv_j\,dv_i. \qquad (1.24)$$

Since the integrals (1.22) and (1.24) are equal, each of them will be equal to one half of the sum of both integrals, i.e.,

$$\frac{1}{2!}\int\psi_i I_{ij}\,dv_i = \frac{1}{2}\iiint(\psi_i - \psi_i')(f_if_j - ff_j)g_{ij}\,b\,db\,dv_j\,dv_i.$$

Summing these integrals over i and j, and using the fact that i and j may be interchanged, we have

$$\frac{1}{2!}\sum_{ij}\int\psi_i I_{ij}\,dv_i = \frac{1}{4}\sum_{ij}\iiint(\psi_i + \psi_j - \psi_i' - \psi_j') \times \qquad (1.25)$$
$$\times (ff_j - f_if_j)g_{ij}\,b\,db\,dv_j\,dv_i.$$

For summation invariants, $\psi_1 + \psi_j = \psi'_1 - \psi'_j$ is equal to zero. Consequently, also the right-hand side of Knokog's generalized transport Equation (1.19) vanishes if ψ_1 is equal to m_1, $m_1 V_1$ or $\frac{1}{2}\,m_1 V_1^2$.

Footnote (3) appears on page 38.

Thus the mass, momentum, or energy transport in a gas mixture are described by the following equation:

$$\frac{\partial}{\partial t} \sum_i n_i \overline{\psi_i} + \frac{\partial}{\partial r} \cdot \sum_i n_i \overline{\psi_i v_i} - \sum_i n_i \left(\overline{\frac{\partial \psi_i}{\partial t}} + \overline{v_i \cdot \frac{\partial \psi_i}{\partial r}} \right) = 0. \qquad (1.26)$$

Now we shall derive transport equations for specific molecular quantities. We set $\psi_i = m_i$. In this case Equation (1.18) becomes

$$\frac{\partial n_i}{\partial t} + \frac{\partial}{\partial r} \cdot (n_i \overline{v_i}) = \sum_j \int I_{ij} dv_i = K_i. \qquad (1.27)$$

The integral $\int I_{ij} dv_i$ is equal to the rate at which the number of particles of the ith type increases due to collisions with particles of jth type in a unit volume (in the absence of chemical reactions the integral vanishes). The quantity

$$\sum_j \int I_{ij} dv_i = K_i$$

gives the total increase in the number of particles of the ith type in a unit volume per unit time due to collisions with all types of particles, including those of the ith type (as a result of chemical reactions). Substituting in Equation (1.27) the expression for $\overline{v_i}$ from Equation (1.6), we obtain the equation of continuity for the ith component of the gas:

$$\frac{\partial n_i}{\partial t} + \frac{\partial}{\partial r} \cdot [n_i(v + \Gamma_i)] = K_i. \qquad (1.28)$$

Passing in Equation (1.28) from n_i to mass concentrations

$$c_i = \frac{n_i m_i}{\sum_i n_i m_i} = \frac{n_i m_i}{nm} = \frac{\rho_i}{\rho}, \quad m = \left(\sum_i \frac{c_i}{m_i} \right)^{-1}. \qquad (1.29)$$

we have

$$\frac{\partial}{\partial t}(\rho c_i) + \frac{\partial}{\partial r} \cdot [\rho c_i(v + \Gamma_i)] = w_i. \qquad (1.30)$$

where $w_i = m_i K_i$ is the mass rate of formation of the ith component in a unit volume.

Summing Equations (1.30) over all i, we obtain an equation of continuity for a mixture of gases

$$\frac{\partial \rho}{\partial t} + \frac{\partial}{\partial r} \cdot (\rho v) = 0, \tag{1.31}$$

since $\sum_i \rho_i \overline{V}_i = 0$ by the definition of the rate of diffusion, and $\sum_i w_i = 0$ by Equations (1.21) and (1.25). The condition

$$\sum_i w_i = 0 \tag{1.32}$$

expresses the conservation of mass of a gas mixture with chemical conversions taking place.

Using the equation of continuity for a mixture of gases (1.31), we put the equation of continuity for the ith component in the form

$$\rho \frac{\partial c_i}{\partial t} + \rho v \cdot \frac{\partial c_i}{\partial r} = w_i - \frac{\partial}{\partial r} \cdot (\rho c_i \overline{V}_i). \tag{1.33}$$

It will be noted that on the right-hand side of Equation (1.33) the quantity to be differentiated was defined earlier [see formula (1.10)] as the mass flux density vector.

To obtain the momentum transport equation we substitute $\psi_i = m_i V_i$ in Equation (1.26), and obtain

$$\sum_i m_i \left[\frac{\partial (n_i \overline{V}_i)}{\partial t} + \frac{\partial}{\partial r} \cdot (n_i \overline{v_i V_i}) - n_i \frac{\overline{\partial V_i}}{\partial t} - n_i \overline{\left(v_i \cdot \frac{\partial}{\partial r} \right) V_i} \right] = 0. \tag{1.34}$$

This equation can be simplified by making use of the relations between velocities (1.5) and (1.6) and the definition of the pressure tensor (1.12). When differentiating, it must only be kept in mind that r, v_i and t are independent variables. After simple transformations, the equation of motion for a mixture of gases will be written in the following form:

$$\frac{\partial v}{\partial t} + \left(v \cdot \frac{\partial}{\partial r} \right) v = - \frac{1}{\rho} \left(\frac{\partial}{\partial r} \cdot P \right). \tag{1.35}$$

The energy transport equation will be obtained by substituting $\psi_1 = \frac{1}{2} m_1 V_1^2$ in Equation (1.26):

$$\sum_i \frac{1}{2} m_1 \left[\frac{\partial (n_i \overline{V_i^2})}{\partial t} + \frac{\partial}{\partial r} \cdot n_i \overline{v_i V_i^2} - n_i \frac{\overline{\partial V_i^2}}{\partial t} - n_i \left(\overline{v_i \cdot \frac{\partial V_i^2}{\partial r}} \right) \right] = 0. \qquad (1.36)$$

Using the relations between the velocities (1.5), (1.6), and the definition of the pressure tensor (1.12), and introducing the energy flux density vector q, defined by Equation (1.14), we shall get the energy balance equation

$$\frac{\partial}{\partial t} (\rho E) + \frac{\partial}{\partial r} \cdot \rho v E + \frac{\partial}{\partial r} \cdot q + \left(P \cdot \frac{\partial}{\partial r} \right) \cdot v = 0. \qquad (1.37)$$

Here

$$E = \frac{1}{\rho} \sum_i m_i n_i V_i^2 \qquad (1.38)$$

is the internal energy of the gas per unit mass, equal to the translational motion of molecules (kinetic energy of the translational motion of a gas stream as a whole is not included in this energy). In the last term on the left-hand side of Equation (1.37) the symbol $P \cdot \frac{\partial}{\partial r}$ means that the tensor P is multiplied by the vector $\frac{\partial}{\partial r}$. We recall that this operation can in general be represented by the expression $T \cdot A$, and the result can be expressed as a vector with components

$$(T \cdot A)_x = T_{xx} A_x + T_{xy} A_y + T_{xz} A_z \quad \text{etc.}$$

Equation (1.37) can be simplified using the equation of continuity for the mixture (1.31). As a result, we have

$$\rho \frac{\partial E}{\partial t} + \rho v \cdot \frac{\partial E}{\partial r} = - \frac{\partial}{\partial r} \cdot q - \left(P \cdot \frac{\partial}{\partial r} \right) \cdot v. \qquad (1.39)$$

Equation (1.39) is also valid for polyatomic gases whose molecules possess internal degrees of freedom. In this case, E should be understood as the sum of energies of translational and internal degrees of freedom of molecules,

$$E = \frac{1}{\rho} \sum_i \frac{1}{2} m_i n_i \overline{V_i^2} + \frac{1}{\rho} \sum_i n_i e_i. \qquad (1.40)$$

and the expression for the energy flux density (1.14) must be
replaced by the expression

$$q = \frac{1}{2} \sum_i m_i n_i \overline{V_i^2 V_i} + \sum_i n_i e_i \overline{V_i}. \qquad (1.41)$$

where e_1 is the energy of the internal degrees of freedom of a
molecule of the ith type.

The energy balance Equation (1.39) can be written in terms of
the temperature. In this case, using the equation of continuity for
the ith component (1.30), we get

$$\rho c_v \left(\frac{\partial T}{\partial t} + v \cdot \frac{\partial T}{\partial r} \right) = - \frac{\partial}{\partial r} \cdot q - \left(P \cdot \frac{\partial}{\partial r} \right) v - \\ - \sum_i w_i E_i + \sum_i E_i \left(\frac{\partial}{\partial r} \cdot n_i V_i \right). \qquad (1.42)$$

Here

$$c_v = \sum_i c_i \left(\frac{\partial E_i}{\partial T} \right)_v = \sum_i c_i c_{vi} \qquad (1.43)$$

is the mean specific heat of the mixture per unit weight at constant
volume.

§4.   Rate of Diffusion, Flux Density Vectors and Transport Coefficients

The basic gas dynamic equations of continuity (1.33), motion
(1.35), and energy (1.39) or (1.42) were obtained from the Boltzmann
equation without specifying the form of the distribution function.
However, an inspection of these equations makes it clear that to use
them in practice one must know the expressions for the rate of
diffusion and the mass, momentum, and energy flux density vectors
in terms of the spatial derivatives of the macroscopic quantities and
transport coefficients.

To determine these quantities, one must solve the Boltzmann equation. A great deal of literature is devoted to the problem of obtaining approximate solutions of the Boltzmann equation[4]. It is impossible to dwell upon this problem in detail in the present volume, and for this reason we shall merely briefly present the ideas involved in a widely known method used to solve the Boltzmann equation, i.e., the Enskog-Chapman method of perturbations.

As we know, a gas which is adiabatically insulated and is not subject to external perturbing influences for a sufficient length of time will finally achieve a certain state of equilibrium. For systems in equilibrium, the distribution function f_1 does not depend on the time, and as a result the right-hand side of the Boltzmann Equation (1.15) vanishes. The vanishing of the right-hand side of the equation expresses the state of equilibrium existing in collision processes, which means that the number of particles of the ith type leaving a certain velocity interval due to collisions is exactly equal to the number of particles entering this interval as a result of collisions. The sufficient condition for equilibrium may be obtained if the integrand on the right-hand side of the Boltzmann equation is assumed to vanish, i.e.,

$$f_i f_j = f_i' f_j'$$

$$(1.44)$$

However, it is not clear whether this condition is necessary, since for the right-hand side of the Boltzmann equation to vanish, it is only necessary that the integrand assume positive and negative values in the region of integration, so that the definite integral will add up to zero. The necessity of the condition (1.44) is proved using Boltzmann's H-theorem, whose proof can be found in the monograph by Hirschfelder, Curtiss, and Bird.

Equation (1.44) can be written as

Footnote (4) appears on page 38.

$$\ln f_i + \ln f_j = \ln f_i + \ln f_j \qquad (1.45)$$

Consequently, logarithms of the distribution functions are summation invariants for molecular collisions. But according to the conservation laws (1.20), the only quantities that can qualify as summation invariants for collisions are the mass m_i, momentum $m_i v_i$, and kinetic energy $\frac{1}{2} m_i v_i^2$. Therefore, in general $\ln f_i$ must be a linear combination of these quantities, i.e.,

$$\ln f_i = a_i m_i + b \cdot (m_i v_i) + c \left(\frac{1}{2} m_i v_i^2\right), \qquad (1.46)$$

where a_i, b and c are constants which depend (through initial distribution functions) on the total number of molecules of the ith type, total momentum, and total energy of the system. Upon determining these constants from the conditions

$$\begin{cases} \int f_i \, dv_i = n_i, \\ \sum_i m_i \int v_i f_i \cdot dv_i = \rho v, \\ \frac{1}{2} \sum_i m_i \int (v_i - v)^2 f_i \, dv_i = \frac{3}{2} nkT, \end{cases} \qquad (1.47)$$

we arrive at the well-known Maxwell distribution function for a system in equilibrium

$$f_i = n_i \left(\frac{m_i}{2\pi kT}\right)^{3/2} \exp\left[-\frac{m_i}{2kT} (v_i - v)^2\right], \qquad (1.48)$$

where $v_i - v = V_i$ is the thermal velocity.

In the case when the gas mixture is not in equilibrium, the distribution function can be found using the Enskog-Chapman method by introducing a perturbation parameter ε in the Boltzmann equation ($1/\varepsilon$ is a measure of the collision frequency). For small ε, collisions occur very frequently, so that the gas may be considered as a continuous medium at each point of which a local equilibrium is established. The distribution function for this case can be expanded into a series in the parameter ε:

$$f_i = f_i^{(0)} + \varepsilon f_i^{(1)} + \varepsilon^2 f_i^{(2)} + \ldots \qquad (1.49)$$

Substituting this series into a rearranged Boltzmann equation

$$\frac{\partial f_i}{\partial t} + v_i \cdot \frac{\partial f_i}{\partial r} = \frac{1}{\varepsilon} \sum_j I_{ij} \qquad (1.50)$$

and equating coefficients of identical powers of ε, we obtain a system of equations for the function $f_i^{(0)}$, $f_i^{(1)}$, etc.:

$$\left. \begin{aligned} & 0 = \sum_j I_{ij}(f_i^{(0)}, f_j^{(0)}), \\ & \frac{\partial f_i^{(0)}}{\partial t} + v_i \cdot \frac{\partial f_i^{(0)}}{\partial r} = \\ & \qquad = \sum_j [I_{ij}(f_i^{(0)}, f_j^{(1)}) + I_{ij}(f_i^{(1)}, f_j^{(0)})] \text{ etc.} \end{aligned} \right\} \qquad (1.51)$$

The solution of the first equation in the system (1.51) is, as is easy to see, in the form of the Maxwell distribution (1.48). The quantities

$$n_i = n_i(r,\ t),\ v = v(r,\ t) \text{ and } T = T(r,\ t),$$

in the expression (1.48) are arbitrary functions of position and time. In order that these quantities may correspond to their local values, it is necessary that the solutions of the remaining equations of the system (1.51) satisfy the conditions (1.47). In other words, the distribution functions, in an approximation of order higher than zero $f_i^{(k)}$, $k = 1, 2, 3, \ldots$, must satisfy the conditions

$$\left. \begin{aligned} & \int f_i^{(k)} dv_i = 0, \\ & \sum_i m_i \int v_i f_i^{(k)} dv_i = 0, \\ & \frac{1}{3} \sum_i m_i \int (v_i - v)^2 f_i^{(k)} dv_i = 0 \\ & \text{for } (k = 1, 2, 3, \ldots \end{aligned} \right\} \qquad (1.52)$$

Using the conditions (1.52) one can obtain solutions of the second equation in the system (1.51), etc. The Enskog-Chapman method which is essentially a method of successive approximations can in principle be extended to systems with larger gradients of thermodynamic and gas-dynamic quantities. However, in order to solve a majority of gas-dynamic problems, it is sufficient to solve the Boltzmann equation to a first approximation. In this case, the law describing the variation of the distribution function differs very little from the Maxwell law (1.48), and the gradients of quantities characterizing the macroscopic properties of a gas turn out to be small in the sense that these quantities do not vary appreciably over a distance on the order of the mean free path of molecules.

Referring the reader who is interested in the details of the mathematical solution of the system (1.51) to the already cited monograph by Hirschfelder et al., we shall indicate some of the results obtained when solving the Boltzmann equation to a first approximation.

The expression for the rate of diffusion has the form

$$\overline{V}_i = \frac{n^2}{\rho n_i} \sum_{j=1}^{N} m_j D_{ij} \left[\frac{\partial}{\partial r} \left(\frac{n_j}{n} \right) + \left(\frac{n_j}{n} - \frac{n_j m_j}{\rho} \right) \frac{\partial \ln p}{\partial r} \right] - \frac{1}{n_i m_i} \mathscr{D}_i^\tau \frac{\partial \ln T}{\partial r}, \qquad i = 1, 2, \ldots, N, \tag{1.53}$$

where D_{ij} and $\mathscr{D}_i^\tau$ are the diffusion and thermal diffusion coefficients for a multicomponent mixture, respectively; p is the pressure. Formula (1.53) shows that in the absence of mass forces, diffusion may occur for three reasons: (1) under the influence of a concentration gradient (mass diffusion), (2) under the influence of a pressure gradient (pressure diffusion), and (3) under the influence of a temperature gradient (thermal diffusion).

It must be emphasized that in the zero[th] approximation [for the Maxwell velocity distribution (1.48)], the rate of diffusion $\overline{V}_i$, and consequently, the mass flux density vector for the ith component, J_i, will be equal to zero.

The expression for the rate of diffusion of the ith component of the mixture (1.53) is usually difficult to use in practical calculations, since it involves a diffusion coefficient for a multi-component mixture, D_{ij}, which to a first approximation can be expressed in the form of determinants of Nth order (N is the number of components in the mixture) in terms of the diffusion coefficients for the binary mixture $\mathscr{D}_{ij}$, and of concentrations and molecular weights of the components.

It is much more convenient, instead of N formulas (1.53), to use N - 1 independent relations

$$\sum_{\substack{j=1 \\ j\neq i}} \frac{n_i n_j}{n^2 \mathscr{D}_{ij}} (\overline{V}_j - \overline{V}_i) = \frac{\partial}{\partial r}\left(\frac{n_i}{n}\right) + \left(\frac{n_i}{n} - \frac{n_i m_i}{\rho}\right)\frac{\partial \ln p}{\partial r} -$$
$$- \frac{\partial \ln T}{\partial r}\sum_{\substack{j=1 \\ j\neq i}}^{N} \frac{n_i n_j}{n^2 \mathscr{D}_{ij}}\left(\frac{\mathscr{D}_j^T}{n_j m_j} - \frac{\mathscr{D}_i^T}{n_i m_i}\right). \tag{1.54}$$

A derivation of these relations, sometimes called the Stefan-Maxwell relations, can be found in the monograph by Hirschfelder, Curtiss, and Bird[5].

If one neglects thermal diffusion and pressure diffusion as compared to mass diffusion, then Equations (1.54) simplify to the form

$$\sum_{\substack{j=1 \\ j\neq i}}^{'N} \frac{n_i n_j}{n^2 \mathscr{D}_{ij}}(\overline{V}_j - \overline{V}_i) = \frac{\partial}{\partial r}\left(\frac{n_i}{n}\right). \tag{1.55}$$

Using the expression for the mass concentration (1.29), we put (1.55) in the form [3]

$$\frac{\partial c_i}{\partial r} = \sum_{j=1}^{N} \frac{c_i c_j m}{m_j \mathscr{D}_{ij}}(\overline{V}_j - \overline{V}_i) - \sum_{k=1}^{N} c_k \sum_{\substack{j=1 \\ j\neq k}}^{N} \frac{c_i c_j m}{m_j \mathscr{D}_{kj}}(\overline{V}_j - \overline{V}_k). \tag{1.56}$$

Making use of Equation (1.56), we can introduce the so-called effective diffusion coefficient $\mathscr{D}_i$ [6]:

$$J_i = -\rho \mathscr{D}_i \frac{\partial c_i}{\partial r}, \tag{1.57}$$

Footnotes (5) and (6) appear on page 38.

where $\mathscr{D}_i$ can be found using one of the following formulas:

$$\frac{1}{\mathscr{D}_i} = \sum_{j=1}^{N} \frac{m}{m_j} \frac{c_j}{\mathscr{D}_{ij}} \left(1 - \frac{\overline{V}_j}{\overline{V}_i}\right) + \sum_{k=1}^{N} c_k \sum_{j=1}^{N} \frac{m}{m_j} \frac{c_i}{\mathscr{D}_{kj}} \frac{\overline{V}_j - \overline{V}_k}{\overline{V}_i} =$$

$$= \sum_{j=1}^{N} \frac{m}{m_j} \frac{c_j}{\mathscr{D}_{ij}} \left(1 - \frac{c_i J_i}{c_j J_i}\right) + \sum_{k=1}^{'N} c_k \sum_{j=1}^{N} \frac{m}{m_j} \left(\frac{c_i J_i}{c_j J_i} - \frac{c_i J_k}{c_k J_i}\right). \tag{1.58}$$

From the definition of the effective diffusion coefficient (1.58), it is clear that generally speaking this coefficient depends not only on the composition of a mixture of gases, but also on the ratios of the diffusive flows of components, i.e., essentially on the defining parameters of a concrete problem. This circumstance, although in certain cases creating inconveniences in the computation process, is not important in boundary layer calculations for multi-component mixtures of gases[7], since in many cases the most convenient method of calculations is the method of successive approximations.

The diffusion coefficient for a binary mixture, $\mathscr{D}_{ij}$, is given by the expression

$$\mathscr{D}_{ij} = 0,0026280 \sqrt{\frac{1}{2}\left(\frac{1}{M_i} + \frac{1}{M_j}\right)} \frac{T^{3/2}}{p \sigma_{ij}^2 \Omega_{ij}^{(1,1)*}(T_{ij}^*)} \frac{cm^2}{sec}. \tag{1.59}$$

Here p is the pressure, in atm; M_i is the molecular weight of the ith component; $\Omega_{ij}^{(1,1)*}(T_{ij}^*)$ is the collision term for mass transfer measuring the deviation from the model in which gas molecules are considered as hard spheres for which $\Omega_{ij}^{(1,1)*} = 1$; T is the temperature, in °K; $T_{ij}^* = kT/\varepsilon_{ij}$ is the characteristic temperature, in °K; ε_{ij}/k is a parameter related to the potential energy of molecules that characterizes the interaction between molecules of the ith and j^{th} type, °K; σ_{ij} is the effective collision diameter for molecules (in angstroms).

The values of the function $\Omega_{ij}^{(1,1)*}(T_{ij}^*)$ for $0.3 \leq T_{ij}^* \leq 400$ are listed in the monograph by Hirschfelder, Curtiss, and Bird.

Footnote (7) appears on page 38.

Formula (1.59) shows that the diffusion coefficients for a binary mixture, $\mathcal{D}_{ij}$, are relatively insensitive to moderate changes in the molecular weights of the components. Therefore, if any gas mixture consists of two types of components, each of which has approximately identical atomic or molecular weight and approximately identical collision cross-sections, then the mixture may be considered to be "effectively" binary in that each group acts as a single component. One must, however, keep in mind that in calculating the energy transfer, one must strictly differentiate between the enthalpies of the individual components.

For a binary mixture, from Equation (1.53) one can easily obtain the following expression for the diffusive flux of the ith component:

$$j_i = m_i n_i \overline{V}_i = -\frac{n^2}{\rho} m_i m_j \mathcal{D}_{ij} \left[\frac{\partial}{\partial r}\left(\frac{n_i}{n}\right) + \left(\frac{n_i}{n} - \frac{n_i m_i}{\rho}\right) \frac{\partial \ln p}{\partial r} - k_T \frac{\partial \ln T}{\partial r} \right]. \tag{1.60}$$

Here

$$k_T = \frac{\rho}{n^2 m_i m_j} \frac{\mathcal{D}_i^T}{\mathcal{D}_{ij}} \tag{1.61}$$

is the ratio of the thermal diffusion coefficient to the binary diffusion coefficient, known as the thermal diffusion ratio. This ratio characterizes the relative significance of the thermal diffusion versus the mass diffusion.

Using Expression (1.29), we shall change in Equation (1.60) to the mass concentration, and we obtain the result

$$j_i = -\rho c_i \mathcal{D}_{ij} \left[\frac{\partial \ln c_i}{\partial r} + \frac{m_j - m_i}{m} c_j \frac{\partial \ln p}{\partial r} + \frac{m_i m_j}{m^2 c_i} k_T \frac{\partial \ln T}{\partial r} \right]. \tag{1.62}$$

In boundary layer type flows, the contribution of the pressure diffusion to mass transfer is always negligibly small as compared to the contribution of the mass diffusion, since with an accuracy on the order of 1/Re, the pressure is constant across a boundary

layer. The term characterizing the thermal diffusion is also usually small as compared to the term describing mass diffusion. In a turbulent boundary layer, where the molecular diffusion needs to be considered only in the laminar sublayer, usually occupying less than one half of the entire boundary layer (although in certain cases the thickness of the sublayer may amount to more than 50% of the thickness of the entire layer), only the mass diffusion must be considered[8]. In this case Equation (1.62) assumes the form known as Fick's law

$$j_i = -\rho \mathcal{D}_{ij} \frac{\partial c_i}{\partial r} . \tag{1.63}$$

Continuing the discussion of the first-order approximations to the solution of the Boltzmann equation, we shall write an expression for the pressure tensor

$$P = p\dot{\mathcal{E}} - 2\mu\dot{S}, \tag{1.64}$$

where

$$p = nkT \tag{1.65}$$

is the equilibrium static pressure for a local temperature and density of particles,

$$\dot{\mathcal{E}} = \begin{pmatrix} 1 & 0 & 0 \\ 0 & 1 & 0 \\ 0 & 0 & 1 \end{pmatrix} \tag{1.66}$$

is the unit tensor, $\dot{S}$ is the rate of strain (displacement) tensor, defined by the expression

$$\dot{S}_{\alpha\alpha} = \frac{\partial v_\alpha}{\partial \alpha} - \frac{1}{3}\left(\frac{\partial}{\partial r} \cdot v\right), \quad \dot{S}_{\alpha\beta} = \frac{1}{2}\left(\frac{\partial v_\beta}{\partial \alpha} + \frac{\partial v_\alpha}{\partial \beta}\right), \tag{1.67}$$
$$\alpha,\beta = 1,2,3,$$

μ is the dynamic viscosity coefficient.

Footnote (8) appears on page 39.

The diagonal and off-diagonal elements of the pressure tensor are

$$P_{\alpha\alpha} = p + \frac{2}{3}\mu\left(\frac{\partial}{\partial r}\cdot v\right) - 2\mu\frac{\partial v_\alpha}{\partial \alpha},$$

$$P_{\alpha\beta} = -\mu\left(\frac{\partial v_\beta}{\partial \alpha} + \frac{\partial v_\alpha}{\partial \beta}\right), \quad \alpha, \beta = 1, 2, 3. \quad (1.68)$$

Equation (1.68) shows that the pressure tensor differs only as to its sign from the stress tensor, as usually defined in the mechanics of continuous media [4].

The dynamic viscosity coefficient introduced above for the case of an N-component gas mixture is defined by the expression[9]

$$\frac{\begin{vmatrix} H_{11} & H_{12} & H_{13} & \ldots & H_{1N} & x_1 \\ H_{12} & H_{22} & H_{23} & \ldots & H_{2N} & x_2 \\ H_{13} & H_{23} & H_{33} & \ldots & H_{3N} & x_3 \\ \cdot & \cdot & \cdot & \cdot & \cdot & \cdot \\ H_{1N} & H_{2N} & H_{3N} & \ldots & H_{NN} & x_N \\ x_1 & x_2 & x_3 & \ldots & x_N & 0 \end{vmatrix}}{\begin{vmatrix} H_{11} & H_{12} & H_{13} & \ldots & H_{1N} \\ H_{12} & H_{22} & H_{23} & \ldots & H_{2N} \\ H_{13} & H_{23} & H_{33} & \ldots & H_{3N} \\ \cdot & \cdot & \cdot & \cdot & \cdot \\ H_{1N} & H_{2N} & H_{3N} & \ldots & H_{NN} \end{vmatrix}} \cdot \quad (1.69)$$

where

$$H_{ii} = \frac{x_i^2}{\mu_i} + \sum_{\substack{k=1 \\ k\neq i}}^{N} \frac{2x_i x_k}{\mu_{ik}} \frac{M_i M_k}{(M_i + M_k)^2}\left[\frac{5}{3A_{ik}} + \frac{M_k}{M_i}\right],$$

$$H_{ij} = -\frac{2x_i x_j}{\mu_{ij}} \frac{M_i M_j}{(M_i + M_j)^2}\left[\frac{5}{3A_{ij}} - 1\right], \quad i \neq j, \quad (1.70)$$

$x_i = n_i/n$ is the molar concentration of the ith component; μ_i is the viscosity coefficient of the ith component, equal to

$$\mu_i \approx 266.93\cdot 10^{-7}\frac{\sqrt{M_i T}}{\sigma_i^2 \Omega_i^{(2,2)*}(T_i^*)}\frac{g}{cm\cdot sec}; \quad (1.71)$$

σ_i is the collision diameter; $T_i^* = kT/\varepsilon_i$ is the characteristic temperature; ε_i/k is the parameter related to the potential function of the intermolecular interaction $\Omega_i^{(2,2)*}$ is the collision term for momentum transport, measuring the deviation from the model in which the molecules of the gas are considered as hard spheres, for which

Footnote (9) appears on page 39.

$\Omega^{(2,2)'} = 1$. The values of the function $\Omega^{(2,2)'}(T_i^*)$ for a wide range of T_1^* are listed in the monograph by Hirschfelder, Curtiss, and Bird; μ_{ij} is a coefficient defined by the expression

$$\mu_{ij} = 266.93 \cdot 10^{-7} \frac{\sqrt{\frac{2M_i M_j T}{M_i + M_j}}}{\sigma_{ij}^2 \Omega_{ij}^{(2,2)'}(T_{ij}^*)} \frac{g}{cm \cdot sec}, \qquad (1.72)$$

where $\Omega^{(2,2)'}_{ij}$ is the collision term for the ith and j^{th} component for the case of momentum transport. The values of this term are also given in the monograph by Hirschfelder et al. The quantity A^*_{ij}, appearing in Equations (1.70), is equal to $\Omega^{(2,2)'}_{ij}/\Omega^{(1,1)'}_{ij}$.

In Equation (1.69) the off-diagonal elements of H_{ij} are usually small as compared to the diagonal elements H_{ii}. In order to make the off-diagonal elements exactly equal to zero, one must set $A^*_{ij} =$ 5/3. If the same assumption is used for diagonal elements, then expression (1.69) becomes

$$\mu = \sum_{i=1}^{N} \frac{x_i^2}{H_{ii}} = \sum_{i=1}^{N} \frac{x_i^2}{\frac{x_i^2}{\mu_i} + 2 \sum_{\substack{k=1 \\ k \neq i}}^{N} \frac{x_i x_k}{\mu_{ik}} \frac{M_k}{M_i + M_k}}. \qquad (1.73)$$

However, formula (1.73) is not in good agreement with experiment. To bring it in agreement with experimental data, it is sufficient to replace the factor 2 in the denominator with the empirical coefficient 1.385, i.e., to write it in the form

$$\mu = \sum_{i=1}^{N} \frac{x_i^2}{\frac{x_i^2}{\mu_i} + 1.385 \sum_{\substack{k=1 \\ k \neq i}}^{N} \frac{x_i x_k}{\mu_{ik}} \frac{M_k}{M_i + M_k}}. \qquad (1.74)$$

A computation of the viscosity of mixtures according to these formulas turns out to be quite laborious. For this reason, in many cases it is advisable to use less exact but simpler relations. In particular, the dynamic viscosity of a pure gas can be computed from the well-known Sutherland formula

$$\mu_i = K' \frac{T^{3/2}}{T + C}. \qquad (1.75)$$

The values of the coefficients K' and C' for certain gases, as well as numerous data on the viscosity of pure gases and mixtures, are given in the monographs [5].

The energy flux density vector q for a multicomponent mixture of mono-atomic gases, obtained as the first approximation to the solution of the Boltzmann equation, has the form

$$q = -\lambda \frac{\partial T}{\partial r} + \sum_i^N \rho c_i \bar{V}_i h_i + \frac{kT}{n} \sum_i^N \sum_{\substack{j \\ j \neq i}}^N \frac{n_j \mathcal{D}_i^T}{m_i \mathcal{D}_{ij}} (\bar{V}_i - \bar{V}_j). \qquad (1.76)$$

Here λ is the heat conductivity coefficient, and h_i is the enthalpy of the ith component per unit weight, equal to

$$h_i = \frac{5}{2} \frac{kT}{m_i}. \qquad (1.77)$$

Expression (1.76) shows that in multicomponent mixtures the energy transport takes place by means of three mechanisms. The first term on the right-hand side of (1.76) characterizes the energy transport due to heat conductivity; the second term — due to mass transport by means of all types of diffusion (mass diffusion, pressure diffusion, and thermal diffusion). The third term characterizes the additional energy flux due to the diffusive thermal effect (Dufour's effect[*]).

For a mixture of polyatomic gases, the energy flux density has the same form as for a mixture of monatomic gases (1.76), with the exception that the enthalpy h_i is understood to be equal to the sum

$$h_i = \left(\frac{5}{2} kT + e_i \right) \frac{1}{m_i}. \qquad (1.78)$$

where e_i is the energy of the internal degrees of freedom of molecules.

---

[*]Translator's Note: When concentration gradients produce non-uniformity of temperature, this is called the Dufour effect.

In boundary-layer type flows, the contribution of the diffusive thermal effect to the energy transport is usually small, and thus with accuracy sufficient in practice we can write the following expression for the energy flux density vector in a multicomponent mixture

$$q = -\lambda \frac{\partial T}{\partial r} + \sum_{i}^{N} \rho c_i \overline{V}_i h_i. \qquad (1.79)$$

If expression (1.53) is used for the mass flux density vector of the ith component, and if it is assumed that thermal diffusion and pressure diffusion are negligibly small, then Equation (1.79) can be written in the form

$$q = -\left(\lambda - \sum_i \sum_j \frac{n^2}{\rho} m_i m_j D_{ij} h_i \frac{\partial x_i}{\partial T}\right) \frac{\partial T}{\partial r}. \qquad (1.80)$$

The quantity in parentheses may be considered to be a certain effective thermal conductivity coefficient, consisting of two parts: λ, which is the heat conductivity of a gas mixture, due to molecular collisions, and

$$\lambda_R = -\sum_i \sum_j \frac{n^2}{\rho} m_i m_j D_{ij} h_i \frac{\partial x_j}{\partial T} \qquad (1.81)$$

which is the heat conductivity due to mass transport, i.e.,

$$\lambda_{eff} = \lambda + \lambda_R. \qquad (1.82)$$

If mass transport makes chemical reactions such as dissociation, ionization, etc., possible, then the heat conductivity coefficient λ is called the heat conductivity coefficient of a gas in a "frozen" state (i.e., in the absence of chemical reactions), and λ_R is the heat conductivity coefficient accounting for chemical reactions.

For a gas consisting of molecules of one type which do not possess any internal degrees of freedom (the internal degrees of freedom are "frozen"), the heat conductivity coefficient can be expressed in the following fashion ($\lambda_R = 0$):

$$\lambda = \frac{5}{2}\mu c_v.$$ (1.83)

where c_v is the heat capacity per unit weight at constant volume.

A gas consisting of molecules of one type that do possess
internal degrees of freedom and are in various excited quantum
states may be considered as a gas which is a chemically reacting
mixture with a large number of components, none of which possesses
any internal degrees of freedom. If we assume that the rate of
energy transport from translational degrees of freedom to internal
degrees is small — or, in other words, the distribution of molecules
over various states is an equilibrium distribution, corresponding
to the local temperature — then for polyatomic molecules (of one
type), we can obtain the following expression for the effective heat
conductivity coefficient[10]

$$\lambda_{eff} = \frac{1}{4}\left[\left(15 - 3\frac{\rho\mathscr{D}}{\mu}\right)\gamma - \left(15 - 10\frac{\rho\mathscr{D}}{\mu}\right)\right]c_v\mu.$$ (1.84)

where $\gamma = c_p/c_v$, $\mathscr{D}$ is the self-diffusion coefficient defined as the
limiting form of the diffusion coefficient for a binary mixture.
The expression for the self-diffusion coefficient can be obtained
from Equation (1.59) by setting $i = j$. The dimensionless quantity
$\rho\mathscr{D}/\mu$ is a function of temperature, and its value is on the order of
unity. By setting this value to unity, we obtain the following
formula for the heat conductivity coefficient for a polyatomic gas

$$\lambda_{eff} = \frac{1}{4}(9\gamma - 5)c_v\mu.$$ (1.85)

The factor $(9\gamma - 5)/4$ is called Aitken's corrective factor. Equations
(1.84) and (1.85) are not in good agreement with experiment at
ordinary temperatures, since the energy transport from the transla-
tional to the internal degrees of freedom at such temperatures is
difficult. However, at high temperatures, Equation (1.84) is
sufficiently accurate.

Footnote (10) appears on page 39.

Today the heat conductivity coefficients for mixtures of mono-
atomic gases can be computed with great accuracy using the Chapman-
Enskog theory. The existing methods of computation, which are a
further development of the Chapman-Enskog methods, make it possible
in principle to compute heat conductivities of mixtures of poly-
atomic gases at high temperatures. To carry out calculations using
these methods, one must know the potential specifying the interaction
between molecules. However, in many practical important cases,
these potentials are not as yet sufficiently known. Our knowledge
is particularly limited when it comes to potentials describing
interactions of electrons with atoms, ions, and molecules. When
calculating viscosity coefficients, we are permitted to neglect
collisions of electrons with other particles since the electrons
carry only a small fraction of the total momentum due to their
small mass. However, when calculating heat conductivities, the
collisions of electrons with other particles cannot be neglected,
since electrons, having a great speed, carry a significant fraction
of the kinetic energy. A detailed discussion of the problem of
determining transport coefficients in the air at high temperatures
can be found in a paper by Hansen [6]. Practical methods of calcula-
tion of heat conductivities in pure gases and mixtures can be found
in the monograph by Bretshnayder which was quoted above[11].

§ 5. Equations of the Dynamics of a Multicomponent, Reacting Gas

The expressions for the mass flux density vector (rate of
diffusion) of the ith component (1.53), pressure tensor (1.64), and
the energy flux density vector (1.76) given in the preceding section
enable us to write the gas dynamic transport equations (Section 3)
in macroscopic form. However, before we do this, we shall first
collect all transport equations, keeping the vector-tensor notation.
The equation of continuity for a mixture of gases is

Footnote (11) appears on page 39.

$$\frac{\partial \rho}{\partial t} + \frac{\partial}{\partial r} \cdot (\rho v) = 0, \tag{1.31}$$

the equation of continuity for the ith component is

$$\rho \frac{\partial c_i}{\partial t} + \rho v \cdot \frac{\partial c_i}{\partial r} = w_i - \frac{\partial}{\partial r} \cdot J_i, \tag{1.33}$$

the equation of motion is

$$\frac{\partial v}{\partial t} + \left(v \cdot \frac{\partial}{\partial r} \right) v = - \frac{1}{\rho} \left(\frac{\partial}{\partial r} \cdot P \right), \tag{1.35}$$

the energy equation is

$$\rho \frac{\partial E}{\partial t} + \rho v \cdot \frac{\partial E}{\partial r} = - \frac{\partial}{\partial r} \cdot q - \left(P \cdot \frac{\partial}{\partial r} \right) \cdot v. \tag{1.39}$$

In order to complete the system of equations (1.31), (1.33), (1.35), and (1.39), that relate the five unknown quantities v, ρ, p, c_i, and E (or T), we must add to this system the equation of state for a mixture of gases

$$p = \rho R T \sum_i^N \frac{c_i}{W_i}. \tag{1.86}$$

Substituting the expression (1.64) for the pressure tensor in the equation of motion (1.35), we obtain the following fundamental form of this equation:

$$\rho \frac{dv}{dt} = - \frac{\partial p}{\partial r} + 2 \frac{\partial}{\partial r} \cdot \mu S. \tag{1.87}$$

Here and below

$$\frac{d}{dt} = \frac{\partial}{\partial t} + v \cdot \frac{\partial}{\partial r}. \tag{1.88}$$

In the energy equation (1.39), we pass from the internal energy E to the enthalpy h, related to the former by

$$h = E + \frac{p}{\rho}. \tag{1.89}$$

simultaneously replacing the pressure tensor by its expression in (1.64). Then we have

$$\rho \frac{dh}{dt} = \frac{dp}{dt} - \frac{\partial}{\partial r} \cdot q + 2\mu \left(S \cdot \frac{\partial}{\partial r} \right) \cdot v. \tag{1.90}$$

Keeping in mind that

$$\left(\dot{S} \cdot \frac{\partial}{\partial r} \right) \cdot v = \dot{S}^2, \tag{1.91}$$

we change Equation (1.90) to the form

$$\rho \frac{dh}{dt} = \frac{dp}{dt} - \frac{\partial}{\partial r} \cdot q + 2\mu \dot{S}^2. \tag{1.92}$$

We shall give still another form of the energy equation that can be easily derived from Equation (1.39) by using Equations (1.35), (1.64), (1.88), and (1.89):

$$\rho \frac{d}{dt} \left(h + \frac{v^2}{2} \right) = \frac{\partial p}{\partial t} - \frac{\partial}{\partial r} \cdot q + 2 \frac{\partial}{\partial r} \cdot (\mu \dot{S} \cdot v). \tag{1.93}$$

The quantity

$$h + \frac{v^2}{2} = H \tag{1.94}$$

will be called below the total enthalpy of a gas.

Now we substitute the expression for the mass flux density vector (1.10) in the equation of continuity for the ith component, also using Equation (1.53) for the rate of diffusion and replacing the molar concentration x_i with the mass concentration c_i according to Equation (1.29). This gives

$$\rho \frac{\partial c_i}{\partial t} + \rho v \cdot \frac{\partial c_i}{\partial r} = w_i - \frac{\partial}{\partial r} \left\{ \frac{\rho m_i}{n i^2} \sum_j D_{ij} \left[\frac{\partial}{\partial r} (c_j m) + c_j (m - m_j) \frac{\partial \ln p}{\partial r} \right] - \mathcal{D}_i^T \frac{\partial \ln T}{\partial r} \right\}. \tag{1.95}$$

If we neglect the pressure diffusion and thermal diffusion as compared to the mass diffusion and replace the diffusion coefficient for a multicomponent mixture, D_{ij}, with the so-called effective diffusion coefficient $\mathcal{D}_i$, defined by Equation (1.58), then Equation (1.95) will become

$$\rho \frac{\partial c_i}{\partial t} + \rho v \cdot \frac{\partial c_i}{\partial r} = w_i + \frac{\partial}{\partial r} \cdot \left(\rho \mathcal{D}_i \frac{\partial c_i}{\partial r} \right). \tag{1.96}$$

In the case of a binary mixture, the coefficient $\mathcal{D}_i$ equals the diffusion coefficient for a binary mixture, $\mathcal{D}_{ij}$, and Equation (1.96) will then be given by

$$\rho \frac{\partial c_i}{\partial t} + \rho v \cdot \frac{\partial c_i}{\partial r} = w_i + \frac{\partial}{\partial r} \cdot \left(\rho \mathcal{D}_{ij} \frac{\partial c_i}{\partial r} \right). \tag{1.97}$$

Now we consider the energy equation in the form (1.93). Substituting in this equation the expressions for the energy and mass flux density vectors, (1.76) and (1.10), (1.53), respectively, we have

$$\rho \frac{dH}{dt} = \frac{\partial p}{\partial t} + 2 \frac{\partial}{\partial r} \cdot (\mu \dot{S} \cdot v) + \frac{\partial}{\partial r} \cdot \left(\lambda \frac{\partial T}{\partial r} \right) -$$
$$- \frac{\partial}{\partial r} \left\{ \frac{\rho^2}{m} \sum_{i=1}^{N} \left[\sum_{j=1}^{N} m_i D_{ij} \left(\frac{\partial}{\partial r} (c_j m) + c_j (m - m_j) \frac{\partial \ln p}{\partial r} \right) - \right. \right.$$
$$\left. - \mathcal{D}_i^T \frac{\partial \ln T}{\partial r} \right] h_i \right\} + \frac{\partial}{\partial r} \cdot \left\{ kT \sum_{i=1}^{N} \frac{\mathcal{D}_i^T}{c_i m} \left[\frac{\partial}{\partial r} (c_i m) + \right. \right. \tag{1.98}$$
$$\left. \left. + c_i (m - m_i) \frac{\partial \ln p}{\partial r} - \frac{\partial \ln T}{\partial r} \sum_{\substack{j=1 \\ j \neq i}}^{N} \frac{m^2}{m_j D_{ij} \rho} (c_i \mathcal{D}_j^T - c_j \mathcal{D}_i^T) \right] \right\}.$$

As noted above in boundary-layer type flows, the contribution of the pressure diffusion to mass and energy transport is very insignificant. The contribution of thermal diffusion to mass and energy transport (diffusive thermal effect) is in many cases also small. Neglecting these effects and using the effective diffusion coefficient instead of the diffusion coefficient for a multicomponent mixture, we obtain the following form of the energy equation:

$$\rho \frac{dH}{dt} - \frac{\partial p}{\partial t} + 2 \frac{\partial}{\partial r} \cdot (\mu \dot{S} \cdot v) +$$
$$+ \frac{\partial}{\partial r} \cdot \left(\lambda \frac{\partial T}{\partial r} + \sum_{i=1}^{N} \rho \mathcal{D}_i h_i \frac{\partial c_i}{\partial r} \right). \tag{1.99}$$

Taking the fact into account that

$$h = \sum_i^N c_i h_i, \qquad h_i = \int_0^T c_{pi} dT + h_i^0 \qquad (1.100)$$

and, consequently,

$$\frac{\partial T}{\partial r} = \frac{1}{c_p} \left(\frac{\partial h}{\partial r} - \sum_{i=1}^N h_i \frac{\partial c_i}{\partial r} \right), \qquad c_p = \sum_{i=1}^{N} c_i c_{pi}, \qquad (1.101)$$

we write Equation (1.99) in the form

$$\rho \frac{dH}{dt} = \frac{\partial p}{\partial t} + 2 \frac{\partial}{\partial r} \cdot (\mu \dot{S} \cdot v) +$$
$$+ \frac{\partial}{\partial r} \left\{ \frac{\mu}{Pr} \left[\frac{\partial h}{\partial r} + \sum_{i=1}^N (Le_i - 1) h_i \frac{\partial c_i}{\partial r} \right] \right\}. \qquad (1.102)$$

Here h_i^0 is the heat of formation of the ith component under standard conditions.

Equation (1.102) involves the parameters: the effective Lewis number and the Prandtl number

$$Le_i = \frac{\rho \mathscr{D}_i c_p}{\lambda}, \qquad Pr = \frac{\mu c_p}{\lambda}. \qquad (1.103)$$

A parameter that can be derived from these two is the effective Schmidt number, defined as the ratio of the Prandtl and Lewis numbers:

$$Sc_i = \frac{Pr}{Le_i} = \frac{\mu}{\rho \mathscr{D}_i}. \qquad (1.104)$$

The effective Lewis and Schmidt numbers introduced in this manner cannot generally be considered, just as the Prandtl number, to be similarity parameters, since the effective diffusion coefficient depends by definition on the diffusion flows of the individual components and thus on the defining parameters of a specific problem. However, in the particular case of a binary mixture, $\mathscr{D}_i$ becomes equal to the diffusion coefficient for a binary mixture, $\mathscr{D}_{ij}$, which, as can be seen from Equation (1.59), does not depend on the defining parameters of a flow. In this case, the Lewis and Schmidt

numbers, formed in terms of the diffusion coefficient for a binary mixture

$$Le = \frac{\rho \mathscr{D}_{ij} c_p}{\lambda}, \quad Sc = \frac{\mu}{\rho \mathscr{D}_{ij}}, \qquad (1.105)$$

may indeed be considered to be similarity parameters.

An inspection of Equation (1.102) shows that, if the Lewis number is equal to unity ($Le_1 = 1$), then the energy equation has the same form as the ordinary energy equation for a gas with homogeneous composition.

FOOTNOTES

Footnote (1) on page 10.   It should be noted that, when comput-
                            ing averages, the integration over V_1
                            is equivalent to integration over v_1,
                            since these velocities differ by a
                            constant and the integration is per-
                            formed over all velocity values.

Footnote (2) on page 10.   In Equation (1.11), the tensor P_1 is
                            regarded as the result of the dyad
                            multiplication of two vectors $V_1 V_1$,
                            where — in contrast with the scalar
                            product $V_1 \cdot V_1$ and the vector product
                            $V_1 \times V_1$ of these vectors — the
                            multiplication sign is not included
                            in the dyad product.

Footnote (3) on page 14.   See [1] on page 39a.

Footnote (4) on page 19.   See, for example, the monographs
                            written by J. Hirschfelder, C. Curtiss,
                            and R. Bird, and by Chapman and Cowling,
                            mentioned before, that contain results
                            of early work. The results of more
                            recent work can be found in a monograph
                            by Kogan, M. N., "Dinamika razrezhennogo
                            gaza" (Dynamics of Rarefied Gas),
                            "Nauka" Publishing House, Moscow, 1967.

Footnote (5) on page 23.   See [1] and [2] on page 39a.

Footnote (6) on page 23.   The concept of the effective diffusion
                            coefficient was applied to practical
                            boundary layer calculations by G. A.
                            Tirskiy. See, for example, Tirskiy,
                            G. A., Determination of the Effective
                            Diffusion Coefficients in a Laminar
                            Boundary Layer, Doklady Akademii Nauk
                            SSSR, Vol. 155, No. 6, 1963, pp. 1278-
                            1282, as well as the above paper by
                            the same author.

Footnote (7) on page 24.   A detailed knowledge of molecular
                            diffusion, just as the knowledge of
                            molecular heat conductivities and
                            viscosities, is very necessary when
                            studying turbulent boundary layers in
                            hypersonic flows, due to the major role
                            played by the laminar sublayer in
                            processes involving heat and mass
                            transfer.

Footnote (8) on page 26.   One exception may be flow of a multi-
                             component gas mixture containing
                             components differing greatly in their
                             molecular weight — such as, for
                             example, hydrogen and air, helium and
                             air.

Footnote (9) on page 27.   Hirschfelder, J. et al., see
                             [1] on page 39a.

Footnote (10) on page 31.   Hirschfelder, J. et al., see [1] on
                             page 39a.

Footnote (11) on page 32.   See [5] on page 39a.

REFERENCES

1) Hirschfelder J. O., Curtiss C. F., Bird R. B., Molecular theory of gases and liquids, New York, Wiley, London, Chapman and Hall, 1954; русский перевод: Гиршфельдер Дж., Кертисс Ч., Берд Р., Молекулярная теория газов и жидкостей, ИЛ, Москва, 1961.

2) Chapman S., Cowling T. G., The mathematical theory of non-uniform gases, Cambridge Univ. Press, 1952; русский перевод: Чепмен С. и Каулинг Т., Математическая теория неоднородных газов, ИЛ, Москва, 1960.

3) Тирский Г. А., Анализ химического состава ламинарного многокомпонентного пограничного слоя на поверхности горящих пластиков, Космические исследования 2, вып. 4, 570—594 (1964).

4) Лойцянский Л. Г., Механика жидкости и газа, «Наука», Москва, 1970.

5) Голубев И. Ф., Вязкость газов и газовых смесей, Физматгиз, Москва, 1959; Бретшнайдер Ст., Свойства газов и жидкостей, «Химия», Москва — Ленинград, 1966.

6) Hansen F., Approximations for the thermodynamic and transport properties of high-temperature air, NASA TR, R-50 (1959).

CHAPTER II

TURBULENCE IN GASDYNAMIC FLOWS

§6. Equations of Turbulent Motion

In turbulent motion the velocity, pressure, temperature, con-
centration fields and those of other gasdynamic quantities have a
very complicated structure. The complex structure of these fields
is due to the extremely irregular and random character of their varia-
tion in space and time. If the space and time scale of turbulence
(i.e., the minimum size of a turbulent inhomogeneity and the charac-
teristic period of turbulent fluctuations) is much greater than the
space and time scale of molecular motion (i.e., the mean free path
of molecules and the mean time between two molecular collisions),
the transport equations obtained in the preceding sections may in
principle be used to describe turbulent motion.

Experiment shows that the space and time scale of turbulence is
always greater by several orders of magnitude than the space and
time scale of molecular motion, and thus a description of turbulent
flows by means of differential transport equations is fully justified.
However, direct use of these equations is in practice impossible,

since the fields of gasdynamic quantities in a turbulent flow, which
are always nonsteady, depend very strongly on the initial conditions
which are usually far from being completely known. This means that
a complete detailed description of turbulent motion is impossible.
However, in practice such a detailed knowledge of the fields of gas-
dynamic quantities is not even necessary in a majority of cases, since
we are merely interested in the average (statistical) characteristics
of these fields. The fact that turbulent motion is described by dif-
ferential transport equations becomes extremely important in this
case. Due to this fact, it becomes nearly possible to establish re-
lationships among the average characteristics of the fields of
gasdynamic quantities.

The techniques that make it possible to establish such relations
in the case of incompressible isothermic fluids were first proposed
by Reynolds [1]. By now these techniques have been described in great
detail in the literature [2], and for this reason we shall only briefly
describe their main features. As we know, Reynolds proposed that the
values of all gasdynamic quantities in a turbulent f'ow be represen-
ted as sums of the average and fluctuating components, and proposed
that only the average quantities which vary relatively smoothly with
position and time be investigated. Reynolds suggested that, in order
to determine the average value of a given quantity, one should apply
ordinary averaging over a certain time interval (time averaging).
It should be noted that, along with this method of averaging, other
methods are also possible, including averaging over a certain region
at a given time instant (space averaging) or averaging for a large
number of fields that vary both from point to point and from one time
instant to another (statistical averaging over ensembles). Without
discussing here the respective merits and drawbacks of various methods
of averaging, we shall only note that procedures most commonly used
in practice enable us to measure time averages of various quantities,
and thus time averaging turns out to be most advisable[1].

Footnote (1) appears on page 69.

Following Reynolds, we shall now write the instantaneous value of each of the unknown quantities or their arbitrary combinations as sums of the average ($\bar{f}$) and fluctuating (f') components:

$$f = \bar{f} + f'.$$ (2.1)

By averaging, we mean time averaging

$$\bar{f} = \frac{1}{\Delta t} \int_{t}^{t+\Delta t} f\, dt.$$ (2.2)

where the averaging interval Δt is assumed to be sufficiently long as compared to the characteristic period of the fluctuating field and significantly smaller than the period of the average field. If the average field is steady, i.e., its period is infinitely long, then the average value of f will be given by

$$\bar{f} = \lim_{\Delta t \to \infty} \left[\frac{1}{\Delta t} \int_{t}^{t+\Delta t} f\, dt \right].$$ (2.3)

As shown by Reynolds, in the process involving any type of averaging (not only time averaging) the following relations must be satisfied, which came to be called the Reynolds relations:

$$
\begin{cases}
1)\ \overline{f + g} = \bar{f} + \bar{g}; \\
2)\ \overline{af} = a\bar{f}, \quad \text{if}\quad a = \text{const}; \\
3)\ \bar{a} = a, \quad \text{if}\quad a = \text{const}; \\
4)\ \overline{\frac{\partial f}{\partial s}} = \frac{\partial \bar{f}}{\partial s}, \text{ where } s \text{ is } x,y,z \text{ or } t; \\
5)\ \overline{\bar{f}g} = \bar{f}\bar{g}.
\end{cases}
$$ (2.4)

Setting $g = 1$, $g = \bar{h}$, and $g = h' = h - \bar{h}$ in succession in Equations (2.4) (the prime will signify from now on that fluctuating components of quantities are meant), we shall obtain the following important consequences of the Reynolds conditions:

$$\bar{\bar{f}} = \bar{f}, \quad \bar{f'} = \overline{\bar{f} - f} = 0, \quad \overline{\bar{f}\bar{h}} = \bar{f}\bar{h}, \quad \overline{\bar{f}h'} = \bar{f}\overline{h'} = 0.$$ (2.5)

Making use of these equations, we shall establish the rules of averaging for products of two and three variables that will be found very useful below

$$\overline{fg} = \overline{(\bar{f} + f')(\bar{g} + g')} = \bar{f}\bar{g} + \overline{f'g'}, \tag{2.6}$$

$$\overline{fgh} = \bar{f}\bar{g}\,\bar{h} + \bar{f}\overline{g'h'} + \bar{g}\overline{f'h'} + \bar{h}\overline{f'g'} + \overline{f'g'h'}. \tag{2.7}$$

The fluctuating component of a product of two variables is obviously equal to

$$\begin{aligned}
(fg)' = fg - \overline{fg} &= (\bar{f} + f')\,(\bar{g} + g') - \overline{fg} = \\
&= \bar{f}\bar{g} + f'\bar{g} + \bar{f}g' + f'g' - \bar{f}\bar{g} - \overline{f'g'} = \\
&= f'\bar{g} + \bar{f}g' + f'g' - \overline{f'g'}.
\end{aligned} \tag{2.8}$$

Now we proceed to derive the averaged equations of turbulent motion for a multicomponent reacting gas mixture[2]. For convenience we shall write the equations of continuity for a mixture and for the ith component, as well as the equations of momentum and energy transfer in tensor notation: subscripts repeated twice will signify summation over 1, 2, 3 corresponding to vector and tensor components along the x, y, and z axes (this rule does not apply to the subscript i).

The equation of continuity for a mixture of gases (1.31) in this notation will become

$$\frac{\partial \rho}{\partial t} + \frac{\partial}{\partial x_j}(\rho v_j) = 0. \tag{2.9}$$

The equation of continuity for the ith component (1.33) will be transformed using Equation (2.9) to the form

$$\frac{\partial}{\partial t}(\rho c_i) + \frac{\partial}{\partial x_j}(\rho v_j c_i) = w_i - \frac{\partial}{\partial x_j}(\rho c_i V_{ij}). \tag{2.10}$$

To write the equations of momentum transport, we shall make use of Equation (2.9) and the expression for the pressure tensor (1.64).

Footnote (2) appears on page 69.

As a result we get

$$\frac{\partial}{\partial t}(\rho v_k) + \frac{\partial}{\partial s_j}(\rho v_j v_k) = -\frac{\partial p}{\partial s_k} + \frac{\partial}{\partial s_j}(2\mu \dot{S}_{jk}). \qquad (2.11)$$

We shall use the form (1.93) of the equation of energy transport. Making use of the expression for the heat flux (1.79), as well as Equation (2.9), we obtain

$$\frac{\partial}{\partial t}\left(\rho h + \frac{\rho v_k^2}{2}\right) + \frac{\partial}{\partial s_j}\left(\rho v_j h + \frac{1}{2}\rho v_j v_k^2\right) = \frac{\partial p}{\partial t} +$$
$$+ \frac{\partial}{\partial s_j}\left(\lambda \frac{\partial t}{\partial s_j} - \sum_i \rho_i V_{ij} h_i + 2\mu \bar{S}_{jk} v_k\right). \qquad (2.12)$$

In these equations, the subscript i signifies the component number, and the subscripts j and k may assume values 1, 2, 3.

Applying the averaging process (2.2) to the equation of continuity (2.9) and assuming that this operation may be interchanged with differentiation with respect to position and time [fourth of the Reynolds conditions (2.4)], we obtain

$$\frac{\partial \bar{\rho}}{\partial t} + \frac{\partial}{\partial s_j}(\overline{\rho v_j}) = 0. \qquad (2.13)$$

Expanding the term $\overline{\rho v_j}$ in accordance with the rule (2.6), we get

$$\overline{\rho v_j} = \bar{\rho}\,\bar{v}_j + \overline{\rho' v_j}. \qquad (2.14)$$

Thus the equation of continuity for a compressible gas becomes

$$\frac{\partial \bar{\rho}}{\partial t} + \frac{\partial}{\partial t}(\bar{\rho}\bar{v}_j) + \frac{\partial}{\partial s_j}(\overline{\rho' v_j}) = 0. \qquad (2.15)$$

In contrast with the equation of continuity for an incompressible fluid, Equation (2.15) involves space derivatives of the average fluxes of fluctuating motion. The incompleteness of our knowledge on the general nature of turbulence does not permit us at the present to give a numerical estimate of the contribution made by the term $\frac{\partial}{\partial s_j}(\overline{\rho' v_j})$ to the equation of continuity. From physical considerations it is clear that

$$\overline{\rho' v_j} < \overline{\rho v_j}.$$

However, the question of under what conditions it is permissible to neglect $\overline{\rho' v_j}$ as compared to $\overline{\rho v_j}$ remains open. These factors give the derivation of the equations of the average turbulent motion for a compressible gas (if density fluctuations are not neglected) an essentially formal character.

Now we take the average of the equation of continuity for the ith component (2.10), and obtain

$$\frac{\partial}{\partial t}\overline{\rho c_i} + \frac{\partial}{\partial x_j}\overline{(\rho v_j)c_i} = \overline{w_i} - \frac{\partial}{\partial x_j}\overline{(\rho V_{ij})c_i}. \tag{2.16}$$

Applying to this equation relation (2.6) and performing differentiation on the left-hand side of the equation, we find

Reproduced from
best available copy.

$$c_i \frac{\partial \bar\rho}{\partial t} + \bar\rho \frac{\partial \bar c_i}{\partial t} + \frac{\partial}{\partial t}\overline{\rho' c_i} + \bar\rho \bar v_j \frac{\partial \bar c_i}{\partial x_j} + \bar\rho \overline{v_j} \frac{\partial c_i}{\partial x_j} + $$
$$+ \bar c_i \frac{\partial}{\partial x_j}(\bar\rho \bar v_j + \overline{\rho' v_j}) + \frac{\partial}{\partial x_j}\overline{(\rho v_j)' c_i} = $$
$$= \bar w_i - \frac{\partial}{\partial x_j}(\overline{\rho V_{ij}})\bar c_i - \frac{\partial}{\partial x_j}\overline{(\rho V_{ij})' c_i} \tag{2.17}$$

Noting that the sum of the first and sixth terms on the left-hand side of Equation (2.17) is zero by virtue of the equation of continuity (2.15), and dropping the last term on the right, since it is negligible compared to the second term on the same side

$$|\overline{(\rho V_{ij})' c_i}| < |(\overline{\rho V_{ij}})\bar c_i|. \tag{2.18}$$

we find[3]

$$\bar\rho \frac{\partial \bar c_i}{\partial t} + \overline{\rho v_j}\frac{\partial \bar c_i}{\partial x_j} = $$
$$= \bar w_i - \frac{\partial}{\partial x_j}[(\overline{\rho V_{ij}})\bar c_i + \overline{(\rho v_j)' c_i}] - \frac{\partial}{\partial t}\overline{\rho' c_i} - \overline{\rho' v_j}\frac{\partial \bar c_i}{\partial x_j} \tag{2.19}$$

Footnote (3) appears on page 69.

Inequality (2.18) holds because in turbulent motion, as we know, the molecular properties of a medium play an important role only in the region immediately adjacent to the wall (laminar sublayer), where turbulent pulsations disappear. Since $\bar{V}_{1j}$ is the rate of molecular diffusion, it is clear that the fluctuating components of the diffusive flow in this region will be small as compared to the average components.

Equation (2.19) shows that in turbulent motion, in addition to the transport of mass due to molecular diffusion, there is also transport of mass due to the mixing produced by fluctuations of the density, velocity, and concentration $\overline{(\rho v_j)' c_i}$. The process of mass transport in a turbulent flow, due to fluctuations of the density, velocity, and concentration, will be called turbulent diffusion in analogy with molecular diffusion.

A derivation of the average equation of motion [Equations (2.11) are the equations we start with] does not involve any new features as compared to the derivation of the averaged equation of continuity (2.19), and is fully analogous to it. Therefore, omitting the intermediate steps, we shall only give these equations in their final form:

$$\bar{\rho}\frac{\partial \bar{v}_1}{\partial t} + \bar{\rho}\bar{v}_j \frac{\partial \bar{v}_1}{\partial x_j} =$$

$$= -\frac{\partial \bar{p}}{\partial x_i} + \frac{\partial}{\partial x_j}[2\bar{\mu} \bar{V}_{ik} - \overline{(\rho v_j)' v_k}] - \frac{\partial}{\partial t}\overline{\rho' v_i} - \overline{\rho' v_j}\frac{\partial \bar{v}_i}{\partial x_j}. \tag{2.20}$$

It should be noted that, in deriving these equations, the terms containing viscosity fluctuations were neglected as compared to the terms containing their average values [for a reason explained in the remark concerning the inequality (2.18)]. Equations (2.20) will be called the Reynolds equations for a compressible gas. In these equations, the quantities $\overline{(\rho v_j)' v_k}$ are understood to be the components of the tensor of additional stresses arising from the presence of turbulent fluctuations in the mass flow and velocity. These additional stresses are usually called the Reynolds stresses.

In obtaining the equations of energy transport in an averaged turbulent motion of a multicomponent reacting mixture, we shall neglect the fluctuations of the viscosity, heat conductivity, diffusion, and specific heat capacity as compared with their average values.

Averaging Equation (2.12) and, as before, interchanging the order of averaging and differentiation with respect to position and time, we obtain

$$\frac{\partial}{\partial t}\overline{\rho h} + \frac{1}{2}\frac{\partial}{\partial t}\overline{\rho v_k v_k} + \frac{\partial}{\partial s_j}\overline{\rho v_j h} + \frac{1}{2}\frac{\partial}{\partial s_j}\overline{\rho v_j v_k^2} =$$
$$= \frac{\partial \overline{p}}{\partial t} + \frac{\partial}{\partial s_j}\left[\overline{\lambda \frac{\partial T}{\partial s_j}} - \sum_i \overline{\rho_i \overline{V_{ij}} h_i} + 2\overline{\mu S_{jk} v_k}\right]. \qquad (2.21)$$

We shall transform separately each of the four terms on the left-hand side of this equation, using Equations (2.6) - (2.8). We thus obtain

$$\frac{\partial}{\partial t}\overline{\rho h} = \frac{\partial}{\partial t}(\overline{\rho}\,\overline{h} + \overline{\rho' h'}) = \overline{\rho}\frac{\partial \overline{h}}{\partial t} + \overline{h}\frac{\partial \overline{\rho}}{\partial t} + \frac{\partial}{\partial t}\overline{\rho' h'},$$

$$\frac{1}{2}\frac{\partial}{\partial t}\overline{\rho v_k v_k} = \frac{1}{2}\frac{\partial}{\partial t}[\overline{\rho}\,\overline{v}_k^2 + \overline{\rho}\,\overline{v_k'^2} + 2\overline{v}_k\overline{\rho' v_k'} + \overline{\rho' v_k'^2}] =$$
$$= \frac{\overline{v}_k^2}{2}\frac{\partial \overline{\rho}}{\partial t} + \overline{\rho}\,\overline{v}_k\frac{\partial \overline{v}_k}{\partial t} + \frac{1}{2}\frac{\partial}{\partial t}\overline{\rho}\,\overline{v_k'^2} + \frac{\partial}{\partial t}\overline{v}_k\overline{\rho' v_k'} + \frac{1}{2}\frac{\partial}{\partial t}\overline{\rho' v_k'^2},$$

$$\frac{\partial}{\partial s_j}\overline{\rho v_j h} = \frac{\partial}{\partial s_j}\overline{(\rho v_j)h} = \frac{\partial}{\partial s_j}[\overline{\rho v_j}\,\overline{h} + \overline{(\rho v_j)' h'}] =$$
$$= \overline{\rho v_j}\frac{\partial \overline{h}}{\partial s_j} + \overline{h}\frac{\partial}{\partial s_j}\overline{\rho v_j} + \frac{\partial}{\partial s_j}\sum_i \overline{(\rho v_j)'(c_i h_i)'} =$$
$$= \overline{\rho}\,\overline{v}_j\frac{\partial \overline{h}}{\partial s_j} + \overline{\rho' v_j'}\frac{\partial \overline{h}}{\partial s_j} + \overline{h}\frac{\partial}{\partial s_j}(\overline{\rho}\,\overline{v}_j + \overline{\rho' v_j'}) +$$
$$+ \frac{\partial}{\partial s_j}\sum_i \overline{c}_i\overline{(\rho v_j)' h_i'} + \frac{\partial}{\partial s_j}\sum_i \overline{h}_i\overline{(\rho v_j)' c_i'} + \frac{\partial}{\partial s_j}\sum_i \overline{(\rho v_j)' c_i' h_i'},$$

$$\frac{1}{2}\frac{\partial}{\partial s_j}\overline{\rho v_j v_k^2} = \frac{1}{2}\frac{\partial}{\partial s_j}\overline{(\rho v_j)v_k^2} =$$
$$= \frac{1}{2}\frac{\partial}{\partial s_j}[\overline{\rho v_j}\,\overline{v}_k^2 + \overline{(\rho v_j)' v_k^2}] =$$
$$= \frac{1}{2}\frac{\partial}{\partial s_j}[\overline{\rho v_j}(\overline{v}_k^2 + \overline{v_k'^2}) + 2\overline{v}_k\overline{(\rho v_j)' v_k'} + \overline{(\rho v_j)' v_k'^2}] =$$
$$= \frac{\overline{v}_k^2}{2}\frac{\partial}{\partial s_j}(\overline{\rho}\,\overline{v}_j + \overline{\rho' v_j'}) + \overline{\rho}\,\overline{v}_j\overline{v}_k\frac{\partial \overline{v}_k}{\partial s_j} + \overline{\rho' v_j'}\overline{v}_k\frac{\partial \overline{v}_k}{\partial s_j} +$$
$$+ \frac{1}{2}\frac{\partial}{\partial s_j}\overline{\rho v_j}\,\overline{v_k'^2} + \frac{\partial}{\partial s_j}\overline{v}_k\overline{(\rho v_j)' v_k'} + \frac{\partial}{\partial s_j}\overline{(\rho v_j)' v_k'^2}.$$

We substitute these expressions in the initial Equation (2.21) and obtain

$$\bar{\rho}\frac{\partial \bar{h}}{\partial t} + \bar{h}\frac{\partial \bar{\rho}}{\partial t} + \frac{\partial}{\partial t}\overline{\rho'h'} + \frac{\bar{v}_k^2}{2}\frac{\partial \bar{\rho}}{\partial t} + \bar{\rho}\bar{v}_k\frac{\partial \bar{v}_k}{\partial t} +$$
$$\text{(1)} \qquad \text{(2)} \qquad \text{(3)} \qquad \text{(4)} \qquad \text{(5)}$$

$$+ \frac{1}{2}\frac{\partial}{\partial t}\overline{\rho v_k'^2} + \bar{v}_k\frac{\partial}{\partial t}\overline{\rho'v_k'} + \frac{1}{2}\frac{\partial}{\partial t}\overline{\rho'v_k'^2} + \bar{\rho}\bar{v}_j\frac{\partial \bar{h}}{\partial s_j} +$$
$$\text{(6)} \qquad \text{(7)} \qquad \text{(8)} \qquad \text{(9)}$$

$$+ \overline{\rho'v_j'}\frac{\partial \bar{h}}{\partial s_j} + \bar{h}\frac{\partial}{\partial s_j}(\bar{\rho}\bar{v}_j + \overline{\rho'v_j'}) + \frac{\partial}{\partial s_j}\sum_i \bar{c}_i\overline{(\rho v_j)'h_i'} +$$
$$\text{(10)} \qquad \text{(11)} \qquad \text{(12)}$$

$$+ \frac{\partial}{\partial s_j}\sum_i \bar{h}_i\overline{(\rho v_j)'c_i'} + \frac{\partial}{\partial s_j}\sum_i \overline{(\rho v_j)'c_i'h_i'} +$$
$$\text{(13)} \qquad \text{(14)}$$

$$+ \frac{\bar{v}_k^2}{2}\frac{\partial}{\partial s_j}(\bar{\rho}\bar{v}_j + \overline{\rho'v_j'}) + \bar{\rho}\bar{v}_j\bar{v}_k\frac{\partial \bar{v}_k}{\partial s_j} + \overline{\rho'v_j'}\bar{v}_k\frac{\partial \bar{v}_k}{\partial s_j} +$$
$$\text{(15)} \qquad \text{(16)} \qquad \text{(17)}$$

$$+ \frac{1}{2}\frac{\partial}{\partial s_j}\overline{\rho v_j v_k'^2} + \frac{\partial}{\partial s_j}\bar{v}_k\overline{(\rho v_j)'v_k'} + \frac{\partial}{\partial s_j}\overline{(\rho v_j)'v_k'^2} + \bar{\rho}\bar{v}_k\frac{\partial \bar{v}_k}{\partial t} =$$
$$\text{(18)} \qquad \text{(19)} \qquad \text{(20)} \qquad \text{(21)}$$

$$= \frac{\partial \bar{p}}{\partial t} + \frac{\partial}{\partial s_j}\bar{\lambda}\frac{\partial \bar{T}}{\partial s_j} - \frac{\partial}{\partial s_j}\sum_i \overline{\rho_i V_{ij} h_i} -$$
$$\text{(1)} \qquad \text{(2)} \qquad \text{(3)}$$

$$- \frac{\partial}{\partial s_j}\sum_i \overline{(\rho_i V_{ij})'h_i'} + 2\frac{\partial}{\partial s_j}\bar{\mu}\bar{S}_{jk}\bar{v}_k + 2\frac{\partial}{\partial s_j}\overline{\mu S_{jk}'v_k'}. \quad (2.22)$$
$$\text{(4)} \qquad \qquad \text{(5)} \qquad \qquad \text{(6)}$$

(2.22)

In the equation thus obtained, the sum of the second, fourth, eleventh, and fifteenth terms on the left-hand side is equal to zero according to the equation of continuity (2.15). The eighth, fourteenth, and twelfth terms on the left-hand side may be dropped due to their smallness, inasmuch as they involve a third power of fluctuations. It is not hard to see that the sixth and the eighteenth terms on the left-hand side may also be neglected, since $\overline{v_k'^2} \ll \bar{v}_k^2$. The fourth and the sixth terms on the right-hand side of the equation may be omitted for the same reason as the last term in Equation (2.17). To further simplify Equation (2.22), we shall group together the fifth, seventh, sixteenth, and seventeenth terms on the left, obtaining the expression

$$\bar{v}_k\left[\bar{\rho}\frac{\partial \bar{v}_k}{\partial t} + \bar{\rho}\bar{v}_j\frac{\partial \bar{v}_k}{\partial s_j} + \overline{\rho'v_j'}\frac{\partial \bar{v}_k}{\partial s_j} + \frac{\partial}{\partial t}\overline{\rho'v_k'}\right],$$

which as can be easily seen from Equation (2.20) is equivalent to the expression

$$\bar{v}_k\left[-\frac{\partial \bar{p}}{\partial s_k} + \frac{\partial}{\partial s_j}(2\bar{\mu}\bar{S}_{jk}) - \frac{\partial}{\partial s_j}\overline{(\rho v_j)'v_k'}\right].$$

Keeping this in mind and making simple rearrangements, we shall change the energy Equation (2.22) to the following form:

$$\bar{\rho}\,\frac{\partial \bar{h}}{\partial t} + \bar{\rho}\bar{v}_j\,\frac{\partial \bar{h}}{\partial s_j} = \frac{\partial \bar{p}}{\partial t} + \bar{v}_k\,\frac{\partial \bar{p}}{\partial s_k} +$$
$$+ [2\bar{\mu}\bar{S}_{jk} - \overline{(\rho v_j)'v_k}]\frac{\partial \bar{v}_k}{\partial s_j} + \frac{\partial}{\partial s_j}\left[\bar{\lambda}\frac{\partial \bar{T}}{\partial s_j} - \sum_i \bar{c}_i\overline{(\rho v_j)'h_i}\right] -$$
$$- \frac{\partial}{\partial s_j}\left[\sum_i \bar{\rho}_i\bar{V}_{ik}\bar{h}_i + \sum_i \bar{h}_i\overline{(\rho v_j)'c_i}\right] -$$
$$- \frac{\partial}{\partial t}\overline{\rho'h'} - \overline{\rho'v_j'}\frac{\partial \bar{h}}{\partial s_j} - \overline{\rho'v_k'}\frac{\partial \bar{v}_k}{\partial t}.$$

$$(2.23)$$

In Equation (2.23), the quantity $\overline{(\rho v_j)'\,h_i'}$ expresses the energy transport of the ith component that is caused by turbulent fluctuations. The term $\sum_i \overline{(\rho v_j)'c_i\bar{h}_i}$ expresses the energy transport due to turbulent mass transport (turbulent diffusion). The term $\overline{(\rho v_j)'v_k}\frac{\partial \bar{v}_k}{\partial s_j}$ gives the conversion rate of the energy of average motion into the energy of turbulence as a result of the Reynolds stresses. The term $\sum_i \bar{c}_i\overline{(\rho v_j)'h_i}$ expresses the total amount of energy transported by all components of the mixture due to turbulent fluctuations.

The process of energy transport in a turbulent flow, which is due to the density, velocity, and enthalpy fluctuations, will be called turbulent heat conductivity in analogy with molecular heat conductivity.

Now we shall perform the averaging process on the equation of state (1.86). Using the rule (2.7) and neglecting third powers of fluctuations, we obtain

$$\bar{p} = \bar{\rho}R\bar{T}\sum_i \frac{\bar{c}_i}{M_i}\left[1 + \frac{\overline{c_i'T'}}{\bar{c}_i\bar{T}} + \frac{\overline{\rho'c_i'}}{\bar{c}_i\bar{\rho}} + \frac{\overline{\rho'T'}}{\bar{\rho}\bar{T}}\right].$$

$$(2.24)$$

Equations (2.15), (2.19), (2.20), (2.23) and (2.24) constitute a system of equations of the average turbulent motion for a multi-component reacting mixture of gases. It must, however, be noted at once that the use of this system at the present time, even within

the framework of the semiempirical theory of the boundary layer, is not possible without a number of assumptions whose validity is in many cases far from obvious. As already noted above, our knowledge of the nature of turbulence does not permit us to estimate the contribution made to the transport process by terms involving density fluctuations. Therefore, in all existing theories that make use of the indicated system of equations or its modifications, the terms involving density fluctuations are neglected. This does not mean, of course, that the density is considered constant. The average density $\bar{\rho}$ is considered to be a variable quantity where it is necessary.

Neglecting in the equations of the average turbulent motion for multicomponent reacting mixture of gases the terms involving fluctuations of the density, and in the equation of state neglecting all fluctuating terms[4], and considering below only the "steady" turbulent flows in which the average velocity, enthalpy, density, etc. do not depend on time, we obtain the following system of equations:

$$\frac{\partial}{\partial s_j}(\bar{\rho}\,\bar{v}_j) = 0,$$

(2.25)

$$\bar{\rho}\bar{v}_j\frac{\partial \bar{c}_i}{\partial s_j} = \bar{w}_i - \frac{\partial}{\partial s_j}(\bar{\rho}\overline{V_{ij}}\bar{c}_i + \bar{\rho}\overline{v_j'c_i'}),$$

(2.26)

$$\bar{\rho}\bar{v}_j\frac{\partial \bar{v}_k}{\partial s_j} = -\frac{\partial \bar{p}}{\partial s_k} + \frac{\partial}{\partial s_j}(2\bar{\mu}\bar{S}_{jk} - \bar{\rho}\overline{v_j'v_k'}),$$

(2.27)

$$\bar{\rho}\bar{v}_j\frac{\partial \bar{h}}{\partial s_j} = \bar{v}_k\frac{\partial \bar{p}}{\partial s_k} + (2\bar{\mu}\bar{S}_{jk} - \bar{\rho}\overline{v_j'v_k'})\frac{\partial \bar{v}_k}{\partial s_j} +$$
$$+ \frac{\partial}{\partial s_j}\left(\bar{\lambda}\frac{\partial \bar{T}}{\partial s_j} - \sum_i \bar{c}_i\bar{\rho}\,\overline{v_i'h_i'}\right) - \frac{\partial}{\partial s_j}\left(\sum_i \bar{\rho}_i\overline{V}_i h_i + \sum_i \bar{h}_i\bar{\rho}\,\overline{v_j'c_i'}\right),$$

(2.28)

$$\bar{p} = \bar{\rho}R\bar{T}\sum_i \frac{\bar{c}_i}{M_i}.$$

(2.29)

Below we formally set

$$-\bar{\rho}\overline{v_j'v_k'} = \varepsilon\frac{\partial \bar{v}_k}{\partial s_j},$$

(2.30)

$$-\bar{\rho}\,\overline{v_j'c_i'} = \bar{\rho}\mathcal{D}_\mathrm{T}\frac{\partial \bar{c}_i}{\partial s_j},$$

(2.31)

$$-\bar{\rho}\overline{v_i'h_i'} = \lambda_\mathrm{T}\frac{\partial \bar{T}}{\partial s_j},$$

(2.32)

Footnote (4) appears on page 69.

where ε, $\mathcal{D}_\tau$ and $\lambda_\mathbb{T}$ are the turbulent viscosity, turbulent diffusion, and turbulent heat conductivity coefficients, respectively. In contrast with the molecular viscosity, diffusion, and heat conductivity coefficients, the turbulent viscosity, diffusion, and heat conductivity coefficients do not describe the physical properties of a gas, but instead the statistical properties of fluctuating motion. Therefore, these coefficients are functions of position and time. It is important to note that far away from a solid surface the turbulent transport coefficients are much greater than the molecular transport coefficients.

By analogy with the molecular Prandtl, Lewis, and Schmidt numbers (1.103) and (1.105), we shall introduce their turbulent analogs

$$Pr_\tau = \frac{\varepsilon \bar{c}_p}{\lambda_\tau},$$

$$(2.33)$$

$$Le_\tau = \frac{\bar{\rho} \mathcal{D}_\tau \bar{c}_p}{\lambda_\tau}.$$

$$(2.34)$$

$$Sc_\tau = \frac{\varepsilon}{\bar{\rho} \mathcal{D}_\tau} = \frac{Pr_\tau}{Le_\tau}.$$

$$(2.35)$$

Although the turbulent transport coefficients ε, $\mathcal{D}_\tau$, and $\lambda_\mathbb{T}$ are in general functions of position and time, their dimensionless combinations Pr_τ, Le_τ and Sc_τ usually are slowly varying quantities which in many practically important cases permits us to consider them constant. The numerical values of Pr_τ, Le_τ and Sc_τ have not as yet been accurately determined. The few experimental data concerning the values of these numbers are extremely inconsistent. Nevertheless, it can be stated that in boundary-layer type flows near a solid surface Pr_τ and Sc_τ are close to unity; in turbulent jet flows they are close to 0.5 – 0.7[5].

Using Equations (2.30) – (2.32), and for simplicity omitting below the averaging symbols, we shall write the system of Equations (2.25) – (2.29) in the form

---

Footnote (5) appears on page 69.

$$-\frac{\partial}{\partial s_j}(\rho v_j) = 0. \tag{2.36}$$

$$\rho v_j \frac{\partial c_i}{\partial s_j} = w_i - \frac{\partial}{\partial s_j}\left(\rho V_{ij}c_i - \rho \mathcal{D}_\tau \frac{\partial c_i}{\partial s_j}\right). \tag{2.37}$$

$$\rho v_j \frac{\partial v_k}{\partial s_j} = -\frac{\partial p}{\partial s_k} + \frac{\partial}{\partial s_j}\left(2\mu \dot{S}_{jk} + \varepsilon \frac{\partial v_k}{\partial s_j}\right). \tag{2.38}$$

$$\rho v_j \frac{\partial i}{\partial s_j} = v_k \frac{\partial p}{\partial s_k} + \left(2\mu \dot{S}_{jk} + \varepsilon \frac{\partial v_k}{\partial s_j}\right)\frac{\partial v_k}{\partial s_j} +$$
$$+ \frac{\partial}{\partial s_j}\left[(\lambda + \lambda_\tau)\frac{\partial T}{\partial s_j}\right] - \frac{\partial}{\partial s_j}\left(\sum_i \rho c_i V_{ij}h_i - \sum_i \rho \mathcal{D}_\tau h_i \frac{\partial c_i}{\partial s_j}\right). \tag{2.39}$$

$$p = \rho R T \sum_i \frac{c_i}{M_i}. \tag{2.40}$$

Making use of Equation (1.101), which in tensor notation has the form,

$$\frac{\partial T}{\partial s_j} = \frac{1}{c_p}\left(\frac{\partial h}{\partial s_j} - \sum_i h_i \frac{\partial c_i}{\partial s_j}\right). \tag{2.41}$$

and also taking into account Equations (2.33) - (2.35), we shall bring the energy Equation (2.39) to the form

$$\rho v_j \frac{\partial h}{\partial s_j} = v_k \frac{\partial p}{\partial s_k} + \left(2\mu \dot{S}_{jk} + \varepsilon \frac{\partial v_k}{\partial s_j}\right)\frac{\partial v_k}{\partial s_j} +$$
$$+ \frac{\partial}{\partial s_j}\left[\left(\frac{\mu}{Pr} + \frac{\varepsilon}{Pr_\tau}\right)\frac{\partial h}{\partial s_j} - \sum_i\left(\rho c_i V_{ij}h_i - \frac{\mu}{Pr}h_i \frac{\partial c_i}{\partial s_j}\right) + \right.$$
$$\left. + \frac{\varepsilon}{Pr_\tau}(Le_\tau - 1)\sum_i h_i \frac{\partial c_i}{\partial s_j}\right]. \tag{2.42}$$

Passing in Equation (2.42) from the enthalpy h to the total enthalpy H, defined by Equation (1.94), and using Equation (2.38), we shall obtain

$$\rho v_j \frac{\partial H}{\partial s_j} = \frac{\partial}{\partial s_j}\left[\left(\frac{\mu}{Pr} + \frac{\varepsilon}{Pr_\tau}\right)\frac{\partial H}{\partial s_j} -\right.$$
$$- \sum_i\left(\rho c_i V_i h_i - \frac{\mu}{Pr}h_i \frac{\partial c_i}{\partial s_j}\right) + \frac{\varepsilon}{Pr_\tau}(Le_\tau - 1)\sum_i h_i \frac{\partial c_i}{\partial s_j} +$$
$$+ \varepsilon\left(1 - \frac{1}{Pr_\tau}\right)\frac{\partial}{\partial s_j}\left(\frac{v^2}{2}\right) + 2\mu v_k \dot{S}_{jk} - \frac{\mu}{Pr}\frac{\partial}{\partial s_j}\left(\frac{v^2}{2}\right)\right]. \tag{2.43}$$

The system (2.36) - (2.40), containing 5 + N + j equations (out of N equations for concentrations, only N - 1 equations are independent

since $\sum_i c_i = 1$), generally speaking, does not completely determine the turbulent flow of an N-component reacting mixture since it involves $5 + N + J$ unknown functions v_j, p, ρ, h, c_i (i = 1, 2, ..., N) and the undetermined turbulent viscosity, diffusion, and heat conductivity coefficients ε, $\mathcal{L}_\tau$, and λ_T, respectively. In other words, the system of Equations (2.36) - (2.40) is open. The fact that the system of equations describing the process of turbulent transport is open up to the present time has made it impossible to create a theory by means of which one could make turbulent flow calculations, even in the simplest case involving flow of a homogeneous incompressible isothermal fluid, using a purely theoretical method. All the existing theories of turbulence in an incompressible homogeneous fluid are semiempirical, since — in addition to certain justified assumptions — they are also based on a number of empirical formulas. The solution of the turbulent flow problem for the more complicated cases involving compressible heat-conducting reacting gases is usually based on a generalization of the semiempirical theories, developed for an incompressible fluid, to the indicated more complicated cases. However, even in this type of a semi-empirical approach, it is difficult to use the system of Equations (2.36) - (2.40) in view of their mathematical complexity. Therefore, in many important cases it is extremely useful to deal with simplifications of this system provided by boundary layer theory.

§ 7. Equations of the Turbulent Boundary Layer in a Multicomponent Reacting Gas

Application of the system of Equations (2.36) - (2.40) to flows in thin boundary layers forming on the walls of channels or on the surface of bodies during motion through a gas medium leads to a considerable simplification of the system. The set of assumptions (first formulated by L. Prandtl) that form the basis of the present-day boundary layer theory is well-known.

Let us consider a steady two-dimensional average flow with average velocities $v_1 = u$ and $v_2 = v$, corresponding to the direction
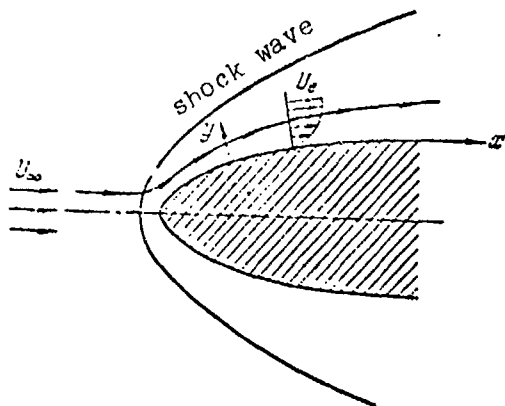
Figure 1

s_1 = x along the surface of the body with the flow and s_2 = y along the normal to the surface of the body (Figure 1).

Following the basic idea advanced by Prandtl, we shall divide the entire flow field into two regions: a thin region of turbulent motion, adjacent to the surface of the body, in which the parameters of the flow deviate sharply from their values on the surface to the values in the external flow (boundary layer), and the region of potential (vortex-free) flow (external flow). The thickness of the boundary layer δ will be assumed to be small as compared to the distance x. The order of x and u will be taken to be unity, i.e.,

$$x \sim O(1) \quad \text{and} \quad u \sim O(1);$$

then

$$y \sim O(\delta) \quad \text{and} \quad v \sim O(\delta)$$

and, consequently,

$$\frac{\partial}{\partial x} \sim O(1) \quad \text{and} \quad \frac{\partial}{\partial y} \sim O\left(\frac{1}{\delta}\right),$$

$$\frac{\partial^2}{\partial x^2} \sim O(1) \quad \text{and} \quad \frac{\partial^2}{\partial y^2} \sim O\left(\frac{1}{\delta^2}\right).$$

The pressure, density, concentration, and enthalpy will be assumed to be on the order of unity:

$$p \sim O(1), \; \rho \sim O(1), \; c_i \sim O(1), \; h \sim O(1).$$

Assuming that the terms in Equations (2.36) - (2.39) which involve $\mu, \lambda, \varepsilon, \mathcal{T}_\tau, \lambda_\tau$ and $\overline{V}_i$ do not exceed the order of the remaining terms, it is not difficult to arrive at the conclusion that $\lambda, \mu, \varepsilon, \mathcal{T}_\tau$ and λ_τ are no greater than $\sim \delta^2$ and $\overline{V}_i$ are no greater than δ.

Using the preceding estimates and retaining in Equations (2.36) - (2.39) terms of the same order, we shall reduce the system to the following form:

$$\frac{\partial}{\partial x}(\rho u) + \frac{\partial}{\partial y}(\rho v) = 0, \tag{2.44}$$

$$\rho u \frac{\partial c_i}{\partial x} + \rho v \frac{\partial c_i}{\partial y} = w_i - \frac{\partial}{\partial y}\left(\rho c_i V_{iy} - \rho \mathcal{T}_\tau \frac{\partial c_i}{\partial y}\right). \tag{2.45}$$

$$\rho u \frac{\partial u}{\partial x} + \rho v \frac{\partial u}{\partial y} = -\frac{\partial p}{\partial x} + \frac{\partial}{\partial y}\left[(\mu + \varepsilon)\frac{\partial u}{\partial y}\right], \tag{2.46}$$

$$0 = -\frac{\partial p}{\partial y}, \tag{2.47}$$

$$\rho u \frac{\partial \lambda}{\partial x} + \rho v \frac{\partial \lambda}{\partial y} = u \frac{\partial p}{\partial x} + (\mu + \varepsilon)\left(\frac{\partial u}{\partial y}\right)^2 +$$
$$+ \frac{\partial}{\partial y}\left[(\lambda + \lambda_\tau)\frac{\partial T}{\partial y} - \sum_i \rho c_i V_{iy} h_i - \rho \mathcal{T}_\tau \sum_i h_i \frac{\partial c_i}{\partial y}\right]. \tag{2.48}$$

Equations (2.42) and (2.43) will then become

$$\rho u \frac{\partial \lambda}{\partial x} + \rho v \frac{\partial \lambda}{\partial y} = u \frac{\partial p}{\partial x} + (\mu + \varepsilon)\left(\frac{\partial u}{\partial y}\right)^2 +$$
$$+ \frac{\partial}{\partial y}\left[\left(\frac{\mu}{Pr} + \frac{\varepsilon}{Pr_\tau}\right)\frac{\partial \lambda}{\partial y} - \sum_i \rho c_i \Gamma_{iy} h_i - \frac{\mu}{Pr}\sum_i h_i \frac{\partial c_i}{\partial y} +\right.$$
$$\left. + \frac{\varepsilon}{Pr_\tau}(Le_i - 1)\sum_i h_i \frac{\partial c_i}{\partial y}\right] \tag{2.49}$$

and

$$\rho u \frac{\partial H}{\partial x} + \rho v \frac{\partial H}{\partial y} = \frac{\partial}{\partial y}\left\{\left(\frac{\mu}{Pr} + \frac{\varepsilon}{Pr_\tau}\right)\frac{\partial H}{\partial y} + \left[\mu\left(1 - \frac{1}{Pr}\right) +\right.\right.$$
$$\left.+ \varepsilon\left(1 - \frac{1}{Pr_\tau}\right)\right]\frac{\partial}{\partial y}\left(\frac{u^2}{2}\right) - \sum_i \rho c_i V_{iy} h_i -$$
$$\left. - \frac{\mu}{Pr}\sum_i h_i \frac{\partial c_i}{\partial y} + \frac{\varepsilon}{Pr_\tau}(Le_i - 1)\sum_i h_i \frac{\partial c_i}{\partial y}\right\}. \tag{2.50}$$

In Equations (2.45) and (2.48) - (2.50), the diffusion rate is generally given by Equation (1.53). However, as noted in Section 3, the effect of pressure and thermal diffusion in the boundary layer is usually small. This is even more true for a turbulent boundary

layer in which a region with significant molecular transport processes occupies only a portion of the entire boundary layer, and a portion at that which is in many cases insignificant. Neglecting the effect of pressure and thermal diffusion on mass transport as compared with mass diffusion, the rate of diffusion will be given here by an expression that can be derived from Equation (1.57). Its y-component will have the form

$$V_{iy} = - \frac{\mathscr{D}_i}{c_i} \frac{\partial c_i}{\partial y}.$$

(2.51)

Here $\mathscr{D}_i$ is the effective diffusion coefficient given by Equation (1.58). In the case of a binary mixture, $\mathscr{D}_i$ becomes the diffusion coefficient for a binary mixture, $\mathscr{D}_{ij}$.

Substituting Equation (2.51) in the equation of continuity for the ith component (2.45) and in the energy Equation (2.48), and omitting the ratio (2.47), the system of equations for a turbulent boundary layer in a multicomponent reacting gas will have the form

$$\frac{\partial}{\partial x}(\rho u) + \frac{\partial}{\partial y}(\rho v) = 0,$$

(2.44)

$$\rho u \frac{\partial u}{\partial x} + \rho v \frac{\partial u}{\partial y} = -\frac{dp}{dx} + \frac{\partial}{\partial y}\left[(\mu + \varepsilon)\frac{\partial u}{\partial y}\right],$$

(2.52)

$$\rho u \frac{\partial c_i}{\partial x} + \rho v \frac{\partial c_i}{\partial y} = w_i + \frac{\partial}{\partial y}\left[\rho(\mathscr{D}_i + \mathscr{D}_\tau)\frac{\partial c_i}{\partial y}\right],$$

(2.53)

$$\rho u \frac{\partial \lambda}{\partial x} + \rho v \frac{\partial \lambda}{\partial y} =$$
$$= u \frac{dp}{dx} + (\mu + \varepsilon)\left(\frac{\partial u}{\partial y}\right)^2 + \frac{\partial}{\partial y}\left\{\left(\frac{\mu}{Pr} + \frac{\varepsilon}{Pr_\tau}\right)\frac{\partial \lambda}{\partial y} + \right.$$
$$\left. + \sum_i\left[\frac{\mu}{Pr}(Le_i - 1) + \frac{\varepsilon}{Pr_\tau}(Le_\tau - 1)\right]h_i\frac{\partial c_i}{\partial y}\right\}.$$

(2.54)

The energy equation in the form (2.50), upon substitution of Equation (2.51), will become

$$\rho u \frac{\partial H}{\partial x} + \rho v \frac{\partial H}{\partial y} = \frac{\partial}{\partial y}\left\{\left(\frac{\mu}{Pr} + \frac{\varepsilon}{Pr_\tau}\right)\frac{\partial H}{\partial y} + \right.$$
$$+ \sum_i\left[\frac{\mu}{Pr}(Le_i - 1) + \frac{\varepsilon}{Pr_\tau}(Le_\tau - 1)\right]h_i\frac{\partial c_i}{\partial y} +$$
$$\left. + \left[\mu\left(1 - \frac{1}{Pr}\right) + \varepsilon\left(1 - \frac{1}{Pr_\tau}\right)\right]\frac{\partial}{\partial y}\left(\frac{u^2}{2}\right)\right\} .$$

(2.55)

It should be noted that in a turbulent boundary layer there is a "transition" (buffer) zone at a certain distance from the wall in which the molecular and turbulent transport coefficients are of the same order. In this region, the above boundary layer equations are inaccurate, since, in deriving the general equations of turbulent motion which in turn were used to deduce the boundary layer equations, we neglected quantities (fluctuations of molecular terms) which in the buffer zone play an important role. Therefore, the equations of motion (2.52), energy (2.54), (2.55), and continuity for the ith component (2.53) in the form in which they are written assume that the boundary layer is divided in two regions with different types of flow: the turbulent core in which $\mu \ll \varepsilon,\ \lambda \ll \lambda_r,\ \mathcal{D}_i \ll \mathcal{I}_r$, and the laminar sublayer in which $\mu \gg \varepsilon,\ \lambda \gg \lambda_r$, and $\mathcal{T}_i \gg \mathcal{D}_r$.

The equations of continuity for the ith component (2.53), written for the mass concentrations of the individual components of the mixture, are inhomogeneous when homogeneous chemical reactions occur in the flow ($w_i \neq 0$). In certain cases, it is more convenient not to write these equations for the mass concentrations of the components, but instead for the mass concentrations of individual chemical elements, regardless of the type of a chemical compound in which a given element is bound. In this case, in the absence of nuclear reactions, the diffusion equations become homogeneous. In fact, if

$$c_{ki} = \frac{m_k N_k}{m_i} \tag{2.56}$$

signifies the concentration of the kth element in the ith component of the mixture, where N_k is the number of atoms of the kth element in the ith component, then $w_i c_{ki}$ will represent the mass rate of transition of the element k into the component i. Since in chemical reactions, the mass of an element is conserved, we have

$$\sum_i c_{ki} w_i = w_k = 0. \tag{2.57}$$

The concentration of the element k in a mixture will obviously be equal to $c_k = \sum_i c_{ki} c_i$. Consequently, multiplying the diffusion Equation

(2.53) by c_{ki} and summing over all components of the mixture, we obtain the equation of continuity for the kth element in the form

$$\rho u \frac{\partial c_k}{\partial x} + \rho v \frac{\partial c_k}{\partial y} = \frac{\partial}{\partial y}\left[\rho(\mathcal{P}_k + \mathcal{D}_\tau)\frac{\partial c_k}{\partial y}\right].$$

$$\mathcal{D}_k = \sum_i \mathcal{P}_i c_{ki}\frac{\partial c_i/\partial y}{\partial c_k/\partial y}.$$ \qquad (2.58)

The equations of the turbulent boundary layer are sometimes conveniently written in terms of variables that were named after L. Crocco. Crocco suggested that the longitudinal velocity component u be used as one of the variables. The formulas describing a transformation from the variables x, y to the Crocco variables $\xi = x$, u are[6]

$$\frac{\partial}{\partial v} = \frac{\partial u}{\partial y}\,\frac{\partial}{\partial u} \, , \quad \frac{\tau}{\mu + \varepsilon}\,\frac{\partial}{\partial u} \, ,$$
$$\frac{\partial}{\partial x} = \frac{\partial}{\partial \xi} - \frac{\partial u}{\partial \xi}\,\frac{\tau}{\mu + \varepsilon}\,\frac{\partial}{\partial u} \, , \qquad (2.59)$$

Upon making the indicated change of variables in the equation of continuity (2.44) and multiplying the latter by $\frac{\mu + \varepsilon}{\tau}$, we obtain

$$\frac{\mu + \varepsilon}{\tau}\,\frac{\partial}{\partial \xi}(\rho u) - \frac{\partial u}{\partial \xi}\,\frac{\partial}{\partial u}(\rho u) + \frac{\partial}{\partial u}(\rho v) = 0. \qquad (2.60)$$

Transforming to the variables ξ, u and dividing through by $\tau/(\mu + \varepsilon)$, the equation of motion (2.52) will become

$$-\rho u \frac{\partial u}{\partial \xi} + \rho v = -\frac{\partial p}{\partial \xi}\,\frac{\mu + \varepsilon}{\tau} + \frac{\partial \tau}{\partial u}. \qquad (2.61)$$

Differentiating both sides of Equation (2.61) with respect to u, we get

$$-\rho u \frac{\partial}{\partial \xi}\left(\frac{\partial u}{\partial u}\right) - \frac{\partial u}{\partial \xi}\,\frac{\partial}{\partial u}(\rho u) + \frac{\partial}{\partial u}(\rho v) =$$
$$= -\frac{\partial p}{\partial \xi}\,\frac{\partial}{\partial u}\left(\frac{\mu + \varepsilon}{\tau}\right) + \frac{\partial^2 \tau}{\partial u^2}.$$

Subtracting term by term both sides of this equation from Equation (2.60) and using $\partial y/\partial u = (\mu + \varepsilon)/\tau$, we eliminate v and find

---

Footnote (6) appears on page 69.

$$u \frac{\partial}{\partial \xi}\left[\frac{(\mu+\varepsilon)\,\nu}{\tau}\right] + \frac{\partial \tau}{\partial u^2} - \frac{dp}{d\xi}\,\frac{\partial}{\partial u}\left(\frac{\mu+\varepsilon}{\tau}\right) = 0. \qquad (2.62)$$

We shall similarly transform the equation of continuity for the ith component (2.53). Rewriting it first in terms of the new variables

$$\rho u \frac{\partial c_i}{\partial \xi} + \left(-\rho u \frac{\partial \nu}{\partial \xi} + \rho \nu\right)\frac{\tau}{\mu+\varepsilon}\frac{\partial c_i}{\partial u} =$$
$$= w_i + \frac{\tau}{\mu+\varepsilon}\frac{\partial}{\partial u}\left[\frac{\rho\,(\mathcal{X}_i+\mathcal{J}_\tau)}{\mu+\varepsilon}\tau\frac{\partial c_i}{\partial u}\right]$$

and then eliminating with the help of (2.61) the expression on the left in parentheses, and taking into account Equations (1.104) and (2.35), we obtain after simple rearrangements

$$\rho u \frac{\mu+\varepsilon}{\tau}\frac{\partial c_i}{\partial \xi} + \left(\frac{\partial \tau}{\partial u} - \frac{dp}{d\xi}\frac{\mu+\varepsilon}{\tau}\right)\frac{\partial c_i}{\partial u} =$$
$$= \frac{\mu+\varepsilon}{\tau}w_i + \frac{\partial}{\partial u}\left[\left(\frac{1}{Sc_i}+\frac{1}{Sc_\tau}\right)\tau\frac{\partial c_i}{\partial u}\right]. \qquad (2.63)$$

Applying the transformation (2.69) to the energy Equation (2.55), and performing, as before, straightforward simplifications, we obtain

$$\rho u \frac{\mu+\varepsilon}{\tau}\frac{\partial H}{\partial \xi} + \left(\frac{\partial \tau}{\partial u} - \frac{dp}{d\xi}\frac{\mu+\varepsilon}{\tau}\right)\frac{\partial H}{\partial u} =$$
$$= \frac{\partial}{\partial u}\left\{\tau\left[\left(\frac{1}{Pr}+\frac{1}{Pr_\tau}\right)\frac{\partial H}{\partial u} + \sum_i\left(\frac{1}{Pr}(Le_i-1)+\right.\right.\right.$$
$$\left.\left.\left.+ \frac{1}{Pr_\tau}(Le_\tau-1)\right)h_i\frac{\partial c_i}{\partial u} + \left(1-\frac{1}{Pr}-\frac{1}{Pr_\tau}\right)u\right]\right\}. \qquad (2.64)$$

Reproduced from best available copy.

The energy equation in the Crocco variables written in terms of the enthalpy h can be easily obtained from Equation (2.64) by substituting the equality (1.94) for H and keeping in mind that $\partial u/\partial u = 0$. Thus we obtain

$$\rho u(\mu+\varepsilon)\frac{\partial h}{\partial \xi} - (\mu+\varepsilon)\left(u+\frac{\partial \tau}{\partial u}\right)\frac{\partial h}{\partial \xi} + \tau\frac{\partial \tau}{\partial u}\frac{\partial h}{\partial u}\times$$
$$\times\left(1-\frac{1}{Pr}-\frac{1}{Pr_\tau}\right) - \tau^2\left[1+\frac{\partial}{\partial u}\left(\frac{1}{Pr}+\frac{1}{Pr_\tau}\right)\frac{\partial h}{\partial u}\right] -$$
$$- \sum_i\left[\frac{1}{Pr}(Le_i-1)+\frac{1}{Pr_\tau}(Le_\tau-1)\right]h_i\frac{\partial c_i}{\partial u} = 0. \qquad (2.65)$$

Equations (2.62), (2.63), (2.64) [or (2.65)], together with the equation of state (2.40) constitute a system of equations of the

turbulent boundary layer in Crocco variables. This system, similar to the system of Equations (2.44), (2.52), (2.53), (2.54) [or (2.55)], assumes that the boundary layer has been divided into two parts — namely, the turbulent core and the laminar sublayer. When applying these equations to the laminar sublayer, one omits terms involving the turbulent transport coefficients and their dimensionless combinations (ε, λ_τ, f_τ, Pr_τ, Le_τ, Sc_τ). In the case of the turbulent core, one similarly omits terms involving the molecular transport coefficients and their dimensionless combinations (u, λ, f_i, Pr, Le_i, Sc_i).

For flows in the boundary layer over axially symmetric bodies of revolution, the equation of continuity is written as

$$\frac{\partial}{\partial x}(r_w \rho u) + \frac{\partial}{\partial y}(r_w \rho v) = 0, \tag{2.66}$$

and to the left-hand side of the equation of motion in the Crocco variables (2.62) one must add the term $\frac{\rho v(\mu - \varepsilon)}{\tau} \frac{1}{r_w} \frac{dr_w}{d\xi}$, thus obtaining

$$u \frac{\partial}{\partial \xi} \left[\frac{(\mu + \varepsilon)\rho}{\tau} \right] + \frac{\partial \tau}{\partial u^2} - \frac{d\rho}{d\xi} \frac{\partial}{\partial u} \left(\frac{\mu + \varepsilon}{\tau} \right) + \\ + \frac{\rho v(\mu + \varepsilon)}{\tau} \frac{1}{r_w} \frac{dr_w}{d\xi} = 0. \tag{2.67}$$

Here $r_w = r_w(x) = r_w(\xi)$ is the radius of the lateral curvature of the body. Equations (2.66) and (2.67) are valid only if the thickness of the boundary layer δ is much smaller than r_w, i.e., $\delta \ll r_w$. This condition no longer holds for the rear portion of long, axially symmetric bodies or for long channels. All the other equations of the turbulent boundary layer on axially symmetric bodies are completely identical with the equations of a flat boundary layer.

§ 6. Semi-empirical Theories of Turbulence.
Reynolds Similitude

The system of equations for a turbulent boundary layer which was obtained in the preceding section is open just like the initial system (2.36) – (2.40), since the number of unknowns exceeds the

number of equations. As we know, in the study of the turbulent motion of an incompressible homogeneous isothermal fluid, we must resort to semi-empirical theories of turbulence in order to close the system of equations. All present-day semi-empirical theories of turbulence of an incompressible fluid are based on a set of assumptions constituting a hypothesis which came to be called "the hypothesis of the local mechanism of turbulent transport" [3]. The most important of these assumptions is the one stating that the mechanism of turbulent momentum transport can be completely specified by giving the local values of the derivatives of the average velocities along the coordinate normal to the direction of the flow and by specifying the physical properties of the fluid. The effect of processes far from the indicated point in the turbulent flow is not taken into account by the localization hypothesis. On the basis of the localization hypothesis and dimensional considerations, one can obtain formulas comprising the semi-empirical theories as proposed by Prandtl and Karman[7].

In Prandtl's theory, it is assumed that a local variation of the average velocity is determined only by the first derivative of the velocity, du/dy. For this reason, dimensional considerations make it necessary for us to introduce the additional concept of the length of "the mixing path" without which it would be impossible to set up a formula for the friction stress. Using dimensional considerations, it can be established that the only possible combination of the fluid density ρ, "mixing path" l, and derivative of the velocity du/dy that can yield the friction stress τ is

$$\tau = \rho l^2 \left(\frac{du}{dy}\right)^2. \tag{2.68}$$

The quantitative expression for l (y) must be determined on the basis of additional considerations.

Footnote (7) appears on page 70.

In Karman's theory, the variation of the average velocity is determined by the first two derivatives of the velocities du/dy and d^2u/dy^2. Similar dimensional considerations lead to a conclusion about the existence and uniqueness of Karman's formula for the friction stress

$$\tau = \rho\varkappa^2 \frac{\left(\frac{du}{dy}\right)^4}{\left(\frac{d^2u}{dy^2}\right)^2}.$$

(2.69)

Application of the semi-empirical theory to processes involving turbulent heat and mass transfer is based on so-called "Reynolds similitude". According to this concept, it is assumed that the turbulent momentum, enthalpy, and mass transport coefficients have identical values. This assumption presupposes the absence of the effect of changes in the enthalpy and concentration of mass in a flow on the mechanism of turbulent mixing, and is probably valid for not too large enthalpy and concentration gradients. The assumption stating that the turbulent momentum, enthalpy, and mass transport coefficients are identical is apparently equivalent to an assumption stating that the turbulent analogs of the Prandtl and Schmidt numbers are equal to unity:

$$Pr_{\tau} = Sc_{\tau} = 1.$$

(2.70)

In quantitative terms, Reynolds similitude can be expressed as

$$\tau = \varepsilon \frac{du}{dy}, \qquad q = \varepsilon \frac{dh}{dy}, \qquad j_{i\tau} = \varepsilon \frac{dc_i}{dy}$$

(2.71)

or

$$\frac{q}{\tau} = \frac{dh}{du}, \qquad \frac{j_{i\tau}}{\tau} = \frac{dc_i}{du}.$$

(2.72)

When studying turbulent flows, in which one must take into account the effects of compressibility, heat and mass transfer, chemical reactions, etc. (all at the same time or some of them), the only

possible method involves an extension of the semi-empirical theories
of turbulence in incompressible fluids to these more complicated
cases. The extension in question usually reduces to direct use of
the semi-empirical formulas of Prandtl (2.68) and Karman (2.69). Here
Prandtl's and Karman's formulas retain their previous form, with the
only exception that the density ρ is considered to be variable.
Regarding the value of the turbulence constant κ (we recall that the
mixing path is usually given by $l = \kappa y$), it should be noted that,
even though there is some experimental evidence that the value in
question is affected by compressibility and heat transfer, at the same
time the evidence we have does not permit us to make any numerical
estimates of this effect[8]. For this reason, the constant κ is
usually given the value it assumes in an incompressible fluid,
$(\kappa = 0.39 - 0.41)$.

§ 9. Integral Momentum and Energy Relations

In the theory of the boundary layer when constructing the so-
called (approximate) integral techniques of friction and heat transfer
calculations, one uses the integral form of the momentum and energy
conservation conditions. In order to obtain these conditions, we
shall set up the boundary conditions at the surface of the body and
at the external boundary of the boundary layer for the velocities,
total enthalpy, and concentrations of components. To make the argu-
ments more general, we shall assume that the surface of the body is
permeable. These conditions are

$$
\begin{aligned}
& u = 0, \quad v = v_w, \quad H = h_w, \quad c_i = c_{iw} \quad \text{for } y = 0; \\
& u \to U_e, \quad H \to H_e, \quad c_i \to c_{ie} \quad \text{for } y \to \infty; \\
& \frac{\partial u}{\partial y} \to 0, \quad \frac{\partial H}{\partial y} \to 0, \quad \frac{\partial c_i}{\partial y} \to 0 \quad \text{for } y \to \infty.
\end{aligned}
\right\} \tag{2.73}
$$

The second condition at the wall, $v = v_w$, describes its permeability.
If the wall is not permeable, then $v_w = 0$. The last three conditions
provide for the smooth transition of the velocity, total enthalpy,
and concentration profiles at the boundary of the boundary layer with
the external flow.

Footnote (8) appears on page 70.

The external flow will be assumed to be isentropic, and thus
the velocity at the outer boundary U_e will be related to pressure on
the surface of the body by the Bernoulli equation

$$-\frac{dp}{dx} = \rho_e U_e \frac{dU_e}{dx}.$$ (2.74)

In deriving the integral relations, we make use of the boundary
layer equations expressed in terms of x, y. Here the equation of
continuity (2.66) will be

$$\frac{\partial}{\partial x}(\rho u) + \frac{\partial}{\partial y}(\rho v) + \rho u \frac{1}{r_w^\nu} \frac{dr_w^\nu}{dx} = 0,$$ (2.75)

where $\nu = 0$ for a plane flow and $\nu = 1$ for an axially symmetric flow
in the boundary layer.

Integral momentum relation. Using Equations (2.74) and (2.75),
we rewrite the equation of motion (2.52) as

$$\frac{\partial}{\partial x}(\rho u^2) + \frac{\partial}{\partial y}(\rho u v) + \rho u^2 \frac{1}{r_w^\nu} \frac{dr_w^\nu}{dx} =$$
$$= \rho_e U_e \frac{dU_e}{dx} + \frac{\partial}{\partial y}\left[(\mu + \epsilon)\frac{\partial u}{\partial y}\right].$$

Multiplying both sides of Equation (2.75) by U_e, we obtain

$$\frac{\partial}{\partial x}(\rho u U_e) + \frac{\partial}{\partial y}(\rho v U_e) + \rho u U_e \frac{1}{r_w^\nu} \frac{dr_w^\nu}{dx} = \rho u \frac{dU_e}{dx}.$$

Subtracting both sides of the preceding equation from this equation,
we arrive at the expression

$$\frac{\partial}{\partial x}\rho u(U_e - u) + \frac{\partial}{\partial y}\rho v(U_e - u) + (\rho_e U_e - \rho u)\frac{dU_e}{dx} +$$
$$+ \rho u(U_e - u)\frac{1}{r_w^\nu}\frac{dr_w^\nu}{dx} = -\frac{\partial}{\partial y}\left[(\mu + \epsilon)\frac{\partial u}{\partial y}\right].$$

Integrating this expression across the boundary layer along y
between 0 and infinity, and introducing the integral thicknesses:

$$\delta^{**} = \int_0^\infty \frac{\rho u}{\rho_e U_e} \left(1 - \frac{u}{U_e}\right) dy \qquad (2.76)$$

which is the momentum loss thickness, and

$$\delta^* = \int_0^\infty \left(1 - \frac{\rho u}{\rho_e U_e}\right) dy \qquad (2.77)$$

which is the displacement thickness, and also using the boundary conditions for the velocity (2.73), we obtain

$$\frac{d}{dx}(\rho_e U_e^2 \delta^{**}) + \delta^* \rho_e U_e \frac{dU_e}{dx} +$$
$$+ \rho_e U_e^2 \delta^{**} \frac{1}{r_w^\nu} \frac{dr_w^\nu}{dx} = \tau_w + \rho_w v_w U_e, \qquad (2.78)$$

where

$$\tau_w = \left(\mu \frac{\partial u}{\partial y}\right)_w$$

is the friction stress at the wall.

Performing differentiation in (2.78), and noting that

$$\frac{\rho_e'}{\rho_e} = -M_e^2 \frac{U_e'}{U_e}, \qquad (2.79)$$

upon dividing both sides of Equation (2.78) by $\rho_e U_e^2$ we obtain the integral momentum relation

$$\frac{d\delta^{**}}{dx} + \frac{U_e'}{U_e}(2 + H^* - M_e^2)\delta^{**} + \frac{\delta^{**}}{r_w^\nu} \frac{dr_w^\nu}{dx} = \frac{\tau_w}{\rho_e U_e^2} + \frac{\rho_w v_w}{\rho_e U_e}. \qquad (2.80)$$

Here

$$H^* = \frac{\delta^*}{\delta^{**}} \qquad (2.81)$$

is the form parameter of the boundary layer, $M_e = U_e/a_e$ is the Mach number, a_e is the velocity of sound at the outer boundary of the boundary layer. The prime indicates a derivative with respect to the

x coordinate. It will be noted that Equation (2.79) can be easily derived from the Bernoulli Equation (2.74), upon writing the latter in the form

$$-\left(\frac{dp}{d\rho}\right)_e \frac{d\rho_e}{dx} = \rho_e U_e \frac{dU_e}{dx}.$$

Now recalling the definition of the velocity of sound

$$a_e^2 = \left(\frac{dp}{d\rho}\right)_e,$$

(2.82)

we arrive at once at (2.79).

The integral momentum relation may also be written in a somewhat different form considering that

$$a_e^2 = \gamma R T_e, \qquad T_e\left(1 + \frac{\gamma-1}{2}M_e^2\right) = \text{const}$$

and, consequently,

$$\frac{U_e'}{U_e} = \frac{(M_e a_e)'}{M_e a_e} = \frac{M_e'}{M_e} + \frac{a_e'}{a_e} = \frac{M_e'}{M_e} + \frac{1}{2}\frac{T_e'}{T_e} =$$
$$= \frac{M_e'}{M_e} - \frac{(\gamma-1)M_e^2}{1+\frac{\gamma-1}{2}M_e^2} \cdot \frac{M_e'}{M_e} = \frac{1}{1+\frac{\gamma-1}{2}M_e^2} \cdot \frac{M_e'}{M_e}.$$

(2.83)

As a result we obtain

$$\frac{d\delta^{\bullet\bullet}}{dx} + \frac{M_e'}{M_e}\frac{2+H^{\bullet}-M_e^2}{1+\frac{\gamma-1}{2}M_e^2}\delta^{\bullet\bullet} + \frac{\delta^{\bullet\bullet}}{r_w^\nu}\frac{dr_w^\nu}{dx} = \frac{c_f}{2} + c_m.$$

(2.84)

Here

$$c_f = \frac{2\tau_w}{\rho_e U_e^2}$$

(2.85)

is the local friction coefficient, and

$$c_m = \frac{\rho_w v_w}{\rho_e U_e}$$

(2.86)

is the relative mass flow across the surface.

Integral energy relation. The energy Equation (2.56) will be transformed with the help of Equation (2.75) into

$$\frac{\partial}{\partial x}(\rho u H) + \frac{\partial}{\partial y}(\rho v H) + \rho u H \frac{1}{r_w^\nu}\frac{dr_w^\nu}{dx} = \frac{\partial}{\partial y}\Big[\Big(\frac{\mu}{Pr} + \frac{\varepsilon}{Pr_\tau}\Big)\frac{\partial H}{\partial y} +$$
$$+ \sum_i\Big[\frac{\mu}{Pr}(Le_i - 1) + \frac{\varepsilon}{Pr_\tau}(Le_\tau - 1)\Big]h_i\frac{\partial c_i}{\partial y} +$$
$$+ \Big[\mu\Big(1 - \frac{1}{Pr}\Big) + \varepsilon\Big(1 - \frac{1}{Pr_\tau}\Big)\Big]\frac{\partial}{\partial y}\Big(\frac{u^2}{2}\Big)\Big].$$

Noting that H_e = const, we shall write the equation of continuity as

$$\frac{\partial}{\partial x}(\rho u H_e) + \frac{\partial}{\partial y}(\rho v H_e) + \rho u H_e\frac{1}{r_w^\nu}\frac{dr_w^\nu}{dx} = 0.$$

Subtracting the preceding equation from the last one and integrating across the boundary layer with respect to y between zero and infinity, in view of the boundary conditions (2.73), we obtain

$$\frac{d}{dx}\int_0^\infty \rho u(H_e - H)\,dy - \rho_w v_w(H_e - H_w) +$$
$$+ \frac{1}{r_w^\nu}\frac{dr_w^\nu}{dx}\int_0^\infty \rho u(H_e - H)\,dy = q_w. \tag{2.87}$$

where

$$q_w = \Big(\frac{\mu}{Pr}\frac{\partial H}{\partial y} + \frac{\lambda}{c_p}\sum_i(Le_i - 1)h_i\frac{\partial c_i}{\partial y}\Big)_w \tag{2.88}$$

is the heat flux from the gas to the wall.

Introducing the integral thickness of the energy loss

$$\delta_H^{**} = \int_0^\infty \frac{\rho u}{\rho_e U_e}\Big(1 - \frac{H}{H_e}\Big)\,dy \tag{2.89}$$

in view of Equation (2.79), we obtain the integral energy relation in the following form:

$$\frac{d\delta_H^{**}}{dx} + \frac{U_e'}{U_e}(1 - M_e^2)\delta_H^{**} + \frac{(r_w^\nu)'}{r_w^\nu}\delta_H^{**} = \frac{q_w + \rho_w v_w(H_e - H_w)}{\rho_e U_e H_e}. \tag{2.90}$$

Introducing the dimensionless heat transfer coefficient (Stanton number), we have

$$c_h = \frac{q_w}{\rho_e U_e (H_r - h_w)},$$ (2.91)

where

$$H_r = h_e + r\frac{U_e^2}{2}$$ (2.92)

is the equilibrium enthalpy of the surface over which the flow occurs without heat transfer, and r is the recovery factor characterizing the nonadiabaticity of motion in the boundary layer. Using Equations (2.83) and (2.86), we bring the integral energy relation (2.90) to the following form:

$$\frac{d\delta_H^{**}}{dx} + \frac{M_e'}{M_e} \cdot \frac{1 - M_e^2}{1 + \frac{\gamma - 1}{2}M_e^2} \delta_H^{**} + \frac{(r_w^\nu)'}{r_w^\nu} \delta_H^{**} =$$

$$= c_h \frac{H_r - h_w}{H_e} + c_m\left(1 - \frac{h_w}{H_e}\right).$$ (2.93)

FOOTNOTES

Footnote (1) on page 41.   A detailed discussion of the methods of
                            computing various averages in the
                            theory of turbulence can be found in
                            the monograph by A. S. Monin and
                            A. M. Yaglom that was quoted above.

Footnote (2) on page 43.   A derivation of the average equations
                            of turbulent motion for a compressible
                            homogeneous gas was first given in the
                            paper: Van Driest, E.R. Turbulent
                            Boundary Layer in Compressible Fluids.
                            Journ. Aero. Sci., Vol. 18, No. 3,
                            1951, pp. 145-160.

Footnote (3) on page 45.   It should be noted that the operation
                            involving averaging the mass rate of
                            formation of the ith component w_i is

                            not written explicitly in this case,
                            since today, when using the averaged
                            equation of continuity of the ith
                            component in turbulent flow, wide use
                            is made of an approximation in which
                            $\bar{w}_i$ is understood to mean the expression

                            for (w_i) in which all variables are

                            time averages. The attempts to take
                            into account the fluctuating terms in
                            the expression for $\bar{w}_i$ lead to difficulties

                            that have not as yet been overcome.

Footnote (4) on page 50.   For the equation of state we use the
                            same approximation as for the mass rate
                            of formation of the ith component w_i

                            (see footnote 3 above).

Footnote (5) on page 51.   Concerning the turbulent Prandtl
                            number, see Section 15.

Footnote (6) on page 58.   For a derivation of the transformation
                            formulas, see the monograph by
                            L. G. Loytsyanskiy "Laminarnyy pogran-
                            ichnyy sloy" (Laminar Boundary Layer),
                            "Fizmatgiz", Moscow, 1962, p. 335.

Footnote (7) on page 61.   For a detailed exposition of Prandtl's
                            and Karman's theories see the monograph
                            by G. Schlichting, "Boundary Layer
                            Theory", "Nauka" Publishing House,
                            Moscow, 1969.

Footnote (8) on page 63.   This question will be considered in
                            detail in Chapter III.

REFERENCES

1) Reynolds O., On the dynamical theory of incompressible viscous fluids and the determination of the criterion, Phil. Trans. Roy. Soc., London 186 (1894); русский перевод в сб. «Проблемы турбулентности», ОНТИ, Москва, стр. 185—227, 1936.

*) Монин А. С., Яглом А. М., Статистическая гидромеханика, часть I, «Наука», Москва, 1965. См. также ранее цитированную книгу Л. Г. Лойцянского (сноска на стр. 32).

*) Лойцянский Л. Г., Гипотеза локальности в турбулентном движении жидкости при наличии вязкости, Прикл. матем. и мех., т. XXII, вып. 5 (1958).

CHAPTER III

TURBULENT BOUNDARY LAYER IN A HOMOGENEOUS GAS FLOW
AT SUPERSONIC VELOCITIES

§10. INTRODUCTION

In this chapter we are going to discuss the theoretical and experimental results of the studies dealing with characteristics of the turbulent boundary layer on a nonpermeable surface in a homogeneous gas flow at supersonic velocities. The homogeneity of the gas flow signifies essentially that no chemical reactions occur in the flow. A majority of the results presented here refer to flows in which the specific heat capacity of the gas may be considered to be constant.

The problem of turbulent boundary layer calculations for supersonic velocities and bodies of arbitrary shape is at the present time still far from completely being solved. As we know, the problem of the separation of the turbulent boundary layer, arising in a study of flows with large positive pressure gradients, does not have a satisfactory solution even for the case of an incompressible fluid. Therefore, existing methods of turbulent boundary layer calculations for supersonic velocities enable us to determine the skin friction and

heat transfer coefficients only for bodies of relatively simple shape
(plates, cones, neighborhood of the critical point of a blunt-nosed
body, etc.). The most significant results (experimental and theoreti-
cal) were obtained when studying the flow near a smooth flat plate
positioned along the flow.

The literature devoted to a computation of the drag coefficient
for a smooth flat plate contains a large number (several dozen) of
approaches. In accordance with the basic assumptions used by various
authors, we can distinguish three directions of research that coexist
at the present time.

The first of these is based on a generalization of the formulas
of the semi-emperical theories of turbulence (2.68) (Prandtl) and
(2.69) (Karman), obtained for an incompressible fluid to the case of
a gas moving at a large velocity. Methods used in this approach can
also be characterized as methods using the logarithmic velocity pro-
file.

The methods comprising the second approach characteristically
use a power-law velocity profile. Both the first and second approach
are a natural extension of the traditional methods of the theory of
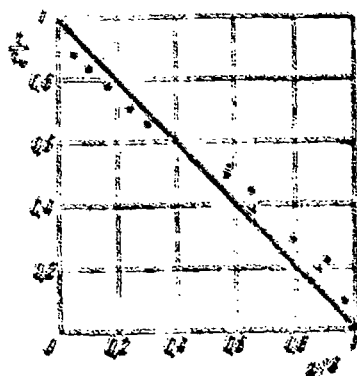turbulent boundary layer to incompressible fluids.

Figure 2

Finally, the third approach may
be called empirical. Its basic
feature is the fact that it uses for-
mulas which are formally identical
with the formulas for an incompres-
sible fluid and involve parameters
with values corresponding to the
so-called "defining" temperature,
selected in a certain fashion.

There also are methods which occupy an intermediate position among
the indicated directions of research.

A majority of papers belonging to the first approach make use of the assumption that the tangential friction stress τ is constant across the boundary layer and equal to its value at the wall, i.e.,

$$\tau = \text{const} = \tau_w. \tag{3.1}$$

In reality, as shown by experiments done by Klebanoff [1], in an incompressible turbulent boundary layer on a flat plate (Figure 2, circles signify the experimental points obtained by Klebanoff), the dependence of the turbulent friction stress on the lateral coordinate is nearly linear (straight line in Figure 2), and can be approximately described by the expression

$$\frac{\tau}{\tau_w} = 1 - \frac{y}{\delta}, \tag{3.2}$$

where δ is the thickness of the boundary layer.

Nevertheless, the assumption (3.1) does not introduce a significant error, as compared with (3.2), into the calculation of the integral characteristics of the boundary layer (friction, displacement thickness, momentum loss thickness, etc.). This becomes easy to see if we consider the momentum loss thickness δ** given by Equation (2.76). Writing this equation in the form

$$\delta^{**} = \int_0^\delta \frac{\tau}{\tau_w} \left(1 - \overline{u}_*\right)\left[\frac{d\overline{u}_*}{dy}\right]^{-1} du_*, \tag{3.3}$$

we note that it is the derivative du/dy that depends on the distribution of the tangential stresses across the boundary layer [this can be seen from Prandtl's and Karman's formulas (2.68) and (2.69)]. The maximum error introduced in it by assumption (3.1) will obviously occur near the external boundary of the boundary layer, where according to (3.1) τ = τ_w, whereas in fact τ → 0 or y → ∞. But in this case the derivative (du/dy)^{-1} is multiplied by a small quantity $(1 - u/U_e)$ (The quantity is small since u → U_e for y → ∞) which in the final analysis results in a small error in δ**. On the other hand, as will be shown

below, the friction coefficient at the wall is of $\sim (\ln \delta^{**})$. This also contributes to a reduction of the error made in the calculation because of the assumption (3.1).

To justify the assumption (3.1), we can also use the following simple arguments. Making use of the usual logarithmic velocity profile [2]

$$\frac{u}{v_*} = 2.5 \ln \left(\frac{y v_*}{\nu}\right) + 5.5, \quad v_* = \left(\frac{\tau_w}{\gamma}\right)^{\frac{1}{2}}, \tag{3.4}$$

it is easy to obtain from Equation (3.2) the following relationship between the friction stress in the boundary layer and the velocity:
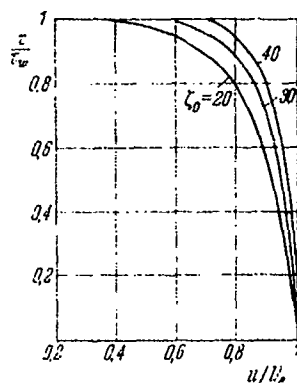
Figure 3

$$\frac{\tau}{\tau_w} = 1 - e^{-0.15\zeta_0(1-\bar{u})} \tag{3.5}$$

$$\zeta_0 = \frac{U_e}{v_*} = \sqrt{\frac{2}{c_{f0}}},$$

$$\bar{u} = \frac{u}{U_e}.$$

The results of the computation based on Equation (3.5) for three values of the friction parameters $\zeta_0 = 20$, 30, 40 are given in Figure 3. As we can see from Figure 3, for example, for $\zeta_0 = 30$ (this means that the Reynolds number is $\sim 10^7$) in the velocity interval $0 \leq \bar{u} \leq 0.8$ the friction stress varies within the range $0.9 \leq \tau/\tau_w \leq 1$ which justifies the use of (3.1) in practical calculations.

When using (3.1) from Prandtl's and Karman's formulas, (2.68) and (2.69), we can obtain the following expressions for the velocity profiles:

$$\eta = \frac{1}{C_1} \exp \varkappa \zeta \int \left(\frac{\rho}{\rho_w}\right)^{\frac{1}{2}} d\bar{u}, \tag{3.6}$$

$$\eta = C_3 + C_2 \zeta \int \exp \left[\varkappa \zeta \int \left(\frac{\rho}{\rho_w}\right)^{\frac{1}{2}} d\bar{u}\right] d\bar{u}. \tag{3.7}$$

Here

$$\eta = \frac{yv_*}{\nu_w}; \quad \varphi - \frac{u}{v_*}; \quad v_* = \left(\frac{\tau_w}{\rho_w}\right)^{1/2};$$
$$\zeta = \frac{U_e}{v_*} = \left(\frac{2}{c_f}\frac{\rho_w}{\rho_e}\right)^{1/2}; \quad \frac{\varphi}{\zeta} = \bar{u}; \quad c_f = \frac{2\tau_w}{\rho_e U_e^2};$$
(3.8)

C_1, C_2, C_3 are constants of integration; x is an empirical constant of turbulence whose value is usually set equal to its value for an incompressible fluid, i.e., $\kappa = 0.39 - 0.41$.

Equations (3.6) and (3.7) lead, respectively, to the following expressions for the momentum loss thicknesses (2.76):

$$\delta^{**} = \frac{\varkappa\zeta^2\mu_w}{\rho_e U_e C_1}\int_0^1\left(\frac{\rho}{\rho_w}\right)^{1/2}\bar{u}(1-\bar{u})\exp\left[\varkappa\zeta\int_0^1\left(\frac{\rho}{\rho_w}\right)^{1/2}d\bar{u}\right]d\bar{u},$$
(3.9)

$$\delta^{**} = \frac{\zeta^2\mu_w C_2}{\rho_e U_e}\int_0^1\frac{\rho}{\rho_w}\bar{u}(1-\bar{u})\exp\left[\varkappa\zeta\int_0^1\left(\frac{\rho}{\rho_w}\right)^{1/2}d\bar{u}\right]d\bar{u}.$$
(3.10)

The differences among studies using the first approach are usually contained in the assumptions regarding the constants of integration C_1, C_2, or regarding the expression for ρ/ρ_w, or finally regarding the methods used to evaluate the integrals in the expressions for the momentum loss thicknesses (3.9) and (3.10)[1].

The paper that started a wide use of the semi-empirical methods in the first approach was written by F. I. Frankl' and V. V. Voyshel' [3]. In this paper, the authors decided to follow the approach of a direct generalization of Karman's method [1]. Unfortunately, the degree of approximation used by Frankl' and Voyshel' [4] enabled them only to perform calculations for Mach numbers not much larger than unity.

The transition to large Mach numbers, apparently, would have required even more complicated computational techniques than those already used by the authors, or it might have required a direct use of numerical methods.

Footnote (1) appears on page 178.

After almost 25 years, the same approach to a generalization of Karman's formula (2.69) to the case of supersonic velocities was taken by Wilson [5], who had analyzed a flow over a thermally insulated plate.

A more general problem of the drag of a plate in a gas flow in the presence of heat transfer but using Prandtl's formula (2.68) was considered by Van Driest [6] almost simultaneously with Wilson. Later Van Driest [7] obtained the formula for friction on the basis of Karman's formula (2.69).

A method developed by V. M. Ievlev has become widely used in practice [8].

The semi-empirical methods have been further developed by I. P. Ginzburg and A. A. Shemets [9], L. Ye. Kalikhman [10], S. S. Kutateladze and A. I. Leont'ev [11], L. G. Loytsyanskiy and Yu. V. Lapin [12], L. M. Zysina-Molozhen and I. N. Soskova [13], and other authors.

Now we shall briefly characterize the methods of the turbulent boundary layer calculations which belong to the second approach. It must be noted that the theory of the isothermic turbulent boundary layer in an incompressible fluid, using a power-law velocity profile, is based on a well-known experimental fact first discovered by Blasius. In a turbulent flow in a straight circular tube, the variation of the velocity across the tube as a function of the distance from the wall and the friction stress at the wall as a function of the Reynolds number, calculated from the velocity on the axis U_a and the tube radius r_0, obey a power law

$$\frac{u}{U_a} = \left(\frac{r}{r_0}\right)^{1/n}, \quad c_f = \frac{A}{\left(\frac{U_a r_0}{\nu}\right)^m}. \tag{3.11}$$

A use of the power-law velocity profile for the case of external flow by an incompressible fluid made it possible to obtain a power-law dependence of the friction coefficient on the Reynolds number,

calculated in terms of the velocity of the oncoming flow and the length of the plate. The value of the exponent in the expression for the velocity profile

$$\frac{u}{U_e} = \left(\frac{y}{\delta}\right)^{1/n}.$$ (3.12)

where δ is the thickness of the boundary layer, is usually selected by demanding that the result agree with the experimental data. It is then explained that the exponent varies depending on the Reynolds number within a fairly wide range: $6 < n < 13$. This fact, however, is of no essential importance since — if other parameters do not affect the value of the exponent — it is always possible to choose the most satisfactory value of the exponent within the required range of the Reynolds number.

The situation is different for a compressible gas. In this case, the exponent is affected not only by the Reynolds number, but also by the Mach number and a temperature factor, which greatly complicates the selection of the correct value for the exponent. This means that some of the theories of turbulent boundary layer in a compressible gas, based on the power-law velocity profile [14], are satisfactory only within a relatively limited range of any given parameter $(Re_x, M_e, T_w/T_e)$.

Among methods that belong in the second approach, we shall mention, in particular, the method of the "effective length" proposed by V. S. Avduyevskiy [15]. The method is based on power-law velocity and enthalpy distributions in a boundary layer written in terms of the Dorodnitsyn variables, and on experimentally established formulas for the drag and heat transfer on a flat plate. A computation of the drag and heat transfer in a turbulent boundary layer of a compressible gas for moderate longitudinal pressure gradients reduces in the final analysis to a calculation using the formulas for a flat plate. Instead of the actual coordinate giving the position of a point on the surface of the body, they use a certain "effective length" which can be

calculated from integral conditions.

The third, so-called empirical, approach to the problem of a turbulent boundary layer in a compressible gas is essentially an attempt at extending the well-known relationships, obtained for incompressible fluids, to the case of a compressible gas by referring the physical parameters of a gas to a certain temperature, selected in some fashion. Thus, as early as in 1935, at the Volta Congress in Rome, Karman [16] proposed a formula for skin friction in a compressible gas flowing over a thermally insulated plate. The formula was set up without any theoretical justification by starting with a simplified assumption stating that it is possible to use the same formula for both large and small velocities, as long as the physical parameters are determined at the temperature of the wall. This formula for the mean friction coefficient has the form

$$\frac{0{,}242}{\sqrt{c_F}}\left(1+\frac{\gamma-1}{2}M_e^2\right)^{-\frac{1}{2}} = \lg(c_F\,\mathrm{Re}_L) - n\lg\left(1+\frac{\gamma-1}{2}M_e^2\right). \qquad (3.13)$$

A comparison of Karman's formula with experiment has shown that the use of the wall temperature as the defining temperature in a boundary layer results in an exaggerated effect of compressibility.

By now, many authors have proposed a large number of empirical formulas for the "defining" temperature. Some of them are given below:

$$\frac{T_{onp}}{T_e} = 1 + \frac{1}{2}\left(\frac{T_r}{T_e}-1\right) \quad \left[T_r = T_e\left(1+r\frac{\gamma-1}{2}M_e^2\right)\right];$$

$$\frac{T_{onp}}{T_e} = 0{,}42 + 0{,}032M_e^2 + 0{,}58\frac{T_w}{T_e} \quad \text{for} \quad M_e < 5{,}5\,^3);$$

$$\frac{T_{onp}}{T_e} = 0{,}70 + 0{,}023M_e^2 + 0{,}58\frac{T_w}{T_e} \quad \text{for} \quad M_e > 5{,}5\,^4).$$

It should be noted that the last two formulas for the defining temperature were obtained from an analysis of the numerical solutions of the equations of a laminar boundary layer. Even though these expressions are used when calculating friction in a turbulent boundary

layer, one should nevertheless keep this circumstance in mind. A
computation using these formulas gives understated values of the
friction coefficient.

A method which is different from others, but still essentially
empirical, was developed by Spalding and Chi [2]. A comparison of
various methods of calculating friction in a turbulent boundary layer
on a flat plate with the existing experimental data, done by Spalding
and Chi in their paper, has shown that the most accurate methods are
those proposed by Wilson, Van Driest [3] (method based on Karman's
formula), Kutateladze and Leont'yev [4], Spalding and Chi.

Taking this into account, Section 12 will describe the semi-
empirical method of calculation, leading in the case of a thermally
insulated plate to Wilson's results and in the case of a flow with
heat transfer, to Van Driest's results. At the same time, we shall
briefly present Spalding and Chi's method (Section 13) which to a cer-
tain extent uses the results of the semi-empirical method. The
simplicity and high accuracy of this method make it very convenient
for engineering calculations.

§11. Experimental Studies of a Turbulent Boundary
Layer in Supersonic Flows (Friction and Velocity Profiles)

Among the numerous problems of experimental aerodynamics, the
problem of determining the turbulent skin friction has been for many
years one of the most urgent and widely studied problems. Without
presenting the experimental results regarding the characteristics of
the turbulent boundary layer in an incompressible fluid, we shall
limit ourselves here to the most important and interesting experimental
results concerning the velocity profiles and skin friction in a

---

Footnote (2) appears on page 178.
Footnote (3) appears on page 178.
Footnote (4) appears on page 178.

turbulent boundary layer of a compressible gas, both on thermally insulated surfaces and on surfaces that can exchange heat with the flowing gas. A majority of the results described below were obtained from 1950 on. It should be noted that the experimental results available today are far from complete. This is particularly true regarding data on the velocity profiles in a boundary layer.

Among papers dealing with the characteristics of the boundary layer on thermally insulated surfaces, we shall consider those by Wilson, Chapman and Kester, Coles, Korkegi, Matting et al., Moor and Harkness. Among papers dealing with surfaces with heat exchange, we shall consider those by Lobb et al., Hill, Sommer and Short, Winkler, Kozlov. The results obtained by other authors will be included in the resultant plots.

Experimental Studies Using Thermally Insulated Surfaces

Wilson's experiments [5]. At certain sections of the boundary later on a thermally insulated flat plate, Wilson measured the velocity
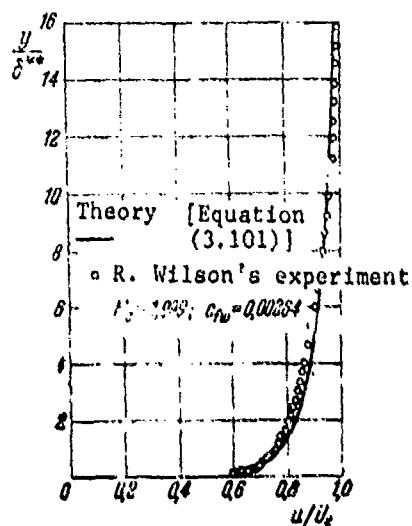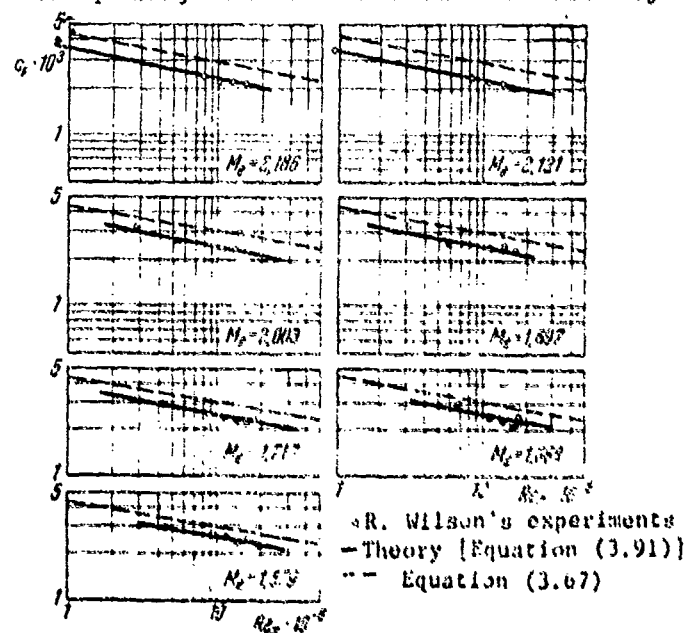

Figure 4

Footnote (5) appears on page 178.

profiles using the Pitot tube. The numbers M_e and Re_x were varied in the experiments within the following ranges:

$$1,579 \leqslant M_e \leqslant 2,186;$$
$$2,2 \leqslant Re_x \cdot 10^{-6} \leqslant 19.$$

As an example, Figure 4 shows the velocity profile for $M_e = 1.999$ (circles signify experimental points; the solid line will be explained below in Section 12). Using the velocity profiles, Wilson determined the momentum loss thickness δ^{**}, and then computed the mean friction coefficient [see Equations (2.76) and (3.64)]. The values of the mean friction coefficients thus found are plotted in Figure 5.

Chapman and Kester's experiments [20]. The measurements of the mean friction coefficient c_F were made on the surface of a long cylindrical body of revolution at subsonic and supersonic flow velocities for the following range of M_e and Re_x: $0.61 \leq M_e \leq 3.60$; $4 \leq Re_x \cdot 10^{-6} \leq 32$. The skin friction force was determined directly by means of tests on two models (models are sketched in Figure 6). The experiments measured the difference between the total drag and wake drag, respectively, for each model of the cone-cylinder and the cone: $(Q_1 - Q_{D1})$ and $(Q_2 - Q_{D2})$.

Transition wire

First model   Housing

Second model
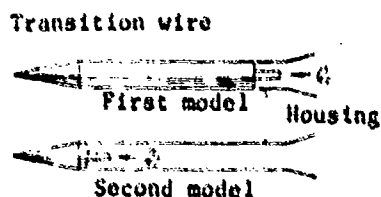
Figure 6

The difference between these two values gives the friction force acting on the surface of the cylinder:

$$F = (Q_1 - Q_{D1}) - (Q_2 - Q_{D2}).$$

The results are shown in Table 1. The value of the mean friction coefficient in an incompressible fluid (c_{F0})exp by which friction coefficients, measured for various values of M_e, were divided was determined experimentally. In the lower row of the table, the same coefficients were divided by the mean friction

coefficient c_{F0} calculated using Karman's formula (3.59).

TABLE 1

M_e	0.51	0.81	1.99	2.49	2.95	3.36	3.60
$c_F/(c_{F0})$exp	0.985	0.929	0.746	0.671	0.623	0.578	0.551
c_F/c_{F0}	0.994	0.924	0.757	0.672	0.630	0.571	0.552

Experimental values of the friction coefficient c_F are plotted in Figure 7 as functions of the Re_x number for various values of M_e. The
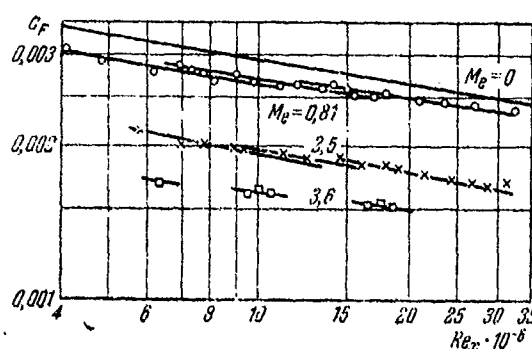

values of the friction coefficient c_{F0} for $M_e = 0$ were found using Karman's formula (3.59). As can be seen in Figure 7, the plots corresponding to various values of M_e are parallel to the curve for $M_e = 0$, which means that the ratio c_F/c_{F0} does not depend on Re_x in the range of Re_x investigated. The layer structure of the experimental data for the same value of M_e is due to the use of cylinders of various lengths (the experiments used cylinders for which the ratio of the length to the diameter was $l/d = 8$, 13, and 23).

Figure 7

Coles' experiments [21]. Coles experimentally determined the values of the local and mean skin friction. Local friction was measured directly by means of a "floating" element built into the surface of a plate placed in the test section of a supersonic aerodynamic tunnel. Mean friction was determined from the momentum loss thickness δ^{**} [Equation (2.76)]. M_e in the experiments ranged from $M_e = 2$ to $M_e = 4.5$, and the Reynolds number — from $3 \cdot 10^6$ to $9 \cdot 10^6$. The experimental results are listed in Table 2.

TABLE 2

M_e	2,57	2,58	3,70	3,70	4,51	4,55	4,50	4,54
$\frac{U_e x}{v_e} \cdot 10^{-6}$	4,84	8,32	3,54	7,25	3,52	6,83	3,37	6,91
$c_f \cdot 10^3$	1,81	1,66	1,62	1,38	1,48	1,22	1,55	1,26
c_f/c_{f_0}	0,705	0,700	0,595	0,570	0,530	0,500	0,535	0,495
c_F/c_{F_0}	0,715	0,710	0,635	0,610	0,590	0,560	0,600	0,560

Korkegi's experiments [22]. The local friction on a flat plate was measured by means of a "floating" element, similar to Coles' studies. M_e was held constant during the experiment (M_e = 5.8), and the Reynolds number, calculated from the parameters on the outer boundary of the boundary layer and the distance from the "floating" element to the front edge of the plate, was varied from 10^6 to 4×10^6. Along with friction, Korkegi also measured the velocity and temperature profiles which were then used to calculate the integral boundary layer thicknesses δ* and δ**, and the parameter H* = δ*/δ**. The experimental results are listed in Table 3.

TABLE 3

M_e	Re**	δ**,δ	δ*,δ	H*	$c_f \cdot 10^3$	(c_f/c_{f_0})Re**	c_f/c_{f_0}
5,787	2477	0,0375	0,520	14,10	1,316	0,403	0,467
5,770	2780	0,0361	0,510	11,38	1,275	0,400	0,463
5,702	3120	0,0357	0,501	15, ..	1,223	0,400	0,463
5,803	401	0,0385	0,501	15,73	1,170	0,317	0,462

In Table 3 in the next to the last column, the ratio c_f/c_{f0} was calculated for a constant value of Re**, i.e., c_{f0} was determined for the same value of Re** as c_f. The ratio c_f/c_{f0} in the last column of Table 3 was computed for

$$\text{Re}_x - \text{const} \qquad (5 \leqslant \text{Re}_x \cdot 10^6 \leqslant 6).$$

The Matting, Chapman, Nyholm, and Thomas experiments [23]. These four authors have performed an extensive and thorough experimental investigation of the turbulent boundary layer on a thermally insulated surface in the absence of a longitudinal pressure gradient. The experiments yielded data on the local friction and velocity profiles for Mach numbers ranging from 0.2 to 9.9 and Reynolds numbers ranging from $2 \cdot 10^6$ to $100 \cdot 10^6$. The working substance for $0.2 \leq M_e \leq 4.2$ was the air, and for $4.2 \leq M_e \leq 9.9$ — helium. Since the adiabatic exponents (ratio of the specific heat capacities at constant pressure and volume) $\gamma = c_p/c_v$ for the air and helium differ significantly from each other ($\gamma_{air} = 1.4$, $\gamma_{He} = 1.66$), the similitude parameter was of the form $(\gamma - 1) M_e^2$. In this case, the experimental results obtained in a helium stream for $(M_e)_{He}$ will be equivalent to the results obtained in an air stream for

$$(M_e)_{air} = (M_e)_{He} \sqrt{\frac{\gamma_{He}-1}{\gamma_{air}-1}} \approx 1.29 (M_e)_{He}.$$

The validity of this relation was confirmed by experiments. In particular, Figure 8 shows the velocity profile in the air ($M_e = 4.2$) and in helium ($M_e = 3.25$) for the same Reynolds number $Re_x = 6.2 \times 10^6$ in the upper drawing and $Re_x = 35 \cdot 10^6$ in the lower one. The velocity profiles determined for various gases are in very good agreement.

The results of the velocity measurements in the boundary layer for various values of $(M_e)_{air}$ are presented in Figure 9. The axes measure the universal coordinates ϕ and η [see Equations (3.8)]. As we can see from Figure 9, in the turbulent core, the Mach number has hardly any effect on the form of the universal profile, which as before is described well by a logarithmic formula. As we approach the wall (in the laminar sublayer), we observe a large scatter of the experimental points and their displacement upward from the curve $\phi = \eta$. In the author's opinion, measurements near the wall are not reliable. An estimate of the laminar sublayer thickness using the experimental data shows that the thickness increases with M_e. For $(M_e)_{air} = 3.4$, it amounts to 10% of the thickness of the entire boundary layer.
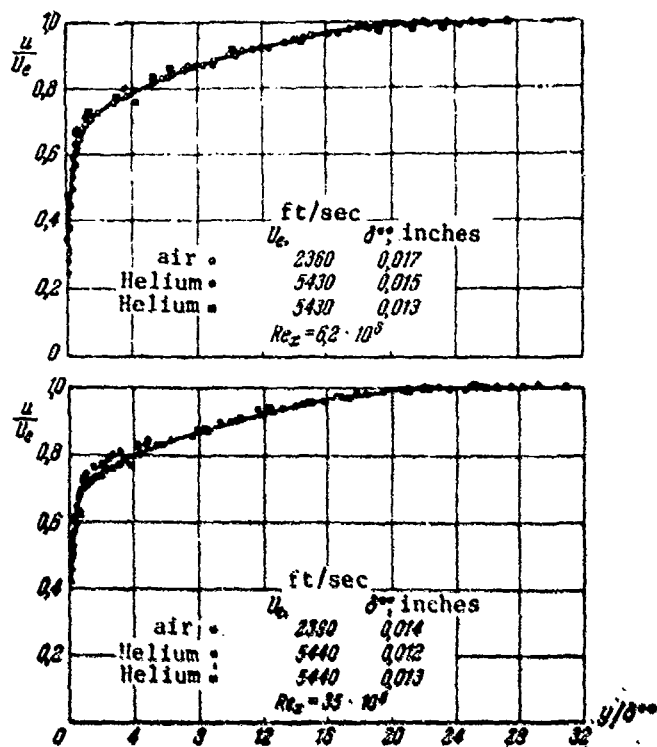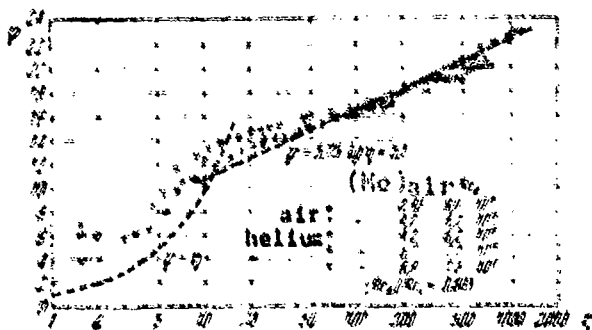
Figure 8

Figure 9

Along with the measurements of the velocity profiles, the authors also measured the local skin friction with the aid of a floating element. The results of these measurements are shown in Figures 10 and 11. As can be seen from Figure 11, the Reynolds number does not affect
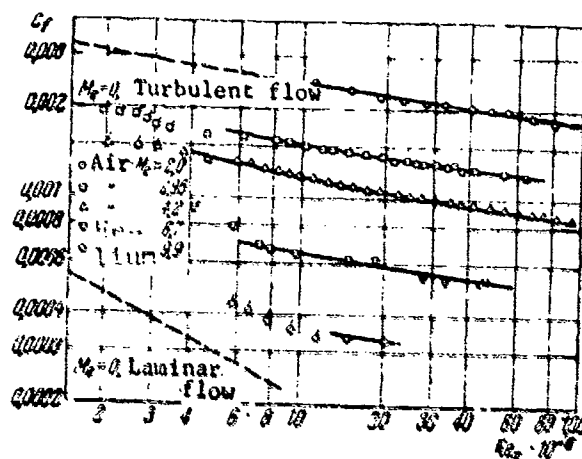
Figure 10
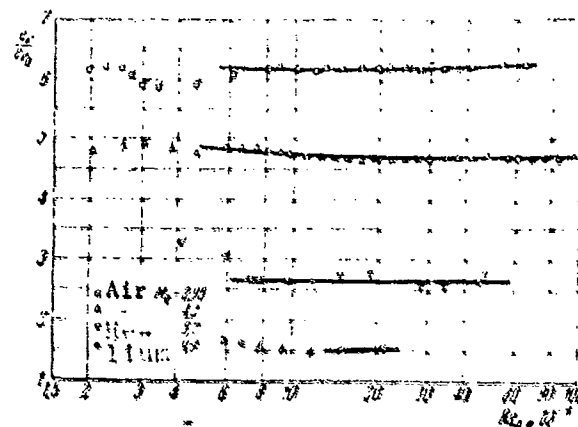
Figure 11

the ratio c_f/c_{f0} in the range investigated. In Figures 10 and 11 "flags" indicate the experimental points obtained for small Reynolds numbers $[(Re_x/Re_L) < 0.6]$ (L is the length of the plate). The authors encountered difficulties when attempting to measure accurately the friction at these points. The difficulties were due to insufficient development of turbulent flow for $(Re_x/Re_L) < 0.6$.

The Moore and Harkness experiments [24]. The paper contains the results of measurements of local friction and velocity profiles on a thermally insulated surface for $M_0 = 2.8$. The distinguishing feature of these measurements is the fact that they encompass a region of very large Reynolds numbers, up to $Re_x = 1.41 \times 10^9$. The local friction was measured by means of a floating element. The results of measuring friction on the wall of a supersonic diffuser section of a wind tunnel are given in Table 4.

TABLE 4

M_e	T_e, °K	δ^{**}, мм	δ^*, мм	δ, мм	$Re^{**} \cdot 10^{-4}$	$Re_x \cdot 10^{-6}$	c_f
2,831	298	1,86	22,7	101,0	4,24	8,27	0,000300
2,843	292	1,61	21,4	116,9	3,26	6,11	0,000953
2,865	2 15	5,01	21,0	101,9	2,12	3,76	0,000958
2,897	249	5,82	23,1	114,6	1,82	3,18	0,001020
2,747	316	6,79	30,8	139,2	5,57	11,2	0,000349
2,901	3'7	6,76	31,1	144,2	4,16	8,73	0,000374
2,824	311	7,04	32,5	140,5	2,79	5,12	0,000346
2,639	305	8,11	34,7	153,5	7,02	14,1	0,000362
2,693	300	8,31	36,0	139,5	5,95	11,8	0,000391

Experimental Investigations with Heat Exchange
Between a Gas and a Surface of Bodies

Lobb, Winkler, and Persch experiments [25]. The papers discussed
in the preceding portion of this section were devoted mainly to the
investigation of skin friction on thermally insulated surfaces, and
yielded relatively little information about characteristics of the
turbulent boundary layer such as velocity and temperature profiles,
laminar sublayer thickness, etc.

The paper written by these three authors is one of those rare
papers in which a determination is made not only of friction, but also
of the indicated characteristics of the turbulent boundary layer. The
investigations of the boundary layer were made on the wall of a flat
nozzle in a supersonic wind tunnel, with a small pressure gradient in
the section under investigation. Local friction was determined from
the velocity gradient near the wall, as well as through the Reynolds
similitude from the measurements of thermal fluxes in the section
investigated.

The results of measurements of local friction and a characteristic
of flow regimes in which the measurements were made are given in
Table 5.

TABLE 5

M_e	4.5?	5.01	5.05	5.66	6.83	6.75	6.55	6.75	7.07
$(T_r - T_w)/T_r$	0	1.23	2.07	2.36	3.05	4.05	4.16	4.63	5.65
Re**	5350	6480	7950	7370	8550	8460	12040	7960	8130
$(c_f/c_{f0})_{Re**}$	0.372	0.3.25	0.3416	0.3517	0.252	0.242	0.233	0.250	—
$c_f \cdot 10^3$	1.11	1.10	0.907	0.930	0.640	0.656	0.590	0.690	—

The value of c_{f0} was found for the same values of Re** for which c_f were measured, using Karman's formula

$$c_{f0} = \frac{0.02932}{\lg(2\,Re^{**})\left[\frac{1}{2}\lg(2\,Re^{**}) + 0.433\right]}. \tag{3.14}$$

The Re** number, calculated from the momentum loss thickness, was chosen as the characteristic Reynolds number due to difficulties that were involved in determining the beginning of the boundary layer on the wall of the tunnel, and due to the fact that it was impossible to use the Re_x number calculated in terms of the length. The dependence of $(c_f/c_{f0})_{Re**}$ on the temperature factor $(T_r - T_w)/T_e$ (T_r is the recovery temperature) is also shown in (Figure 12). As can be seen from the plot, the ratio $(c_f/c_{f0})_{Re**}$ depends slightly on heat exchange.
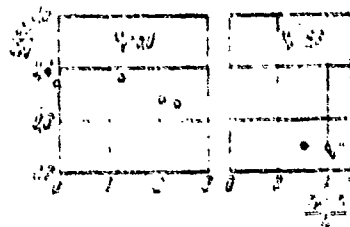
Figure 12

Of greatest interest in the paper under consideration are measurements of the velocity profiles in the boundary layer.

Figure 13 shows the velocity profile for M_e = 6.8 and two values of the heat exchange factor (the largest and the smallest for the given Mach number M_e). In order to show the difference between the velocity profiles, the distance in millimeters was plotted in the figure on the horizontal axis. As can be seen from Figure 13, the velocity profiles in the turbulent core change very little with the heat exchange factor, whereas the curvature

Figure 13

of the curve in the laminar sub-layer increases with an increase in heat exchange.

The same velocity profiles as well as profiles for $M_e = 5$, represented in terms of the universal variables ϕ and η in Figures 14 and 15, exhibit a considerable displacement upward of the curves in the turbulent core of the layer when the heat exchange factor increases.

Figure 14

Figure 15

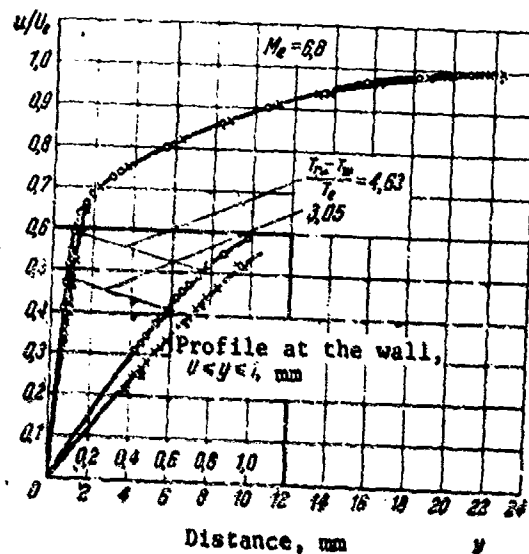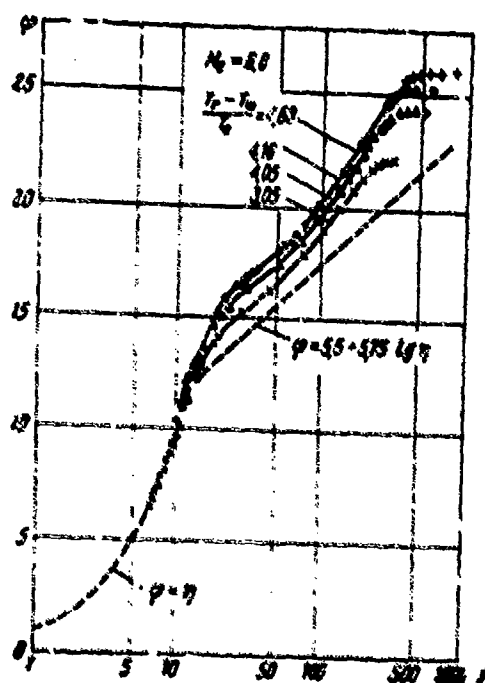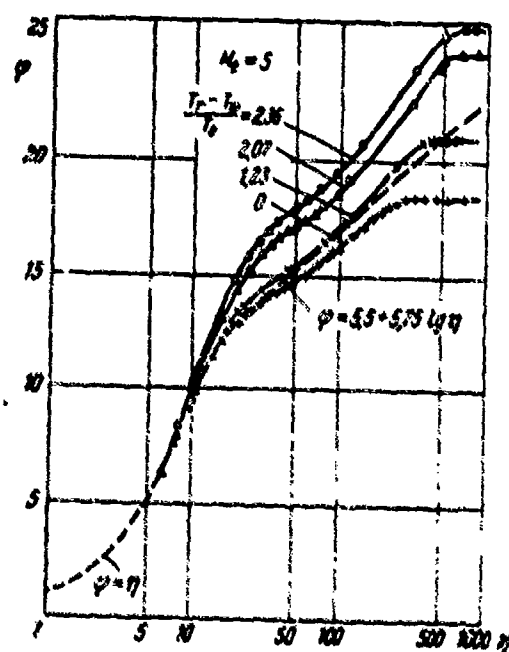The velocity profile in the laminar sublayer for all values of the heat exchange factor is well described by the equality $\phi = \eta$. However, the thickness of the sublayer, as seen in Figure 14 and Figure 15, increases with an increase of the heat exchange factor. The value of the parameters η_l which determines the thickness of the laminar sublayer and plays an important role in the turbulent boundary layer theory, turns out to be equal to its corresponding value for incompressible fluids ($\eta_l = 11.9 = \alpha$) only if there is no heat exchange [see in Figure 15 the curve for $M_e = 5$; $(T_{i \cdot} - T_w)/T_e = 0$].
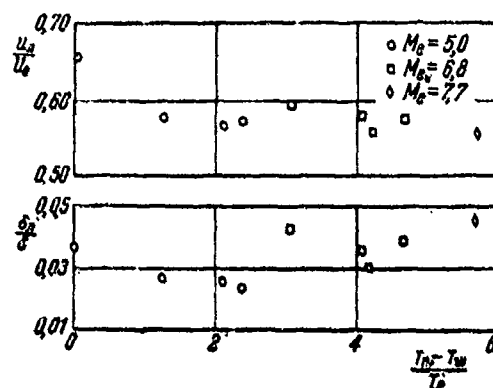
Figure 16

The results of the measurement of the laminar sublayer thickness and the velocity on its boundary are given in Figure 16. Although the scatter of points is quite significant (partly this is due to the difference in the Reynolds numbers), nevertheless it is permissible to draw the conclusion that, with an increase in the heat exchange, the relative velocities on the boundary of the laminar sublayer and the sublayer thickness decrease. The same figure shows that, when the M_e number increases from 5 to 6.8, the thickness of the laminar sublayer in the boundary layer increases approximately by a factor of 2.

Hill's experiments [26]. The experiments were made with a conical nozzle with the M_e number at the exit equal to 9.1. At several sections of the nozzle, the Pitot tube and a thermocouple were used to measure the velocity and temperature profiles in the boundary layer. The conditions in the nozzle differed somewhat from the conditions of flow on a flat plate, since the walls of the nozzle were tilted to its axis at the angle of 6°, and there was a small negative longitudinal pressure gradient.

The magnitude of local friction was determined from the slope of the velocity profiles near the wall by means of the formula $\tau_w = \left(\mu \frac{\partial u}{\partial y}\right)_w$. The overall data on skin friction are listed in Table 6 (where c_f is the coefficient of friction calculated in terms of the parameters of the oncoming flow).

TABLE 6

M_e	T_w/T_e	Re^{**}	$c_f \cdot 10^4$	$(c_f/c_{f0})Re^{**}$
8,99	7,68	1245	7,899	0,197
9,04	7,97	1607	8,910	0,235
9,07	8,28	1908	8,505	0,234
9,10	8,69	2287	8,000	0,227
8,22	7,17	2081	9,240	0,257
8,25	7,26	2498	9,102	0,265
8,27	7,34	2885	8,695	0,259
8,29	7,37	3202	8,202	0,247
8,29	7,41	3451	7,709	0,239

In the last column of Table 6, the friction coefficient c_f was divided by the friction coefficient c_{f0} calculated according to Karman's formula (3.14) for the values of the Reynolds numbers Re^{**} given in the Table.

When comparing the experimental data on friction with theoretical calculations, one must keep in mind that, according to an estimate given by Hill, the experimental values of the friction coefficient may exceed by 20% the friction coefficient on a flat plate due to the effect of the negative pressure gradient.

The results of measurements of the velocity profiles in various sections of the boundary layer in the nozzle are given in Figure 17, where the universal coordinate ϕ and η were plotted on the axes. As can be seen from the figure, in the laminar sublayer ($\lg \eta < 1.1$), the experimental points are distributed near the curve $\phi = \eta$ (solid line). In the turbulent core, the experimental points are located practically
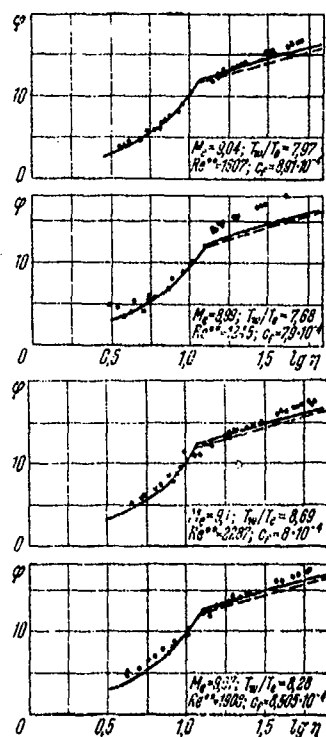
Figure 17

along a straight line, which is displaced upward from the dotted line constructed according to Equation (3.4) for the velocity profile in an incompressible fluid (the solid line in the turbulent core will be explained in Section 12). Among the given velocity profiles, the profile for $M_e = 8.99$ differs considerably from the profiles for other values of the Mach number. The reason, as noted by Hill, is that the section in question was located in a region of an insufficiently developed turbulence. Among other peculiarities of the velocity profiles, we should note the thickening of the laminar sublayer. According to Hill's data, the laminar sublayer for $M_e = 9$ occupies about 15% of the thickness of the boundary layer.

The Sommer and Short experiments [27]. Free-flight determination of friction was made measuring drag on hollow cylindrical models shot through a supersonic wind tunnel. Here the numbers $M_e = 2.8$ and 3.9 were obtained when shooting through stationary air, and the number $M_e = 7.2$ was achieved when shooting against an air stream moving at the velocity $M_e = 2$. The number $M_e = 5.6$ was obtained using models with a faired leading edge which lowered the Mach number from $M_e = 7$ to 5.6 on the outer boundary of the boundary layer. The drag was calculated from the deceleration of the models, which was in turn determined on the basis of chronograph readings and shadow photographs.

A turbulent boundary layer was produced using vortex generators in the form of threaded cuts on the outer and inner surfaces of the

model. To account for the thickening of the boundary layer and the additional drag caused by the turbulence-producing threading, the so-called "effective" Reynolds number was calculated (in Table 7, Re_{eff}), from which the friction coefficient for an incompressible fluid, c_{f0}, was determined. Without going into details of how Re_{eff} was calculated, we will only mention that this Reynolds number was constructed from the length of the turbulent boundary layer necessary for the formation of the momentum loss thickness which would be obtained if the additional drag, caused by the vortex generator, were attributed only to the friction in the boundary layer.

The results of the measurements of the friction coefficient are given in Table 7. The values of the friction coefficients for incompressible fluids were determined using Karman's formula (3.59).

TABLE 7[1]

M_e	T_w/T_e	$Re_{\varphi\varphi\varphi} \cdot 10^{-4}$	$Re_c \cdot 10^{-4}$	c_f	c_f/c_{f0}
2,81	1,03	62,3	3,00	0,00284	0,867
3,82	1,05	84,0	4,07	0,00237	0,730
5,63	1,29	72,0	4,71	0,00170	0,562
6,60	1,60	82,0	4,06--6,01	0,00125	0,401--0,451
7,00	1,75	123,5	6,06--9,02	0,00115	0,395--0,446
3,78	1,05	84,0	4,02	0,00201	0,604
3,67	1,05	78,5	3,73	0,00240	0,724

[1] In this table, Re_c is the Reynolds number constructed from the parameters of the oncoming flow and the length measured from the beginning of the formation of the turbulent boundary layer.

Winkler's experiments [28]. An investigation was made of the characteristics of the turbulent boundary layer on a cooled flat plate for M_e = 5.2 and three values of the temperature factor. Measurements in the boundary layer were made using full-pressure nozzles (Pitot tubes) and thermocouples. The friction stress on the walls τ_w was determined in parallel using two methods: from the slope of the

velocity profile at the wall $\tau_w = \mu_w (\partial u / \partial y)_w$ and from the measured values of the thermal flux from the gas to the wall using the relationship, proposed by Kol'bern, between friction and heat transfer $c_f = 2c_h Pr^{2/3}$, where c_h is the heat loss coefficient (so-called generalized Reynolds similitude).

The results of the friction measurements using the two methods are given in Table 8 (here T_e^* is the deceleration temperatures; c_f is the friction coefficient constructed from the parameters of the on-coming flow; Re_x is the Reynolds number constructed from the parameters of the oncoming flow). As seen in the table, the values obtained using the two different methods coincide in a majority of cases to within $\pm 4\%$. At the same time it should be noted that Winkler's data on the

TABLE 8

$c_f \cdot 10^2 \rho$ (1)	$c_f \cdot 10^2 \rho$ (2)	M_e	T_w / T_e^*	$Re_x \cdot 10^{-6}$	Re^{**}	λ^{**}, мм	δ^*, мм	$c_f \cdot 10^4$ (1)	$c_f \cdot 10^4$ (2)
0,187	0,194	5,21	0,801	2,72	20,0	0,166	1,66	11,65	11,87
0,184	--	5,15	0,875	3,36	2835	0,149	1,57	13,63	--
0,500	0,178	5,20	0,810	4,07	3173	0,238	2,46	11,32	13,18
0,185	0,192	5,36	0,815	5,01	3890	0,241	2,86	13,16	13,13
0,192	0,180	5,31	0,815	5,01	4300	0,332	4,00	13,04	12,78
0,133	0,136	1,05	0,757	2,29	1990	0,170	1,66	13,33	13,18
0,530	--	5,18	0,711	2,54	1742	0,119	1,33	10,60	--
0,137	0,107	5,20	0,733	3,81	2850	0,227	2,31	12,48	11,63
0,111	0,121	5,21	0,773	4,55	3155	0,280	3,23	11,51	11,76
--	0,340	5,31	0,765	5,11	3740	0,330	3,86	--	10,63
0,117	0,351	5,17	0,663	3,01	1035	0,111	1,23	11,07	15,17
0,131	0,370	5,16	0,546	2,57	1632	0,188	3,05	13,23	13,33
0,112	--	5,10	0,574	2,75	1735	0,181	1,93	13,35	--
0,422	0,436	5,11	0,565	3,37	2184	0,241	3,81	12,36	12,75
0,430	--	5,20	0,549	3,57	2182	0,268	3,74	13,03	--
0,375	0,343	5,14	0,605	4,22	3250	0,313	3,71	10,51	10,73

effect of the temperature factor on friction are in disagreement with the results of the calculations and the experimental data provided by other authors. The results of the velocity profile measurements in the boundary layer for $M_e = 5.2$ and three values of the temperature factor are given in Figure 18. An approximate calculation of the laminar sublayer thickness using the data of the figure shows that the
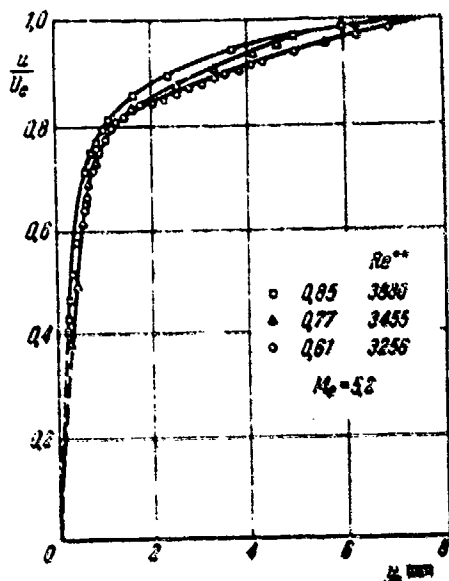
Figure 18

laminar sublayer occupies about 9% of the thickness of the entire boundary layer.

L. V. Kozlov's experiments [29]. A technique involving a floating element was used to measure local friction on a flat plate in a supersonic flow with intensive heat transfer between the flow and the wall. The mach number of the oncoming flow in the experiments was equal to 2.9. The Reynolds number varied within the intervals $1.5 \leq Re_x \cdot 10^{-7} \leq 2.5$. On the basis of the analysis of experimental data, the author recommends the following empirical formula for the friction coefficient:

$$c_{fw} = \frac{2\tau_w}{\rho_e U_e^2} = 0.055 Re_{xw}^{\ldots} \left(\frac{T_w}{T_e}\right)^{\ldots} \left(\frac{T_r}{T_e}\right)^{\ldots}. \tag{3.15}$$

where $Re_{xw} = \frac{\rho_e U_e x}{\mu_w}$, $T_r = T_e\left(1 + r\frac{k-1}{2} M_e^2\right)$, $r = 0.89$.

The author notes that the mean square deviation of the experimental points from the curve calculated using formula 3.15 was $\pm 5\%$ within the experimental range of the Reynolds number and the temperature factor.

Some comments regarding the results of the experimental investigations of the turbulent boundary layer at supersonic velocities. The results of the velocity profile measurements for various values of the Mach number of the oncoming flow and the temperature factor, given in the present section in Figures 8, 13-15, 17, indicate that in a laminar sublayer the velocity profiles can be satisfactorily described by the linear relationship $\phi = \eta$.
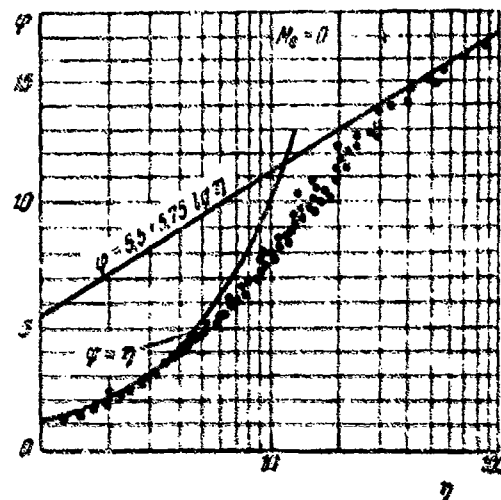
Figure 19
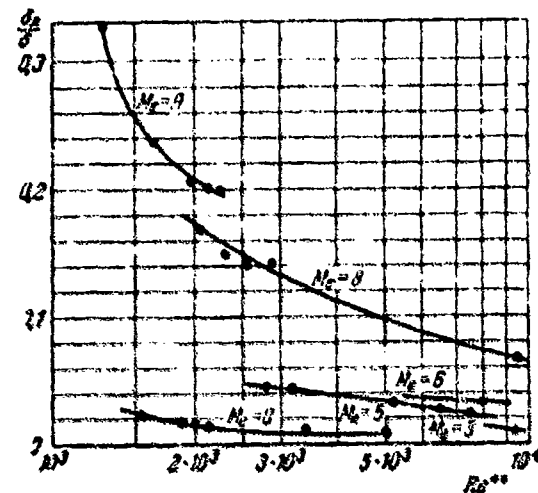
Figure 20

In the turbulent core, the velocity profile is logarithmic
(Figures 9, 17). In the case of a thermally insulated surface, the
profile slope (Figure 9) turns out to be the same as for an incompres-
sible fluid. In the presence of heat transfer (Figure 17), the slope
of the velocity profile in this region turns out to be greater than
for an incompressible fluid (one must, however, keep in mind that in
Hill's experiments in Figure 17, the increase in the slope of the pro-
file can be explained partially as being due to the effect of the
negative pressure gradient). An increase in the intensity of heat
transfer between a gas and the wall may lead, as can be seen in Figures
14 and 15, to a change in the slope of the velocity profile (the
deformation of the profile at the junction of the laminar sublayer
and the turbulent core may be explained as being caused by the pres-
sure gradient, since the experiments were made on the surface of a
flat nozzle).

A comparison of the velocity profiles for large Mach numbers
(Figure 17) and for an incompressible fluid (Figure 19, dots signify
the experimental data obtained by Nikuradse [30]) shows that for large
Mach numbers, the transitional (buffer) zone between the laminar

sublayer and the turbulent core is considerably reduced. If for an incompressible fluid, the buffer zone begins at $\eta = 5$ and ends at $\eta = 30 - 50$, then for large Mach numbers (for example, Hill's experiments) the buffer zone almost completely disintegrates and the transition from the laminar sublayer to the turbulent core is a sharp one. This justifies the use of the double layer Prandtl scheme in the theory of the turbulent boundary layer for large supersonic velocities.

Another important feature of the velocity profiles in supersonic flows is the increase in thickness of the laminar sublayer with an increase in the Mach number. The change of the relative thickness of the laminar sublayer with an increase in the Mach number for various Reynolds numbers may be judged using Figure 20 (this figure contains the experimental data obtained by Hill, Lobb, Winkler, and Persch, as well as by Ye. U. Repik). As can be seen from the figure, for an incompressible fluid, the thickness of the laminar sublayer does not exceed 3% of the thickness of the entire layer δ. For $M_e = 9$ δ_l, it may occupy 30% and more of the total layer thickness, where the rate of increase of the relative thickness of the laminar sublayer increases with increase in the Mach number. A decrease in the Reynolds number Re^{**} also leads to an increase in δ_l/δ.
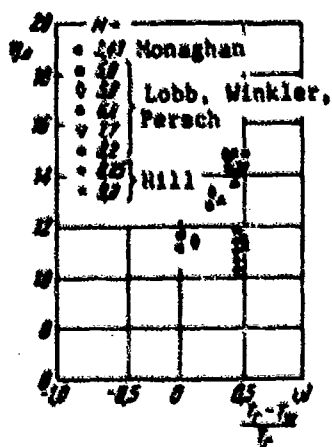

Figure 21

Figure 21 shows the data obtained by Lobb et al., Hill, Monaghan [31] on the universal coordinate η on the boundary of the laminar sublayer, denoted by η_l. As can be seen in Figure 21, the experimental evidence available today is insufficient to provide a numerical estimate of the effect of a certain factor on the value of this parameter.

This fact explains why, in a majority of the existing theories of the turbulent boundary layer in a compressible gas, the value of n_l is set equal to its value in an incompressible fluid, i.e.,

$$n_l = \alpha = 10.8 - 12.5^{(6)}$$

§12. Semiempirical Method of Calculation of Friction on a Flat Plate [32]

Let us consider flow over a smooth impermeable plate of a supersonic gas stream (Figure 22). If the plate is oriented at zero angle of attack (Figure 22, a), then the velocity on the outer boundary of the boundary layer will be constant and equal to the velocity of the oncoming flow at infinity: $U_e = U_\infty^{(7)}$. When the flow is over a plate at the angle of attack (or a wedge) with an associated discontinuity on the lower surface and a fan of rarefaction waves on the upper surface (Figure 22, b), the velocity on the outer boundary of the boundary layer will also be constant and equal to the velocity behind the discontinuity or the fan of rarefaction, respectively. The magnitude of the velocity behind the associated oblique shock wave and the fan of the rarefaction waves can be determined using well known gasdynamic relations [33].
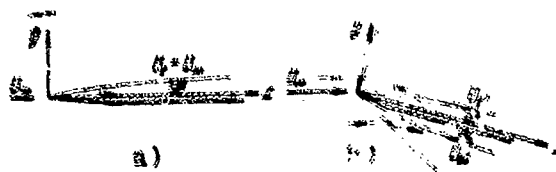

Figure 22

In the case under consideration involving a plane flow with constant velocity (U_e = const, dU_e/dx = 0) over a nonpermeable wall (u_w = 0), the integral momentum relation (2.80) will become

---

Footnote (6) appears on page 178.
Footnote (7) appears on page 178.

$$\frac{d\delta^{**}}{dx} = \frac{\tau_w}{\rho_e U_e^2}. \tag{3.16}$$

Here δ^{**} is the momentum loss thickness given by Equation (2.76). The parameters referred to the outer boundary of the boundary layer will, as before, be denoted with a subscript e, keeping in mind that only in the particular case involving flow over a flat plate at the zero angle of attack are these parameters equal to the parameters of the oncoming flow at infinity.

Introducing the Reynolds numbers, constructed using the momentum loss thickness

$$Re^{**} = \frac{U_e \rho_e \delta^{**}}{\mu_e} \tag{3.17}$$

and the running coordinate of a point on the plate

$$Re_x = \frac{U_e \rho_e x}{\mu_e}. \tag{3.18}$$

we shall write Equation (3.16) in the form

$$d Re_x = \left(\frac{\rho_e}{\rho_w}\right) \zeta^2 d Re^{**}. \tag{3.19}$$

where ζ is the friction parameter given by Equation (3.8). Rewriting Equation (3.19) in integral form, we obtain

$$Re_x = \frac{\rho_e}{\rho_w} \int_0^{Re^{**}} \zeta^2 d Re^{**}. \tag{3.20}$$

As implied by Equation (3.20), in order to solve the problem thus formulated, one must find a relationship between ζ and Re^{**}, i.e., one must establish a "drag law". To establish this law, we turn to the expression for the momentum loss thickness (2.76), writing it in terms of the universal coordinates φ and η, introduced by Equations (3.8), in the form

$$\delta^{**} = \frac{\nu_w \varphi}{U_e} \int_0^1 \frac{\rho}{\rho_e} \frac{u}{U_e}\left(1 - \frac{u}{U_e}\right)\frac{d\eta}{d\varphi} d\left(\frac{\varphi}{\eta}\right). \tag{3.21}$$

In view of Equations (3.17) and (3.8), we put (3.21) in the form

$$Re^{**} = \zeta^2 \frac{\mu_w}{\mu_e} \int_0^1 \frac{\rho}{\rho_w} \bar{u}(1-\bar{u})\frac{d\eta}{d\varphi}\,d\bar{u}. \qquad (3.22)$$

We use the two-layer model of the turbulent boundary layer: laminar-turbulent core (for a justification of this model for supersonic flows see Section 11).

To determine the function $\frac{d\eta}{d\phi}$ ($\bar{u}$) in the turbulent core, we shall make use of Formula (2.69) in Karman's semiempirical theory. As far as the turbulence constant κ in this formula is concerned, we shall assume that it does not depend on compressibility (on the M_e number) or on heat transfer (on the temperature factor T_w/T_e), and has the same numerical value as for an incompressible fluid, i.e., $\kappa = 0.4$. Passing to the universal coordinates (3.8) in Karman's Formula (2.69), we bring it to the form

$$\frac{\varphi''^2}{\varphi'^4} = \kappa^2 \frac{\frac{\rho}{\rho_w}}{\frac{\tau}{\tau_w}}, \qquad (3.23)$$

where the prime denotes a derivative with respect to η.

Taking the root of both sides of the question thus obtained, we have

$$\frac{\varphi''}{\varphi'^2} = -\kappa \Psi, \qquad (3.24)$$

where

$$\Psi = \sqrt{\frac{\frac{\rho}{\rho_w}}{\frac{\tau}{\tau_w}}}. \qquad (3.25)$$

The minus sign on the right-hand side of Equation (3.24) was chosen since on the plate $\phi'' < 0$ (the condition of the convexity of the velocity profile).

Interchanging in (3.24) the argument and the function, we obtain the equation

$$\frac{\frac{d^2\eta}{d\varphi^2}}{\frac{d\eta}{d\varphi}} = \varkappa\Psi',$$

(3.26)

whose first integral is

$$\frac{d\eta}{d\varphi} = C_1 \exp\left(\varkappa\zeta \int \Psi\, d\bar{u}\right).$$

(3.27)

To determine the constant of integration C_1 the value of the derivative $d\phi/d\eta$ at the boundary of the laminar sublayer on the side of the turbulent core must be given. The simplest assumption here is a requirement that $\partial\phi/d\eta$ have the same value as for an incompressible fluid, i.e.,

$$[\varphi'(\eta)]_{\eta_{\wedge}+0} = f = \frac{1}{\varkappa\alpha};$$

In other words, it is assumed that $\varphi'(\eta_l + 0)$ does not depend on the compressibility and heat transfer (α is an empirical constant for the laminar sublayer, η_l is a coordinate specifying the boundary of the laminar sublayer). This assumption leads to the following result:

$$\frac{d\eta}{d\varphi} = \frac{1}{f} \exp\left(\varkappa\zeta \int_{\bar{u}_l}^{\bar{u}} \Psi\, d\bar{u}\right).$$

(3.28)

Here $\bar{u}_l = u_l/U_e$ is the dimensionless velocity at the boundary of the laminar sublayer (a definition of this quantity will be given later).

Upon performing integration in (3.28) and determining the constant of integration from the condition at the boundary of the laminar sublayer ($u = u_l$ at $\eta = \eta_l$), we obtain an expression for the velocity profile in the turbulent core

$$\eta = \eta_{\wedge} + \frac{\zeta}{f} \int_{\bar{u}_{\wedge}}^{\bar{u}} \exp\left(\varkappa\zeta \int_{\bar{u}_{\eta}}^{\bar{u}} \Psi\, d\bar{u}\right) d\bar{u}.$$

(3.29)

Here Ψ is given by Equation (3.25). In the laminar sublayer we assume a linear relation for the velocity profile

$$\varphi = \eta, \tag{3.30}$$

from which follows an expression for the velocity at the boundary of the laminar sublayer[8]

$$\bar{u}_{\pi} = \frac{\varphi_{\pi}}{\zeta} = \frac{\eta_{\pi}}{\zeta} = \frac{\alpha}{\zeta}. \tag{3.31}$$

Thus, the derivative $\frac{d\eta}{d\varphi}$ $(\bar{u})$ which is necessary to determine the Reynolds number **Re**** (3.22) is given for the turbulent core by Equation (3.22), and for the laminar sublayer, according to (3.30), by the equality

$$\frac{d\eta}{d\varphi} = 1. \tag{3.32}$$

Turning now to the expression for **Re**** (3.22), we note that, when evaluating the integral on the right-hand side of the equation, the integration interval must, strictly speaking, be divided into two segments: laminar sublayer $(0 \le \bar{u} \le \bar{u}_l)$ and turbulent core $(\bar{u}_l \le \bar{u} \le 1)$. A proper value of $d\eta/d\varphi$ should be substituted in each of these segments, using the Expression (3.32) in the first segment, and (3.28) in the second. However, such calculations result in a fairly complicated expression for **Re**** and are not necessary in those cases when the relative thickness of the laminar sublayer is not very large $[(\delta_l/\delta) < 0.10 - 0.15]$. In this case, one may omit the first segment and continue the second all the way to the wall. Calculations show that, for large values of the friction parameter ζ, the error involved in such an approximation is insignificant. Following this reasoning, we shall substitute the expression for $d\eta/d\varphi$ (3.28) in (3.22). As a result we obtain the following expression for the Reynolds number **Re****:

Footnote (8) appears on page 173.

$$Re^{**} = \frac{\mu_\varphi}{\mu_\varphi} \frac{\zeta^2}{l} \int_0^1 \Phi(\bar{u}) \exp\left(\varkappa\zeta \int_{\bar{u}_n}^{\bar{u}} \Psi(\bar{u}) \, d\bar{u}\right) d\bar{u}. \qquad (3.33)$$

Here we introduce the notation[9]

$$\Phi(\bar{u}) = \frac{\rho}{\rho_w} \bar{u}(1 - \bar{u}). \qquad (3.34)$$

For later use it is convenient to write (3.33) in the form

$$Re^{**} = \exp\left[-\varkappa\zeta I(\bar{u}_n)\right] \frac{\mu_w}{\mu_\varphi} \frac{\zeta^2}{l} \int_0^1 \Phi(\bar{u}) \exp\left[\varkappa\zeta I(\bar{u})\right] d\bar{u}, \qquad (3.35)$$

where

$$I(\bar{u}) = \int_0^{\bar{u}} \Psi(\bar{u}) \, d\bar{u} = \int_0^{\bar{u}} \sqrt{\frac{\rho/\rho_w}{\tau/\tau_w}} \, d\bar{u}, \qquad (3.36a)$$

$$I(\bar{u}_n) = \int_0^{\bar{u}_n} \Psi(\bar{u}) \, d\bar{u} = \int_0^{\bar{u}_n} \sqrt{\frac{\rho/\rho_w}{\tau/\tau_w}} \, d\bar{u}. \qquad (3.36b)$$

Regarding the friction stress τ in the boundary layer, we shall make the assumption (3.1) (a justification of this assumption was given in Section 10). In this case, we have

$$I(\bar{u}) = \int_0^{\bar{u}} \sqrt{\frac{\rho}{\rho_w}} \, d\bar{u}. \qquad (3.37)$$

When determining $I(\bar{u}_l)$, we shall approximately set the density in the laminar sublayer equal to a constant — namely, its value at the wall ρ_w. In this case, in view of (3.31), we find

$$I(\bar{u}_n) = \bar{u}_n = \frac{\alpha}{\zeta}. \qquad (3.38)$$

In order to evaluate the integral in the Expression (3.35), we use the fact that ζ is much greater than unity ($\zeta \gg 1$). In this case, the integral may be represented by an asymptotic series obtained as a result of integration by parts:

Footnote (9) appears on page 179.

$$\int \Phi(\bar{u}) \exp\left[\varkappa\zeta\, I(\bar{u})\right] d\bar{u} = \frac{\exp\left[\varkappa\zeta\, I(\bar{u})\right]}{\varkappa\zeta\,\Psi} \left(\Phi - \frac{F_1}{\varkappa\zeta} + \frac{F_2}{\varkappa^2\zeta^2} - \frac{F_3}{\varkappa^3\zeta^3} + \dots\right). \qquad (3.39)$$

Here

$$\begin{aligned}
\Psi &= \left(\frac{\rho}{\rho_w}\right)^{1/2}, \quad F_1 = \frac{1}{\Psi}\left(\Phi' - \frac{\Phi\Psi'}{\Psi}\right), \\
F_2 &= \frac{1}{\Psi^2}\left(\Phi'' - \frac{\Phi\Psi'' + 3\Phi'\Psi'}{\Psi} + \frac{3\Phi\Psi'^2}{\Psi^2}\right), \\
F_3 &= \frac{1}{\Psi^3}\left(\Phi''' - \frac{6\Phi'\Psi' + 4\Phi'\Psi'' + \Phi\Psi'''}{\Psi} + \right. \\
&\qquad\qquad \left. + \frac{15\Phi'\Psi'^2 + 10\Phi\Psi'\Psi''}{\Psi^2} - \frac{15\Phi\Psi'^3}{\Psi^3}\right).
\end{aligned} \right\} \qquad (3.40)$$

Here primes denote derivatives with respect to $\bar{u}$.

We determine the values of the functions $\Phi\,(\bar{u})$ and $\Psi\,(\bar{u})$ and their derivatives for $\bar{u} = 1$:

$$\begin{aligned}
\Phi(1) &= 0; \qquad \Phi'(1) = -\frac{\rho_e}{\rho_w}; \\
\Phi''(1) &= -2\left(\frac{\rho}{\rho_w}\right)_e' - 2\left(\frac{\rho_e}{\rho_w}\right); \\
\Psi(1) &= \left(\frac{\rho_e}{\rho_w}\right)^{1/2}; \quad \Psi'(1) = \frac{1}{2}\left(\frac{\rho}{\rho_w}\right)_e'\left(\frac{\rho_e}{\rho_w}\right)^{-1/2}.
\end{aligned} \right\} \qquad (3.41)$$

It is not necessary to calculate the values of the functions Φ and Ψ and their derivatives at $\bar{u} = 0$, since it is obvious beforehand that the contribution of the series (3.39) for $\bar{u} = 0$ to the value of the integral is immeasurably smaller than the contribution of the same series for $\bar{u} = 1$, due to the presence in the latter of a large exponential factor. In view of Equations (3.37), (3.38), (3.40) and (3.41), we shall evaluate the definite integral occurring on the right-hand side of (3.35) with the aid of (3.39). Retaining only the terms up to $\varkappa^3\zeta^3$ in the denominator, we obtain the following expression for Re**:

$$\mathbf{Re^{**}} = \frac{\rho^{*2}}{\jmath x^2} \cdot \frac{\mu_w}{\mu_e} \exp\left[\varkappa\zeta\int_0^1\left(\frac{\rho}{\rho_w}\right)^{1/2} d\bar{u}\right] \times$$
$$\times \left[1 - \frac{2 + \frac{1}{2}\left(\frac{\rho_w}{\rho_e}\right)\left(\frac{\rho}{\rho_w}\right)_e'}{\left(\frac{\rho_e}{\rho_w}\right)^{1/2}\varkappa\zeta}\right]. \qquad (3.42)$$

Now let us consider the Reynolds number constructed with the displacement thickness δ^* (2.77):

$$\text{Re}^* = \frac{U_e \rho_e \delta^*}{\mu_e}.$$

(3.43)

Following the same reasoning as in determining Re^{**}, we find

$$\text{Re}^* = \frac{e^{-\varkappa x}}{f x^2} \frac{\mu_w}{\mu_e} \exp\left[\varkappa \zeta \int\limits_0^1 \left(\frac{\rho}{\rho_w}\right)^{1/2} d\bar{u}\right]\left[1 + \left(\frac{\rho}{\rho_w}\right)'_e \left(\frac{\rho_e}{\rho_w}\right)^{-1} - \right.$$
$$\left. - \frac{1}{\varkappa \zeta}\left(\frac{\rho_e}{\rho_w}\right)^{-1/2}\left[\frac{1}{2}\left(\frac{\rho}{\rho_w}\right)'_e + \left(\frac{\rho}{\rho_w}\right)''_e - \frac{3}{2}\left(\frac{\rho}{\rho_w}\right)'^2_e \left(\frac{\rho_e}{\rho_w}\right)^{-1}\right]\right].$$

(3.44)

Forming the ratio $\text{Re}^*/\text{Re}^{**}$, we obtain an expression for the form parameter $H^* = \delta^*/\delta^{**}$:

$$H^* = \left\{1 + \left(\frac{\rho}{\rho_w}\right)'_e \left(\frac{\rho_e}{\rho_w}\right)^{-1} - \frac{1}{\varkappa \zeta}\left(\frac{\rho_e}{\rho_w}\right)^{-1/2}\left[\frac{1}{2}\left(\frac{\rho}{\rho_w}\right)'_e + \left(\frac{\rho}{\rho_w}\right)''_e - \right.\right.$$
$$\left.\left. - \frac{3}{2}\left(\frac{\rho}{\rho_w}\right)'^2_e \left(\frac{\rho_e}{\rho_w}\right)^{-1}\right]\right\}\left\{1 - \frac{1}{\varkappa \zeta}\left(\frac{\rho_e}{\rho_w}\right)^{-1/2}\left[2 + \frac{1}{2}\left(\frac{\rho_w}{\rho_e}\right)\left(\frac{\rho}{\rho_w}\right)'_e\right]\right\}^{-1}.$$

(3.45)

The Expression (3.42) that relates the Reynolds number Re^{**} (3.17) with the friction parameter ζ (3.8) is essentially a "drag law". It is important to emphasize that this law was obtained without any assumptions about the density variation in the boundary layer, and can be used to solve problems of flow over impermeable surfaces for an arbitrary variation of density in the boundary layer.

Now we proceed to establish the relationship between density and velocity, which will be necessary below. We note that from the equation of state (1.86) and the condition that pressure be constant across the boundary layer, we can deduce the following simple relation between the density and temperature

$$\frac{\rho}{\rho_w} = \left(\frac{T}{T_w}\right)^{-1}.$$

(3.46)

In the simplest form, the relationship between the temperature and velocity in the boundary layer can be obtained by assuming that the Prandtl number Pr and its turbulent analog Pr_T are equal to unity,

and the specific heat capacity of the gas is constant. In this case,
we obtain a particular integral of the energy equation, called
the Crocco integral:

$$\frac{T}{T_w} = 1 - \omega \bar{u} - \beta \bar{u}^2.$$

(3.47)

Here

$$\omega = 1 - \frac{T_e^*}{T_w}, \quad \beta = \frac{\gamma-1}{2} M_e^2 \frac{T_e}{T_w}, \\
T_e^* = T_e \left(1 + \frac{\gamma-1}{2} M_e^2\right)$$

(3.48)

(T_e^* is the deceleration temperature).

Sometimes, in order to account for a deviation of the Prandtl
numbers (Pr and Pr_T) from unity, one artificially introduces the
recovery factor r[10] in the expression for ω and β (3.48). In this
case we have

$$\omega = 1 - \frac{T_r}{T_w}, \quad \beta = r \frac{\gamma-1}{2} M_e^2 \frac{T_e}{T_w}, \\
T_r = T_e \left(1 + r \frac{\gamma-1}{2} M_e^2\right)$$

(3.49)

(T_r is the recovery temperature).

A basis for this modification of the Crocco integral is provided
by a simple reasoning according to which, in the absence of heat of
transfer between the gas and the wall, the coefficient ω must vanish
regardless of the values of the Prandtl numbers (Pr, Pr_T). When the
Prandtl numbers deviate from unity, the condition in question will be
satisfied only if, in the expression for ω (3.48), T_e^* will signify
the equilibrium temperature of the thermally insulated wall, T_r. As
a result, in the expression for β (3.48) to satisfy the conditions on
the outer boundary ($T = T_e$ for $\bar{u} = 1$) one must introduce the recovery
factor r, which brings β to its form in (3.49).

Footnote (10) appears on page 179.

Using Equations (3.47) and (3.46), we find the desired relation-
ship between the density and the velocity in the boundary layer:

$$\frac{\rho}{\rho_w} = (1 - \omega\bar{u} - \beta\bar{u}^2)^{-1}. \tag{3.50}$$

Substituting Equation (3.50) in (3.37), and performing the
resultant integration, we find an expression for the function $I(\bar{u})$
which will be important later:

$$I(\bar{u}) = \frac{1}{\sqrt{\beta}}\left(\arcsin\frac{\sqrt{\beta}\,\bar{u} + \frac{\omega}{2\sqrt{\beta}}}{\sqrt{1 + \frac{\omega^2}{4\beta}}} - \arcsin\frac{\frac{\omega}{2\sqrt{\beta}}}{\sqrt{1 + \frac{\omega^2}{4\beta}}}\right). \tag{3.51}$$

Furthermore noting that the function $I(\bar{u})$ enters the exponents
in Equations (3.42) and (3.44), and performing the indicated calcula-
tions on the right-hand sides of these equations and taking account
of (3.50), we find the following expressions for Re** and Re*:

$$\mathbf{Re^{**}} = \frac{e^{-\varkappa z}}{\int \varkappa^2}\frac{\mu_w}{\mu_e}\exp\left[\varkappa\zeta I(1)\right]\left[1 - \frac{2 - 1{,}5\,\omega - \beta}{\varkappa\zeta\sqrt{1 - \omega - \beta}}\right],$$

$$\mathbf{Re^*} = \frac{e^{-\varkappa z}}{\int \varkappa^2}\frac{\mu_w}{\mu_e}\exp\left[\varkappa\zeta I(1)\right]\left[\frac{1 + \beta}{1 - \omega - \beta}\right] \times \tag{3.52}$$

$$\times\left[1 - \frac{\beta\left(3 - 1{,}5\omega - \beta + \frac{\omega}{2\beta}\right)}{\varkappa\zeta(1 + \beta)\sqrt{1 - \omega - \beta}}\right] \tag{3.53}$$

Here

$$I(1) = \frac{1}{\sqrt{\beta}}\left(\arcsin\frac{\sqrt{\beta} - \frac{\omega}{2\sqrt{\beta}}}{\sqrt{1 + \frac{\omega}{4\beta}}} - \arcsin\frac{\frac{\omega}{2\sqrt{\beta}}}{\sqrt{1 + \frac{\omega^2}{4\beta}}}\right). \tag{3.54}$$

Forming the ratio of Equations (3.53) and (3.52), we find an
expression for the form parameter $H^* = \delta^*/\delta^{**}$:

$$H^* = \frac{(1 + \beta)\left[1 - \frac{\beta\left(3 - 1{,}5\omega - \beta + \frac{\omega}{2\beta}\right)}{\varkappa\zeta(1 + \beta)\sqrt{1 - \omega - \beta}}\right]}{(1 - \omega - \beta)\left[1 - \frac{2 - 1{,}5\omega - \beta}{\varkappa\zeta\sqrt{1 - \omega - \beta}}\right]}. \tag{3.55}$$

In the limiting case of an incompressible gas ($\beta = 0$) and in the absence of heat transfer ($\omega = 0$), we obtain an expression

$$H_0^* = \frac{1}{1 - \frac{2}{x_{50}}},\qquad(3.56)$$

which for the Reynolds numbers 10^5 - 10^7 gives the value $H_0^* + 1.36 - - 1.23$, which is in good agreement with experiment.

Having obtained the drag law (3.52) that establishes a relation between the Reynolds numbers Re** (3.17), constructed from the momentum loss thickness, and the friction parameter ζ (3.8), it is not difficult, using the momentum equation in the form (3.20), to establish the required relationship between the friction coefficient c_f and the Reynolds number Re_x (3.18), constructed from the running coordinate of a point on the plate. In establishing this relationship, it is convenient to use a rough approximation for Re** in which one neglects the second term on the right-hand side of Equation (3.52) as compared with unity. This approximation will simplify considerably the final formula for the friction coefficient c_f. However, the error introduced in the formula for c_f can be to a considerable extent compensated by a suitable choice of the constant of integration[11]. Substituting the expression for Re**, with the approximation described above, in Equation (3.20) and performing the integration with the boundary condition $Re_x = 0$ at $\zeta = 0$ (the condition that the turbulent boundary layer will begin at the leading edge of the plate), we obtain approximately

$$C_1 \frac{\cdots}{\cdots}\frac{\cdots}{\cdots}\frac{\cdots}{\cdots}\,\zeta^2 \exp[x\zeta/(1)] = Re_x.\qquad(3.57)$$

The constant C_1 has been introduced in (3.57) to "compensate" for the approximation used for Re**.

Passing in Formula (3.57) from ζ to c_f according to (3.8), using Equation (3.50), and taking the logarithm, we obtain

Footnote (11) appears on page 170.

$$x(\lg e)\sqrt{2}\sqrt{1-\omega-\beta}\,I(1)(c_f)^{-1/2} = 2\lg(Re_x c_f) - $$
$$ - \lg\left(\frac{\mu_w}{\mu_e}\right) + C_2. \qquad (3.58)$$

where I (1) is given by Equation (3.54), and

$$C_2 = -\lg\left[\frac{C_1 \, 2e^{-\kappa z}}{\beta \kappa^2}\right].$$

Setting in (3.58) $\kappa = 0.4$ and determining the constant C_2 from the condition that for $\omega = \beta = 0$, Formula (3.58) turn into Karman's formula for an incompressible fluid

$$\frac{0.242}{\sqrt{c_{f0}}} = 0.41 + \lg(Re_x c_{f0}). \qquad (3.59)$$

We obtain the following expression for the local skin friction coefficient for a flat plate in a compressible gas:

$$\frac{0.242\sqrt{1-\omega-\beta}}{\sqrt{c_f}\,\sqrt{\beta}}\left(\arcsin\frac{\sqrt{\beta}+\frac{\omega}{2\sqrt{\beta}}}{\sqrt{1+\frac{\omega^2}{4\beta}}} - \arcsin\frac{\frac{\omega}{2\sqrt{\beta}}}{\sqrt{1+\frac{\omega^2}{4\beta}}}\right) = $$
$$ = 0.41 + \lg(Re_x c_f) - \lg\left(\frac{\mu_w}{\mu_e}\right). \quad (3.60) \qquad (3.60)$$

To calculate the dynamic viscosity of the gas, one can use either the Sutherland Formula (1.75), or the power law

$$\frac{\mu}{\mu_e} = \left(\frac{T}{T_e}\right)^n. \qquad (3.61)$$

where the exponent n is usually taken equal to 0.76.

Now we proceed to determine the mean coefficient of skin friction

$$c_f = \frac{1}{Re_x}\int_0^{Re_x} c_f \, dRe_x. \qquad (3.62)$$

For this purpose, we use the integral momentum relation in the form (3.19), first transforming it to the form

$$\frac{\mu_w}{\mu_e}\frac{1}{c_f}\,dRe_x = dRe^{**}. \qquad (3.63)$$

Passing on the left-hand side of Equation (3.63) from ζ to c_f with the help of Equation (3.8) and performing the resultant integration under the condition $\mathbf{Re}^{**} = 0$ for $\mathbf{Re}_x = 0$ in view of Equation (3.62), we obtain

$$c_f \, \mathbf{Re}_x = 2 \, \mathbf{Re}^{**}. \tag{3.64}$$

Substituting in the right-hand side of Formula (3.64), the approximate expression for $\mathbf{Re}^{**}$ (3.52), we have

$$c_f \, \mathbf{Re}_x = C_3 \frac{2c}{h^2} \frac{\mu_\infty}{\mu_r} \exp[x\zeta/(1)]. \tag{3.65}$$

The constant C_3 has been introduced here, just as in relation (3.57), to "compensate" for the approximate expression for $\mathbf{Re}^{**}$.

Comparing Equation (3.65) with Equation (3.57), put in the form

$$c_f \, \mathbf{Re}_x = C_1 \frac{2c}{h^2} \frac{\mu_\infty}{\mu_r} \exp[x\zeta/(1)].$$

It is not difficult to note that, for the large values of the parameter ζ that are considered here, the coefficients c_p and c_f differ by a constant. Consequently, one may conclude that the expression for the mean friction coefficient has the form (3.60), although with a different constant, i.e.,

$$\frac{0.242}{\sqrt{s}} \sqrt{\frac{1}{c_f}} \frac{\mathrm{arcsin}\,1/(1)}{} \quad \lg(\mathbf{Re}_x \, c_f) = \lg \frac{\mu_\infty}{\mu_r} \quad C_4 \tag{3.66}$$

The constant C_4 will be determined by requiring that for $\omega = \beta = 0$, Equation (3.66) will pass into the Karman law for the mean skin friction coefficient in the case of an incompressible fluid, namely:

$$\frac{0.242}{\sqrt{c_f}} = \lg(\mathbf{Re}_x \, c_f) \tag{3.67}$$

Upon determining the constant C_4, we obtain the following final formula for the mean skin friction coefficient:

$$\frac{0.212\sqrt{1-\omega-\beta}}{\sqrt{c_F}\sqrt{\beta}}\left(\arcsin\frac{\sqrt{\beta}+\frac{\omega}{2\sqrt{\beta}}}{\sqrt{1+\frac{\omega^2}{4\beta}}}-\arcsin\frac{\frac{\omega}{2\sqrt{\beta}}}{\sqrt{1+\frac{\omega^2}{4\beta}}}\right)=$$

$$= \lg(Re_x c_F)-\lg\left(\frac{\mu_w}{\mu_e}\right). \quad (3.68) \qquad (3.68)$$

Let us consider two practically important particular cases of a flow over a flat plate.

Thermally insulated plate. In this case, $T_w = T_r$, $\omega = 0$

$$\beta = \frac{\frac{\gamma-1}{2}M_e^2}{1+\frac{\gamma-1}{2}M_e^2} \quad \text{for} \quad Pr = Pr_T = 1, \qquad (3.69a)$$

$$\beta = \frac{r\frac{\gamma-1}{2}M_e^2}{1+r\frac{\gamma-1}{2}M_e^2} \quad \text{for} \quad Pr \neq Pr_T \neq 1. \qquad (3.69b)$$

Formulas (3.60) for the local friction coefficient and (3.68) will become, respectively,

$$\frac{0.212}{\sqrt{c_f}}\sqrt{\frac{1-\beta}{\beta}}\arcsin\sqrt{\beta}=0.41+\lg(Re_x c_f)-\lg\left(\frac{\mu_r}{\mu_e}\right) \qquad (3.70)$$

and

$$\frac{0.212}{\sqrt{c_F}}\sqrt{\frac{1-\beta}{\beta}}\arcsin\sqrt{\beta}=\lg(Re_x c_F)-\lg\left(\frac{\mu_r}{\mu_e}\right). \qquad (3.71)$$

Plate with heat transfer in a stream of an incompressible fluid. In this case, setting β to 0, we obtain

$$\frac{0.424(\sqrt{1-\omega}+\omega-1)}{\sqrt{c_f}\,\omega}=0.41+\lg(Re_x c_f)-\lg\left(\frac{\mu_w}{\mu_e}\right), \qquad (3.72)$$

$$\frac{0.424(\sqrt{1-\omega}+\omega-1)}{\sqrt{c_F}\,\omega}=\lg(Re_x c_F)-\lg\left(\frac{\mu_w}{\mu_e}\right). \qquad (3.73)$$

The relationships between the friction coefficients and the parameters of the oncoming flow and the conditions at the wall, obtained in an implicit form, are not always convenient in practice. It is not hard to show by means of simple rearrangements that these relationships can be made explicit. For this purpose, we turn to

Equation (3.57), which in the case of an incompressible fluid and the absence of heat transfer between the gas and the wall becomes

$$C_1 \frac{e^{-x_2}}{7x^2} \, \overline{\omega} e^{x_2} \cdot Re_x.$$

(3.74)

Dividing both sides of Equation (3.57), respectively, by both sides of Equation (3.74), we have

$$\left(\frac{\zeta}{\nu'}\right)^2 \exp[x\zeta I(1) - x\zeta_0] = \frac{\mu_e \rho_w}{\mu_w \rho_e}.$$

(3.75)

Passing in the Expression (3.75) from ζ to c_f with the help of (3.8), and taking the logarithm, we obtain

$$-\lg \frac{c_f}{c_{f0}} = FK \bigg/ \sqrt{\frac{c_{f0}}{c_f}} \quad F + G.$$

(3.76)

where

$$F = \frac{0.313}{\sqrt{c_{f0}}}.$$

(3.77)

$$G = \lg\left(\frac{\mu_e}{\mu_w}\right).$$

(3.78)

$$K = \sqrt{\frac{1-\omega-3}{3}} \left(\arcsin\frac{\sqrt{3}+\frac{\omega}{2\sqrt{3}}}{\sqrt{1+\frac{\omega^2}{3}}} - \arcsin\frac{\frac{\omega}{2\sqrt{3}}}{\sqrt{1+\frac{\omega^2}{3}}}\right).$$

(3.79)

To determine the friction coefficient c_{f0} one can use either the Karman Formula (3.59) or the simpler explicit relations

$$c_{f0} = 0.0263 \, Re_x^{0.1}, \quad c_{f0} = 0.0131 \, Re_x \qquad \omega_x \quad (12)$$

(3.80)

Equation (3.76) can be reduced to a transcendental equation with one parameter. For this purpose, we rewrite this equation in the form

$$2\lg\frac{1}{\sqrt{\frac{c_f}{c_{f0}}}} + \frac{FK}{\sqrt{\frac{c_f}{c_{f0}}}} = F + G$$

Footnote (12) appears on page 179.

and then add $2 \lg \frac{FK}{2}$ to both sides of the equation thus obtained, obtaining

$$\lg\left(\frac{FK}{2\sqrt{\frac{c_i}{c_{i0}}}}\right) + \frac{FK}{2\sqrt{\frac{c_i}{c_{i0}}}} = \lg\frac{FK}{2} + \frac{F+G}{2}. \tag{3.81}$$

Introducing the notation

$$N = \frac{FK}{2\sqrt{\frac{c_i}{c_{i0}}}}, \tag{3.82}$$

$$Q = \lg\frac{FK}{2} + \frac{F+G}{2}. \tag{3.83}$$

we shall have instead of Equation (3.81) the following equation:

$$\lg N + N = Q. \tag{3.84}$$

Thus, this expression for the friction coefficient can be written in the form

$$\frac{c_i}{c_{i0}} = \left(\frac{FK}{2N}\right)^2, \tag{3.85}$$

where F and K are determined from Equations (3.77) and (3.79), and N can be found solving Equation (3.84). Determination of N is not difficult, and can be easily done using tables of decimal logarithms or graphically.

If for the dynamic viscosity we use the power law (3.61), then the expression for the function G, which together with F and K determines N, becomes

$$G = n \lg\left(\frac{T_\delta}{T_w}\right). \tag{3.86}$$

It is interesting to note that, when Prandtl's Formula (2.68) is used instead of Karman's Formula (2.69), the expression for the friction coefficient thus obtained is the same as the Expression (3.85),

with the only difference that the function G is not given by (3.86), but instead by

$$G = \left(n + \frac{1}{2}\right) \lg \left(\frac{T_e}{T_w}\right).$$ (3.87)

Considering Formula (3.85), it may be noted that for large Reynolds numbers, the ratio c_f/c_{f0} depends slightly on the Reynolds number. In fact, by letting the Reynolds number approach infinity ($Re_x \to \infty$) or, which is the same thing, $F \to \infty$, we obtain the following limiting formula for the ratio c_f/c_{f0}

$$\frac{c_f}{c_{f0}} = K^2,$$ (3.88)

K, given by Equation (3.79), depends only on the compressibility of the medium (β) and the heat transfer (ω), and does not depend on the Reynolds number.

The existence of the limiting Formula (3.88) was established, and then widely used to construct semiempirical methods of turbulent boundary layer calculations by S. S. Kutateladze, A. I. Leont'yev, and others [34].

When Formula (3.85) is used for computing the friction coefficient, it is useful, just as before, to consider certain particular cases.

In the case of a thermally insulated plate ($\omega = 0$), the coefficient β is given by Equations (3.69a) and (3.69b), and the determining function K has the form

$$K = \sqrt{\frac{1-\beta}{\beta}} \arcsin \sqrt{\beta}.$$ (3.89)

For an incompressible fluid in the presence of heat transfer, by letting β go to zero, we obtain

$$K = \frac{2(\sqrt{1-\omega}+\omega-1)}{\omega}.$$ (3.90)

In order to calculate the mean friction coefficient for a flat plate, one can easily establish the validity of a formula or the same form as Formula (3.85), namely

$$\frac{c_F}{c_{F0}} = \left(\frac{FK}{2N}\right)^2,$$

(3.91)

where K and N are given by the same equations as before, namely (3.79) and (3.84), and F has the form

$$F = \frac{0,242}{\sqrt{c_{F0}}}.$$

(3.92)

To determine the friction coefficient c_{F0}, one can use either Karman's Formula (3.67), or the simpler power-law relation

$$c_{F0} = 0,0307\, Re_x^{-1/7}.$$

(3.93)

Formulas (3.85) and (3.91) obtained above permit us to calculate the ratios of the local and mean friction coefficient if we are given the values of the Mach number M_e, the temperature factor T_w/T_r, and the Reynolds number Re_x, to the local and mean friction coefficients for an incompressible fluid ($M_e = 0$, $T_w/T_r = 1$) for the same value of the Reynolds number Re_x. However, in certain cases, particularly when analyzing experimental data, it may be more convenient to use the Reynolds number constructed from the momentum loss thickness, Re**, as the characteristic Reynolds number. This is expedient, for example, in those cases when it is difficult to determine the initial point of the boundary layer on the wall of a tunnel, and consequently, it is impossible to use the Reynolds number constructed from the running coordinate, Re_x. In those cases, in order to compare theory with experiment, it is useful to have the ratios c_f/c_{f0} and c_F/c_{F0} in which c_f and c_{f0}, c_F and c_{F0} have been calculated for the same values of the Reynolds number Re**.

To obtain these ratios, we turn to the expression for the Reynolds number Re**, (3.53), which, for an incompressible fluid, becomes

$$Re^{**} = \frac{e^{-\varkappa\chi}}{f\varkappa^2}e^{\varkappa\zeta_0}\left(1 - \frac{2}{\varkappa\zeta_0}\right).$$ (3.94)

Similarly, as was done when deriving Equations (3.85) and (3.91), we shall use a rough approximation for the Reynolds number Re^{**} in which we neglect on the right-hand sides of Equations (3.52) and (3.94) terms containing $1/\zeta$ ($1/\zeta_0$), as they are negligible compared to unity. Then dividing as before, both sides of Equation (3.52) by both sides of Equation (3.94), respectively, and passing from ζ to c_f according to (3.8), we obtain after simple rearrangements

$$\left(\frac{c_f}{c_{f0}}\right)_{Re^{**}} = \left(\frac{K}{1+\frac{G}{F}}\right)^2.$$ (3.95)

where the functions F, K, and G are as before given by Equations (3.77) - (3.79).

The expression for $(c_F/c_{F0})_{Re^{**}}$ has the same form as in (3.95), except that the function F is in this case given by Equation (3.92).

Letting in Equation (3.95) the Reynolds number Re^{**} go to infinity, we arrive at the limiting Formula (3.88) obtained above.

Now we proceed to determine the velocity profile in a boundary layer. In the laminar sublayer, the velocity profile is described by a linear relation (3.30). To find the velocity profile in the turbulent core of the boundary layer, we turn to Equation (3.29), first writing the latter in the form

$$\eta = \eta_a + \frac{\zeta}{f}\exp\left[-\varkappa\zeta\int_0^{\bar{u}_n}\Psi\,d\bar{u}\right]\left\{\int_0^{\bar{\bar{u}}}\exp\left[\varkappa\zeta\int_0^{\bar{\bar{u}}}\Psi\,d\bar{u}\right]d\bar{u} - \int_0^{\bar{\bar{u}}_n}\exp\left[\varkappa\zeta\int_0^{\bar{\bar{u}}}\Psi\,d\bar{u}\right]d\bar{u}\right\}.$$ (3.96)

Here ψ is given by Equation (3.25).

Making the assumption (3.1) for the friction stress as before, and assuming that the density in the laminar sublayer (for $0 \leq \bar{u} \leq \bar{u}_l$) is constant and equal to its value at the wall, we obtain from the preceding equation

$$\eta = \frac{e^{-\varkappa\alpha\zeta}}{f} \int_0^{\bar{u}} \exp\left[\varkappa\zeta I\left(\bar{u}\right)\right] d\bar{u}. \tag{3.97}$$

Here $I\left(\bar{u}\right)$ is given by Equation (3.51).

Substituting in the Expression (3.97) the value of $I\left(\bar{u}\right)$ from Equation (3.51) and performing integration, we obtain the following expression for the velocity profile in the turbulent core:

$$\eta = \frac{e^{-\varkappa\alpha}}{f\varkappa}\left(\frac{\sqrt{1-\omega\bar{u}-\beta\bar{u}^2}+\frac{\beta}{\varkappa\zeta}\bar{u}+\frac{\omega}{2\varkappa\zeta}}{1+\frac{\beta}{\varkappa^2\zeta^2}}\right) \times$$
$$\times \exp\left[\frac{\varkappa\zeta}{\sqrt{\beta}}\left(\arcsin\frac{\sqrt{\beta}\bar{u}+\frac{\omega}{2\sqrt{\beta}}}{\sqrt{1+\frac{\omega^2}{4\beta}}}-\arcsin\frac{\frac{\omega}{2\sqrt{\beta}}}{\sqrt{1+\frac{\omega^2}{4\beta}}}\right)\right]. \tag{3.98}$$

Upon a substitution in (3.98) of the corresponding values of the empirical constants (α = 11.5, κ = 0.4, f = $1/\kappa\alpha$ = 0.218) and taking the logarithm, we express the velocity profile in the following form:

$$\frac{\zeta}{\sqrt{\beta}}\left(\arcsin\frac{\sqrt{\beta}\bar{u}+\frac{\omega}{2\sqrt{\beta}}}{\sqrt{1+\frac{\omega^2}{4\beta}}}-\arcsin\frac{\frac{\omega}{2\sqrt{\beta}}}{\sqrt{1+\frac{\omega^2}{4\beta}}}\right)+$$
$$+5{,}75\lg\left[\left(1+\frac{6{,}25\beta}{\zeta^2}\right)^{-1}\left(\sqrt{1-\omega\bar{u}-\beta\bar{u}^2}+\frac{2{,}5\beta\bar{u}}{\zeta}+\frac{1{,}25\omega}{\zeta}\right)\right]=$$
$$= 5{,}75\lg\eta+5{,}5. \tag{3.99}$$

For the limiting case of an incompressible fluid (β = 0) and in the absence of heat transfer (ω = 0), Equation (3.99) turns into the well-known logarithmic velocity profile

$$\varphi = 5{,}75\lg\eta+5{,}5. \tag{3.100}$$

When the Expression (3.52) for the Reynolds number Re** is used, the velocity profile (3.98) can be easily transformed to the following

form, which is useful in certain practical applications:

$$
\frac{\zeta}{\sqrt{\beta}}\left(\arcsin\frac{\sqrt{\beta}\,\bar{u}+\frac{\omega}{2\sqrt{\beta}}}{\sqrt{1+\frac{\omega^2}{4\beta}}}-\arcsin\frac{2\frac{\omega}{\sqrt{\beta}}}{\sqrt{1+\frac{\omega^2}{4\beta}}}\right)+5{,}75\times
$$

$$
\times\lg\frac{0{,}4\zeta\left(\sqrt{1-\omega a-\beta a^2}+\frac{2{,}5\beta a}{\zeta}+\frac{1{,}25\omega}{\zeta}\right)}{\left(1+\frac{6{,}25\beta}{\zeta^2}\right)\left(\sqrt{1-\omega-\beta}-\frac{5}{\zeta}+\frac{3{,}75\omega}{\zeta}+\frac{2{,}5\beta}{\zeta}\right)\sqrt{1-\omega-\beta}}
$$

$$
=5{,}75\lg\left(\frac{y}{\delta^{**}}\right). \tag{3.101}
$$

The semiempirical method of calculating friction in the turbulent boundary layer on a flat plate, as presented in the present section, is illustrated by the plots given in Figures 23 - 26. For comparison, the experimental data obtained by various workers are also given therein.

Figure 23 gives the results of calculating the local friction coefficient for a thermally insulated plate for three Reynolds numbers: 10^6, 10^7, 10^8. The subscript ∞ means that a curve in question has been plotted according to the limiting Formula (3.88). In addition to the experimental points obtained by the authors whose papers were discussed in Section 11, Figure 23 also contains points obtained by Lipmann and Dhavan [35].

Figure 24 gives the results of calculating the mean friction coefficient on a thermally insulated surface. In addition to the experimental data taken from the papers discussed earlier, the results obtained by Pappas [36] are also used here. It should be noted that here, just as in Figure 23, the data points obtained by Coles lie above the theoretical curves.

Figure 25 gives the results of calculating the local friction coefficient for a plate that can exchange heat with gas (thermal flux is directed from the gas to the wall).

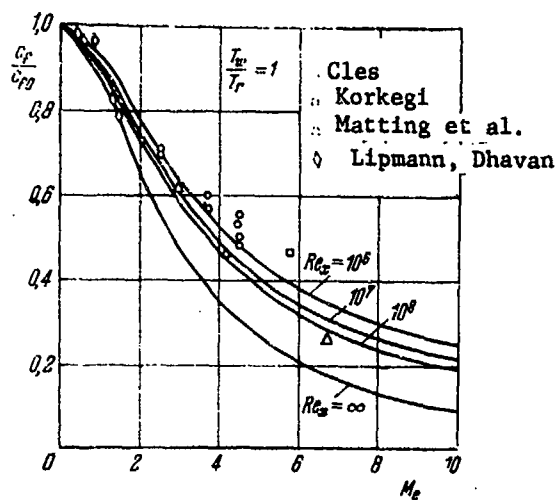Figure 26 gives the results of calculating the ratio of the local friction coefficient in a compressible gas to the friction
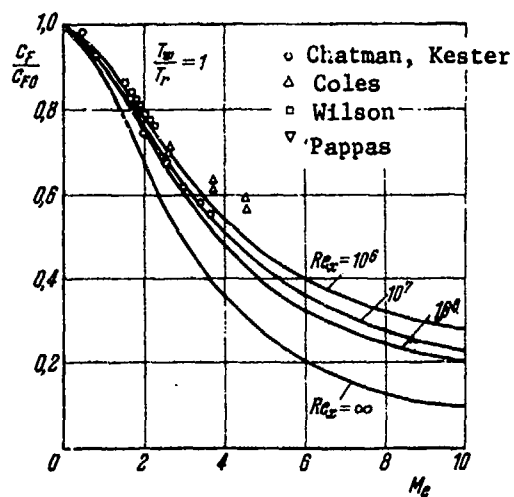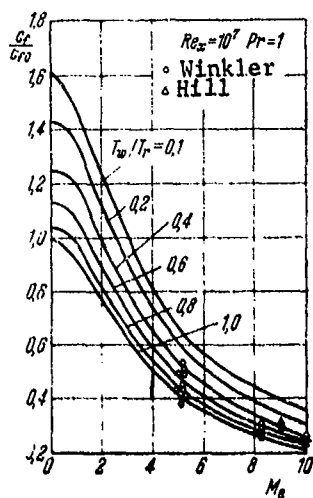
Figure 23

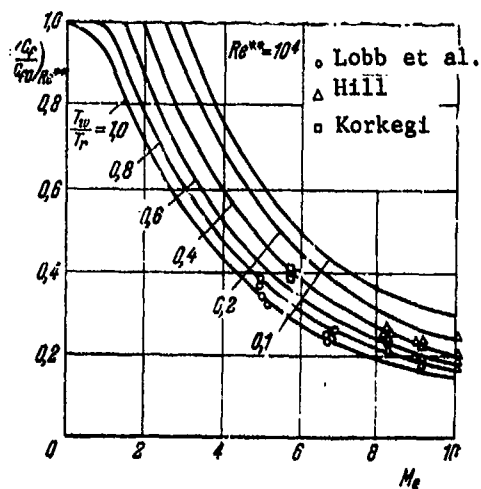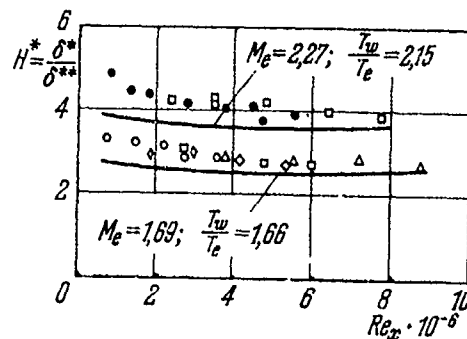

Figure 24

Figure 25

Figure 26

Figure 27

coefficient in an incompressible fluid, where both coefficients were computed for the same Reynolds number constructed from the momentum loss thickness [Formula (3.95)]. Figure 26, along with the data points taken from Hill's paper discussed in Section 11, also contains data points for $M_e = 10$ from a later paper of the same author.

Figure 27 is a comparison of the form parameter H^*, calculated using Equation (3.55), with the values of this form parameter obtained from Pappas' experiments [37]. As can be seen from the graph, the theoretical and experimental data are in better agreement for larger Reynolds numbers.

Figure 17 also includes the theoretical profiles along with the experimental velocity profiles, obtained experimentally by Hill. Solid lines indicate the velocity profiles calculated using Formulas (3.30) (laminar sublayer) and (3.99) (turbulent core). Dotted lines indicate the logarithmic velocity profile obtained for an incompressible fluid using Formula (3.100). A comparison of the solid lines with the experimental points shows that Formula (3.99) gives a good qualitative account of the effects of compressibility and temperature on the form of the velocity profile. One should not expect full agreement between the theoretical and experimental velocity profiles, if one recalls that certain simplifying assumptions [in particular, assumption (3.1) about a constant stress friction across the boundary layer] were made in developing the computational technique delineated above.

§ 13. The Effect of Compressibility and Heat Transfer on the Laminar Sublayer

The problem of determining the thickness of the laminar sublayer and the velocity at its boundary is of great importance in turbulent boundary layer theory, since the "laws" of drag and heat transfer greatly depend on the choice of these parameters. It will be recalled that in the theory of the turbulent boundary layer for an incompressible fluid the thickness of the laminar sublayer is determined from simple dimensional considerations. In fact, if it is assumed that the flow in the laminar sublayer is determined by the friction stress at the wall τ_w, viscosity μ, and the density of the medium, ρ, then dimensional considerations imply [38] that

$$\delta_{.l} = \alpha \frac{\nu}{\sqrt{\tau_w/\rho}}, \quad \nu = \frac{\mu}{\rho}, \tag{3.102}$$

where α is a dimensionless empirical constant.

The value of the constant α cannot be calculated theoretically and must be determined from experiments. Measurements done by Nikuradze which involved the flow of water in long cylindrical tubes have shown that the value of α is close to 11.5. The subsequent measurements done by other authors resulted in values of α ranging from 10 to 13.5.

The assumption that the friction stress (τ = const = τ_w) yields a linear distribution of the velocities in the laminar sublayer and the Newton formula (3.105) for friction lead to a linear velocity distribution in a laminar sublayer:

$$u = \frac{\tau_w}{\mu} y. \tag{3.103}$$

In terms of the universal coordinates, the equality becomes

$$\varphi = \eta. \tag{3.30}$$

and at the boundary of the sublayer according to (3.102)[13]

$$\eta_1 = \frac{\delta_1 \sqrt{\frac{\tau_w}{\rho}}}{\nu} = \varkappa.$$ (3.104)

When considering the flow in the turbulent boundary layer of a compressible gas, one can obviously obtain a formula similar to Formula (3.102) by starting with the same dimensional considerations. However, due to the variation of μ and ρ across the sublayer, it is unclear how one should choose the values of viscosity and density in this formula. It is also not clear whether the empirical constant α depends on the Mach number and the temperature factor. Usually, in Formula (3.102), μ and ρ are either taken at a certain "defining" temperature or are obtained by averaging over the sublayer. In particular, in Wilson's and Van Driest's papers, which were quoted above, the defining temperature was that of the wall.

In L. Ye. Kalikhman's paper[14] the following averaging law was used for viscosity

$$\mu_{cp} = \mu_w \frac{T_{cp}}{T_w},$$

$$T_{cp} = \frac{\int_0^{\delta_1} \rho u T \, dy}{\int_0^{\delta_1} \rho u \, dy},$$

and for the density and velocity

$$\rho_1 u_1 \delta_1 = \int_0^{\delta_1} \rho u \, dy.$$

One can also give examples of other methods of averaging; however, today there is no necessity of using them. It is perfectly clear that, at the present time, it is not possible to give a definite answer to the question of the "defining" temperature or the law of averaging. This circumstance, as noted above, has led to a great number of ways of determining the thickness of the laminar sublayer.

Footnotes (13) and (14) appear on page 179.

As always in such cases, the criterion that should be used when selecting the "defining" temperature or the law of averaging is a comparison with experiment. However, the lack of sufficient experimental evidence does not permit us to make this comparison today. Until enough experimental data are accumulated, preference in selecting a hypothesis about the "defining" temperature (method of averaging) should apparently be given to a hypothesis that leads to the simplest results.

The flow in the laminar sublayer in a compressible gas can be most simply described when the temperature of the wall is used as the "defining" temperature. In this case, the velocity profile is described by the same linear relation (3.30) as in the case of an incompressible fluid. The experimental data on velocity profiles given in Section 11 indicate that this relation is also well-satisfied at supersonic gas velocities.

The above methods of accounting for the effects of compressibility and heat transfer on the parameters of the laminar sublayer by selecting a "defining" temperature or by averaging over the sublayer do not facilitate a detailed analysis. A much greater amount of information on velocity profiles in the laminar sublayer can be obtained if one takes into account the actual variation of the gas viscosity with the temperature across the sublayer. This has been done by Czarnecki and Monta [39]. Following this paper, we shall rewrite Newton's formula for the friction stress

$$\tau = \mu \frac{du}{dy} \tag{3.105}$$

in the form

$$\tau = \tau_w \left(\frac{\mu}{\mu_w}\right) \frac{d\xi}{d\eta} . \tag{3.106}$$

where ξ and η are the universal coordinates defined in Equations (3.8).

Making the assumption (3.1) that the friction stress is constant in the sublayer and that the dependence of viscosity on temperature can be expressed in the form of a power law (3.61), and using the Crocco integral (3.47) relating the temperature to velocity, one can obtain the following expression for the velocity profile in the laminar sublayer from Formula (3.106):

$$\eta = \int_0^\varphi \left[1 - \frac{\omega}{\zeta}\varphi - \frac{\beta}{\zeta}\varphi^2 \right]^n d\varphi. \qquad (3.107)$$

where ω, β and ζ are given by Equations (3.49) and (3.8).

The results of calculations based on Formula (3.107) for the Mach number $M_e = 9$, the numbers $Re_x = 10^6$, 10^7, 10^8, and two values of the temperature factor $T_w/T_e = 15.1$ (thermally insulated surface) and $T_w/T_e = 2.6$ (strongly cooled surface) are given in Figure 28.
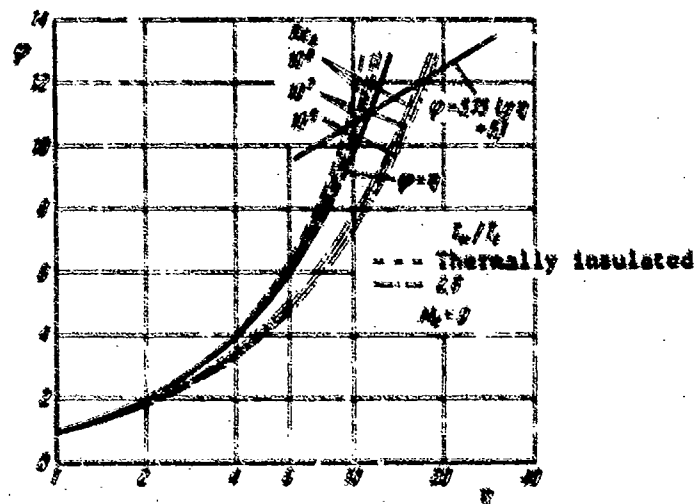

Figure 28

Figure 28 makes it clear that on a thermally insulated plate, the compressibility hardly affects the form of the velocity profile: all the curves (for the three Reynolds numbers) lie close to the curve

$\phi = \eta$. As a result, the value of the coordinate η_l characterizing the boundary of the laminar sublayer, is close to its value in an incompressible fluid ($\eta_l = 10 - 11$). When the plate is strongly cooled ($T_w/T_e = 2.6$), the velocity profiles become flatter and are noticeably displaced relative to the profile $\phi = \eta$. The values of the coordinate η_l increase considerably in this case[15].
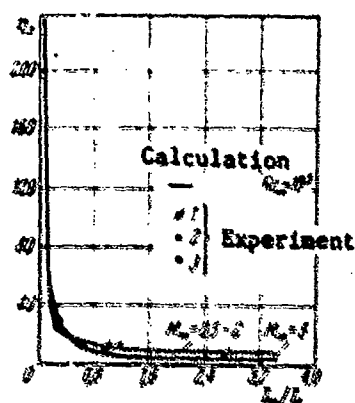

Figure 29

Similar results were obtained by L. M. Zysina-Molozhen and I. N. Soskova[16]. They assumed a linear dependence of viscosity on temperature ($n = 1$). The velocity profile in this case has the form

$$\eta = \phi\left[1 - \frac{\omega}{\zeta}\frac{\phi}{2} - \frac{\beta}{6}\frac{\phi^2}{3}\right], \quad (3.108)$$

where ω and β are given by Equations (3.48). Using the profile (3.108) for the laminar sublayer, and Van Driest's velocity profile[17] for the turbulent core, the authors of the paper determined the value of the coordinate η_l for various values of the Mach number and the temperature factor by combining these profiles (Figure 29). Here 2 represents the experimental data obtained by Lobb, Winkler, and Persch for $M_\infty = 5$; 1 and 3 represent the experimental data obtained by L. M. Zysina-Molozhen and I. N. Soskova for $M_\infty = 1.45$ and $M_\infty = 0.2$, respectively. As can be seen in Figure 29, with strong cooling the value of the parameter η_l increases substantially[18]. A similar tendency was noted in the paper by Lobb, Winkler, and Persch (Figure 21), whereas in Hill's experiments, as can be seen in the same Figure 21, this phenomenon was not observed. The above discussion implies that on thermally insulated surfaces in the presence of heat transfer from the surface of the body to the gas the value of the coordinate η_l is close to its

Footnotes (15), (16), (17) and (18) appear on pages 179 - 180.

value in an incompressible fluid. A final judgment as to the effect of compressibility and heat transfer on the parameter n_π c·· apparently be made only if a sufficiently great amount of experimental data is accumulated. Until the problem is solved experimentally, one should apparently use for $n_l = \alpha$ those values of the parameter that were obtained in experiments with an incompressible fluid, i.e., $\alpha = 11.5$.

§ 14. Empirical Method of Calculating Friction on a Flat Plate[19]

The method is based on the assumption that we have the following functional relationship:

$$\tfrac{1}{2}c_j F_c = \psi^{**}\,(Re^{**}F_{k e^{**}}), \qquad (3.109)$$

where the function ψ^{**} depends only on the Reynolds number Re^{**}, constructed from the momentum loss thickness, and the functions F_c and $F_{Re^{**}}$ depend only on the Mach number M_e and the temperature factor T_w/T_e. The functions F_c and $F_{Re^{**}}$ are such that

$$\left.\begin{aligned}F_c = F_c\left(M_e,\tfrac{T_w}{T_e}\right) = 1,\\[4pt]F_{ke^{**}} = F_{ke^{**}}\left(M_e,\tfrac{T_w}{T_e}\right) = 1\end{aligned}\right\}\ \text{for }\ M_e = 0\ \text{and}\ \tfrac{T_w}{T_e} = 1. \qquad (3.110)$$

The reasoning that leads to Equation (3.109) becomes obvious if the relation is written in the form

$$\left(\tfrac{c_h}{c_{h 0}}\right)_{k e^{**}} = \tfrac{F_{ke^{**}}}{F_c}. \qquad (3.111)$$

where

$$c_h = 2\psi^{**}Re^{**}. \qquad (3.112)$$

Comparing Equations (3.111) with the Expression (3.95) in Section 12, we note that, in contrast with (3.95), the right-hand side of

Footnote (19) appears on page 180.

FTD-HC-23-723-71   127

Equation (3.111) does not depend on the Reynolds number Re**, which holds for sufficiently large Reynolds numbers [see the limiting Formula (3.88)].

To establish the dependence of the friction coefficient c_f on the Reynolds number, constructed in terms of the distance from the leading edge of the plate, Re_x, we shall use the integral momentum Equation (3.20) in the form

$$Re_x = \int_0^{Re^{**}} \frac{2}{c_f} dRe^{**}.$$

(3.113)

Multiplying both sides of this equation by $F_{Re^{**}}/F_c$, we obtain

$$\frac{F_{Re^{**}}}{F_c} Re_x = \int_0^{F_{Re^{**}}Re^{**}} \frac{2}{c_f F_c} d(F_{Re^{**}}Re^{**}).$$

(3.114)

Introducing the notation

$$F_{Re_x} = \frac{F_{Re^{**}}}{F_c} = F_{Re_x}\left(M_e, \frac{T_w}{T_e}\right)$$

(3.115)

and noting that in accordance with the relation (3.109) there is a unique relation between $(c_f F_c)$ and $(F_{Re^{**}} Re^{**})$, we conclude that there is a relation

$$\frac{1}{2} c_f F_x = \psi_x (Re_x, F_{Re_x}),$$

(3.116)

where the function ψ_x depends only on the number Re_x, and does not depend on the Mach number M_e and the temperature factor T_w/T_e, and

$$F_{Re_x} = F_{Re_x}\left(M_e, \frac{T_w}{T_e}\right) = 1$$
$$\text{for } M_e = 0, \frac{T_w}{T_e} = 1.$$

(3.117)

Similarly one can obtain

$$\frac{1}{2} c_f F_c = \bar{\psi}(Re_x, F_{Re_x}).$$

(3.118)

where $\bar{\psi}$ again does not depend on M_e and T_w/T_e.

Equations (3.116) and (3.118) can be written in the form

$$\left(\frac{c_f}{c_{f0}}\right)_{Re_x} = \frac{F_{Re_x}}{F_c}.$$ (3.119)

$$\left(\frac{c_F}{c_{F0}}\right)_{Re_x} = \frac{F_{Re_x}}{F_c}.$$ (3.120)

Comparing the Expressions (3.119) and (3.120) with their analog (3.95), we note that, in contrast with (3.95), the right-hand sides of (3.119) and (3.120) do not depend on the Reynolds number Re_x. As a result, in this method of calculation we have equality of the ratios

$$\left(\frac{c_f}{c_{f0}}\right)_{Re_x} = \left(\frac{c_F}{c_{F0}}\right)_{Re_x}.$$

To determine the functions ψ^{**}, ψ_x and $\bar{\psi}$, the authors use the relations

$$Re^{**} = \frac{1}{6}\zeta_0^3 + \frac{1}{\varkappa\alpha}\left[\left(2 - \frac{3}{\varkappa\zeta_0}\right)\exp(\varkappa\zeta_0) + \frac{3}{\varkappa\zeta_0} + 1 - \frac{1}{6}(\varkappa\zeta_0)^2 - \frac{1}{12}(\varkappa\zeta_0)^3 - \frac{1}{40}(\varkappa\zeta_0)^4 - \frac{1}{180}(\varkappa\zeta_0)^5\right],$$ (3.121)

$$Re_x = \frac{1}{12}\zeta_0^3 + \frac{1}{\varkappa\alpha}\left[(6 - \varkappa\zeta_0 + (\varkappa\zeta_0)^2)\exp\varkappa\zeta_0 - 6 - 2\varkappa\zeta_0 - \frac{1}{12}(\varkappa\zeta_0)^4 - \frac{1}{30}(\varkappa\zeta_0)^5 - \frac{1}{90}(\varkappa\zeta_0)^6 - \frac{1}{252}(\varkappa\zeta_0)^7\right],$$ (3.122)

$$\frac{1}{2}c_{f0} = \frac{Re^{**}}{Re_x}.$$ (3.123)

where $\varkappa = 0.4$, $\alpha = 12$, $\zeta_0 = \sqrt{2/c_{f0}}$.

The form of one of the two unknown functions F_c and $F_{Re^{**}}$ (or F_{Re_x}), which determine the friction coefficient — namely, the function F_c — was selected on the basis of an analysis of the existing semiempirical methods of computation. The analysis of the semiempirical methods, done by the authors, showed that those methods give the highest accuracy. The results, written in the form (3.111), (3.119), or (3.120), lead to the following expression for F_c:

$$F_c = \frac{1}{K^2},$$

<div align="right">(3.124)</div>

where K is given by Equation (3.79), and the coefficients ω and β, appearing in (3.79), are defined by Formulas (3.49). In other words, the function F_c is determined in exactly the same way as was done in the semi-empirical method presented in Section 12.

The second unknown function F_{Re**} was determined empirically by using the experimental data on the friction coefficient. It was assumed that the function F_{Re**} has the form

$$F_{Re**} = \left(\frac{T_w}{T_e}\right)^p \left(\frac{T_r}{T_w}\right)^q.$$

<div align="right">(3.125)</div>

The considerations leading to the Expression (3.125) were also based on an analysis of the existing semi-empirical methods.

Using the functions ψ_{Re**}, ψ_x, ψ, and F_c, defined above, as well as numerous experimental data, the authors of the method found the values of p and q by minimizing the mean-square value of

$$\frac{c_{f,\text{эксп}} - c_{f,\text{теор}}}{c_{f,\text{теор}}}$$

As a result, it turned out that p = 00.702, and q = 0.772. Accordingly, the expression for F_{Re**} has the form

$$F_{Re**} = \left(\frac{T_w}{T_e}\right)^{-0,702} \left(\frac{T_r}{T_w}\right)^{0,772}.$$

<div align="right">(3.126)</div>

TABLE 9. VALUES OF THE FUNCTION F_c FOR VARIOUS VALUES OF M_e and T_w/T_e.

T_w/T_e \ M_e	0	1	2	3	4	5	6	7
0,05	0,3743	0,4036	0,4884	0,6222	0,7999	1,0184	1,2759	1,5713
0,1	0,4331	0,4625	0,5477	0,6829	0,8628	1,0842	1,3451	1,6444
0,2	0,5236	0,5530	0,6358	0,7756	0,9584	1,1836	1,4491	1,7534
0,3	0,5989	0,6283	0,7145	0,8523	1,0370	1,2649	1,5 37	1,8418
0,4	0,6662	0,6957	0,7821	0,9208	1,1069	1,3370	1,6083	1,9194
0,5	0,7286	0,7580	0,8446	0,9839	1,1713	1,4031	1,6767	1,9903
0,6	0,7873	0,8168	0,9036	1,0434	1,2318	1,4651	1,7405	2,0564
0,8	0,8972	0,9267	1,0137	1,1544	1,3445	1,5802	1,8539	2,1785
1	1,0000	1,0295	1,1167	1,2581	1,4494	1,6871	1,9684	2,2913
2	1,4571	1,4867	1,5744	1,7176	1,9130	2,1572	2,4472	2,7869
3	1,8660	1,8956	1,9836	2,1278	2,3254	2,5733	2,8687	3,2092
4	2,2500	2,2796	2,3678	2,5126	2,7117	2,9621	3,2611	3,6066
5	2,6180	2,6477	2,7359	2,8812	3,0813	3,3336	3,6355	3,9847
6	2,9747	3,0044	3,0927	3,2384	3,4393	3,6930	3,9971	4,3493
8	3,6642	3,6938	3,7823	3,9284	4,1305	4,3863	4,6937	5,0505
10	4,3311	4,3608	4,4493	4,5958	4,7986	5,0559	5,3657	5,7259
12	4,9821	5,0117	5,1003	5,2470	5,4504	5,7088	6,0204	6,3832
14	5,6208	5,6505	5,7391	5,8860	6,0898	6,3491	6,6621	7,0271
16	6,2500	6,2797	6,3683	6,5153	6,7196	6,9795	7,2937	7,6603
18	6,8713	6,9010	6,9897	7,1368	7,3413	7,6019	7,9170	8,2851
20	7,4861	7,5157	7,6045	7,7517	7,9564	8,2175	8,5334	8,9027
25	9,0000	9,0297	9,1184	9,2658	9,4711	9,7330	10,0505	10,4222
30	10,4886	10,5183	10,6071	10,7546	10,9602	11,2228	11,5415	11,9149

T_w/T_e \ M_e	8	9	10	11	12	13	14	15
0,05	1,9041	2,3738	2,6803	3,1233	3,6027	4,1186	4,6707	5,2591
0,1	1,9812	2,3552	2,7660	3,2134	3,6976	4,2180	4,7748	5,3680
0,2	2,0958	2,4750	2,8925	3,3462	3,8366	4,3636	4,9269	5,5267
0,3	2,1882	2,5723	2,9937	3,4522	3,9074	4,4793	5,0475	5,6523
0,4	2,2692	2,6569	3,0820	3,5443	4,0435	4,5704	5,1518	5,7608
0,5	2,3429	2,7336	3,1620	3,6276	4,1303	4,6097	5,2458	5,8584
0,6	2,4115	2,8040	3,2362	3,7048	4,2105	4,7531	5,3324	5,9483
0,8	2,5379	2,9360	3,3721	3,8459	4,3570	4,9051	5,4901	6,1117
1	2,6542	3,0562	3,4966	3,9748	4,4905	5,0434	5,6333	6,2590
2	3,1564	3,5725	4,0282	4,5228	5,0556	5,6263	6,2345	6,8801
3	3,5929	4,0184	4,4846	4,9904	5,5353	6,1187	6,7401	7,3993
4	3,9904	4,4290	4,9030	5,4176	5,9719	6,5653	7,1972	7,8673
5	4,3792	4,8174	5,2970	5,8196	6,3817	6,9833	7,6240	8,3033
6	4,7477	5,1905	5,6764	6,2041	6,7727	7,3814	8,0297	8,7109
8	5,4549	5,9050	6,3994	6,9368	7,5161	8,1305	8,7972	9,4977
10	6,1347	6,5904	7,0913	7,6363	8,2241	8,8539	9,5247	10,2359
12	6,7955	7,2556	7,7618	8,3129	8,9077	9,5452	10,2245	10,9449
14	7,4422	7,9058	8,4164	8,9727	9,5734	10,2174	10,9040	11,6321
16	8,0779	8,5444	9,0587	9,6194	10,2251	10,8748	11,5676	12,3026
18	8,7045	9,1737	9,6912	10,2556	10,8657	11,5204	12,2187	12,9598
20	9,3238	9,7952	10,3154	10,8832	11,4971	12,1562	12,8595	13,6050
25	10,8467	11,3225	11,8482	12,4227	13,0446	13,7128	14,4263	15,1841
30	12,3418	12,8200	13,3509	13,9305	14,5586	15,2339	15,9550	16,7235

TABLE 10. VALUES OF THE FUNCTION F_{Re**} FOR VARIOUS VALUES OF M_e AND T_w/T_e.

T_w/T_e \ M_e	0	1	2	3	4	5	6	7
0,05	82,7405	93,8950	125,3092	173,1153	234,1633	306,3489	388,2642	478,9229
0,1	29,7852	33,8006	45,1092	62,3185	84,2949	110,2803	139,7684	172,4040
0,2	10,7221	12,1676	16,2385	22,4336	30,3447	39,6990	50,3142	62,0625
0,3	6,8983	6,6934	8,9323	12,3407	16,6926	21,8384	27,6779	34,1406
0,4	3,8598	4,3801	5,8456	8,0757	10,9236	14,2910	18,1123	22,3414
0,5	2,2779	3,1524	4,2071	5,8121	7,9618	10,2353	13,0355	16,0792
0,6	2,1233	2,4095	3,2157	4,4424	6,0091	7,8615	9,9636	12,2900
0,8	1,3395	1,5768	2,1043	2,9071	3,9323	5,1445	6,5201	8,0425
1	1,0000	1,1348	1,5145	2,0923	2,8301	3,7025	4,6926	5,7883
2	0,3600	0,4085	0,5452	0,7532	1,0184	1,3328	1,6892	2,0837
3	0,1980	0,2247	0,2999	0,4143	0,5604	0,7332	0,9292	1,1462
4	0,1296	0,1471	0,1963	0,2711	0,3667	0,4798	0,6081	0,7501
5	0,0933	0,1058	1,1412	0,1951	0,2639	0,3453	0,4377	0,5393
6	0,0713	0,0809	0,1080	0,1491	0,2017	0,2639	0,3345	0,4126
8	0,0466	0,0529	0,0706	0,0976	0,1320	0,1727	0,2189	0,2700
10	0,0336	0,0381	0,0508	0,0702	0,0950	0,1243	0,1575	0,1943
12	0,0257	0,0291	0,0339	0,0537	0,0726	0,0950	0,1204	0,1485
15	0,0204	0,0232	0,0310	0,0429	0,0579	0,0757	0,0959	0,1143
16	9,0168	0,0191	0,0254	6,0351	0,0475	0,0622	0,0788	0,0972
18	0,0141	0,0160	0,0214	0,0295	0,0400	0,0523	0,0662	0,0817
20	0,0121	0,0137	0,0183	0,0253	0,0342	0,0447	0,0567	0,0700
25	0,0087	0,0099	0,0132	0,0182	0,0246	0,0322	0,0408	0,0503
30	0,0066	0,0075	0,0101	0,0139	0,0188	0,0246	0,0312	0,0385

T_w/T_e \ M_e	8	9	10	11	12	13	14	15
0,05	577,5949	683,7102	796,8344	916,5708	1042,029	1174,722	1312,620	1456,116
0,1	207,9243	240,1261	286,8407	320,9519	375,3286	422,8794	472,5207	524,1767
0,2	74,8492	88,6012	103,2599	118,7770	135,1119	152,2295	170,0993	188,6946
0,3	41,1745	48,7395	56,8032	65,3392	74,3250	83,7414	93,3716	103,6000
0,4	28,9444	31,8949	37,1718	42,7577	48,6340	54,8000	61,3129	67,0248
0,5	19,3920	22,9549	26,7527	30,7739	35,0050	39,4398	44,0696	48,8873
0,6	14,8221	17,5454	20,4482	23,5210	26,7557	30,1455	33,6942	37,3665
0,8	9,6995	11,4810	13,3312	15,3920	17,5088	19,7271	22,0423	24,4525
1	6,9808	8,2434	9,6305	11,0777	12,6012	14,1077	15,6643	17,5946
2	2,5130	2,9747	3,4008	3,9878	4,5382	5,1109	5,7109	6,3352
3	1,3824	1,6364	1,9071	2,1937	2,4954	2,8115	3,1416	3,4850
4	0,9040	1,0708	1,2480	1,4355	1,6330	1,8398	2,0554	2,3409
5	0,6511	0,7707	0,8982	1,0332	1,1752	1,3241	1,4706	1,6413
6	0,4976	0,5891	0,6862	0,7897	0,8983	1,0121	1,1309	1,2545
8	0,3238	0,3855	0,4493	0,5188	0,5878	0,6623	0,7401	0,8210
10	0,2344	0,2774	0,3233	0,3719	0,4231	0,4767	0,5326	0,5909
12	0,1791	0,2121	0,2471	0,2843	0,3234	0,3643	0,4071	0,4516
14	0,1427	0,1690	0,1969	0,2265	0,2576	0,2903	0,3244	0,3598
16	0,1172	0,1358	0,1617	0,1860	0,2116	0,2384	0,2664	0,2955
18	0,0985	0,1137	0,1359	0,1564	0,1779	0,2004	0,2239	0,2484
20	0,0844	0,0990	0,1164	0,1339	0,1523	0,1716	0,1917	0,2127
25	0,0607	0,0719	0,0838	0,0964	0,1096	0,1235	0,1380	0,1531
30	0,0404	0,0549	0,0640	0,0737	0,0834	0,0944	0,1053	0,1170

TABLE 11.   VALUES OF THE FUNCTIONS $F_c c_f$, $F_c c_F$, $F_{Re**}Re**$ AND $F_{Re_x}Re_x$.

$F_c c_f$	$F_c c_F$	$F_{Re_x**}Re**$	$F_{Re_x}Re_x$	$F_c c_f$	$F_c c_F$	$F_{Re_x**}Re**$	$F_{Re_x}Re_x$
0,0010	0,001117	$2,873 \cdot 10^7$	$5,758 \cdot 10^{10}$	0,0060	0,008205	233,0	$5,679 \cdot 10^4$
0,0015	0,001716	$3,955 \cdot 10^4$	$4,610 \cdot 10^8$	0,0065	0,009105	177,6	$3,901 \cdot 10^4$
0,0020	0,002333	$5,425 \cdot 10^4$	$4,651 \cdot 10^7$	0,0070	0,010012	140,4	$2,796 \cdot 10^4$
0,0025	0,002967	$1,386 \cdot 10^4$	$9,310 \cdot 10^8$	0,0075	0,011014	114,4	$2,078 \cdot 10^4$
0,0030	0,003621	5030	$2,778 \cdot 10^6$	0,0080	0,012016	95,62	$1,592 \cdot 10^4$
0,0035	0,004299	2253	$1,063 \cdot 10^6$	0,0085	0,01304	82,40	$1,251 \cdot 10^4$
0,0040	0,005006	1208	$4,828 \cdot 10^5$	0,0090	0,01409	73,91	$1,006 \cdot 10^8$
0,0045	0,005747	718,0	$2,492 \cdot 10^5$	0,0095	0,01516	62,53	$8,253 \cdot 10^3$
0,0050	0,006528	462,3	$1,417 \cdot 10^5$	0,0100	0,01624	55,47	$6,883 \cdot 10^3$
0,0055	0,007345	319,4	$8,897 \cdot 10^4$	0,0105	0,01742	30,46	$5,838 \cdot 10^3$

In the case of a flow near a thermally insulated wall, we have

$$F_{**} = \left(\frac{T_w}{T_e}\right)^{-n,w}. \qquad (3.127)$$

A comparison of this method with the experimental data, done by the authors of the method, showed that it resulted in a mean-square error which was smallest as compared with the other methods — namely, 9.9%.

To simplify the computation, the necessary auxiliary functions have been tabulated (Tables 9 – 11).

The computational procedure according to the above method is as follows. Given the Mach number M_e and the temperature factor T_w/T_e, we use Table 9 to determine the function F_c. Then using

Equation (3.126) or Table 10, we find the function F_{Re*}, and then — using Formula (3.115) — $F_{Re_{e_x}}$. Finally, from the given Reynolds ($Re**$ or Re_x) and functions F_{Re_x} (or F_{Re**}) and F_c, determined earlier, we use Table 11 to find the values of c_f and c_F.

This method of calculating friction in the turbulent boundary layer on a flat plate does not involve any new physical hypotheses. The expression for the function F_c was assumed to be the same as in the semi-empirical method considered in Section 12. The function F_{Re**} was found in a purely empirical way. All in all, the method can be recommended as a simple engineering method for calculating friction on a flat plate.

§ 15. Relationship between Friction and Heat Transfer on a Flat Plate (Reynolds Similitude). Recovery Factor

The specific thermal flux between a gas and a wall according to the Fourier law can be written in the form

$$q_w = \left(\lambda \frac{\partial T}{\partial y}\right)_w. \tag{3.128}$$

Passing in this equation from the temperature to enthalpy $\left(h = \int_0^T c_p \, dT\right)$ and performing simple rearrangements, we get

$$q_w = \left(\frac{\lambda}{c_p} \frac{\partial h}{\partial y}\right)_w = \frac{\tau_w}{h} \frac{h_e}{U_e} \left(\frac{\partial \bar{h}}{\partial \bar{u}}\right)_w. \tag{3.129}$$

Here

$$\bar{h} = \frac{h}{h_e}, \quad \bar{u} = \frac{u}{U_e}. \tag{3.130}$$

To find the derivative $(\partial \bar{h}/\partial \bar{u})$, we turn to the energy equation in the Crocco variables (2.65)[20]. In the case of a flow of a

Footnote (20) appears on page 180.

homogeneous gas $(\partial c_i/\partial u = 0)$ over a flat plate positioned at a zero angle of attack $(dp/d\xi = 0)$ the equation becomes

$$\rho u (\mu + \varepsilon) \frac{\partial h}{\partial \xi} + \left(1 - \frac{1}{Pr_m}\right) \tau \frac{\partial \tau}{\partial u} \frac{\partial h}{\partial u} - \tau^2 \left[1 + \frac{\partial}{\partial u}\left(\frac{1}{Pr_m} \frac{\partial h}{\partial u}\right)\right] = 0. \qquad (3.131)$$

Here $Pr_m = Pr$ in the laminar sublayer and $Pr_m = Pr_T$ in the turbulent core [see Formulas (1.103) and (2.33)].

Below, for simplicity, we shall assume that the enthalpy h is a function of the velocity u alone, and does not depend on the longitudinal coordinate ξ, i.e., h = h (u). The assumption may be justified if one notes that it is strictly satisfied if the Prandtl number and its turbulent analog are equal to unity. In this case, as we know, we have the Crocco integral. Consequently, one can expect that, for a small deviation of the Prandtl number and its turbulent analog from unity, the dependence of enthalpy on the longitudinal coordinate will be insignificant. Taking advantage of this assumption $(\partial h/\partial \xi = 0)$, we bring (3.131) to the form

$$\left(\frac{\bar{h}'}{Pr_m}\right)' + (1 - Pr_m)\frac{\bar{\tau}'}{\bar{\tau}}\left(\frac{\bar{h}'}{Pr_m}\right) = -\frac{U_e^2}{h_e}. \qquad (3.132)$$

Here

$$\bar{\tau} \cdot \frac{\tau}{\tau_w},$$

and the prime denotes a derivative with respect to the dimensionless velocity $\bar{u}$. The boundary conditions for Equation (3.132) are

$$\left.\begin{array}{l} h = h_w \quad \text{for} \quad \bar{u} = 0, \\ \bar{h} = 1 \quad \text{for} \quad \bar{u} = 1. \end{array}\right\} \qquad (3.133)$$

Integrating Equation (3.132) once, we get

$$\frac{\bar{h}'}{\bar{h}_w} = \exp\left[-\int_0^{\bar{u}}(1 - Pr_m)\frac{d\bar{\tau}}{\bar{\tau}}\right] \times \qquad (3.134)$$

$$\times \left[\left(\frac{\bar{h}'}{\bar{h}_w}\right)_w - \frac{U_e^2}{h_e}\int_0^{\bar{u}}\exp\left(\int_0^{\bar{u}}(1 - Pr_m)\frac{d\bar{\tau}}{\bar{\tau}}\right)d\bar{u}\right].$$

An integration of (3.134) leads to the relation

$$\overline{h}(\overline{u}) = \overline{h}_w + \frac{(\overline{h}')_w}{\Pr_m S(\overline{u})} - \frac{U_e^2}{h_e} R(\overline{u}), \qquad (3.135)$$

where

$$S(\overline{u}) = \left\{ \int_0^{\overline{u}} \Pr_m \exp\left[-\int_1^{\overline{\tau}} (1 - \Pr_m) \frac{d\overline{\tau}}{\overline{\tau}} \right] d\overline{u} \right\}^{-1}, \qquad (3.136)$$

$$R(\overline{u}) = \int_0^{\overline{u}} \Pr_m \exp\left[-\int_1^{\overline{\tau}} (1 - \Pr_m) \frac{d\overline{\tau}}{\overline{\tau}} \right] \times$$
$$\times \left\{ \int_0^{\overline{u}} \exp\left[\int_1^{\overline{\tau}} (1 - \Pr_m) \frac{d\overline{\tau}}{\overline{\tau}} \right] d\overline{u} \right\} d\overline{u}. \qquad (3.137)$$

Using the second of the boundary conditions (3.133), we find from Equation (3.134) the derivative $(h')_w$, which is necessary to determine the thermal flux:

$$(\overline{h}')_w = \Pr_m S(1) \left[1 - \overline{h}_w + \frac{U_e^2}{h_e} R(1) \right]. \qquad (3.138)$$

Substituting the expression (3.138) into the relations (3.134) and (3.129), we obtain

$$\overline{h}(\overline{u}) = \overline{h}_w - (\overline{h}_w - 1)\frac{S(1)}{S(\overline{u})} + \frac{U_e^2}{h_e}\left[\frac{S(1)}{S(\overline{u})} R(1) - R(\overline{u}) \right], \qquad (3.139)$$

$$q_w = -\tau_w S(1) \left[h_e + 2R(1)\frac{U_e^2}{2} - h_w \right] \frac{1}{U_e}. \qquad (3.140)$$

The quantity

$$H_r = h_e + 2R(1)\frac{U_e^2}{2} \qquad (3.141)$$

is usually called the equilibrium enthalpy of a thermally insulated surface or the enthalpy of recovery. The factor

$$r = 2R(1), \qquad (3.142)$$

in the expression for the equilibrium enthalpy (3.141) is called
the recovery factor. The recovery factor characterizes the differ-
ence between the value of the equilibrium enthalpy H_r and the
enthalpy of an adiabatically and isentropically decelerated gas
$He = h_e + Ue^2/2$. In other words, it characterizes the nonadiabaticity
of the flow processes in a boundary layer.

Let us introduce the dimensionless heat transfer coefficient
(Stanton number)

$$c_h = \frac{q_w}{\rho_e U_e (H_r - h_w)}.$$

(3.143)

Then, using the expression for the local friction coefficient c_f
(2.85), we find the following relation from Equation (3.140):

$$\frac{2c_h}{c_f} = S(1).$$

(3.144)

The quantity $S(1)$ is called the Reynolds similitude parameter.

Thus, in order to calculate the local heat flux q_w, one must
know the recovery factor r, the Reynolds similitude parameter $S(1)$,
and the local friction coefficient c_f:

$$q_w = \frac{c_f}{2} \rho_e U_e S(1)\left(h_e + r \frac{U_e^2}{2} - h_w\right).$$

(3.145)

The recovery factor. The general expression for the recovery
factor with a variable Prandtl number Pr_m, in view of Equations
(3.142) and (3.137), has the form

$$r = 2\int_0^1 Pr_m \exp\left[-\int_1^{\bar{u}}(1-Pr_m)\frac{d\bar{\tau}}{\bar{\tau}}\right] \times$$
$$\times \left\{\int_0^{\bar{u}}\exp\left[\int_1^{\bar{u}}(1-Pr_m)\frac{d\bar{\tau}}{\bar{\tau}}\right]d\bar{u}\right\}d\bar{u}.$$

(3.146)

If the generalized Prandtl number Pr_m can be considered constant
over the cross section of a boundary layer, then Equation (3.146)
will be considerably simplified, and after simple rearrangements it
will become

$$r = 2\,\mathrm{Pr}_m \int_0^1 \bar{\tau}^{-\mathrm{Pr}_m - 1} \left(\int_0^{\bar{u}} \bar{\tau}^{-\mathrm{Pr}_m - 1}\,d\bar{u} \right) d\bar{u}.$$

(3.147)

When the generalized Prandtl number is equal to unity ($\mathrm{Pr}_m = 1$) — which, within the framework of the double-layer Prandtl model of the turbulent boundary layer, means that the Prandtl number (Pr) in the laminar sublayer and its turbulent analog (Pr_T) in the turbulent core have been assumed constant and equal to unity — the recovery factor turns out to be equal to unity ($r = 1$), as can be seen from expression (3.147). In this case, the equilibrium enthalpy of a thermally insulated surface is equal to the enthalpy of an adiabatically and isentropically decelerated gas: $H_r = H_e$. Thus, it is only in the case $\mathrm{Pr} = \mathrm{Pr}_T = 1$ that the flow in the boundary layer becomes similar to adiabatic flow.

In the case $\mathrm{Pr}_m = \mathrm{const} \neq 1$ and in order to determine the recovery factor, as can be seen from Equation (3.147), one must know the distribution of the tangential stresses across the boundary layer $\bar{\tau} = \bar{\tau}(\bar{u})$.

As was already noted in Section 10, there is very little information about the character of this distribution, even in the case of an incompressible fluid. According to the experimental data obtained by Klebanov and shown in Figure 2, the relationship between the friction stress and the lateral coordinate is close to linear, and can be approximately described by the expression (3.2). The dependence of the friction stress on the velocity in the turbulent core of the boundary layer has the approximate form shown in Figure 3, and is described by Equation (3.5). As can be seen in Figure 3, for the value $\zeta_0 = 30$ and the velocity range $0 \leq \bar{u} \leq 0.8$, the friction stress varies within the range $0.9 \leq \bar{\tau} \leq 1$, which makes it possible to consider the friction stress in the boundary layer to be approximately constant and equal to its value at the wall. If we make this assumption, then, within the framework of the double-layer model, Equation (3.147) leads to the following expression for the recovery factor:

$$r = Pr_T - (Pr_T - Pr)\,\bar{u}_l^2. \tag{3.148}$$

Here $\bar{u}_l$ is the dimensionless velocity at the boundary of the laminar sublayer, defined by Equation (3.31). We note that in obtaining (3.148) the integration interval $0 \le \bar{u} \le 1$ was subdivided into two intervals: $0 \le \bar{u} < \bar{u}_l$ — laminar sublayer, where $Pr_m = Pr$, and $\bar{u}_l \le \bar{u} \le 1$ — turbulent core, where $Pr_m = Pr_T$[21].

Unfortunately, up to the present time there has been a lack of sufficiently reliable data on the value of the turbulent Prandtl number. The attempts to directly estimate the value of Pr_T from the measurements of the velocity and temperature profiles for a flow of air in tunnels and channels lead to values of Pr_T which are somewhat smaller than unity. However, in experiments on heat transfer in liquid metals one observed $Pr_T > 1$. This deviation of Pr_T from unity is apparently due to the diverse effects of the molecular transfer inside the carriers of turbulent transfer — i.e., finite gas volumes participating in turbulent mixing — on the mechanism of momentum and heat transfer. A certain indeterminacy of the value of Pr_T is sometimes used to obtain a better agreement between theory and experiment through a suitable choice of the Prandtl number. Until the problem of the value of Pr_T is ultimately solved experimentally, one should, as many authors often do, set its value to unity.

Letting $Pr_T = 1$ in the expression for the recovery factor (3.148), we get[22]

$$r = 1 - (1 - Pr)\,\bar{u}_l^2. \tag{3.149}$$

For Prandtl numbers close to unity for the velocity at the boundary of the laminar sublayer $\bar{u}_l$ ranging from 0.2 to 0.8, Equation (3.149) may to within $\pm 10\%$ be replaced by the following simple formula:

Footnotes (21) and (22) appear on pages 180 – 181.

$$r = 1 - (1 - Pr)\,\bar{u}_1^2 \simeq Pr^{\prime\prime}. \tag{3.150}$$

For $Pr = 0.72$ (air), Formula (3.150) leads to a value of the recovery factor $r = 0.895$, which is in good agreement, as will be shown below, with the experimental data.

In addition to using the double-layer model and simple assumptions about the distribution of the friction stresses in the boundary layer, attempts were also made to calculate the recovery factor using a more complex three-layer Karman model [40].

It will be recalled that according to this model [41] the velocity profile in the turbulent boundary layer of an incompressible fluid is divided into three segments: 1) laminar sublayer in which

$$\varphi = \eta \quad \text{for} \quad 0 \leqslant \eta \leqslant 5; \tag{3.151a}$$

2) buffer zone in which

$$\varphi = 5\left[1 + \ln\frac{\eta}{5}\right] \quad \text{for} \quad 5 \leqslant \eta \leqslant 30; \tag{3.151b}$$

3) fully turbulent region:

$$\varphi = 5.5 + 2.5\ln\eta \quad \text{for} \quad \eta > 30. \tag{5.151c}$$

In the paper by Van Driest [42], in the first two regions the friction stress was assumed to be constant and equal to its value at the wall. In the third region, the distribution of the tangential stresses was represented in the form (3.5). The final formula for the recovery factor, obtained by Van Driest, has the form

$$r = Pr_t\left[1 + \frac{2}{\varkappa}\sqrt{\frac{\tau_w}{2}}(1 - Pr_t)\left\{\frac{\varkappa^2}{6} + \frac{3}{2}(1 - Pr_t)\right\} + \right.$$
$$+ 25\frac{\tau_w}{2}\left\{\frac{Pr}{Pr_t} - 1 + 2\ln\left[1 + \frac{5}{6}\left(\frac{Pr}{Pr_t} - 1\right)\right] + \tag{3.152}$$
$$\left. + (\ln 6)\ln\left[1 + \frac{7}{8}\left(\frac{Pr}{Pr_t} - 1\right)\right] - (\ln 6)\ln\left[1 + \frac{1}{4}\left(\frac{Pr}{Pr_t} - 1\right)\right]\right\}\right]$$

140

This formula, as implied by the above discussion, refers to a flow of an incompressible fluid. As shown by Van Driest, Formula (3.152) can be generalized to the case of a compressible gas (without heat transfer) if instead of c_{f0} the quantity c_f multiplied by $(1 + r\frac{\tau-1}{2}M_e^2)$ is introduced in it, where c_f is understood to be the local friction coefficient for a compressible gas. In calculations based on Formula (3.152), it turned out that if the friction coefficient for an incompressible flow, c_{f0}, is used and the value of the turbulent Prandtl number is taken as 0.86, then, within the Reynolds number range $10^5 \leq Re_x \leq 10^8$, the recovery factor will be a constant equal to 0.88. Here the value of the Prandtl number was set equal to 0.71.

The result of taking into account the effect of compressibility on the value of r in Formula (3.152), by having introduced in this formula the friction coefficient c_f for a compressible flow multiplied by $(1 + r\frac{\tau-1}{2}M_e^2)$, is that the values of the recovery factor depend only slightly on the Mach number (for $0 < M_e < 5$) (Figure 30). Figure 30 shows two theoretical curves. The first curve (1) was calculated for the conditions of a wind tunnel (stagnation temperature $T^*_e = 311^\circ$ K), the second for free flight conditions (temperature at infinity $T_\infty = 222^\circ$ K). The difference between these curves is explained by Van Driest as due to the different character of the variation of the molecular Prandtl number in a wind tunnel as compared with free flight.
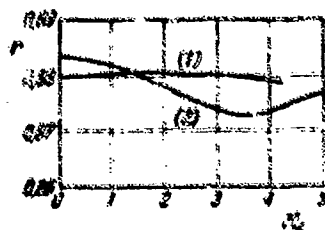

Figure 30.

Experimental data on the recovery factor. The first measurements of the recovery factor were made more than a quarter of century ago. In L. Crocco's paper [42], published in 1941, it was established experimentally — by studying the turbulent boundary layer in a supersonic flow — that the recovery factor ranged from 0.91 to 0.98, where a noticeable dependence of r on the Mach number M_e was observed.

Later a whole series of experimental studies aimed at determining the recovery factor were made. The results of some of those studies, done between 1749 and 1951), are listed in Table 12 which is reprinted from a paper by Kaye [43].

The most accurate measurements of the recovery factor have been made during the past ten-fifteen years.

TABLE 12

Authors	Year	Model	$Re_x \cdot 10^{-6}$	M_e	r
Wimdrow	1949	cone, paraboloid	2.7 4.8 -	2 1.5 2.0	0.885 ± 0.008 0.902 ± 0.005 0.894 ± 0.008
Stolder Rubezin Tendeland	1950	plate	7	2.4	(0.884-0.897 ± 0.007
Hilton	1951	plate	10	2.0	0.880 ± 0.004
Eber	1952	cone, cone-cylinder	1.0 0.25	2.87 4.25	0.92 0.97
Kliris, Sternberg	1952	cone, cone-cylinder	7	2-3.4	0.882 ± 0.007
Sleck	1952	plate	3	2.4	0.906
Stein Scherer	1952	10° cone 40° cone-cylinder	0.4-4 0.3-1	2-3.8 3-3.8	0.882 ± 0.008 0.885 ± 0.011

Pappas' experiments[23]. In the course of the experiments, measurements were made of the surface temperature of a thermally insulated plate and of the Mach number on the outer edge of the boundary layer. The recovery factor was calculated from the formula

Footnote (23) appears on page 181.

$$r = \frac{T_r}{T_e^*} \frac{1 + 0,2 M_e^2}{0,2 M_e^2} - \frac{1}{0,2 M_e^2} \, , \qquad (3.153)$$

where T_e^* is the temperature of an adiabatically and isentropically decelerated gas. The measurements were made at the Mach numbers $M_e = 1.69$ and $M_e = 2.27$. The Reynolds number was varied from 10^6 to 10^7. The results of the measurements are shown in Figures 31 and 32. As can be seen from the diagrams, the recovery factor decreases with an increase of the Reynolds number approximately from 0.90 to 0.89, and a majority of the experimental points lies near the value 0.89.
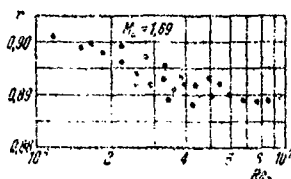
Figure 31
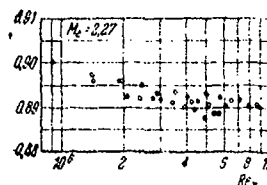
Figure 32.

The Shoulberg, Hill, and Rivas experiments [44]. In the experiments, the recovery factor was measured on a flat plate placed in a wind tunnel. The experimental and computational technique used was the same as in Pappas' paper just considered. The measurements were made within the following range of the Mach and Reynolds number: $1.9 \leq M_e \leq 3.14 \cdot 10^6 \leq Re_x \leq 17 \cdot 10^6$. The results of the experiments are shown in Figures 33 and 34. As can be seen in Figure 33, the recovery factor decreases somewhat with an increase of the Reynolds number. Even though the decrease in the Reynolds number range investigated is only about 0.5%, nevertheless, the tendency toward a decrease can be seen very clearly. As far as the effect of the Mach number on the recovery factor is concerned, as seen in Figure 34, the effect in question is absent in the range of the M_e numbers investigated. The experimental value of the recovery factor (Figure 33) is smaller than its value calculated using Formula (3.150), in which the Prandtl number was determined at the temperature at the wall $T_w = T_r$, by approximately 1%.
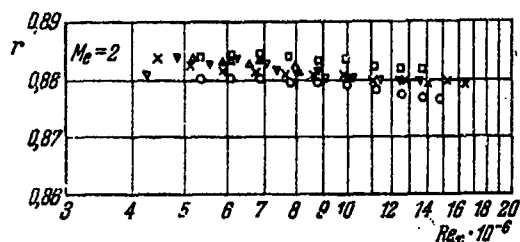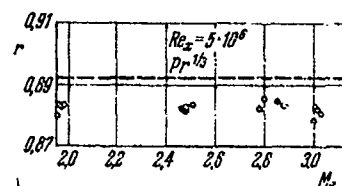
Figure 33

Figure 34

Tendeland's experiments [45]. The measurements were made on the surface of a cylindrical model with a conical nose (cylinder diameter was two inches, cylinder length was 14.75 inches, the cone angle was 20°) in a flow of air with the Mach numbers M_∞ = 3; 3.44; 4.08; 4.56 and 5.04. The local Reynolds numbers per 1 foot (Re_x/foot) were equal to $3 \cdot 10^6$; $4 \cdot 10^6$; $3.6 \cdot 10^6$, $2.8 \cdot 10^6$ and $2.3 \cdot 10^6$, respectively. The recovery factors were calculated from the temperatures measured along the model under equilibrium conditions. The local values of the recovery factors were determined after making corrections for the relatively small radiation losses to the cold lateral wall of the wind tunnel on the basis of the local values of temperatures, local values of the Mach numbers M_e, and the values of the deceleration temperature.

The results of the measurements are shown in Figure 35. The abscissa axis in this figure measures the distance from the nose of the model in diameters. The plots make it clear that, for M_∞ = 3.00, 3.44 and 4.08, the recovery factor varies approximately from 0.88 to 0.89, where the values of r on the conical nose are somewhat smaller than those on the cylindrical portion of the model. For M_∞ = 4.56 and 5.04, the values of r near the junction of the nose with the cylindrical portion are much smaller. This phenomenon is explained by the author of the paper as due to the large pressure drop at the junction and the temperature gradient along the axis of the model, which resulted in a reduction of temperature, and as a result, in a significant error in the determination of r in the region of the junction.
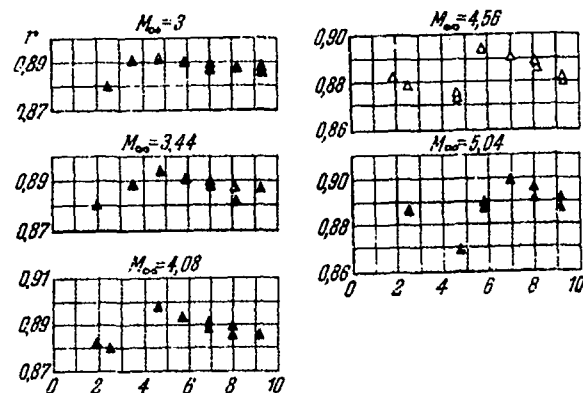
Figure 35.

The Adcock, Peterson, and McRee experiments [46]. The paper presents the results of an experimental investigation of a turbulent boundary layer on a cylinder for the Mach number $M_e = 6$ and the Reynolds numbers, constructed in terms of the distance from the leading edge, $5 \leq Re_x \cdot 10^{-6} \leq 33$. The dependence of the recovery factor on the distance from the leading edge of the model is plotted in Figure 36. Just as in the papers by Pappas, Shoulberg et al. that have been considered above, one observes a tendency toward a decrease of r with an increase of the Reynolds number. The values of the recovery factor in the Reynolds number range investigated lie within $0.875 \leq r \leq 0.895$.
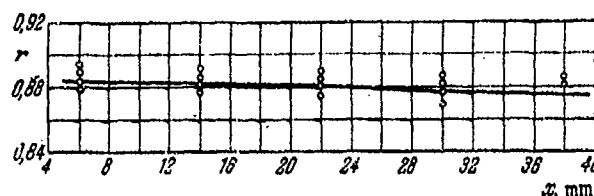
Figure 36.

Summarizing the experimental data obtained by various authors which were discussed above, we can draw the conclusion that the recovery factor depends very slightly on the local Reynolds number Re_x and does not depend at all on the Mach number. In the Reynolds number and Mach number ranges investigated (up to $M_e = 6$), the values

of the recovery factor lie within $0.88 \leq r \leq 0.90$. We should observe the satisfactory agreement between the Van Driest Formula (3.152) and the experimental data in the Mach number range investigated.

In order to develop sufficiently reliable theoretical methods of calculating the recovery factor for supersonic velocities, detailed experimental studies must first be made of the structure of the laminar sublayer and the buffer zone, as well as of the distribution of the friction stresses in the turbulent boundary layer at those velocities.

Until a satisfactory theory of the recovery factor is created and the experimental data at high supersonic velocities are obtained, one should use $0.88 \leq r \leq 0.90$ in calculations.

The Reynolds similitude parameter. A general expression for the Reynolds similitude coefficient, in view of Equations (3.144) and (3.136), has the form

$$\frac{2c_h}{c_f} = \left\{ \int_0^1 Pr_m \exp\left[-\int_1^{\bar{\tau}} (1 - Pr_m) \frac{d\bar{\tau}}{\bar{\tau}} \right] d\bar{u} \right\}^{-1}. \tag{3.154}$$

If the generalized Prandtl number Pr_m is constant, then Equation (3.154) becomes

$$\frac{2c_h}{c_f} = \left(Pr_m \int_0^1 \bar{\tau}^{Pr_m - 1} d\bar{u} \right)^{-1}. \tag{3.155}$$

If the generalized Prandtl number is equal to unity ($Pr_m = 1$), which within the framework of the double-layer Prandtl model implies the assumption

$$Pr = Pr_{\tau} = 1,$$

Equation (3.155) leads to a classical expression for the Reynolds similitude

$$c_h = \frac{1}{2} c_f. \tag{3.156}$$

146

For $Pr_m = const \neq 1$, in order to determine the Reynolds similitude parameter, it is necessary, just as in a calculation of the recovery factor r, to have the distribution of the tangential stresses in the boundary layer, $\bar{\tau}(\bar{u})$. Under the assumption (3.1) ($\tau = const = \tau_w$) and using the double-layer model of the turbulent boundary layer, we obtain from Equation (3. 5) the following expression for the Reynolds similitude parameter

$$\frac{2c_h}{c_f} = [Pr_T - (Pr_T - Pr)\bar{u}_n]^{-1}. \tag{3.157}$$

The turbulent Prandtl number is taken as equal to unity ($Pr_T = 1$). Then expression (3.157) will become

$$\frac{2c_h}{c_f} = [1 - (1 - Pr)\bar{u}_n]^{-1}. \tag{3.158}$$

When $\bar{u}_l$ ranges from 0.4 to 0.9 and the Prandtl numbers are close to unity, the relation (3.158) can, to within $\pm$ 10%, be written more simply as

$$\frac{2c_h}{c_f} = [1 - (1 - Pr)\bar{u}_n]^{-1} \approx Pr^{-k_1}. \tag{3.159}$$

For $Pr = 0.72$ Formula (3.159) gives the value $2 c_h/c_f = 1.24$. Using the same assumptions as those involved in a derivation of Formula (3.152) for the recovery factor, Van Driest[24] obtained the following expression for the Reynolds similitude parameter:

$$\frac{2c_h}{c_f} = \frac{1}{Pr_T}\left[1 + 5\sqrt{\frac{c_f}{2}}\left\{\frac{1}{Pr_T}(1 - Pr_T)\left[\frac{Pr^4}{6} + \frac{3}{2}(1 - Pr_T)\right] + \frac{Pr}{Pr_T} - 1 + \ln\left[1 + \frac{5}{6}\left(\frac{Pr}{Pr_T} - 1\right)\right]\right\}\right]^{-1}. \tag{3.160}$$

This formula, as noted by its author, is valid for $0.7 \leq Pr_T \leq 1$. In it, just as in the calculation of r using Formula (3.152), it is recommended that the turbulent Prandtl number equal to 0.86 be used.

To account for the effect of compressibility and heat transfer on the Reynolds similitude parameter one should, according to Van Driest, introduce in the expression (3.160) a factor $(T_w/T_r)\left[1 + r\frac{k-1}{2}M^2\right]$.

Footnote (24) appears on page 161.

multiplying c_f. c_f should be understood to mean the local coeffi-
cient in a compressible gas.

The results of the calculation of $2c_h/c_f$ according to Formula
(3.160) for the conditions present in a wind tunnel ($T^*_e = 338°$ K,
curve 1) and in free flight ($T_e = 500°$ K, curve 2) for various Mach
numbers are shown in Figure 37. Figure 38 shows the results of
calculations based on Formulas (3.157), (3.158), (3.159) and (3.160)
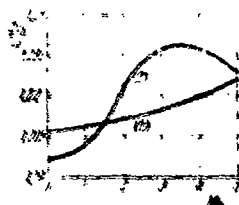for a flow of an incompressible fluid as functions of the Reynolds
number.

Figure 37
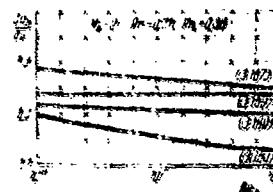
Figure 38

To evaluate the accuracy of the formulas given above, let us
turn to the experimental data.

<u>Experimental data on the Reynolds similitude parameter</u> $2c_h/c_f$.
The experimental data on heat transfer and friction obtained by
various workers up to 1954 have been analyzed by Seiff [47]. On the
basis of the results of this analysis (see Figure 39), Seiff arrived
at the conclusion that in the turbulent boundary layer the experi-
mental data can be represented by the formula to within 15 - 20%:

$$\frac{2c_h}{c_f} = Pr^{-0.67}$$ (3.161)

or

$$\frac{2c_h}{c_f} = 1.22.$$

It should be noted that the experimental data used by Seiff were
obtained for the following Mach number range $0 \le M_e \le 4$.
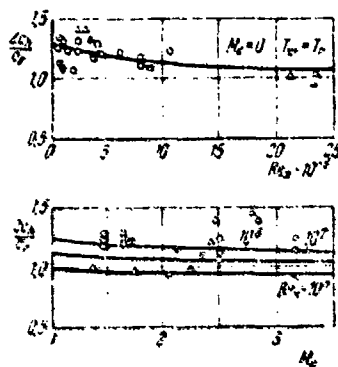
Figure 39

Due to the scarcity of the experimental data and their low accuracy, Seiff failed to establish a relation between the Reynolds similitude coefficient $2c_h/c_f$, on one hand, and the Reynolds, Mach numbers and the temperature factor, on the other.

Relatively recently, L. V. Kozlov [48], on the basis of an analysis of experiments involving a direct simultaneous measurement of the local values of the thermal fluxes and friction, proposed the following more accurate relation between the Reynolds similitude parameter and the parameters listed above:

$$\frac{2c_h}{c_f} = Pr_w^{-0.41} \, 0.695 \, Re_{xw}^{0.20-0.04} \cdots Re_{xw} \left(\frac{T_p}{T_e}\right)^{-0.60}. \tag{3.162}$$

For $T_w/T_e = 1$, $M_e = 0$ and $Re_{xw} = 4.37 \cdot 10^6$, Formula (3.162) changes into Formula (3.161), and the latter has been thoroughly verified in numerous experiments on the flow of an incompressible fluid in tubes and over flat plates.

Formula (3.162) was obtained by L. V. Kozlov for the following parameter ranges: $1.7 \leq M_e \leq 4$; $5 \cdot 10^5 < Re_{xw} < 2 \cdot 10^7$; $0.5 \leq T_w/T_p \leq 1$. The effect of the individual parameters on ratio $2c_h/c_f$ can be seen in Figure 40, in which, just as in Figure 39, all plots were obtained on the basis of Formula (3.162), and c_h and c_f were determined from the conditions on the boundary of the boundary layer.

Figures 40 and 39 imply that, with an increase of the Mach and Reynolds numbers, M_e and Re_x, the value of $2c_h/c_f$ decreases, approaching values close to unity. The fact that at large Mach numbers the Reynolds similitude parameter is close to unity has also been confirmed by the experimental data obtained by Hill on a flat plate for
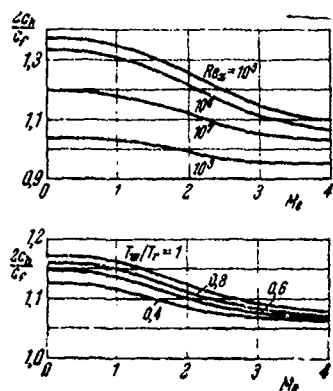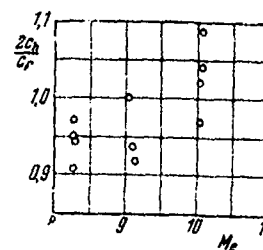
Figure 40

Figure 41

$8 \leq M_e \leq 10$ (Figure 41). The values of the parameter $2c_h/c_f$, as seen in Figure 41, lie in the range $0.9 \leq 2c_h/c_f \leq 1.1$.

An analysis of the theoretical and experimental data given above shows that, in spite of the well-known achievements in this area, the problem of the relationship between heat transfer and friction as a whole requires further theoretical and experimental investigation.

§ 16. Turbulent Boundary Layer on a Cone at Zero Angle of Attack

Along with a flow near a flat plate, another case simple enough for theoretical analysis involves a flow near a cone, positioned at zero angle of attack, if the cone angle is such that the front shock wave forming the head of the cone is attached (Figure 42). In this case, the flow of a gas behind the shock wave will be "conical", and the pressure on the surface of the cone will be constant. This makes the flow in a boundary layer on a cone resemble a flow near a flat plate. As shown by Van Driest [49], there is a simple approximate rule for converting the local friction coefficient for a plate to the analogous coefficient for a cone.

In order to establish this rule, let us turn to the integral momentum relation (2.80). In the case of a cone with an impermeable

surface ($v_w = 0$), the relation takes the form

$$\frac{d\delta^{\bullet\bullet}}{dx} + \frac{\delta^{\bullet\bullet}}{x} = \frac{\tau_w}{\rho_e U_e^2}. \qquad (3.163)$$

Here we used the fact that $r_w = x \sin \theta$ (Figure 42): θ is the half-angle at the vertex. Equation (3.163) can be easily transformed to the form

$$\mathrm{Re}_x \, d\,\mathrm{Re}_x = \frac{\rho_e}{\rho_w} \zeta^2 d\,(\mathrm{Re}^{\bullet\bullet} \mathrm{Re}_x). \qquad (3.164)$$

where the parameter ζ is given by Equation (3.8), and the Reynolds numbers Re_x and Re^{**} are given by Equations (3.18) and (3.17).

If we assume that the mechanisms of flow in the boundary layers around a cone and on a plate are identical (have vanishing gradients, i.e., $dp/dx = 0$), then one may expect that the functional expressions for the velocity profile and the momentum loss thickness for these bodies will also be the same. In this case Equation (3.52), obtained for a flat plate, may be used for the Reynolds number Re^{**}. Making a somewhat rough approximation (just as in Section 12), i.e., neglecting the second term on the right-hand side of Equation (3.52), we obtain

$$\mathrm{Re}^{\bullet\bullet} \approx \frac{e^{\kappa_1}}{\beta \kappa^2} \frac{\rho_w}{\mu_w} \exp\left[\kappa \zeta I\left(1\right)\right]. \qquad (3.165)$$

Figure 42

Upon substituting expression (3.165) in Equation (3.164) and integrating the latter with the same accuracy as in Section 12, we obtain an analog of Equation (3.57) for a cone:

$$C_1 \frac{e^{-\kappa_1}}{\beta \kappa^2} \frac{\rho_w}{\mu_w} \frac{\mu}{\mu_w} \zeta^2 \exp\left[\kappa \zeta I\left(1\right)\right] = \frac{1}{2}\,\mathrm{Re}_x. \qquad (3.166)$$
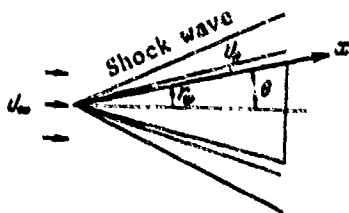
Since the parameter ζ is equivalent to the local friction coefficient c_f [see Formula [3.81)], then a comparison of Equations (3.166) and (3.57) yields a simple rule according to which the local friction coefficient for a cone is equal to the value of this coefficient for a flat plate calculated for the Reynolds number Re_x equal to one half of its value for the cone, and the same values of the temperature factor and the Mach number at the outer boundary of the boundary layer.

If one compares the local friction coefficients for a cone and a plate at identical Reynolds numbers and identical values of the temperature factor, and the Mach numbers at the outer boundary, then it turns out that, for a cone, these coefficients exceed their values for a flat plate by 10 - 15%.

An analysis of the relationship between the local and average friction coefficients for a cone and a plate involving the use of the integral momentum relation, power-law velocity profiles, and the drag law was done by Bradfild [50]. As a result, he obtained the relation

$$\frac{c_{fk}}{c_{fu\,t}} = \left[\frac{2(n+2)}{n+1}\right]^{\frac{2}{n+3}}, \qquad (3.167)$$

where $1/n$ is the exponent in the expression for the velocity profile $u/U_e = (u/\delta)^{1/n}$. For $n = 7$, Equation (3.167) yields $c_{fk}/c_{fpl} = 1.18$. When n changes from 5 to 10, the ratio c_{fk}/c_{fpl} changes from 1.13 to 1.23.

For the average friction coefficients, it was established that

$$\frac{c_{Fk}}{c_{F\,u\,t}} = 2\left[\frac{n+1}{2(n+2)}\right]^{\frac{n+1}{n+3}}. \qquad (3.168)$$

For $5 < n < 10$ Equation (3.168) implies that $1.035 < c_{Fk}/c_{F\,pl}$; for $n = 7$, $c_{Fk}/c_{F\,pl} = 1.06$.

Along with the analysis mentioned above, Bradfild's paper gives the results of measurements of the local friction coefficient for a cone with tha half angle at the vertex equal to 15°, Mach number $M_e = 3.7$, and various Reynolds numbers. The results of the measurements are shown in Figure 43 (open circles), solid circles indicate the results of the measurements done by Coles[25] on a flat plate under the same conditions; the dashed line represents the plot of $c_{fk} = 1.18 c_{fpl}$. As seen in Figure 43, friction on a cone exceeds the friction on a plate by approximately 28%. Apparently, both the Van Driest rule and Bradfild's relation (3.167) result in magnitudes of friction on a cone that are somewhat understated as compared with their actual values.

A more definite conclusion regarding the problem in question can, apparently, be drawn only after new experimental data are obtained.

§ 17. Turbulent Boundary Layer in the Presence
of a Longitudinal Pressure Drop

The problem of the turbulent boundary layer calculations in the presence of an arbitrary distribution of the longitudinal velocity component at the outer boundary of the layer, including the most difficult part of the problem — namely, a determination of the point (line) of separation — even for an incompressible fluid is still far from a complete solution[26].

The effects of compressibility and heat transfer between gas and a surface complicate the problem even more, leading to additional difficulties whose character was described in the preceding sections. The existing methods used in turbulent boundary layer calculations for high-velocity gas flows in the presence of a longitudinal pressure drop and heat transfer between the gas and the surface usually represent a generalization and a further development

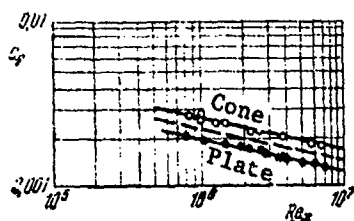Footnotes (25) and (26) appear on page 181.

153

Figure 43.

of the methods used in turbulent boundary layer calculations for an incompressible fluid. A characteristic feature of a majority of these methods is the fact that they use integral relations (for momentum, energy, angular momentum). The number of unknowns appearing in those integral relations usually exceeds the number of equations. Therefore, it is of basic importance in these methods to select families of the velocity and temperature profiles that could be used for substitution in the integral relations, instead of the actual ones that remain unknown. In the present state of the theory, even that selection is a difficult problem. In order to specify the velocity fields, in addition to the semi-empirical theory of turbulence proposed by Prandtl and Karman, sometimes single-term power-law formulas with a constant[27] or variable exponent depending on various parameters are used.

Detailed development of the semi-empirical method for turbulent boundary layer calculations in a gas in the presence of heat transfer and arbitrary pressure distribution in the outer flow was given by L. Ye. Kalikhman [51]. According to this method, based on the formula used in Prandtl's semi-empirical theory, a determination of friction and heat transfer in a boundary layer reduces to solving linear differential equations which are approximately equivalent to the integral momentum and energy relations, followed by a transition from the functions found to those that are still unknown (i.e., friction and heat transfer coefficients) using auxiliary tables and graphs.

A method proposed by S. S. Kutateladze and A. I. Leont'yev [52], based on the limiting laws of friction and heat transfer,

---

Footnote (27) appears on page 181.

and designed for turbulent boundary layer calculations on a curvi-
linear surface, is essentially akin to the semi-empirical methods.

The papers by McLafferty and Barber [53] and by Sasman and
Cresci [54] are an example of the empirical approach to the problem
in question. In the latter paper, the well-known empirical formula
proposed by Ludwig and Tillman which related the drag coefficient
to the momentum loss thickness δ^{**} and the form parameter $H^* = \delta^*/\delta^{**}$
in the theory of the turbulent boundary layer for an incompressible
fluid is used as the drag law. A generalization of this formula to
include a flow with variable density is done using the defining
temperature method, proposed by Eckert [55]. Characteristics of the
turbulent boundary layer in Sasman and Cresci's paper are found by
simultaneously solving the integral momentum and angular momentum
relations.

Among other methods used in the theory of the turbulent boundary
layer in the presence of a longitudinal pressure gradient, one
should mention a method proposed by V. M. Ievlev [56].

Referring the reader for details to the original sources, we
should note a feature which is characteristic of a majority of the
methods. It is the fact that single-parameter families of velocity
profiles are used. This is apparently one of the main reasons for
the unsatisfactory results obtained in many cases when these methods
of boundary layer calculations are applied to pre-separation regions.
As far as the two- and many-parameter methods are concerned, they are
at the present time in their beginning stage of development.

In evaluating the state of the problem as a whole, we can con-
clude that the existing methods used in the theory of the turbulent
boundary layer in supersonic gas flows for an arbitrary pressure
distribution in the outer flow and heat transfer between a gas and a
surface lead to more or less satisfactory results only in those
cases when the effect of the longitudinal pressure gradient on the
form of the velocity profile is small.

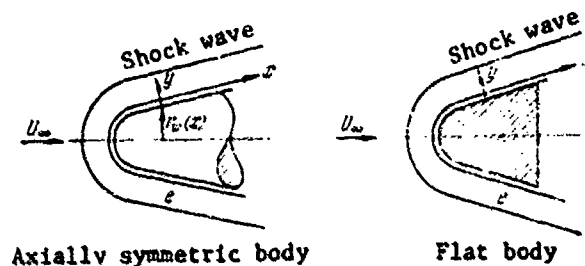Axially symmetric body   Flat body

Figure 44

Taking the above into account, we shall limit our attention here to a presentation of those computational methods in which the effect of the longitudinal pressure gradient on friction is accounted for only through the integral momentum relation, and the direct effect of the pressure gradient on the velocity profile is neglected. These assumptions, as shown in experiments, are approximately valid for flows with negative and small positive pressure gradients. The latter restriction means essentially that pre-separation and separated flows are excluded from the discussion.

Computational method based on the linearized integral momentum relation. Let us consider a steady gas flow over a curvilinear surface (Figure 44). We shall introduce a curvilinear coordinate system. The position of a point in the flow will be characterized by the x coordinate measured along the surface from the critical point, and the y coordinate measured along the normal to the surface.

Let us turn to the integral momentum relation (2.80), which in the case of a flow near an impermeable surface ($v_w = 0$) becomes

$$\frac{d\delta^{**}}{dx} + \frac{u'_e}{U_e}(2 + H^* - M_e^2)\delta^{**} = \frac{\tau_w x}{\rho_e} \delta^{**} - \frac{\tau_w}{\rho_e U_e^2} . \tag{3.169}$$

For later discussion, it is convenient to write Equation (3.169) in a somewhat modified form which is obtained by eliminating the term involving M_e^2 from this equation with the aid of Equation (2.79). Omitting these simple rearrangements, the result is

$$\frac{1}{\rho_e U_e}\frac{d}{dx}(\rho_e U_e \delta^{**}) + \delta^{**}\left[\frac{U_e'}{U_e}(1+H^*) + \frac{(r_w^\nu)'}{r_w^\nu}\right] = \frac{1}{\zeta^2}\frac{\rho_w}{\nu_e}.$$
(3.170)

Here ζ is given by Equation (3.8).

Furthermore, applying the technique introduced by L. Ye. Klikhman in the paper already quoted in this section, we introduce a new variable

$$z = \rho_e U_e \delta^{**}\zeta^2.$$
(3.171)

The first term on the left-hand side of Equation (3.170) can with the aid of (3.171) be written as

$$\frac{1}{\rho_e U_e}\frac{d}{dx}(\rho_e U_e \delta^{**}) = \frac{1}{\rho_e U_e \zeta^2 A}\frac{dz}{dx}.$$
(3.172)

Here we use the notation

$$A = \frac{d \ln z}{d \ln (\rho_e U_e \delta^{**})} = 1 + \frac{2}{\frac{d \ln (\rho_e U_e \delta^{**})}{d \ln \zeta}}.$$
(3.173)

Using Equation (3.172), we transform the integral momentum relation (3.170) to the following form

$$\frac{dz}{dx} + A\left[\frac{U_e'}{U_e}(1+H^*) + \frac{(r_w^\nu)'}{r_w^\nu}\right]z = \rho_w U_e A.$$
(3.174)

It should be noted that the differential Equation (3.174) for the function z is just as exact as the starting Equation (3.169).

Before proceeding to the question of integration of Equation (3.174), one must establish the dependence of parameters A and H*, involved in this equation, on the unknown function z. To establish this dependence, one must know the drag "law", i.e., the relationship between the momentum loss thickness (δ^{**}) and friction (ζ). Since here we only discuss those flows in which the direct effect of a longitudinal pressure gradient on the form of the velocity profile is

significant, then it is obvious that the drag law for a flat plate
(3.52), established in Section 12, may be used as the drag law here.
One must only keep in mind that the parameters $U_e(x)$, $\omega(x)$, $\beta(x)$,
etc. at the outer boundary of the boundary layer are in this case
variables. In addition, just as in Section 12, we use the "approxi-
mate" expression for the drag law for simplicity, omitting the second
term in brackets in Equation (3.52). In order to compensate for the
error thus introduced, we put a certain constant C_1 in the drag law,
whose reasonable selection will enable us later to make the result
obtained more accurate [it will be noted that a similar technique was
used by Karman in deriving the drag law (3.59)]. The drag law thus
transformed will have the form

$$\delta^{**} = C_2 \frac{\mu_w}{\rho_e U_e} \exp\left[\varkappa \zeta I(1)\right], \quad C_2 = C_1 \frac{e^{-\varkappa \varkappa}}{\varkappa^2}. \tag{3.175}$$

Here $I(1)$ is given by Equation (3.54), and ω and β, involved in the
expression (3.54), are given by the ratios (3.48) or (3.49).

Substituting the expressions for the momentum loss thickness
(3.175) in Equation (3.174), we obtain a relation between z and the
friction parameter ζ:

$$z = C_2 \mu_w \zeta^2 \exp\left[\varkappa \zeta I(1)\right]. \tag{3.176}$$

As seen from Equations (3.176), the dependence of the friction
parameter ζ on z is essentially logarithmic, and this enables us
to limit ourselves to an approximate determination of the function
$z(x)$. As a result, in calculating the parameter H^*, one can use
its expression applicable to a flat plate (3.55), which is fully
justified in the approximate approach taken here.

The expression for the function A (3.173), upon substitution
of the drag law (3.175) in it, becomes

158

$$A = 1 + \frac{1}{x\zeta I(1)}.$$

<div align="right">(3.177)</div>

The dependence of the functions H^* and A on the friction parameter ζ, and consequently, through Equation (3.176), on the unknown function z reduces the problem of determining this function to integration of a very complicated nonlinear equation (3.174). Exact integration of this equation is very difficult, and, as will be seen below, is not necessary. A simplification may be achieved due to the fact that the functions H^* and A depend on the friction parameter ζ very slightly. This permits us to approximately determine H^* and A for the values of the parameter ζ calculated using the formulas for the flat plate (Section 12). Regarding the parameters β and ω [see Equations (3.48), (3.49)] on which, along with the parameter ζ, H^* and A are dependent, they must be computed for each section of the boundary layer from the local values of the Mach number M_e and the temperature factor T_w/T_e. Thus, the functions A and H^* may be considered to be known functions of the longitudinal x coordinate before we proceed to integrate Equation (3.174).

This approximate method of determining the parameters A and H^*, as shown by estimates given below, will not result in any significant errors, and the function $z(x)$ is determined from Equation (3.174).

Let us determine the expression for the parameter A in the case of flow of an incompressible fluid over a flat plate under isothermal conditions. Noting that in this case $I(1) = 1$, and using the drag Formula (3.80), we obtain from (3.177)

$$A = 1 + \frac{2}{x\zeta_0} = 1 + 3{,}54\sqrt{c_{f0}} = 1 + 0{,}575 \mathrm{Re}_x^{-1/14}.$$

<div align="right">(3.178)</div>

Expression (3.178) implies that, when the Reynolds number changes by two orders (from 10^5 to 10^7), the value of A changes by 6% (from 1.25 to 1.18). In the general case of compressible gas flow in the presence of heat transfer between the gas and the surface, the

parameter A will not vary too significantly under real conditions.

The results of calculating the parameter H* from Formula (3.55) for the case of air flow over a flat plate for

$$M_e = 1.69, \quad T_w/T_e = 1.66 \qquad \text{and} \qquad M_e = 2.27, \quad T_w/T_e = 2.15$$

are given in Figure 27. The same figure includes the experimental points obtained by Pappas for the same flow conditions. As seen in Figure 27, the parameter H* hardly depends on the Reynolds number, and, consequently, hardly depends on the friction parameter ζ. The fact that H* hardly depends on the parameter ζ has been amply verified by experiment also in the case of flow of an incompressible fluid over a plate. Thus, measurements done by Schultz-Grunow [57] and Hama [58] on flat plates indicate that, when the parameter ζ_0 changes from 18 to 30, the parameter H* changes from 1.5 to 1.25. The results of applying Formula (3.55) to a flow of an incompressible fluid are also in satisfactory agreement with the experimental data.

The results of this analysis of the behavior of H* and A can be written in the form

$$\left. \begin{aligned} H^* &\left[M_e, \frac{T_w}{T_e}, \zeta\left(M_e, \frac{T_w}{T_e}, \mathrm{Re}_x\right) \right] \approx \\ &\approx H^*\left[M_e, \frac{T_w}{T_e}, \zeta_{\mathrm{pl}}\left(M_e, \frac{T_w}{T_e}, \mathrm{Re}_x\right) \right], \\ A &\left[M_e, \frac{T_w}{T_e}, \zeta\left(M_e, \frac{T_w}{T_e}, \mathrm{Re}_x\right) \right] \approx \\ &\approx A\left[M_e, \frac{T_w}{T_e}, \zeta_{\mathrm{pl}}\left(M_e, \frac{T_w}{T_e}, \mathrm{Re}_x\right) \right]. \end{aligned} \right\} \qquad (3.179)$$

In these formulas, the subscript "pl" indicates that the quantity in question should be determined, using formulas obtained for flow over a flat plate.

If we use the approximate method of determining the parameters H* and A, as expressed in Equations (3.179), then the problem of finding z(x) reduces to integration of the following linear differential equation of first order with variable coefficients:

$$\frac{dz}{dx} + P(x)\,z = Q(x).$$

$$(3.180)$$

where

$$P(x) = A\left[\frac{U_e'}{U_e}(1 + H^*) + \frac{(r_w^v)'}{r_w^v}\right], \quad Q(x) = \rho_w U_e.1.$$

$$(3.181)$$

Integrating (3.180), we obtain

$$z = \exp\left[-\int_{x_t}^{x} P(x)\,dx\right]\left\{\int_{x_t}^{x} Q(x)\exp\left[\int_{x_t}^{x} P(x)\,dx\right]dx + C\right\}.$$

$$(3.182)$$

Here x^t is the coordinate specifying the location of the point where the laminar boundary layer changes into the turbulent layer. The constant of integration C follows, as usual, from the continuity condition for the momentum loss thickness δ** at the transition point. As a result, we obtain

$$z = \exp\left[-\int_{x_t}^{x} P(x)\,dx\right]\times$$
$$\times\left\{\int_{x_t}^{x} Q(x)\exp\left[\int_{x_t}^{x} P(x)\,dx\right]dx + \rho_w U_{et}\zeta_t\delta_t^{**}\right\},$$

$$(3.183)$$

where the parameters ζ_t and δ_t^{**} must be found from the theory of the laminar boundary layer.

If the laminar region is absent (for $x_t = 0$ $\delta_t^{**} = 0$), then Equation (3.183) is somewhat simpler and becomes

$$z = \exp\left[-\int_0^x P(x)\,dx\right]\int_0^x Q(x)\exp\left[\int_0^x P(x)\,dx\right]dx.$$

$$(3.184)$$

The integrals appearing in Equations (3.183) and (3.184) can be evaluated using either numerical or graphic methods.

For flow over a flat plate at zero angle of attack ($dU_e/dx = 0$, $v = 0$), Equation (3.184), in view of Equations (3.181) and (3.177), becomes

$$z = \rho_e U_e\int_0^x A\,dx = \rho_e U_e\int_0^x\left[1 + \frac{2}{x_t^v}I(1)\right]dx.$$

$$(3.185)$$

For an incompressible fluid, if the expression in (3.178) is used for
A, the integral on the right-hand side of Equation (3.185) is easily
evaluated, whereupon we obtain

$$z_0 = \rho_e U_e x \, (1 + 0.62 \, \mathrm{Re}_x^{-1/14}). \qquad (3.186)$$

When the Reynolds number (Re_x) varies from 10^5 to 10^7, the expression
in parentheses in Equation (3.186) varies from 1.27 to 1.20. Conse-
quently, we see that with a sufficient degree of accuracy

$$z_0 = 1.24 \rho_e U_e x. \qquad (3.187)$$

After the distribution of the parameter $z(x)$ over the surface
of a body is found from Equation (3.183) (of (3.184, Formula (3.176)
can be used to determine the dependence of the friction parameter ζ
on the longitudinal coordinate, and then Equation (3.8) can be used
to yield the friction coefficient $c_f(x)$. However, a direct use of
Equation (3.176) is inconvenient because it involves the solution of
a logarithmic equation. In order to simplify the calculation of
friction, we shall write expression in (3.176) in a different form.

Taking the logarithm of Equation (3.176), and passing from ζ
to c_f with the help of Equation (3.8), we obtain

$$\varkappa \sqrt{2}(\lg e)\left(\frac{\mu_w}{\mu_e}\right)^{1/2} I(1) c_f^{1/2} + 2\lg(c_f^{1/2}) = C_3 + \lg\left(\frac{\rho_e}{\rho_w}\frac{z}{\mu_w}\right),$$
$$C_3 = \lg C_1.$$

Upon performing simple calculations and introducing

$$K = \left(\frac{\mu_w}{\mu_e}\right)^{1/2} I(1). \qquad (3.188)$$

we obtain

$$\frac{0.219 K}{\sqrt{c_f}} + 2\lg\frac{1}{\sqrt{c_f}} = C_3 + \lg\left(\frac{\rho_e}{\rho_w}\frac{z}{\mu_w}\right). \qquad (3.189)$$

The constant C_3 can be determined from the condition that Formula
(3.189) coincide with Karman's Formula (3.59) for a flat plate in an

incompressible fluid. In view of Equation (3.187), upon comparing
Equation (3.189) with Equation (3.59), we find that $C_3 = 0.30$.
Equation (3.189) can be reduced to an equation with one parameter.
Dividing both sides of this equation by two and then adding $\lg(0.121\ K)$
to both sides, we get

$$N + \lg N = -0{,}767 + \lg\left(K\sqrt{\frac{\rho_e}{\rho_w}\frac{z}{\mu_w}}\right),\tag{3.190}$$

where

$$N = \frac{0{,}121 K}{\sqrt{c_f}}.\tag{3.191}$$

Solving Equation (3.191) for c_f, we get

$$c_f = \left(\frac{0{,}121 K}{N}\right)^2.\tag{3.192}$$

The function N can be easily found from Equation (3.190) in terms of
the known right hand side of this equation with the help of a table of
decimal logarithms.

An even greater simplification of the computational procedure can
be achieved by replacing the left-hand side of Equation (3.190) with
a simpler approximate expression. As shown in the calculations,
when N ranges from 1 to 4 (which in flow over a flat plate corresponds
to a variation of the Reynolds, Mach numbers and the temperature
factor within the ranges: $10^5 \le \mathrm{Re}_x \le 10^8;\ 0 \le M_e \le 10;\ 0.1 \le T_w/T_r \le 1$)
the left hand side of Equation (3.190) can be written with a
sufficient degree of accuracy in the form

$$N + \lg N = 0{,}15 + 1{,}2N.\tag{3.193}$$

The maximum error made in such approximation is 5% for N = 1. On the
average, however, the error varies from 2 to 1%.

Using Equation (3.193), after simple calculations, we obtain
instead of (3.192) the following expression for the friction coeffi-
cient:

$$c_f = \left[\frac{0.145K}{\lg\left(0.242K\sqrt{\frac{\rho_e}{\rho_w}\frac{z}{\mu_w}}\right)} \right]^2.$$

(3.194)

Closing this presentation of the computational procedure, we note that one of the functions of N, which determines friction, is related to z in an almost logarithmic fashion. This fact justifies the approximate method of determining z on the basis of linearization of the integral momentum relation that was used here.

In closing, we shall briefly list the basic steps of the calculation using the method presented above.

1. Given the parameters of the external flow [M_e (x) and T_e (x)] and the conditions at the wall (T_w), Formulas (3.48) and (3.49) are used to determine $\beta(x)$ and $\omega(x)$. The recovery factor r in Formulas (3.49) should be taken as equal to 0.89.

2. Given $\beta(x)$ and $\omega(x)$ and the local Reynolds number $Re_x = U_e \rho_e x/\mu_e$, Formula (3.85) is used to find the local friction coefficient at the plate $c_{f\,pl}$, and Formula (3.8) — to find the friction parameter $\zeta_{pl}(x)$. We determine the functions I(1) [Equation (3.54)] and K(x) [Formula (3.79)] which are needed later. The density ratio ρ_w/ρ_e is found from Equation (3.50), the viscosity μ — from Equation (3.61).

3. From $\beta(x)$, $\omega(x)$ and $\zeta_{pl}(x)$ we determine H*(x) and A(x) using Formulas (3.55) and (3.177).

4. Formulas (3.181) are used to calculate the coefficients P(x) and Q(x). Here $U_e(x)$, $U'_e(x)$, $r_w(x)$ and $r'_w(x)$ must be known.

5. From Equation (3.183) [or (3.184) if the laminar and buffer zones are absent from the boundary layer], we determine the function z(x). The integrals in Equation (3.183) [or in Equation [3.184)]

are found using numerical or graphic methods.

6. Formula (3.194) is used to determine the distribution of the local friction coefficient $c_f(x)$ over the surface of a body. If the friction coefficient is determined using the more accurate Formula (3.192), then it is necessary to first determine the function $N(x)$ from Equation (3.190) in terms of its known right-hand side. Equation (3.190) is solved using the tables of decimal logarithms.

The following data must be given initially: $U_e(x)$, $U'_e(x)$, $r_w(x)$, $r'_w(x)$, $T_e(x)$ and T_w. Instead of $U_e(x)$ and $U'_e(x)$, we may be given the Mach number at the outer boundary of the boundary layer, $M_e(x)$, and its derivative with respect to the longitudinal coordinate, $M'_e(x)$, which are related to the former by Equation (2.83).

From the distribution $c_f(x)$ thus found, one can determine the friction coefficient using the parameters of the oncoming flow:

$$c_{f\infty} = \frac{2\tau_w}{\rho_\infty U_\infty^2} = c_f \frac{\rho_e}{\rho_\infty} \left(\frac{U_e}{U_\infty} \right)^2. \tag{3.195}$$

Method of successive approximations. On the basis of the same initial assumptions as in the preceding method, i.e., considering only flow with moderate longitudinal pressure gradients, one can propose the following method of calculation based on a simple transformation of the integral momentum relation to a form permitting a determination of friction by the method of successive approximations. The first such transformation was used by K. K. Fedyayevskiy and A. S. Ginevskiy [59] to calculate friction in a turbulent boundary layer of an incompressible fluid, and then applied by Yu. V. Lapin to calculate friction in a compressible gas [60].

Let us turn to the momentum Equation (3.170). Introducing in it the new variable

$$\theta = \rho_e U_e \delta^{**} e^\Omega, \quad \Omega = \int_{x_1}^{x} \left[\frac{U'_e}{U_e} (1 + H^*) + \frac{(r_w^*)'}{r_w^*} \right] dx, \tag{3.196}$$

we reduce it to the form

$$\frac{d\theta}{dx} = \frac{e^{\Omega}}{\zeta^2} \rho_w U_e.$$ (3.197)

Integrating Equation (3.197) and passing from θ back to δ^{**}, we obtain

$$\rho_e U_e \delta^{**} = e^{-\Omega} \left(\int_{x_t}^{x} \frac{e^{\Omega}}{\zeta^2} \rho_w U_e dx + \rho_{et} U_{et} \delta_l^{**} \right),$$ (3.198)

where the subscript t signifies that the parameters refer to the point where the laminar layer transfers into the turbulent layer, where δ_t^{**} is determined using the theory of the laminar layer.

Substituting now the expression for the momentum loss thickness (3.175) in the left-hand side of (3.198), we obtain

$$C_2 \mu_w \exp\left[\varkappa \zeta I(1)\right] = e^{-\Omega} \left(\int_{x_t}^{x} \frac{e^{\Omega}}{\zeta^2} \rho_w U_e dx + \rho_{et} U_{et} \delta_l^{**} \right).$$ (3.199)

Taking the logarithm of (3.199), and passing from ζ to c_f with the aid of (3.8), we obtain after simple rearrangements

$$\frac{0.242K}{\sqrt{c_f}} = C_3 + E,$$ (3.200)

where K is given by Equation (3.79), and the function E involving the unknown friction coefficient c_f has the form

$$E = \lg\left[\frac{e^{\Omega}}{\mu_w} \left(\frac{1}{2} \int_{x_t}^{x} e^{\Omega} \rho_e U_e c_f dx + \rho_{et} U_{et} \delta_l^{**} \right) \right].$$ (3.201)

The value of the constant C_3 must be taken the same as in the preceding method, i.e., $C_3 = 0.3$. Having this in mind, it is easy to obtain from Equation (3.200) the following expression for the friction coefficient:

$$c_f = \left(\frac{0.242K}{0.3 + E} \right)^2.$$ (3.202)

In the case where there are no laminar and buffer zones in the boundary layer ($x_t = 0$, $\delta_t^{**} = 0$), the expression for the function E simplifies to

$$E = \lg\left(\frac{1}{2} \frac{c}{\mu_w} \Omega \int_0^x c_f \rho_e U_e c^\Omega dx\right). \qquad (3.203)$$

The exponent Ω, given by the second of Equations (3.196), involves the parameter $H^* = \delta^*/\delta^{**}$. This parameter can be calculated, just as in the preceding method, using Formula (3.55).

Equation (3.202) enables us to use the method of successive approximations in calculating friction. As the zero-order approximation for the friction coefficient c_f, it is natural to take the value of this coefficient for a flat plate, i.e., $c_f^{(0)} = d_{f\ pl}$. Given the parameters at the outer boundary of the boundary layer, $c_{f\ pl}$ can be computed by a method presented in Section 12. Upon finding $c_f^{(0)}(x)$, one can successively find: $\zeta^{(0)}(x)$ by means of Equation (3.8), $H^{*(0)}$ using Equation (3.55), $\Omega^{(0)}(x)$ by means of Equation (3.196), $E^0(x)$ from the relation (3.201) [or (3.203)], $c_f^{(')}(x)$ from the expression (3.202), etc.

The fact that the unknown function c_f occurs on the right-hand side of Equation (3.203) in the integrand and under the sign of the logarithm guarantees the normal fast convergence of the iterative process.

In conclusion, we note that, as was shown in the calculations, both of the methods of turbulent boundary layer calculations, presented in this section (the method based on a linearization of the integral momentum relation, and the method of successive approximations) lead to similar results. Attempts to use these methods for calculating the friction coefficient in pre-separation flow regions have shown that, in those cases, the friction coefficients thus obtained are much too high.

§ 18.   Turbulent Boundary Layer on a Sphere

Among bodies with various shapes of their nose section, bodies
with a spherical surface have attracted the greatest interest among
engineers and researchers. This interest is due to the wide use of
blunt bodies in the construction of various types of aircraft. One
of the main advantages that blunt bodies have to offer, compared to
bodies of a sharp profile, is the fact that the specific thermal
fluxes transferred to blunt bodies are much smaller than those trans-
ferred to bodies of sharp profile. For a laminar flow in the boundary
layer in the neighborhood of the front stagnation point, the thermal
flux to the wall turns out be be inversely proportional to the square
root of the radius of curvature: $q_w \sim 1/\sqrt{R}$.

At the present time, the problem of flow in the laminar boundary
layer in the neighborhood of the front stagnation point of blunt
bodies at supersonic velocities has been thoroughly investigated
both theoretically and experimentally.

Much less research has been done in the area of turbulent flows
over blunt bodies at supersonic velocities. This is due to the fact
that, at the front stagnation point and in its immediate neighborhood,
the flow in the boundary layer, in view of the smallness of the
Reynolds numbers, always remains laminar. If the laminar character
of the flow is also preserved farther along the body, then the thermal
flux attains a maximum at the front stagnation point. The available
experimental data, however, show that the laminar character of flow
in the boundary layer on blunt bodies does not always extend very
far. In particular, the experimental data obtained by Stetson [61]
indicate that it is possible for the laminar layer to pass into a
turbulent layer in the neighborhood of the sonic point (line) [sonic
point (line) is defined as the point (line) at which the velocity at
the outer boundary of the boundary layer becomes equal to the local
velocity of sound]. In this case, the maximum heat flux occurs in
the neighborhood of the sonic point (line). This circumstance
explains why there is particular interest in turbulent boundary
layers on blunt bodies.

Among the wide class of blunt-nosed bodies, the flow pattern near spherical bodies has been studied to the greatest extent. A diagram of flow near a sphere is shown in Figure 45. In a supersonic
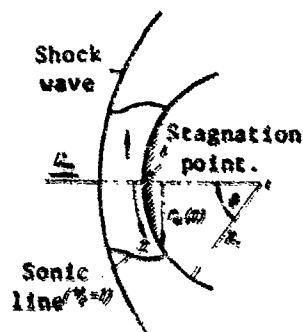
flow over a spherical body, a separated shock wave forms in front of the body. The stream upon passing through the direct shock wave in the neighborhood of the front stagnation point is decelerated to zero velocity, and then accelerated near the body, reaching the local velocity of sound at a certain line (sonic line). As shown by experiment and theory, the sonic line lies near the point having the angular coordinate $\theta = 45°$.

Figure 45

A theoretical investigation of the flow near the front stagnation point of a sphere was, in particular, done by Li Ting-Yi and Geiger [62], and an experimental study was done by Korobkin and Gruenewald [63]. In their investigation, Li Ting-Yi and Geiger found that the velocity gradient of the external flow at the front stagnation point of a sphere is

$$\beta_s = \left(\frac{du}{dx}\right)_s = \frac{u_\infty}{R_s}\sqrt{\frac{\rho_\infty}{\rho_s}\left(2 - \frac{\rho_\infty}{\rho_s}\right)}.$$ (3.204)

where R_s is the radius of curvature of the body at the front stagnation point, ρ_∞ is the density of the gas in the oncoming flow (before the shock wave), ρ_s is the gas density behind the direct shock wave. The ratio of densities before and after the shock, ρ_∞/ρ_s, as implied by the theory of normal shock waves, depends on the Mach number of the oncoming flow and is given by

$$\frac{\rho_\infty}{\rho_s} = \frac{(\gamma + 1)M_\infty^2}{(\gamma - 1)M_\infty^2 + 2}\left[1 + \frac{\gamma - 1}{2}\frac{(\gamma - 1)M_\infty^2 + 2}{2\gamma M_\infty^2 - (\gamma - 1)}\right]^{-1}.$$ (3.205)

Figure 46 gives the results of the calculation of $\frac{2R_s}{U_\infty}\left(\frac{dU_e}{dz}\right)_s$ using Equations (3.204) and (3.205). The same figure contains the experimental data obtained by Korobkin and Gruenewald. One must admit that the agreement between theory and experiment is good.

Figure 47 implies that, with an increase of the Mach number M_∞, the parameter $\frac{2R_s}{U_\infty}\left(\frac{dU_e}{dz}\right)_s$ tends asymptotically to a certain limit which depends on the adiabatic exponent γ.
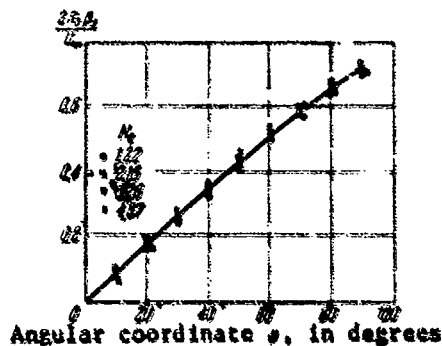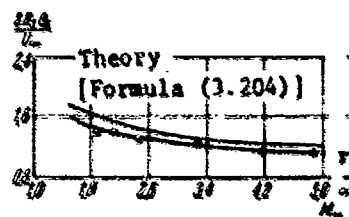

Figure 46

Figure 47

It should be noted that for $M_\infty > 4$ one can calculate the value of $\left(\frac{dU_e}{dz}\right)_s$ with high accuracy using the corrected Newton's formula [64]. In this case, the velocity gradient at the stagnation point is given by the expression

$$\lambda = \left(\frac{dU_e}{dz}\right)_s = \frac{1}{R_s} \sqrt{\frac{2(p_s - p_\infty)}{\rho_s}}. \tag{3.206}$$

For our purposes, we are interested not only in the velocity gradient at the front stagnation point, but also in the variation of the flow velocity along the surface of the sphere in general, and in the neighborhood of the sonic point in particular. The experimental data on the velocity distribution along a sphere, obtained by Korobkin and Gruenewald for the Mach numbers of the oncoming flow ranging from 1.22 to 4.87 (Figure 46), indicate that the dependence of the velocity on the longitudinal coordinate is close to linear: $U_e \sim x$. The velocity gradient along the surface of the sphere turns

out to be very close to the value of this gradient at the stagnation point. According to an estimation by Sibulkin [65] the difference between the velocity gradients at the front stagnation point and at the sonic point does not exceed 3% (for γ = 1.4). All the data available enable us to draw a conclusion that the velocity distribution along the surface of a sphere (0 $\leq$ θ $\leq$ 90°) is described well by the linear relation

$$U_e = \left(\frac{dU_e}{dx}\right)_s x = \beta_s x.$$

The value of $(dU_e/dx)_s$ can be determined either using Formula (3.204) or the plot in Figure 47, or using Formula (3.206) if the Mach number M_∞ > 4.

Calculation of skin friction on a sphere. Now we proceed to calculate the friction distribution along the surface of a sphere. For this purpose, we shall use a method based on the linearization of the momentum equation (Section 17), first making some preliminary simplifying assumptions regarding the behavior of the parameter H* and the function A. Thus we shall assume that both of these quantities are constant. An inspection of Equations (3.55) and (3.173) will provide a justification for this assumption. In fact, as implied by the results of the analysis in the preceding section, H* and Λ hardly depend on the friction parameter ζ. Therefore, one can expect that — if the compressibility parameter β and the heat transfer parameter ω [see Equations (3.48) or (3.49)] change little along the surface — then also the functions H* and A will change very little. The compressibility parameter β in the case of a flow near a sphere will be small, since the Mach numbers at the outer edge of the boundary layer will not exceed 1.5 - 2. In this connection we shall encounter the experimental fact, already mentioned above, according to which the Mach number M_e attains a value of unity at the point with the angular coordinate θ = 45°. Consequently, the effect of the compressibility parameter on H* and A will be insignificant. As far as the heat transfer parameter ω is concerned, its value may turn out

to be quite large. However, if the temperature of the wall is
constant, then the variation of this parameter along the surface of
the sphere will be insignificant, since the temperature at the outer
edge of the boundary layer near the sphere changes very little. Thus,
we have every reason to consider H^* and A to be constant in the case
of a flow over a sphere. If, in addition, we assume approximately
that $r_w(x) \approx x$, then the coefficients of Equation (3.180), $P(x)$
and $Q(x)$ given by Equation (3.181) become

$$P(x) = A(2 + H^*)\frac{1}{x}, \quad Q(x) = \rho_w \beta_s A x. \tag{3.207}$$

Substituting the values of these coefficients in the expression for
the function z, (3.183), we find upon integration

$$z = \left(\frac{x}{x_t}\right)^{-A(2+H^*)} \left[\frac{\beta_s \rho_w \cdot 1 x_t^2}{A(2+H^*)+2} \left[\left(\frac{x}{x_t}\right)^{A(2+H^*)+2} - 1 \right] + \right. \tag{3.208}$$
$$\left. + \rho_e U_{st\omega i} \delta_t^{**} \right]. \quad (3.2$$

If the laminar and transition regions are absent from the boundary
layer, ($x_t = 0$, $U_{et} = 0$), then Equation (3.208) becomes somewhat
simplified, namely

$$z = \frac{\beta_s \rho_w A}{A(2+H^*)+2} x^2. \tag{3.209}$$

Having the function $z(x)$, it is easy to calculate the distribu-
tion of the skin friction coefficient $c_f(x)$, using Formulas (3.192)
or (3.194) of the preceding section.

For a fully turbulent boundary layer upon a substitution of
Equation (3.209) in Equation (3.194), one can obtain the following
relation for the local friction coefficient

$$c_f = \frac{0.29K}{[\lg \{0.556K^2 Re_x (\mu_e/\mu_w) A [A(2+H^*)+2]^{-1}\}]^2}, \tag{3.210}$$

where

$$Re_x = \frac{\beta_s \rho_e x^2}{\mu_e}, \tag{3.211}$$

and K, H*, and A are given by Equations (3.188), (3.55), (3.177), respectively.

For convenience in calculations, Figure 48 gives a plot of the expression $A/A(2 + H^*) + 2$ versus the temperature factor T_w/T_e for the Mach numbers $M_e = 0$; 2. The character and the limits of the variation of this expression confirm the correctness of the assumption about constant A and H*. It should be noted that expression $A/A(2 + H^*) + 2$ depends not only on the parameters T_w/T_e and M_e, but also on the Reynolds number. However, this dependence turns out to be extremely weak, and for this reason the plots given in Figure 48 (they were constructed for $Re_x = 10^7$; $r = 0.89$) can be used with great accuracy within a wide range of the Reynolds numbers ($\sim$ from 10^5 to 10^9).
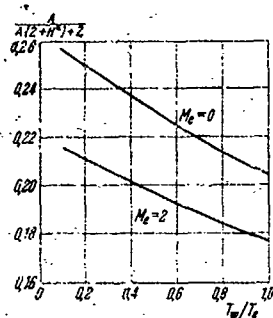

Figure 48.

Figures 49 and 50 give the results of calculating the distributions of certain parameters and local friction coefficients over the surface of a sphere for various flow conditions[28].

The calculations whose results are given in Figure 49 were done for a flow of air of Mach number $M_\infty = 3$ at the altitude 20 km (according to the standard atmosphere) over a sphere of diameter $d = 2$ m. The surface of the sphere was assumed to be thermally insulated. The figure gives, in particular, the distribution of the Mach numbers M_e and the Reynolds numbers Re_x [see Formula (3.211)] at the outer edge of the boundary layer. The presence of a maximum is characteristic of the variation of the Reynolds number. The maximum is due to the fact that, within the initial segment, the increase of the longitudinal coordinate x is the dominant factor, which accounts for the rise of the Reynolds number. Within the final segment, the gas density ρ, which sharply
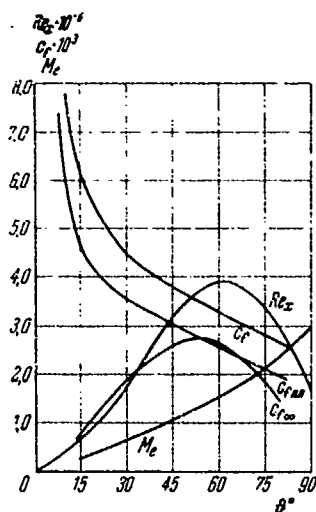

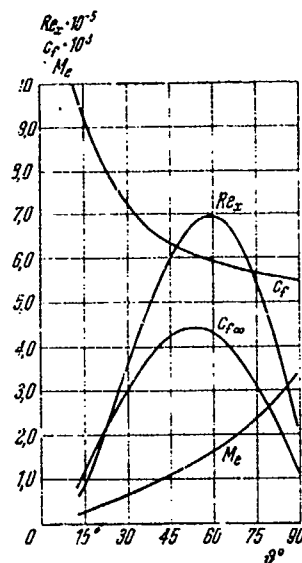
Footnote (28) appears on page 181.

Figure 49

Figure 50

decreases as a result of a isentropic expansion of flow along the surface of the sphere, is such a factor. Figure 49 also gives the distributions of the local friction coefficients over the surface of a sphere, c_f [see Formula (3.210)] and $c_{f\infty}$ [see Formula (3.195)]. The same figure also contains the plot of the friction coefficient $c_{f\ pl}$, calculated using the flat plate formulas for the local values of the Mach and Reynolds numbers, M_e and Re_x, at the outer edge of the boundary layer.

Figure 50 gives the analogous results obtained for flow of Mach number $M_\infty = 11$ at the altitude 25 km for the temperature factor $T_w/T_{e0} = 0.327$ (T_{e0} is the stagnation temperature) in a flow over a sphere of diameter d = 1.07 m.

Figures 49 and 50 show that, in both cases of a flow over a sphere, the local friction coefficient $c_{f\infty}$, determined from the parameters of the oncoming flow [see Formula (3.195)], is largest in the region of flow adjacent to the sonic line.

Calculation of heat transfer for a sphere. Upon a determination of the friction coefficient according to the method described above

one can find, using the Reynolds similitude (3.144), the local heat
transfer coefficient (Stanton number). The expression for the local
thermal flux, in view of the Reynolds similitude, becomes

$$q_w = \frac{1}{2} c_f \rho_e U_e S(1) \left(h_e + r \frac{U_e^2}{2} - h_w \right).$$ (3.145)

Here $S(1)$ and r are the Reynolds similitude parameter and the
recovery factor, respectively. The values of these coefficients can
be determined from Formulas (3.150) and (3.159). Using these
formulas and Equation (3.207), we reduce the expression for the heat
flux on a sphere to the form

$$q_w = \frac{1}{2} c_f \, \mathrm{Pr}^{-2/3} \rho_e \beta_s x \left(h_e + \frac{1}{2} \mathrm{Pr}^{1/3} \beta_s^2 x^2 - h_w \right).$$ (3.212)

Along with the method described above, there are other approxi-
mate methods for calculating heat transfer on spherical surfaces.
The results of some of them are given below.

Van Driest [66] using the power-law velocity profile with the
exponent 1/7, obtained the following expression for the local heat
transfer coefficient:

$$c_{h\infty} = 0{,}042 \, \mathrm{Pr}^{-2/3} \left(\frac{\beta_s d}{U_\infty} \right)^{4/5} \left(\frac{\rho_\infty U_\infty d}{\mu_\infty} \right)^{-1/5} \left(\frac{\rho_e}{\rho_\infty} \right)^{4/5} \left(\frac{\mu_e}{\mu_\infty} \right)^{1/5} \left(\frac{x}{d} \right)^{3/5}.$$ (3.213)

Here the heat flux was given by

$$q_w = c_{h\infty} \rho_\infty U_\infty (H_r - h_w).$$ (3.214)

It should be noted that Formula (3.213) was obtained under the
assumption that the turbulent boundary layer begins at the front
stagnation point.

Arthur and Williams [67], using the Van Driest Formula (3.213),
the power-law dependence of viscosity on temperature, $\mu \sim T^{0.76}$, and
the assumption about the isentropic expansion of the gas along the
surface of the sphere, have found that in this case the maximum value

of the heat transfer coefficient $(c_{h\infty})_{max}$ is achieved at the point $x/d = 0.322$, which corresponds to the angular coordinate $\vartheta = 37°$. The maximum heat flux for $\mathbf{Pr} = 0.75$ turns out to be

$$(q_w)_{max} = 0.0195 \left(\frac{\beta_s d}{U_\infty}\right)^{4/5} \left(\frac{\rho_s}{\rho_\infty}\right)^{4/5} \left(\frac{\mu_s}{\mu_\infty}\right)^{1/5} \times$$
$$\times \left(\frac{\rho_\infty U_\infty d}{\mu_\infty}\right)^{-1/5} \rho_\infty U_\infty (H_r - h_w), \quad (3.215)$$

where the subscript s denotes parameters at the front stagnation point.

A relation equivalent to (3.213) was obtained by Sibulkin[29] who investigated heat transfer at the sonic point. Just like Van Driest, Sibulkin used a power-law velocity profile. In calculating friction, he made use of the Blasius power-law formula, widely used in the theory of the turbulent boundary layer of an incompressible fluid, in which the flow parameters were calculated using Eckert's arbitrary temperature method[30].

In the conclusion of this section, we shall give a formula for calculating turbulent heat transfer in the neighborhood of the stagnation point of an axially symmetric body, proposed by V. S. Avduyevskiy [68]:

$$q_w = 3600 g c_p \rho_e \beta_s x \, 0.040 \left(\frac{\beta_s x^2 \rho_e}{\mu_e}\right)^{-0.2} \times$$
$$\times \left(\frac{T_w}{T_r}\right)^{-0.16} \mathbf{Pr}^{-0.6} (T_r - T_w) \; \frac{kcal}{m^2 hr}. \quad (3.216)$$

Formula (3.216) was obtained by solving the integral energy relation with the aid of the experimental relation between the heat flux and the local characteristics of the boundary layer, established for a flat plate. In deriving Formula (3.216), it was assumed that $\rho_e(x) = $ const.

Figures 51 and 52 give the results of calculating the heat transfer coefficients c_h and $c_{h\infty}$ on the surface of a sphere for the flow conditions indicated in the explanations of Figures 49 and 50,

---

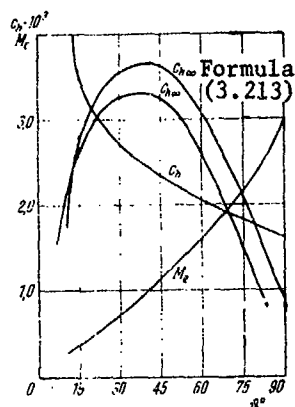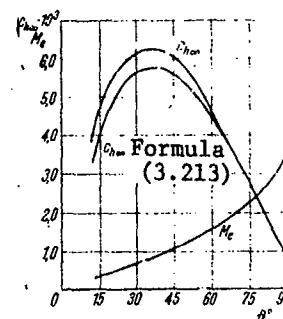Footnotes (29) and (30) appear on page 181.

Figure 51

Figure 52

respectively. The local heat transfer coefficient c_h, determined using the parameters on the outer edge of the boundary layer [see Formula (3.143)], was computed from Equation (3.159). The local heat transfer coefficient $c_{h\infty}$ was determined from the relation

$$c_{h\infty} = c_h \frac{\rho_e}{\rho_\infty} \frac{U_e}{U_\infty}.$$

Figures 51 and 52 also give the distributions of the local heat transfer coefficients $c_{h\infty}$, obtained using the Van Driest Formula (3.213). As can be seen in these figures, both methods lead to similar results. The maximum heat transfer occurs near the sonic line.

FOOTNOTES

Footnote (1) on page 76.   A detailed analysis of various
                            methods used in turbulent boundary
                            layer calculations for the case of a
                            flat plate can be found in:
                            Spalding, D. B., S. W. Chi. The
                            Drag of a Compressible Turbulent
                            Boundary Layer on a Smooth Flat Plate
                            with and without Heat Transfer,
                            Journ. of Fluid Mechan., Vol. 18,
                            Part 1, 1964, pp. 117-143; Russian
                            translation: Mekhanika, No. 6 (88),
                            Foreign Literature Press (IL), 1964.

Footnote (2) on page 80.   See footnote on foreign page 78.

Footnote (3) on page 80.   For a footnote on papers by Wilson
                            and Van Driest, see [5,6,7] on page 182.

Footnote (4) on page 80.   See footnote on foreign page 80.

Footnote (5) on page 81.   See [11] on page 182.

Footnote (6) on page 99.   This question will be discussed in
                            detail in Section 13.

Footnote (7) on page 99.   For large supersonic velocities, it may
                            be necessary to consider the interaction
                            of the boundary layer with the outer
                            nonviscous flow. Due to this inter-
                            action, the magnitude of the pressure,
                            and consequently, also the velocity
                            on the outer boundary of the boundary
                            layer, may noticeably differ from the
                            values of these parameters at infinity.
                            For more details, see, for example,
                            Heis, W. D., R. F. Probstain. "Theory
                            of Hypersonic Flow", IL, Moscow, 1962.
                            In the present chapter, when discussing
                            flows at relatively small supersonic
                            velocities, the viscous interaction
                            does not have to be taken into account.

Footnote (8) on page 103.   A detailed justification of Equations
                            (3.30) and (3.31), as well as a
                            discussion of the questions involved
                            in determining the thickness of the
                            laminar sublayer and questions related
                            to the effect of various factors on the
                            sublayer parameters, will be given in
                            Section 13.

Footnote (9) on page 104.   The function Φ generally depends on two variables x and u, since $\rho = \rho(x,u)$. However, in connection with the approximate calculation given below, where we assume $\rho \approx \rho(\bar{u})$, $\Phi \approx \Phi(\bar{u})$.

Footnote (10) on page 107.   For a detailed discussion of the recovery factor in the turbulent boundary layer, see Section 15.

Footnote (11) on page 109.   It will be recalled that a similar technique was used when deriving the well-known Karman formula for the friction coefficient on a flat plate in an incompressible fluid. See, for example, Sovremennoye sostoyaniye gidroaerodinamiki vyazkoy zhidkosti (Present State of the Hydroaerodynamics of a Viscous Fluid), Vol. II, edited by S. Gol'dshteyn, IL, Moscow, 1948.

Footnote (12) on page 113.   See [29] on the paper L. V. Kozlov on page 183.

Footnote (13) on page 123.   From Equations (3.104) and (3.30) it is easy to obtain the relation $\dfrac{\rho u_l \delta_l}{\mu} = \alpha$

which some authors used as the reason for considering α^2 as the critical Reynolds number (Re_{cr}) that determines the transition from laminar flow in the sublayer to turbulent flow in the core.

Footnote (14) on page 123.   See [5] on page 182.

Footnote (15) on page 126.   Here it is proper to note that the estimates of the effect of compressibility and heat transfer on the coordinate n_1, presented here, are not strictly justified, since the values of the coordinates n_1 in the paper by Czarnecki and Monta have been obtained by joining the velocity profile (3.07) in the laminar sublayer to the logarithmic velocity profile in an incompressible fluid. This fact does not permit us to draw any numerical conclusions on the basis of this type of

179

analysis. However, this analysis is undoubtedly useful in revealing tendencies in the effect that compressibility and heat transfer have on the thickness of the laminar sublayer. Of course, the numerical dependence of the thickness of the laminar sublayer (η_1) on the Mach number and the

temperature factor can at the present time be studied only experimentally.

Footnote (16) on page 126.   See [11] on page 182.

Footnote (17) on page 126.   See [5] on page 182.

Footnote (18) on page 126.   Regardless of the fact that the use of Van Driest's velocity profile is more natural than that of the logarithmic velocity profile in an incompressible fluid, the comment made earlier with respect to Figure 28 is valid also in this case.

Footnote (19) on page 127.   See the paper by Spalding and Chi, which was already cited in this chapter.

Footnote (20) on page 134.   See a paper by Van Driest: [4].

Footnote (21) on page 139.   Here it is proper to note that the deviation of the Prandtl number from unity leads — within the framework of the double-layer model of the turbulent boundary layer — to a situation in which the dynamic and thermal thicknesses of the laminar sublayer turn out to be different. If one takes this discrepancy strictly into account, this will lead to substantially more complicated calculations of heat transfer, and is not necessary if the Prandtl number is not too different from unity. In this connection, it will be recalled that calculation of heat transfer within the framework of the double-layer Prandtl model generally leads to satisfactory results only if the Prandtl number is close to unity. If the Prandtl number is substantially different from unity, better results are obtained by using the more complex three-layer Karman model. For more details about this and also about a

calculation of heat transfer for very large Prandtl numbers, see Loytsyanskiy, L. G., "Semi-empirical Theories of the Interaction of the Processes of Molecular and Molar Exchange in a Turbulent Flow of a Fluid", Trudy Vsesoyuznogo S'yezda po teoricheskoy i prikladnoy mekhanike, 27. I - 3. II 1960, Academy of Sciences of the USSR, Moscow-Leningrad, 1962.

Footnote (22) on page 139.

Apparently, the first expression for the recovery factor, similar to expression (3.149), was obtained by M. F. Shirokov in a paper published in "Zhurnal Tekhnicheskoy Fiziki", Vol. III, No. 12, 1936. See also a monograph by the same author: "Fizicheskiye Osnovy Gazodinamiki" (Physical Foundations of Gas Dynamics), Fizmatgiz, Moscow, 1958.

Footnote (23) on page 142.

See a paper by this author that was mentioned in Section 12.

Footnote (24) on page 147.

See the earlier noted paper of 1955. (Footnote on foreign page 153).

Footnote (25) on page 153.

See [12] of Coles' paper on page 182.

Footnote (26) on page 153.

For more details on this subject see, for example, Rotta, I. K., Turbulentnyi pogranichnyy sloy v neszhimayemoy zhidkosti (Turbulent Boundary Layer in an Incompressible Fluid), "Sudostroyeniye", Leningrad, 1967.

Footnote (27) on page 154.

See the paper by V. S. Avdureyskiy which was already quoted in this chapter ([15] on page 182).

Footnote (28) on page 173.

Calculations were done at the request of the author G. V. Semenova.

Footnote (29) on page 176.

See [65] on page 185.

Footnote (30) on page 176.

See [55] on page 184.

REFERENCES

1) K l e b a n o f f P. S., Characteristics of turbulence in a boundary layer with zero pressure gradient, NACA Rep., № 1247, 1135—1153 (1955).

2) Лойцянский Л. Г., Механика жидкости и газа, Гостехиздат, Москва, 1957.

3) Франкль Ф. И., Войтель В. В., Трение в турбулентном пограничном слое около пластинки в плоскопараллельном потоке сжимаемого газа при больших скоростях, Тр. ЦАГИ, № 321 (1937).

4) Современное состояние гидроаэродинамики вязкой жидкости, под ред. С. Гольдштейна, т. II, ИЛ, Москва, 1948.

5) W i l s o n R. E., Turbulent boundary layer characteristics at supersonic speed-theory and experiment, Journ. Aero. Sci. 17, № 9, 585—595 (1950).

6) V a n D r i e s t E. R., Turbulent boundary layer in compressible fluids, Journ. Aero. Sci. 18, № 3, 145—160 (1951); русский перевод: Механика, № 1, ИЛ, 1952.

7) V a n D r i e s t E. R., The turbulent boundary layer with variable Prandtl number, в сб. «50 Jahre Grenzschichtforschung», Braunschweig, 1955; русский перевод: Проблема пограничного слоя и вопросом теплопередачи, Энергоиздат, Москва — Ленинград, 1960.

8) И е в л е в В. М., Некоторые вопросы гидродинамической теории теплообмена при течении газа, ДАН СССР 86, № 1 (1952).

9) Г и н з б у р г И. П., Ш о м е ц А. А., Турбулентный пограничный слой пластинки в сжимаемой жидкости. Ученые записки ЛГУ, № 280, серии матем., вып. 35 (1960).

10) К а н и х м а н Л. Е., Турбулентный пограничный слой на плоской пластине, обтекаемой газом, ДАН СССР 106, № 1 (1956).

11) К у т а т е л а д з е С. С., Л е о н т ь е в А. И., Турбулентный пограничный слой сжимаемого газа, СО АН СССР, Новосибирск, 1962.

12) Л о й ц я н с к и й Л. Г., Л а в и к Ю. В., Применение метода Кармана к расчету турбулентного пограничного слоя на пластине в газовом потоке, Тр. Ленингр. политехн. ин-та им. М. И. Калинина, № 217, Машгиз, Москва — Ленинград (1961).

13) З м е н и н а - М о л о ж е н Л. М., С о с к о в а Л. Н., Исследование теплообмена и сопротивления при турбулентном течении сжимаемого газа, Тепломассоперенос 1, «Энергия», Минск, 1968.

14) P e r s c h J., A theoretical investigation of turbulent boundary layer flow with heat transfer at supersonic and hypersonic speeds, Proceed. of the Fourth Midwestern conference on fluid mechanics, Lafayette, 8—9, 1955.

15) А в д у е в с к и й В. С., Метод расчет. пространственного турбулентного пограничного слоя в сжимаемом газе, Изв. АН СССР, ОТН, Мех. и машиностр., № 4 (1962).

16) К а р м а н Т., Проблема сопротивления в сжимаемой жидкости, сб. «Газовая динамика», ГОНТИ, стр. 56—89, 1939.

17) T u c k e r M., Approximate calculation of turbulent boundary layer development in compressible flow, NACA TN, № 2337 (1951).

18) R u b e s i n M. W., J o h n s o n H. A., Critical review of skin-friction and heat-transfer solution of the laminar boundary layer of a flat plate, Transact. of the ASME 71, № 4 (1949).

19) Y o u n g G. B. W., J a n s s e n E., The compressible boundary layer, Journ. Aero. Sci. 19, № 4 (1952).

20) C h a p m a n D. R., K e s t e r R. M., Measurements of turbulent skin friction on cylinders in axial flow at subsonic and supersonic velocities, Journ. Aero. Sci. 20, № 7, 441—449 (1953).

21) C o l e s D., Measurements of turbulent friction on a smooth flat plate in supersonic flow, Journ. Aero. Sci. 21, № 7, 433—449 (1954).

22) K o r k e g i R. M., Transition studies and skin-friction measurements on an insulated flat plate at a Mach number of 5.8, Journ. Aero. Sci. 23, № 2, 97—108 (1956).

23) M a t t i n g F. W., C h a p m a n D. R., N y h o l m J. A., T h o m a s A. G., Turbulent skin-friction at high Mach numbers and Reynolds numbers in air and helium, NASA TR, № 82 (1961).

24) M o o r e, D. R., H a r k n e s s J., Experimental investigations of the compressible turbulent boundary layer at very high Reynolds numbers, AIAA Journ. 3, № 4 (1965); русский перевод: Ракетн. техн и космонавт., № 4, 1965.

25) L o b b R. K., W i n k l e r E. M., P e r s c h J., Experimental investigations of turbulent boundary layers in hypersonic flow, Journ. Aero. Sci. 22, № 1, 1—10 (1955); русский перевод: Вопр. ракетн. техн., № 5, ИЛ, 1955.

26) H i l l F. K., Boundary layer measurement in hypersonic flow, Journ. Aero. Sci. 23, № 9, 35—42 (1956); русский перевод: Вопр. ракетн. техн., № 1, ИЛ, 1957.
Рекомендуем читателю также по рассматриваемом в настоящем параграфе более позднюю работу того же автора: H i l l F. K., Turbulent boundary layer measurements at Mach numbers from 8 to 10, The Physics of Fluids 2, № 6 (1959).

27) S o m m e r S. C., S h o r t B. J., Free-flight measurements of skin friction of turbulent boundary layers with high rates of heat transfer at high supersonic speeds, Journ. Aero. Sci. 23, № 6 (1956); русский перевод: Вопр. ракетн. техн., № 4, ИЛ, 1957.

28) W i n k l e r E. M., Investigation of flat plate hypersonic turbulent boundary layers with heat transfer, ARC Paper, № 859-59 (1959).

29) К о з л о в Л. В., Экспериментальное исследование поверхностного трения на плоской пластине в сверхзвуковом потоке при наличии теплообмена, Изв. АН СССР, ОТН, Мех. и маш., № 2 (1963).

30) N i k u r a d s e J., Gesetzmässigkeiten der turbulenten Strömung in glatten Röhren, VDI Forschungsheft 356 (1932); русский перевод: в сб. «Проблемы турбулентности», ОНТИ, Москва, 1936.

31) M o n a g h a n R., The measurement of heat transfer and skin friction at supersonic speeds, ARC CP, №№ 139, 140 (1953).

32) Л о й ц я н с к и й Л. Г., Л о н н Ю. В., Применение метода Кармана к расчету турбулентного пограничного слоя на пластине в газовом потоке, Тр. Ленингр. политехн. ин-та им. М. И. Калинина, № 217, Машгиз, Москва—Ленинград (1961).

33) См., например, S t a f f A. K., Equations, tables and charts for compressible flow, NACA Rep., № 1135 (1953).

34) Теплообмен и трение в турбулентном пограничном слое, под ред. С. С. К у т а т е л а д з е, СО АН СССР, Новосибирск, 1964.

К у т а т е л а д з е С. С., Л е о н т ь е в А. И., Турбулентный пограничный слой сжимаемого газа, СО АН СССР, Новосибирск, 1962.

35) L i p m a n n H. W., D h a w a n C., NACA TN, № 1117 (1952).

36) P a p p a s C. C., Measurement of heat transfer in the turbulent boundary layer on a flat plate in supersonic flow and comparison with skin friction results, NACA TN, № 3222 (1954).

37) H i l l F. K., Turbulent boundary layer measurements at Mach numbers from 8 to 10, The Physics of Fluids 2, № 6, 668—680 (1959).

38) Л о й ц я н с к и й Л. Г., Механика жидкости и газа, Гостехиздат, Москва, 1957.

39) C z a r n e c k i K. R., M o n t a W. J., Effects of compressibility and heat transfer of the laminar sublayer at the turbulent boundary layer, NASA TN, D-1938 (1964).

40) Ван Дрийст Е. Р., Конвективная теплопередача в газах, в сб. «Турбулентные течения и теплопередача», под ред. Лина Цзя-цзяо, ИЛ, Москва, 1963.

41) Современное состояние аэродинамики больших скоростей, т. II, под ред. Л. Хоуарта, ИЛ, Москва, 1956.

42) Crocco L., Boundary layer of gases along a flat plate, Rend. Mat. Univ. Roma 12 (1941).

43) Kaye J., Survey of friction coefficients recovery factors and heat-transfer coefficients for supersonic flow, Journ. Aero. Sci. 21, № 2, 117—129 (1954).

44) Shoulberg R. H., Hill J. A. F., Rivas M. A., An experimental determination of flat plate recovery factors for Mach numbers between 1,9 and 3,14, Journ. Aero. Sci. 21, № 11, 763—771 (1954).

45) Tendeland T., Effects of Mach numbers and wall-temperature ratio on turbulent heat transfer at Mach numbers from 3,0 to 5, NASA TR, № 16 (1939).

46) Adcock J. B., Peterson J. B., McRee D. T., Experimental investigation of a turbulent boundary layer of Mach 6, high Reynolds numbers and zero heat transfer, NASA TN, D-290 (1965).

47) Seiff A., Examination of the existing data on the heat transfer of turbulent boundary layers, NACA TN, № 3284 (1954).

48) Козлов Л. В., Связь аэродинамического нагрева с поверхностным трением, Изв. АН СССР, Мех. и маш., № 4 (1963).

49) Van Driest E. R., Turbulent boundary layer on a cone in a supersonic flow at zero angle of attack, Journ. Aero. Sci. 19, № 1, 55—57 (1952).

50) Bradfild W. S., Conical turbulent boundary layer experiments and a correlation with flat plate data, Trans. of the ASME, Journ. of Heat Transfer, ser. C., May, 22—33 (1960).

51) Калихман Л. Е. Турбулентный пограничный слой на криволинейной поверхности, обтекаемой газом, Оборонгиз, Москва, 1956.

52) Кутателадзе С. С., Леонтьев А. И., Турбулентный пограничный слой сжимаемого газа, СО АН СССР, Новосибирск, 1962.

53) McLafferty G. H., Barber R. E., The effect of adverse pressure gradients on the characteristics of turbulent boundary layers in supersonic streams, Journ. Aero-Space Sci., 29, № 1 (1962).

54) Sasman P. K., Cresci R. J., Compressible turbulent boundary layer with pressure gradient and heat transfer, AIAA Journ. 4, № 1 (1966); русский перевод: Ракетн. техн. и космонавт., № 1, 1966.

55) Eckert E. R. G., Engineering relations for friction and heat transfer to surfaces in high velocity flow, Journ. Aero. Sci. 22, 585—588 (1955).

56) Неелов В. И., Некоторые вопросы гидродинамической теории теплообмена при решении методических задач, ДАН СССР, 46, № 6 (1962). См. также сноску на стр. 72

57) Schultz-Grunow F., Entstehung von Längswirbeln in Grenzschichten, ZAMM 36, 65—65 (1958).

58) Hama F. R., Boundary layer characteristics for smooth and rough surfaces, Trans. Soc. Naval Architects and Marine Engrs. 62, 333—358 (1954).

59) Федяевский К. К., Гиневский А. С., Метод расчета турбулентного пограничного слоя при наличии продольного градиента давления, Журн. техн. физики 27, № 2, 309—328 (1957).

60) Ланин Ю. К., Турбулентный пограничный слой в газовом потоке при наличии теплопереноса и также Прандтля, отличного от единицы, Тр. Ленингр. политехн. ин-та им. М. И. Калинина, № 217, Машгиз, Москва—Ленинград (1961).

61) S t e t s o n K. F., Boundary layer transition on blunt bodies with highly cooled boundary layers, Journ. Aero-Space Sci. **27**, № 2, 81—92 (1960).

62) T i n g - Y i L i, G e i g e r R. E., Stagnation point of a blunt body in hypersonic flow, Journ. Aero. Sci. **24**, № 1, 25—33 (1957).

63) K o r o b k i n I., G r u e n e w a l d K., Investigation of local laminar heat transfer on a hemisphere for supersonic Mach numbers at low rates of heat flux, Journ. Aero. Sci. **24**, № 3, 188—194 (1957).

64) Ч е р н ы й Г. Г., Течения газа с большой сверхзвуковой скоростью, Физматгиз, Москва, 1959.

65) S i b u l k i n M., Estimation of turbulent heat transfer of the sonic point of a bluntnosed body, Jet Prop. **28**, № 8, 548—554 (1958); русский перевод: Вопр. ракетн. техн., № 3, ИЛ, 1959.

66) V a n D r i e s t E. R., The problem of aerodynamic heating, Aeron. Engng. Rev. **15**, № 10 (1956).

67) A r t h u r P. D., W i l l i a m s J. C., Maximum turbulent boundary layer heating rates on a hemispherical nose, ARS Journ. **30**, № 2, 207—208 (1960).

68) А в д у е в с к и й В. С., Д а н и л о в Ю. И., К о ш к и н В. К., К у т ы р и н И. Н., М и х а й л о в а М. М., М и х е е в Ю. С., С е р г е л ь О. С., Основы теплопередачи в авиационной и ракетной технике, Оборонгиз, Москва, 1960.

CHAPTER IV

TURBULENT BOUNDARY LAYER IN A DISSOCIATING GAS

§ 19. Certain Comments Regarding the Thermodynamic Properties of the Air at High Temperatures[1]

The increase of the velocities of aircraft from low subsonic to moderate supersonic velocities has made it necessary to consider the dependence of the density of air and transport coefficients (viscosity and heat transfer) on the temperature when dealing with such velocities. The specific heat capacity of the air increases with temperature due to the excitation of the vibrational degrees of freedom (Figure 53). However, if the temperature gradient in the boundary layer is not very high, then in approximate calculations the heat capacity of the air may be considered constant, and equal to a value corresponding to certain average temperature of the flow.

The methods used in turbulent boundary layer calculations for bodies of various shapes were discussed in the preceding chapter based on the assumption that the heat capacity of the gas is constant.

Footnote (1) appears on page 269.
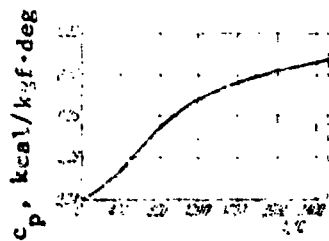
Figure 53

A further increase of the velocities of aircraft is accompanied by such a high increase of the gas temperature that, along with the fact that the density and transport coefficients are variable, it may also become necessary to consider the dependence of the heat capacity on the temperature. Here one must keep in mind that it is not the absolute value of the temperature, but the temperature gradient in the boundary layer (in other words, the difference between the maximum and minimum temperature) that is of basic importance. The flow of a gas with variable heat capacity can be analyzed both by generalizing the methods discussed in the preceding chapter (such a generalization in many cases reduces formally to replacing the temperature with the enthalpy) and by applying methods that will be presented in this chapter.

A transition to hypersonic velocities causes such an enormous increase in the temperature of the gas that thermochemical processes begin to occur in it. They include the dissociation of the gas molecules, ionization of the atoms, formation of oxides, radiation, etc.
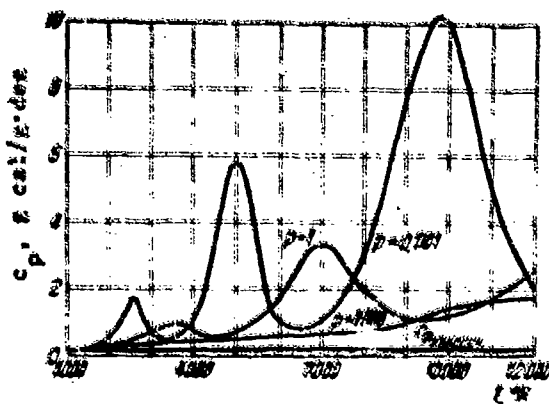
Figure 54

Some concept of the effect of these processes on the "effective" heat capacity of the air in equilibrium may be obtained from Figure 54 [1], which gives the plots of the heat capacity c_p versus temperature for various pressure ("effective" heat capacity is usually defined as the heat capacity which, together with the ordinary heat capacity, includes the thermal effects of the thermochemical processes in a gas).

Figure 55 has been reprinted from the paper by Ye. V. Stupochenko et al., which was quoted above. The figure gives the molar concentrations of the molecular and atomic components of the air and electrons, computed for the conditions of thermodynamic equilibrium, as functions of the temperature for three values of pressure p = 0.001; 1 and 1000 atm. As seen in Figure 55, at high temperatures the air is a multicomponent mixture, consisting of the molecules of oxygen O_2, nitrogen N_2, nitrogen oxide NO, atomic oxygen O, nitrogen N, argon Ar, and electrons e^-. In addition to those components, the mixture contains positively charged ions of oxygen O^+, nitrogen N^+, and nitrogen oxide NO^+ (in Figure 55 the concentrations of these components are not given).

The argon and nitrogen oxide content does not exceed 1% within a wide temperature and pressure range, and for this reason we may neglect the existence of these components in approximate calculations.

Calculations of the equilibrium composition of the air show [2] that, due to a considerable difference in the dissociation energy of oxygen and nitrogen (5.08 eV for O_2 and 9.756 eV for N_2), the dissociation of oxygen is essentially terminated before nitrogen dissociation begins. In addition, due to the high ionization potential for oxygen
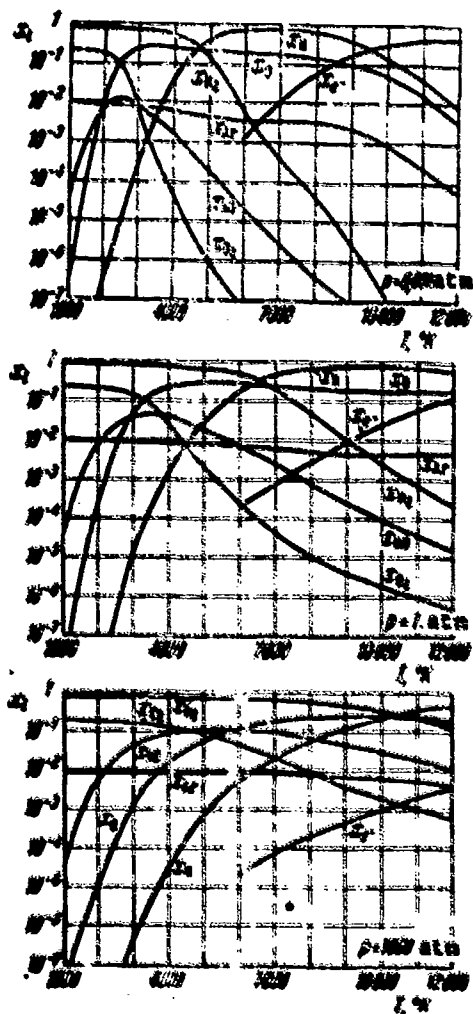

Figure 55

and nitrogen (13.62 eV for Oa and 14.55 eV for N), the dissociation of the oxygen and nitrogen molecules is to a large extent terminated before the ionization of O and N atoms begins.

These features of the flow of chemical reactions in the air at high temperatures enable us to approximately distinguish temperature and pressure ranges in each of which a certain reaction is dominant (Figure 56)[2]. The subdivision into regions, given in Figure 56, permits a considerable simplification of the air flow calculations at high temperatures.
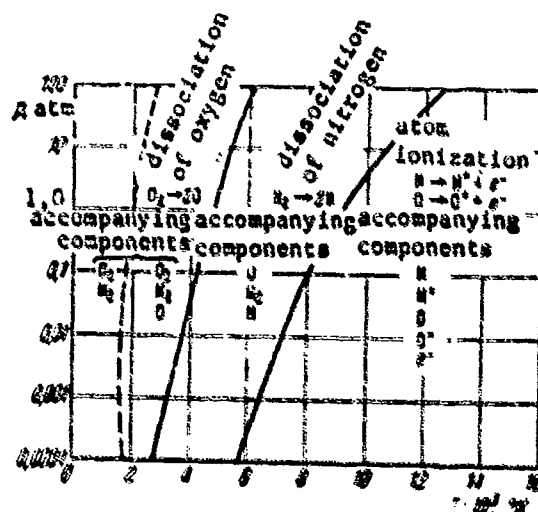

Figure 56

In the present chapter, we shall consider those methods of turbulent boundary layer calculations that are applicable to flows in which the effect of the ionization processes may be neglected (see Figure 56).

§ 20. Elements of the Kinetics of Chemical Reactions

In the present section, we shall give certain basic information on the formal kinetics of homogeneous chemical reactions [3] and, in particular, some information concerning the kinetics of the dissociation reactions of the basic components of the air (oxygen and nitrogen). We shall limit our attention to material that will be found necessary below. We shall also describe a model of an "ideally dissociating gas", proposed by Lighthill [4], which has become widely used in various gasdynamic studies. We shall also devote some space to a model of a partially excited dissociating gas. A brief treatment of the kinetics of heterogeneous (surface) chemical reactions will be given as well.

Footnote (2) appears on page 269.

Definitions. The processes of chemical interaction among the molecules of a gas mixture are a result of collisions among the reacting molecules. Depending on systems in which the reactions take place, they may be of two types: homogeneous and heterogeneous.

Homogeneous reactions are those that occur in a homogeneous medium (for example, in a mixture of reacting gases or in a solution). Usually, when we say homogeneous reactions we mean reactions occurring in finite volumes of gases, solutions, etc. Moreover, if the gases participating in a reaction are contained in a vessel, then the rate of a homogeneous reaction does not depend on the surface area of the vessel. An example of a homogeneous reaction is the dissociation of the oxygen and nitrogen molecules and high temperatures.

Heterogeneous reactions are those that occur in an inhomogeneous medium, at the interface of interacting components which occur in different phases — for example, solid and gaseous (recombination reactions at a catalytic surface), liquid and gaseous, (carbon burnout at the surface of the protective film made of certain materials used for shielding spacecrafts from heat), etc. The heterogeneous reactions are also usually said to include reactions occurring in narrow (as compared with the volume occupied by gases) regions, which form when reacting gases (not previously mixed) are brought in contact. In the limiting case when the rate of a chemical reaction is infinitely large as compared with the rate of diffusion (the rate of delivery and removal of reactants and products of reaction) such a region may be considered to be a surface (reaction front). An example of such a reaction may be provided by the oxidation reaction (combustion) of gaseous carbon when high-temperature air flows over a carbon surface. In this case, the gaseous carbon which is formed as a result of a sublimation of solid carbon diffuses from the surface of the wall to the outer edge of the boundary layer, toward oxygen which diffuses in the opposite direction. If the temperature in the boundary layer is sufficiently high, then the oxidation rate (combustion) of carbon will be very large, and the reaction zone (combustion front) will be

so thin, as compared with the thickness of the boundary layer, that in practice such a reaction may be considered heterogeneous.

A reaction is called endothermic if it involves absorption of heat (for example, the dissociation of oxygen molecules), and exothermic if it involves release of heat (for example, recombination of the oxygen atoms).

The law of mass action. Every chemical reaction obeys the law of constant multiple proportions, and can be generally described by the following stoichiometric equation:

$$\sum_{k=1}^{N} \nu_k' A_k \underset{k''}{\overset{k'}{\rightleftharpoons}} \sum_{k=1}^{N} \nu_k'' A_k, \tag{4.1}$$

where ν_k' and ν_k'' are the stoichiometric coefficients for reactants (prime), and reaction products (double prime); A_k are the chemical symbols of the reactants. N is the total number of the chemical species, and k' and k" are the rate constants of the direct and reverse reactions, respectively, which are functions of temperature.

The law of mass action is the basic relation describing the rate of a chemical reaction (the rate of formation or disintegration of species i). According to the law of mass action, the rate of formation of a species is proportional to the product of the concentrations of the reacting species, where each concentration in the product is raised to a power equal to its stoichiometric coefficient. According to this law for the equation of a chemical reaction (4.1), the rate of the reaction going from left to right can be given by the expression

$$\left(\frac{d[n_i]}{dt}\right)' = k'(T) \prod_{k=1}^{N} [n_k]^{\nu_k'}. \tag{4.2}$$

and the rate of the reaction going from right to left by

$$\left(\frac{d[n_i]}{dt}\right)'' = k''(T) \prod_{k=1}^{N} [n_k]^{\nu_k''}. \tag{4.3}$$

Here $[n_i]$ gives the number of moles per unit volume of species i. The derivative $d[n_i]/dt$ represents the rate of change of the number of moles per unit volume of species i as a result of the chemical reaction. It will be noted that Equations (4.2) and (4.3) were written for one mole. If a reaction is such that reactants are present on both sides of the equation of reaction, then the expressions for the reaction rates must be written in the form

$$\left(\frac{d[n_i]}{dt}\right)' = (v_i'' - v_i')k'(T)\prod_{k=1}^{N}[n_k]^{v_k'},$$ (4.4)

$$\left(\frac{d[n_i]}{dt}\right)'' = (v_i'' - v_i')k''(T)\prod_{k=1}^{N}[n_k]^{v_k''}.$$ (4.5)

These equations were written for $(v_i'' - v_i')$ moles.

The total rate of formation of species i is equal to the difference between the rates of the forward and reverse reactions:

$$\frac{d[n_i]}{dt} = (v_i'' - v_i')k'(T)\prod_{k=1}^{N}[n_k]^{v_k'} - (v_i'' - v_i')k''(T)\prod_{k=1}^{N}[n_k]^{v_k''}.$$ (4.6)

In chemical equilibrium, no changes occur in the composition of a mixture, i.e., the rates of the forward and reverse reactions are equal ($d[n_i]/dt = 0$). Consequently, in this case

$$\frac{k'(T)}{k''(T)} = \prod_{k=1}^{N}[n_k^{(e)}]^{v_k''-v_k'} = K_n(T),$$ (4.7)

where $K_n(T)$ is an equilibrium constant, and the subscript (e) signifies the equilibrium values of $[n_k]$.

Equation (4.7) is the most general equation that can be used to determine the composition of the reaction products in chemical equilibrium. This equation relates the ratio of the kinetic parameters k' and k" to the equilibrium constant $K_n(T)$, which may be calculated exactly using thermodynamic and quantum-mechanical methods.

Equation (4.6) can also be written, in view (4.7), in the form

$$\frac{d[n_i]}{dt} =$$

$$= (v_i^{\cdot} - v_i)k'(T)\prod_{k=1}^{N}[n_k]^{v_k^{\cdot}}\left[1 - \frac{1}{K_n(T)}\prod_{k=1}^{N}[n_k]^{v_k^{\cdot}-v_k}\right]. \qquad (4.8)$$

If a number of reactions occur simultaneously in a system, then — in calculating the total rate of formation of species 1 — one can use the principle of independence of individual reactions. According to this principle, if a number of reactions occur within a system, then each of them occurs independently of the rest, and each is subject to the law of mass action. The total rate of formation of species 1 is equal to the sum of the rates of formation of species 1 in each of the reactions

$$\frac{d[n_i]}{dt} = \sum_{s=1}^{a}\left(\frac{d[n_i]}{dt}\right)_s =$$

$$= \sum_{s=1}^{a}(v_{is}^{\cdot} - v_{is})k_s^{\cdot}\prod_{k=1}^{N}[n_k]^{v_{ks}^{\cdot}}\left[1 - \frac{1}{K_{ns}}\prod_{k=1}^{N}[n_k]^{v_{ks}^{\cdot}-v_{ks}}\right]. \qquad (4.9)$$

where a is the number of independent reactions, s is the reaction number.

For an ideal gas whose state is described by the Clapeyron equation, we have

$$[n_i] = \frac{p_i}{RT}. \qquad (4.10)$$

Here p_i is the partial pressure of species 1, R is the universal gas constant (if $[n_i]$ is measured in moles/cm^3 and pressure in atm, then the gas constant is R = 82.05 cm^3 atm-mole^{-1} · °K^{-1}).

At equilibrium

$$[n_i^{(r)}] = \frac{p_i^{(r)}}{RT}. \qquad (4.11)$$

In chemical kinetics along with the equilibrium constant K_n, expressed in terms of the number of moles (Equation 4.7), one often uses the equilibrium constant K_p, expressed in terms of partial pressures:

$$K_p = \prod_{k=1}^{N} (p_k^{(o)})^{\dot{v}_k - \dot{v}_k}. \tag{4.12}$$

It is easy to see, in view of Equation (4.11), that the equilibrium constants K_n and K_p are related as follows

$$K_n = K_p (RT)^{-\Delta v}, \quad \Delta v = \sum_{k=1}^{N} (v_k' - v_k). \tag{4.13}$$

The ratio of the number of moles of species i per unit volume (or of the partial pressure of species i) to the total number of moles per unit volume (to the total pressure of the mixture) is called the molar concentration of species i:

$$z_i = \frac{[n_i]}{[n]} = \frac{p_i}{p}. \tag{4.14}$$

Here $[n] = \sum_{k=1}^{N} [n_k]$ is the total number of moles per unit volume, and p is the pressure of the gas mixture.

The expression for the equilibrium constant in terms of the equilibrium molar concentrations has the form

$$K_z = \prod_{k=1}^{N} (z_k^{(o)})^{\dot{v}_k - \dot{v}_k}. \tag{4.15}$$

Similarly, one can introduce the equilibrium constant, expressed in terms of the equilibrium mass concentrations:

$$K_c = \prod_{k=1}^{N} (c_k^{(o)})^{\dot{v}_k - \dot{v}_k}. \tag{4.16}$$

Here

$$c_i = \frac{\rho_i}{\rho}, \quad \rho_i = \frac{p_i}{RT} M_i = [n_i] M_i. \tag{4.17}$$

Using these relations, it is easy to show that we have the following relations among the equilibrium constants:

$$\frac{\nu}{k^*} = K_a = K_p(RT)^{-\Delta v} = K_x\left(\frac{p^{(e)}}{RT}\right)^{\Delta v} =$$
$$= K_c(\rho^{(e)})^{\Delta v}\left[\prod_{k=1}^{N}(M_k)^{\dot{v}_k - \dot{v}_k}\right]^{-1}. \tag{4.18}$$

As seen from Equations (4.15) and (4.16), the equilibrium constants K_x and K_c are always dimensionless parameters. As far as K_n and K_p [Equations (4.7) and (4.12)] are concerned, these equilibrium constants are dimensionless only under the condition that $\Delta v = 0$. In order to use any of the above equilibrium constants in the expression for the rate of a chemical reaction (4.8), it is useful to note that the expression

$$\frac{k^*}{k^*}\prod_{k=1}^{N}(n_k)^{\dot{v}_k - \dot{v}_k}$$

is always dimensionless.

Introducing, by analogy with the equilibrium constant, the quantities

$$K_n^* = \prod_{k=1}^{N}(n_k)^{\dot{v}_k - \dot{v}_k}, \quad K_p^* = \prod_{k=1}^{N}(p_k)^{\dot{v}_k - \dot{v}_k},$$
$$K_x^* = \prod_{k=1}^{N}(x_k)^{\dot{v}_k - \dot{v}_k}, \quad K_c^* = \prod_{k=1}^{N}(c_k)^{\dot{v}_k - \dot{v}_k},$$

we obtain

$$\frac{k^*}{k^*}\prod_{k=1}^{N}(n_k)^{\dot{v}_k - \dot{v}_k} = \frac{K_n^*}{K_n} = \frac{K_p^*}{K_p} = \frac{K_x^*}{K_x} = \frac{K_c^*}{K_c}\left(\frac{\rho}{\rho^{(e)}}\right)^{\Delta v} = \frac{K_c^*}{K_c}$$
$$(x = n, \, p, \, c) \tag{4.19}$$

In view of Equation (4.19), we obtain the following equivalent expressions for the rate of a chemical reaction:

$$\frac{d(n_i)}{dt} = (\dot{v}_i - \dot{v}_i)k^*\left(1 - \frac{K_n^*}{K_n}\right)\prod_{k=1}^{N}(n_k)^{\dot{v}_k} \dots$$
$$= (\dot{v}_i - \dot{v}_i)k^*(RT)^{-\Phi}\left(1 - \frac{K_p^*}{K_p}\right)\prod_{k=1}^{N}(p_k)^{\dot{v}_k} \dots$$

(equation continued on next page)

$$= (v_i^{\cdot} - v_i) k' [n]^{\sigma} \left(1 - \frac{K_a^{\cdot}}{K_a}\right) \prod_{k=1}^{N} (x_k)^{v_k^{\cdot}} =$$

$$= (v_i^{\cdot} - v_i) k' \rho^{\sigma} \left(1 - \frac{K_a^{\cdot}}{K_a}\right) \prod_{k=1}^{N} \left(\frac{c_k}{M_k}\right)^{v_k^{\cdot}}.$$

$$\sigma = \sum_{k=1}^{N} v_k^{\cdot}. \tag{4.20}$$

Equilibrium constants. Statistical thermodynamics [5] leads to the following expression for the equilibrium constant:

$$\ln K_p = -\frac{\Delta E_0}{RT} + \sum_{k=1}^{N} v_k^{\cdot} \ln Q_p(A_k^{\cdot}) - \sum_{k=1}^{N} v_k \ln Q_p(A_k). \tag{4.21}$$

where

$$\Delta E_0 \equiv \sum_{k=1}^{N} v_k^{\cdot} E_0(A_k^{\cdot}) - \sum_{k=1}^{N} v_k E_0(A_k) \tag{4.22}$$

is the difference between the energies of the products and the energies of the reactants at a zero temperature point, where the reactant and the reaction products are considered to be in states with unit concentrations at normal pressure; Q_p is the partition function for a gas at unit pressure; E_0 is the energy of the gas at zero absolute temperature.

The partition function for a gas at unit pressure is related to the total partition function Q (a basic quantity in statistical thermodynamics) by the equation

$$Q_p = \rho Q. \tag{4.23}$$

The partition function Q is given by

$$Q = \sum_i g_i e^{-\frac{\varepsilon_i}{kT}}. \tag{4.24}$$

where ε_i is the energy of a particle in the ith state; g_i is the

statistical weight or degeneracy of the energy levels, i.e., the
number of states of a particle with energy levels near ε_i.

According to present-day concepts, the energy of gas molecules
consists of the translational energy ε_i, rotational energy ε_r, the
intramolecular vibration energy, i.e., vibrations of atoms and groups
of atoms in a molecule, ε_v, the electron excitation energy ε_e, and
the nuclear excitation energy. For the temperatures occurring in
gasdynamics, the energy of the nuclear excitation may be neglected.
If we assume that the different forms of energy are independent, then
the partition function will be given by the product

$$Q = Q^i Q^r Q^v Q^e. \tag{4.25}$$

The factors on the right-hand side of Equation (4.25) are the
partition functions for the translational, rotational, vibrational,
and electron levels of energy, respectively. In statistical mechanics,
it is shown that for two-atomic molecules these factors are equal to

$$Q^i_{A_2} = \left(\frac{2\pi m_{A_2} kT}{h^2}\right)^{3/2} \frac{RT}{P}, \tag{4.26a}$$

$$Q^r_{A_2} = \frac{1}{2}\frac{8\pi I kT}{h^2} = \frac{1}{2}\frac{T}{T_r}, \tag{4.26b}$$

$$Q^v_{A_2} = \left(1 - e^{\frac{hv}{kT}}\right)^{-1} = \left(1 - e^{-\frac{T_v}{T}}\right)^{-1}, \tag{4.26c}$$

$$Q^e_{A_2} = \sum_{i=0}^{\infty} g_i e^{-\frac{\varepsilon_i}{kT}}. \tag{4.26d}$$

Here m_{A_2} is the mass of the molecule, I is the moment of inertia of
the molecule, h is Planck's constant, v is the vibrational frequency,
T_r is the characteristic temperature of rotation, T_v is the charac-
teristic vibrational temperature.

The expression for $Q^r_{A_2}$ was written for a two-atomic molecule
consisting of identical atoms. For monoatomic molecules that do not
have rotational and vibrational degrees of freedom, the corresponding
partition functions will become equal to unity. The partition func-
tions for the translational and electron degrees of freedom for
monatomic molecules have the same form as Expressions (4.26a) and
(4.26d), except that m_{A_2} in (4.26a) must be replaced by m_A.

Rate constants of homogeneous reactions. The expressions for
the rate constants of chemical reactions can be obtained either using
the collision theory (Arrhenius theory) [6], or using the theory of
absolute reaction rates [7] (sometimes the theory of absolute reaction
rates is called the activated complex method).

Collision theory, which is a part of formal kinetics, does not
go into the mechanism of collisions, and gives a numerical description
of only the results of an interaction of particles. Arrhenius is the
founder of collision theory. According to Arrhenius, every reaction
goes through an intermediate stage involving the formation of active
molecules, i.e., molecule e- that possess excess energy sufficient to
overcome the energy barrier. In order that an elementary chemical
interaction process may occur, it is necessary that the molecules of
the reactants come close together. Here, regardless of whether the
process involves release or absorption of energy, as a rule, when
molecules approach one another, repulsive forces arise, and a definite
energy is needed to overcome them. As an example, Figure 57 gives a
diagram of the variation of the energy of a reacting system. The
ordinate axis measures the potential energy of the system, and on the
axis of abscissas we plot a coordinate characterizing the relative
spatial distribution of the atoms. Region I refers to the initial
particles, II refers to active particles, III refers to the products
of the reaction. The energy difference between the initial and the
final states of the system is equal to the energy effect of the
reaction. (ΔE_0). E_a is the activation energy, i.e., the minimum value
of the total energy of the
colliding molecules which is
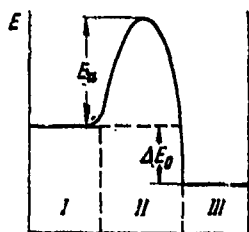necessary for a reaction to take
place.

Figure 57

The reaction rate constant
is directly related to the number
of collisions of the active mole-
cules. Therefore, its value turns

out to be proportional to the Boltzmann factor $(-E_a/RT)$. The question
of which collisions should be considered active must be solved experi-
mentally. A comparison of calculations, based on different hypotheses,
with the experimental data showed that for simple molecules, active
collisions are those in which a component of the kinetic energy of
relative motion along the line joining the mass centers exceeds the
activation energy. In this case, we obtain the following expression
for the reaction rate constant[3]:

$$\bar{k} = 2r_{12}^2 \left(\frac{2\pi kT}{\bar{m}} \right)^{1/2} \exp\left(-\frac{E_a}{RT} \right) = b(T)\exp\left(-\frac{E_a}{RT} \right)$$
$$(\bar{k} = k', k'').$$

Here r_{12} is the sum of the radii of the colliding particles,
$\bar{m} = \left(\frac{1}{m_1} + \frac{1}{m_2} \right)^{-1}$ is the reduced mass of the particles, k is the Boltzmann
constant.

The above expression for the reaction rate constant does not
always lead to results that are in good agreement with experiment,
particularly if complex molecules participate in a reaction. This is
due to the fact that not all active collisions lead to a chemical
transformation. In order to account for this possibility, the expres-
sion for the reaction rate constant must include an additional factor
P which gives the probability that an active collision will result
in a chemical transformation (sometimes P is called a steric factor).
In this case, the expression for $\bar{k}$ becomes

$$\bar{k} = Pb(T)\exp\left(-\frac{E_a}{RT} \right).$$

$$(4.27)$$

If all active collisions result in a reaction, then H = 1. In
reactions in which complex molecules participate, the value of P may
be very small (on the order of 10^{-8}).

Instead of the Expression (4.27), one most often makes use of
the expression

Footnote (3) appears on page 269.

$$\bar{k} = Z(T)\exp\left(-\frac{E_a}{RT}\right),$$

(4.28)

which was introduced by Arrhenius. The value of the factor $Z(T)$ that multiplies the exponent is usually determined experimentally, and for some of the not too complex reactions, it may be computed on the basis of the theory of absolute reaction rates[4].

Heterogeneous chemical reactions[5]. In chemical kinetics, the term "heterogeneous" refers to reactions which occur on the separating surfaces, i.e., on phase boundaries. Depending on the character of the surface participation in the reaction, the heterogeneous reactions that are of greatest interest can be of two types.

In one case, the surface plays the role of a catalyst for the reactants existing in the gas phase. Here the products of a heterogeneous catalytic reaction do not contain the elements of which the surface is composed. In the course of such a reaction, neither the properties of the catalyst nor the shape of the catalytic surface undergo any change. An example of such a reaction is provided by the catalytic recombination of atoms.

In the second case, the surface plays an active rule in the reaction. An example is the combustion of a carbon surface which is submerged in a stream of high-temperature air. In the course of such a reaction, the shape of the surface may change due to the removal of the combustion products by the air stream.

The chemical process occurring in heterogeneous reactions is localized in a thin (monomolecular) layer at the surface. The volume of the layer is determined by the area of the surface and the dimensions of the reacting molecules. The monomolecular layer holds on to the surface as a result of the forces of chemical adsorption, whose

---

Footnotes (4) and (5) appear on page 269.

nature is similar to the forces of valence bonding (physical, or Van der Waals, adsorption rarely leads to heterogeneous reactions).

A reaction occurring at a solid surface may be divided into the following stages: 1) transport of the reactants to the surface, 2) chemical adsorption of the reactants by the surface, 3) chemical reaction between the reactants, adsorbed at the surface or between the adsorbed species and the species in the gas phase, 4) desorption of the reaction products from the surface, 5) removal of the reaction products from the surface.

As an example let us consider the surface reaction of the recombination and dissociation of oxygen. One of the possible mechanisms of this reaction, bearing the name of Langmuir-Hinshelwood [8], may be described by the following system of equations:

$$O + W \rightleftarrows OW, \tag{4.29}$$

$$OW + OW \rightleftarrows O_2 + W + W. \tag{4.30}$$

Equation (4.29) describes the adsorption (forward reaction) and desorption (reverse reaction) of the oxygen atom. W denotes the so-called active portion of the surface, and OW denotes the adsorbed oxygen atom, i.e., the atom which is chemically bound to the surface. Equation (4.30) describes a reaction between the neighboring adsorbed atoms, as a result of which an oxygen molecule is formed and released (desorbed), and the active segments (W) become free.

Another possible mechanism of the reaction, sometimes called the Ridil-Eli mechanism [8], is described by the equations

$$O + W \rightleftarrows OW, \tag{4.29}$$

$$O + OW \rightleftarrows O_2 + W. \tag{4.31}$$

Equation (4.31) describes a reaction between an adsorbed oxygen atom and the oxygen atom in the gas phase.

In both first and second cases, the reaction rates depend on the type of surface and the conditions on it.

In gasdynamic applications it is usually assumed for simplicity that the adsorption reaction (4.29) occurs very fast, and thus does not determine the rate of the entire process as a whole. In this case, reactions of the type (4.30) and (4.31) will be decisive. Schematically, both of these reactions can be written in the form

$$A_i \underset{k_{wj}}{\overset{k_{wi}}{\rightleftarrows}} A_j, \tag{4.32}$$

where k_{wi} and k_{wj} are the rates of the forward and reverse surface catalytic reactions. The expression for the rate of formation of species A_i, provided by formal kinetics, can be written as

$$g_{A_{iw}} = \frac{d[A_i]_w}{dt} = k_{wi}[A_i]_w^{n_i} - k_{wj}[A_j]_w^{n_j}, \tag{4.33}$$

where n_i and n_j are the orders of the forward and reverse reactions, respectively. $[A_i]_w$ and $[A_j]_w$ are the concentrations of the reactant and the reaction product at the wall. The dimensionality of the rates k_{wi} (or k_{wj}) depends on the dimensionality of the concentrations of the reactant and the reaction product.

Taking into consideration the equilibrium constant

$$K_w = \frac{k_{wj}}{k_{wi}} = \frac{\{[A_i]_w^{n_i}\}^{(e)}}{\{[A_j]_w^{n_j}\}^{(e)}} \tag{4.34}$$

[here the superscript (e) denotes parameters in the state of thermodynamic equilibrium], we write Equation (4.33) in the form

$$g_{A_{iw}} = \frac{d[A_i]_w}{dt} = k_{wi}\{[A_i]_w^{n_i} - K_w[A_j]_w^{n_j}\}. \tag{4.35}$$

Under stationary conditions, the rate of formation of a species is equal to the diffusive flux of the species toward the surface:

$$j_{A_{i}w} = - k_{wi}\{[A_i]_w^{n_i} - K'_w[A_j]_w^{n_j}\}. \tag{4.36}$$

Equation (4.36) may be used as a boundary condition in solving boundary layer problems involving surface catalytic reactions.

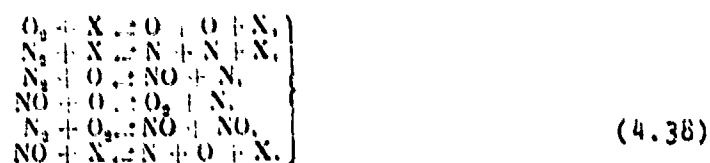The temperature dependence of the constant k_{wi} is in many cases well described by the Arrhenius law

$$k_{wi} = k_{0i}\exp\left(-\frac{E_{aw}}{RT_w}\right). \tag{4.37}$$

Here k_{0i} is a constant of the reactant-catalyst system which is under consideration; E_{aw} is the activation energy. The ratio of E_{aw} to the universal gas constant R may be viewed as the "characteristic" temperature T_{aw} of the reactant-catalyst system.

Kinetics of dissociation and recombination reactions in the air. The air under normal conditions is primarily a mixture of two-atomic molecules of nitrogen and oxygen.

The fractions of carbon dioxide, water vapor, argon, and other admixtures are so small that their presence in the air may be neglected in a majority of practically important cases.

In the temperature range from 2000 to 8000° K, the three-atomic species such as O_3, NO_2, and some other multi-atomic nitrogen oxides, as well as the ionization process, do not play an important role. The following reactions are fundamental in the temperature range indicated [9]:

$$\left.\begin{array}{l} O_2 + X \rightleftarrows O + O + X, \\ N_2 + X \rightleftarrows N + N + X, \\ N_2 + O \rightleftarrows NO + N, \\ NO + O \rightleftarrows O_2 + N, \\ N_2 + O_2 \rightleftarrows NO + NO, \\ NO + X \rightleftarrows N + O + X. \end{array}\right\} \tag{4.38}$$

Here X stands for the catalyst molecule.

Out of the six reactions given, the last four, involving nitrogen oxide NO, play a secondary role as compared with the first two reactions, because the equilibrium content of nitrogen oxide is usually small (no greater than 1%). Therefore, in performing approximate calculations when the basic objective is to obtain integral characteristics (friction, heat flux), one may in many cases consider only the first two reactions. It was already noted above that molecular oxygen is almost completely dissociated (equilibrium dissociation is being considered) before nitrogen begins to dissociate. This fact permits us to consider air as a binary mixture of atoms and molecules. It is only necessary in this case to consider the difference in the dissociation energies of oxygen and nitrogen.

In nonequilibrium dissociation, the binary model of the air may in certain cases turn out to be insufficient due to the difference in the recombination rates k_r for reactions in which different catalyst molecules (X) participate. The values of the constants k_r for various reactions and different catalyst molecules are given in Table 13, adapted from the book by Chung [10]. As is seen in Table 13, the basic scheme which the dissociation reactions follow can be written in the form

$$A_2 + X \underset{k_r(X)}{\overset{k_d(X)}{\rightleftharpoons}} A + A + X. \tag{4.39}$$

Here A_2 denotes a two-atom molecule, A denotes an atom, X represents a catalyst particle (atom or molecule).

The process of dissociation and recombination, occurring according to the scheme $A_2 \rightleftharpoons A + A$, i.e., without the participation of the particle X, does not play an important role. The rate of the forward reaction is small, since the direct disintegration of a strongly excited molecule is very unlikely. The rate of the reverse reaction is also small, since the molecules forming as a result of combinations involving two atoms possess a very large energy. Due to this fact, a majority of such molecules dissociate upon the first collision with other particles.

TABLE 13

Reaction	D, e	X	$cm^2/mole^2$ sec
$O_2 + X \rightleftarrows O + O + X$	5.1	O O_2 N_2 N, NO	$0.23 \cdot 10^{10} \cdot T^{-1}$ $0.8 \cdot 10^{10} \cdot T^{-1}$ $6.19 \cdot 10^{10} \cdot T^{-1}$ $3.02 \cdot 10^{10} \cdot T^{-1}$
$N_2 + X \rightleftarrows N + N + X$	9.8	N N_2 O_2, O, NO	$2.36 \cdot 10^{10} \cdot T^{-1}$ $2.7 \cdot 10^{10} \cdot T^{-1}$ $1.09 \cdot 10^{10} \cdot T^{-1}$
$NO + X \rightleftarrows N + O + X$	6.5	NO O, N, O_2, N_2	$2 \cdot 10^{10} \cdot T^{-1}$ $1.03 \cdot 10^{10} \cdot T^{-1}$
$O + N_2 \rightleftarrows NO + N$	3.3		$1.63 \cdot 10^{10} \quad \dfrac{cm^3}{mole \cdot sec}$

Table 13 indicates that the recombination rates for oxygen and nitrogen may differ significantly depending on the type of the catalyst particle (X) participating in the reaction. The reaction rate constants, for reactions which differ only in the type of the catalyst particle, depend solely on the temperature and are related to each other by a relation which follows from the principle of detailed balance:

$$\frac{k_a(T, X)}{k_r(T, X)} = K_n(T). \qquad (4.40)$$

where $K_n(T)$ is an equilibrium constant given by Equation (4.17)

Using the relations obtained earlier in this section, it is not difficult to write an expression for the mass rate of formation of the atomic species w_A in a reaction described by the stoichiometric Equation (4.39). Here if the mixture consists of N species, then in a general case the mass rate of formation w_A can be obtained, in accordance with the principle of the independence of reactions (4.9),

by summing the rates of formation in each of the reactions (in this case the number of reactions s is equal to the number of species N). For later use, it is convenient to obtain an expression for w_A in terms of the mass concentrations of species. Therefore, we shall use the last of Equations (4.20) for the rate of formation $d[n_A]/dt$, and Equation (4.16) and the last of Equations (4.19) for the equilibrium constant and the ratio K_a^*/K_a, respectively. Taking into account the fact that for all N reactions of the type (4.39), differing only in the catalyst particle X, the stoichiometric coefficients are identical and equal to $v_{A.} = 1, v_X' = 1, \quad v_A' = 0, \quad v_{A.}' = 0, \quad v_X'' = 1, v_A = 2$, and also the fact that

$$s = \sum_{k=1}^{N} v_k' = 2, \quad \Delta v = \sum_{k=1}^{N} (v_k'' - v_k') = 1.$$

we obtain

$$w_A = \sum_{s=1}^{N} w_{A_s} = M_A \sum_{s=1}^{N} \left(\frac{d[n_A]}{dt} \right)_s =$$
$$= \rho^e r_A \left(1 - \frac{1}{K_c} \frac{c_A^2}{c_{A_s}} \frac{\rho}{\rho^{(e)}} \right) \sum_{s=1}^{N} k_{ds} \frac{c_{X_s}}{M_{X_s}} \quad . \tag{4.41}$$

Here and below the superscript (e) denotes the equilibrium parameters; c_{X_s} is the mass concentration of the catalyst (X) in the sth reaction; N is the number of species (reactions).

Sometimes the mass rate of formation of the atomic species w_A may be more conveniently expressed not in terms of the dissociation rate constants k_{ds}, as in the Expression (4.41), but in terms of the recombination rates k_{rs}. In this case, in view of Equation (4.40) and the relation between the constants K_n and K_c, given by Equation (4.18), it is not hard to obtain the result

$$w_A = 2M_A^2 \rho^e c_{A_s} \left(K_c \frac{\rho^{(e)}}{\rho} - \frac{c_A^2}{c_{A_s}} \right) \sum_{s=1}^{N} k_{rs} \frac{c_{X_s}}{M_{X_s}}. \tag{4.42}$$

In the case of reaction (4.39), the equilibrium constant K_c, generally given by Equation (4.16), becomes

$$K_c = \frac{c_A^{(o)}}{c_{A_2}^{(o)}}.$$

(4.43)

In order to determine the equilibrium constant we turn to Equation (4.21). For the reaction (4.39), the former equation becomes

$$\ln K_p = -\frac{\Delta E_0}{RT} + 2\ln Q_p(A) - \ln Q_p(A_2).$$

(4.44)

Let us substitute the expressions for the partition functions of the molecules (4.26) and atoms in the preceding equation (the partition function for the translational energy levels for atoms, Q_A^t, is defined in the same way as $Q_{A_2}^t$, except that m_{A_2} must be replaced with m_A). Upon substitution and changing from K_p to K_c, by Equation (4.18), we obtain

$$K_c = \frac{\exp\left(-\frac{T_d}{T}\right)}{\rho^{(o)}}\left\{m_A\left(\frac{\pi m_A k}{h^2}\right)^{\frac{3}{2}}(T_r T_v^{\frac{3}{2}})\left(\frac{T}{T_o}\right)^{\frac{3}{2}}\left[1 - \exp\left(-\frac{T_v}{T}\right)\right]\frac{(Q_A')^2}{Q_{A_2}'}\right\}.$$

(4.45)

Here T_d is the characteristic dissociation temperature, equal to

$$T_d = \frac{D}{\frac{R}{2N_A}}, \qquad D = \frac{\Delta E_0}{2N_A}.$$

(4.46)

D is the dissociation energy per unit molecule mass, ΔE_0 is the dissociation energy per mole of the starting substance (molecules).

Thus, to determine the equilibrium constant K_c it is necessary to know the characteristic temperatures: of dissociation, T_d, of vibration, T_v, of rotation, T_r, as well as the electron partition functions for the basic components of the air. Data on the characteristic temperatures are given in Table 14 [11].

The electron partition functions are written in the form (see the paper by Hansen which was quoted)

$$Q_{O_2}^e = 3 + 2\exp\left(-\frac{11\,390}{T}\right) + \exp\left(-\frac{18\,990}{T}\right),$$

$$Q_O^e = 5 + 3\exp\left(-\frac{223}{T}\right) + \exp\left(-\frac{326}{T}\right) +$$

$$+ 5\exp\left(-\frac{22\,800}{T}\right) + \exp\left(-\frac{48\,600}{T}\right),$$

$$Q_{N_2}^e = 1,$$

$$Q_N^e = 4 + 10\exp\left(-\frac{27\,700}{T}\right) + 6\exp\left(-\frac{41\,500}{T}\right). \tag{4.47}$$

TABLE 14

	$M_i, \frac{g}{\text{mole}}$	m_i, g	$T_d, °K$	$T_v, °K$	$T_r, °K$
O_2	32	$5.312 \cdot 10^{-23}$	59 000	2270	2.08
N_2	28	$4.648 \cdot 10^{-23}$	113 200	3390	2.89

Equations (4.47) imply that in the temperature range under consideration, (2000 - 8000° K), the ratios of the electron partition functions for oxygen and nitrogen, which are necessary in calculating the equilibrium constants, are only insignificantly modified. Therefore, we can write approximately

$$\frac{(Q_O^e)^2}{Q_{O_2}^e} \approx 27, \qquad \frac{(Q_N^e)^2}{Q_{N_2}^e} \approx 16. \tag{4.48}$$

If we made the assumption (4.48) — namely, that the ratios of the electron partition functions are constant (for nitrogen this assumption is satisfied to a high degree of accuracy and for oxygen the error does not exceed 10 - 12%) — then the expression for the equilibrium constant (4.45) may be written in the following form:

$$K_c = 2\frac{\rho_d}{\rho^{(A)}}\left(\frac{T}{T_v}\right)^{3/2}\left[1 - \exp\left(-\frac{T_v}{T}\right)\right]\exp\left(-\frac{T_d}{T}\right). \tag{4.49}$$

Here

$$\rho_d = \frac{m_A}{2}\left(\frac{\pi m_A k}{h^2}\right)^{3/2}(T_r T_v^{3/2})\frac{(Q_A^e)^2}{Q_{A_2}^e} \tag{4.50}$$

is the so-called characteristic density. A dissociating gas whose equilibrium state is described by Equation (4.49) (ρ_d = const) has come to be called a "partially excited dissociating gas" [12]. For oxygen, assuming Equation (4.48) is satisfied, ρ_d = 151 g/cm^3. For nitrogen under the same assumption, ρ_d = 107 g/cm3 [12].

If we compute the expression

$$\rho_{dL} = 2\rho_d \left(\frac{T}{T_v}\right)^{1/2}\left[1 - \exp\left(-\frac{T_v}{T}\right)\right]. \tag{4.51}$$

which appears on the right-hand side of Equation (4.49) then we see that, for gases such as oxygen and nitrogen, the value of ρ_{dL} varies relatively little within a wide temperature range. This can be seen in the Table 15, adapted from the work by Lighthill, which was already quoted in this section.

TABLE 15

T, °K		1000	2000	3000	4000	5000	6000	7000
ρ_{dL}, $\dfrac{g}{cm^3}$	O$_2$	145	170	166	156	144	133	123
	N$_2$	113	135	136	133	124	123	118

This feature of the behavior of ρ_{dL} was used by Lighthill, who proposed a model of an "ideally dissociating gas" in which one of the basic assumptions is the assumption that the value of ρ_{dL}, which just like ρ_d has the dimensions of density, is constant. ρ_{dL} came to be called the characteristic density of an ideally dissociating gas. For oxygen and nitrogen, the values of ρ_{dL} may be taken to be equal to 150 g/cm^3 and 130 g/cm^3, respectively (other properties of an ideally dissociating gas, just as the properties of a partially excited dissociating gas, will be considered in the following section). Thus, for an ideally dissociating gas the Expression (4.49) for the equilibrium constant K_c, in view of Equation (4.51), becomes

$$K_c = \frac{\rho_{dL}}{\rho^{(r)}} \exp\left(-\frac{T_d}{T}\right) \quad (\rho_{dL} = \text{const}). \tag{4.52}$$

Now substituting the Expression (4.52) for the equilibrium constant K_c into Equations (4.41) and (4.42), we obtain the following equivalent relations for the mass rate of formation of the atomic species:

$$w_A = \rho^2 c_{A_2}\left[1 - \frac{\rho}{\rho_{dL}} \exp\left(\frac{T_d}{T}\right) \frac{c_A^2}{c_{A_2}}\right] \sum_{i=1}^{N} k_{di} \frac{c_{X_i}}{M_{X_i}}, \tag{4.53}$$

$$w_A = 2\rho^2 c_{A_2} M_A^{-1}\left[\frac{\rho_{dL}}{\rho} \exp\left(-\frac{T_d}{T}\right) - \frac{c_A^2}{c_{A_2}}\right] \sum_{i=1}^{N} k_{ri} \frac{c_{X_i}}{M_{X_i}}. \tag{4.54}$$

For a binary mixture consisting of atoms and molecules of a single gas ($c_A + c_{A_2} = 1$), the preceding expressions will become

$$w_A = \rho^2(1 - c_A) M_A^{-1}\left[1 - \frac{\rho}{\rho_{dL}} \exp\left(\frac{T_d}{T}\right) \frac{c_A^2}{1 - c_A}\right] \times$$
$$\times \left[k_d(A)c_A + \frac{1}{2}(1 - c_A)k_d(A_2)\right]. \tag{4.55}$$

$$w_A = 2\rho^2(1 - c_A) M_A^{-1}\left[\frac{\rho_{dL}}{\rho} \exp\left(-\frac{T_d}{T}\right) - \frac{c_A^2}{1 - c_A}\right] \times$$
$$\times \left[k_r(A)c_A + \frac{1}{2}(1 - c_A)k_r(A_2)\right]. \tag{4.56}$$

In those cases when the difference between the dissociation rate constant (or, which is the same thing, recombination rate constants) is insignificant and one can limit himself to just one constant, Equations (4.55) and (4.56) will be written in the form

$$w_A = \frac{1}{2}\rho^2(1 - c_A^2) M_A^{-1} k_d\left[1 - \frac{\rho}{\rho_{dL}} \exp\left(\frac{T_d}{T}\right) \frac{c_A^2}{1 - c_A}\right]. \tag{4.57}$$

$$w_A = \rho^2(1 - c_A^2) M_A^{-1} k_r\left[\frac{\rho_{dL}}{\rho} \exp\left(-\frac{T_d}{T}\right) - \frac{c_A^2}{1 - c_A}\right]. \tag{4.58}$$

Using Equations (4.43) and (4.45), it is not hard to reduce the last two expressions for the mass rate of formation of the atomic species to the form

$$w_A = -\frac{1}{2}\rho^2 M_A^{-1} k_d \left(1 - \frac{c_A^2}{c_A^{(e)2}}\right). \tag{4.59}$$

$$w_A = \rho^2 M_A^{-2} k_r (1 + c_A) \frac{c_A^{(e)2} - c_A^2}{1 - c_A^{(e)2}}. \tag{4.60}$$

Equating the right-hand sides of Equations (4.59) and (4.60), we find after simple algebra an expression for the equilibrium constant

$$K_n = \frac{k_d}{k_r} = \frac{4p}{RT} \frac{c_A^{(e)2}}{1 - c_A^{(e)2}}. \tag{4.61}$$

The reaction rate constants generally depend on the temperature according to the Arrhenius law [see Equation (4.28)], i.e., they increase exponentially with the temperature. The atom recombination rate constant is an exception to this rule, since the recombination reaction proceeds without energy losses to activation ($E_{ar} = 0$). The expression for the recombination rate constant has the form

$$k_r = Z_r(T). \tag{4.62}$$

For recombination reactions, occurring in the air, k_r is satisfactorily approximated by a power-law dependence on temperature, of the form (see Table 12)

$$k_r = A_r T^{-n} \qquad (0 \leqslant n \leqslant 2). \tag{4.63}$$

The equilibrium constants K_n for the more important reactions, occurring in the air at temperatures ranging from 3000 to 8000° K, were approximated by Ree (see the work by Ree, already quoted in this section) by relations of the form

$$K_n = A T^n \exp\left(-\frac{\Delta E_0}{RT}\right).$$

The results of the approximation (with an error less than 10%) are given in Table 16.

TABLE 16

Reaction	Equilibrium constant K_n	Dimension-ality
$O_2 + X \rightleftarrows O + O + X$	$1{,}2 \cdot 10^9 T^{-1/2} \exp(-118\,000/RT)$	$mole/cm^3$
$N_2 + X \rightleftarrows N + N + X$	$18 \exp(-224\,900/RT)$	$mole/cm^3$
$NO + X \rightleftarrows N + O + X$	$4{,}0 \exp(-150\,000/RT)$	$mole/cm^3$
$N_2 + O \rightleftarrows NO + N$	$4{,}5 \exp(-75\,000/RT)$	1
$NO + O \rightleftarrows O_2 + N$	$0{,}24 \exp(-32\,020/RT)$	1
$N_2 + O_2 \rightleftarrows NO + NO$	$19 \exp(-42\,980/RT)$	1

Table 17 lists the values of the rate constants for reactions occurring in the air, which were recommended in the monograph by Ye. V. Stupochenko et al. [13].

The boundary conditions at a catalytic surface generally have the form (4.36). For catalytic recombination reactions, the conditions at the surface are usually far from thermodynamic equilibrium, $[A]_w \gg [A]^{(e)}$. Therefore, the second term on the right-hand side of Equation (4.36) may usually be neglected as compared with the first. In this case, Equation (4.36) becomes

$$J_{A_i w} = -k_w (\rho c_A)_w^n. \qquad (4.64)$$

Using the expression for the diffusive flow of species i (1.57), we write Equation (4.64) in the form

$$\left(\rho \mathscr{D}_i \frac{\partial c_A}{\partial y} \right)_w = k_w (\rho c_A)_w^n. \qquad (4.65)$$

Here K_w is the rate of the catalytic recombination, which depends on the temperature according to the Arrhenius law (4.37); n is the order of the reaction.

TABLE 17

	Reaction	x	k_i cm³/mole·sec
1)	$O_2 + X \rightarrow$ $\rightarrow O + O + X$ $\Delta E_0 =$ $= 118$ kcal/mole	O_2	$5.2 \cdot 10^{10} T^{1/2} \left(\dfrac{\Delta E_0}{RT}\right)^2 \exp\left(\dfrac{-\Delta E_0}{RT}\right)$
		N_2	$2.5 \cdot 10^{11} T^{1/2} \left(\dfrac{\Delta E_0}{RT}\right)^{1.5} \exp\left(\dfrac{-\Delta E_0}{RT}\right)$
		O	$6.25 \cdot 10^{12} T^{1/2} \left(\dfrac{\Delta E_0}{RT}\right)^{1.5} \exp\left(\dfrac{-\Delta E_0}{RT}\right)$
		N, NO	$k_i(O_2)$
		Ar	$4.2 \cdot 10^{11} T^{1/2} \left(\dfrac{\Delta E_0}{RT}\right) \exp\left(\dfrac{-\Delta E_0}{RT}\right)$
2)	$N_2 + X \rightarrow$ $\rightarrow N + N + X$ $\Delta E_0 =$ $= 225$ kcal/mole	N_2	$4.25 \cdot 10^{11} T^{1/2} \left(\dfrac{\Delta E_0}{RT}\right)^{?,?} \exp\left(\dfrac{-\Delta E_0}{RT}\right)$
		N	$1.85 \cdot 10^{1?} T^{1/?} \left(\dfrac{\Delta E_0}{RT}\right)^{1.5} \exp\left(\dfrac{-\Delta E_0}{RT}\right)$
		O_2, NO, O	$k_i(N_2)$
		Ar	$6.8 \cdot 10^{11} T^{1/2} \left(\dfrac{\Delta E_0}{RT}\right)^{1.5} \exp\left(\dfrac{-\Delta E_0}{RT}\right)$
3)	$NO + X \rightarrow$ $\rightarrow N + O + X$ $\Delta E_0 =$ $= 150$ kcal/mole	O_2, N_2, Ar	$7 \cdot 10^{10} T^{1/2} \left(\dfrac{\Delta E_0}{RT}\right)^2 \exp\left(\dfrac{-\Delta E_0}{RT}\right)$
		NO, O, N	$20 k_i(Ar)$
4)	$O + N_2 \rightarrow$ $\rightarrow NO + N$ $N + O_2 \rightarrow$ $\rightarrow NO + O$ $N_2 + O_2 \rightarrow$ $\rightarrow NO + NO$		$7 \cdot 10^{13} \exp T (-75\,500/RT)$ $1.3 \cdot 10^{10} T \exp(-7100/RT)$ $9.1 \cdot 10^{13} T^{-1/2} \exp(128\,500/RT)$

If the wall temperatures are not too high, reactions of the type (4.32) proceed in the first order, i.e., $n = 1$.

Equation (4.65) implies that for $k_W = 0$

$$(\partial \, [c_A]/\partial y)_w = 0,$$

which corresponds to a chemically insulated (absolutely noncatalytic) surface; for $k_w \to \infty \, c_{Aw} \to 0$, which corresponds to an absolutely catalytic surface.

At the present time, information regarding the rate of the catalytic recombination reactions for nitrogen and oxygen at various surfaces is very limited. Some of the available results are plotted in Figure 58, adapted from the work [14]. The abscissa axis in that figure measures the catalytic ability γ_W, related to the constant k_W by

$$\gamma_w = k_w \left(\frac{2\pi M_A}{RT} \right). \qquad (4.66)$$
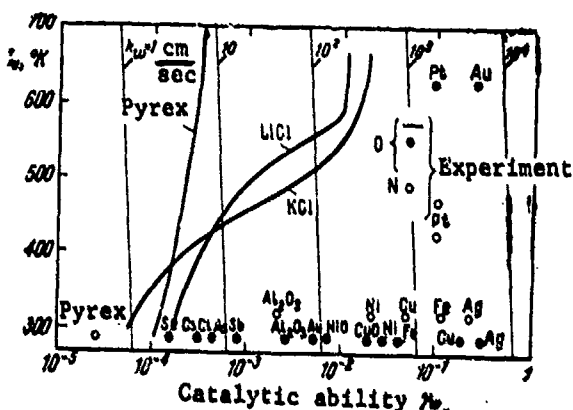
Figure 58

On the ordinate axis, we plot the wall temperature $\blacklozenge_{\!\!j}$. The figure includes the lines of constant k_W, which for oxygen and nitrogen are practically identical.

It should be noted that the data given in Figure 58 were obtained for a recombination of pure nitrogen and oxygen. The processes of catalytic recombination for a mixture of nitrogen and oxygen have not been sufficiently investigated.

§ 21. The Properties of Partially Excited, Dissociating and Ideally Dissociating Gases

In the preceding section, we obtained the expressions for the equilibrium constants for a partially excited dissociating gas (4.49) and an ideally dissociating gas (4.52), as well as the expressions for the mass rates of formation of atomic components.

For a partially excited dissociating gas, consisting of atoms and molecules (binary mixture), the equilibrium composition can be determined from the following relation:

$$\frac{c_A^{(e)'}}{1 - c_A^{(e)}} = 2 \frac{\rho_d}{\rho^{(e)}} \left(\frac{T}{T_v}\right)^2 \left[1 - \exp\left(-\frac{T_v}{T}\right)\right] \exp\left(-\frac{T_d}{T}\right), \qquad (4.67)$$

which was obtained from Equations (4.43) and (4.49). The value of the characteristic density ρ_d, generally given by Equation (4.50), for oxygen may be taken to be equal to $\rho_d(O_2) = 151 \text{ g/cm}^3$, and for nitrogen — $\rho_d(N_2) = 107 \text{ g/cm}^3$.

For an ideally dissociating gas, Equations (4.43) and (4.52) imply that

$$\frac{c_A^{(e)'}}{1 - c_A^{(e)}} = \frac{\rho_{dL}}{\rho^{(e)}} \exp\left(-\frac{T_d}{T}\right), \qquad (4.68)$$

where ρ_{dL} is given by Equation (4.51).

For oxygen, we take $\rho_{dL} = 150 \text{ g/cm}^3$ and for nitrogen $\rho_{dL} = 130 \text{ g/cm}^3$.

For later use, let us consider the thermodynamic properties of dissociating gasses.

Statistical thermodynamics leads to the following expressions for the enthalpy and the integral energy of a gas mixture:

$$h = \sum_i c_i h_i = \sum_i c_i \left[-\frac{R}{M_i} T^2 \left(\frac{\partial \ln Q_{ip}}{\partial T} \right) + h_i^0 \right], \tag{4.69}$$

$$E = \sum_i c_i E_i = \sum_i c_i \left[-\frac{R}{M_i} T^2 \left(\frac{\partial \ln Q_{ic}}{\partial T} \right) + h_i^0 \right]. \tag{4.70}$$

Here Q_{ip} is the partition function of species i in a gas mixture at unit pressure, defined by Equations (4.23) - (4.26); Q_{ic} is the partition function for the ith component of the gas mixture of unit concentration

$$Q_{ic} = \frac{p}{RT} Q_i, \tag{4.71}$$

Q_i is given by Equations (4.24) - (4.26); h_i^0 is the formation energy of species i per unit mass at a temperature equal to absolute zero.

For a binary mixture of atoms and molecules with ground electron states, substitution of Q_{ip} and Q_{ic} into Equations (4.69) and (4.70), respectively, gives

$$h = \left[\frac{7}{2} + \frac{3}{2} c_A + (1 - c_A) \frac{\frac{T_v}{T}}{e^{T_v/T} - 1} \right] \frac{R}{2M_A} T + c_A D, \tag{4.72}$$

$$E = \left[\frac{5}{2} + \frac{1}{2} c_A + (1 - c_A) \frac{\frac{T_v}{T}}{e^{T_v/T} - 1} \right] \frac{R}{2M_A} T + c_A D. \tag{4.73}$$

In the above expressions for the enthalpy and internal energy of a partially exicted dissociating gas, the third term in brackets describes the contribution of the vibrational degrees of freedom to the enthalpy and internal energy. The magnitude of this term for the temperature changing from 0 to ∞ varies from zero to $(1 - c_A)$. The maximum contribution of the vibrational degrees of freedom occurs at $c_A = 0$, and amounts to about 20% of the total enthalpy and 30% of the total internal energy.

At high temperatures, when dissociation becomes noticable, Equations (4.72) and (4.73) may be simplified by setting $[T_v/T]$ [exp $(T_v/T) - 1] = 1/2$. According to this assumption — which provides,

along with the assumption about the constant characteristic density (ρ_{dL} = const), a basis for the Lighthill model of an ideally dissociating gas — it is assumed that the vibrational degrees of freedom of gas molecules are excited regardless of the temperature by an amount equal to one half the value of the "classical" vibrational excitation of molecules. This assumption does not lead to a great error at high temperatures, since with a temperature increase, the molecule concentration $(1 - c_A)$ decreases and the contribution of the term $c_A D$ increases. Thus for an ideally dissociating gas we have

$$h = (4 + c_A) \frac{R}{2M_A} T + c_A D, \tag{4.74}$$

$$E = 3 \frac{R}{2M_A} T + c_A D. \tag{4.75}$$

Next, having the expressions for the enthalpy and the internal energy of partially excited dissociating and ideally dissociating gases, let us determine the "effective" specific heat capacities of a gas at constant pressure and constant volume.

By definition, the specific heat capacities of a mixture of gases at constant pressure, c_p, and constant volume, c_v, are given by

$$c_p = \left(\frac{\partial h}{\partial T} \right)_p, \quad c_v = \left(\frac{\partial E}{\partial T} \right)_\rho. \tag{4.76}$$

Substituting in Equations (4.76) the expressions for h and E (4.69) and (4.70), and taking Equation (4.67) into account, we find the "effective" specific heat capacities of a partially excited dissociating gas in a state of equilibrium

$$\frac{c_p}{\frac{R}{2M_A}} = \frac{7}{2} + \frac{3}{2} c_A + (1 - c_A) \frac{\frac{T_v}{T}}{1 - e^{-T_v/T}} + \tag{4.77}$$

$$+ \frac{1}{2} c_A (1 - c_A^2) \left(\frac{3}{2} + \frac{T_d}{T} - \frac{\frac{T_v}{T}}{1 - e^{-T_v/T}} \right)^2,$$

$$\frac{c_v}{\dfrac{R}{2M_A}} = \frac{5}{2} + \frac{1}{2}c_A + (1-c_A)\frac{\frac{T_v}{T}}{1-e^{-T_v/T}} +$$

$$+ \frac{c_A(1-c_A)}{2-c_A}\left(\frac{1}{2} + \frac{T_d}{T} - \frac{\frac{T_v}{T}}{1-e^{-T_v/T}}\right)^2. \qquad (4.78)$$

Similarly, using Equations (4.68) and (4.74) - (4.76), we obtain the "effective" specific heat capacities of an ideally dissociating gas in thermodynamic equilibrium

$$\frac{c_p}{\dfrac{R}{2M_A}} = 4 + c_A + \frac{1}{2}c_A(1-c_A^2)\left(1 + \frac{T_d}{T}\right)^2, \qquad (4.79)$$

$$\frac{c_v}{\dfrac{R}{2M_A}} = 3 + \frac{c_A(1-c_A)}{2-c_A}\left(\frac{T_d}{T}\right)^2. \qquad (4.80)$$

From the last two equations, it follows that the assumption about constant excitation of the vibrational degrees of freedom implies that the ratios of the specific heat capacities of an ideally dissociating gas before the onset of dissociation is c_p/c_v = 1.33, and not 1.4, as in the case of real two-atomic gases in the absence of an excitation of vibrational degrees of freedom. In addition, it is not hard to see that for an ideally dissociating gas, the specific heat capacities at constant volume per unit mass for molecules and atoms turn out to be identical: $c_vA = c_vA_2$, since the number of the degrees of freedom of the molecules (6) is twice as large as the number of degrees of freedom of atoms (3).

In various gas-dynamic investigations, including studies of boundary layers in dissociating gases, it is useful to introduce the characteristic pressure of an ideally dissociating gas, p_d

$$p_d = \frac{R}{2M_A}\rho_{dL}T_d. \qquad (4.81)$$

The values of p_d for oxygen and nitrogen, along with other quantities describing the properties of ideally dissociating oxygen and nitrogen, are given in Table 18.

TABLE 18

	T_d, °K	ρ_{dL}, g/cm^3	p_d, atm
O$_2$	59 000	150	$2.3 \cdot 10^7$
N$_2$	113 200	130	$4.1 \cdot 10^7$

An expression for the equilibrium concentration of atoms in an ideally dissociating gas as a function of temperature can be easily obtained from Equation (4.68) by using the equation of state for a binary mixture, transformed with the aid of Formula (4.81), to the form

$$\frac{p}{p_d} = \frac{\rho}{\rho_{dL}} \frac{T}{T_d}(1 + c_A).$$
(4.82)

Eliminating the density ρ for Equations (4.68) and (4.82), after simple transformations we obtain

$$c_A = \left[1 + \frac{p}{p_d} \frac{T_d}{T} \exp \frac{T_d}{T}\right]^{-1/2}.$$
(4.83)

In concluding this section (see Figure 59), we shall give the results of calculating the equilibrium concentration of oxygen atoms
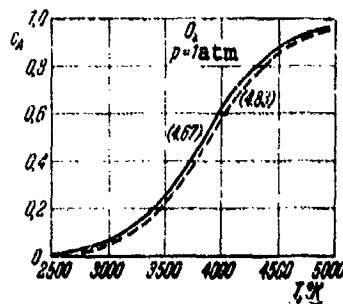
Figure 59

at the pressure p = 1 atm and various temperatures for an ideally dissociating gas [dashed curve corresponds to Formula (4.83), ρ_{dL} = 150 g/cm^3] and for a partially excited dissociating gas [solid curve corresponds to Formula (4.67), ρ_d = 151 g/cm^3].

As seen in Figure 59, adapted from an earlier quoted paper by Glass and Takano, the difference between the equilibrium concentrations of an ideally dissociating and partially excited dissociating gas is small.

§ 22. Statement of the Problem of a Turbulent Boundary Layer in a Dissociating Gas

Remarks concerning the dynamic structure of a turbulent boundary layer at high supersonic velocities. The results of measuring velocity profiles in a turbulent boundary layer on a flat plate for large Mach numbers (up to $M_e = 10$) and various values of the temperature factor (see Section 11) indicate that the velocity profile — constructed in terms of universal coordinates — in a laminar sublayer can be satisfactorily described by a linear relationship, and in a turbulent core (at least in its internal portion) it is of the logarithmic type.

As already noted above, a characteristic feature of velocity profiles for large Mach numbers is the fact that the width of the buffer zone between the laminar sublayer and the turbulent core is very small. The buffer zone is in essence almost completely non-existent, and there is a sharp transition from the sublayer to the core.

Another important feature of velocity profiles at large Mach numbers is the increase in the relative thickness of the laminar sublayer with increasing Mach number. In an incompressible fluid, the thickness of the laminar sublayer, as we know, does not exceed 2 - 3% of the thickness of the entire boundary layer. According to the data obtained by Hill and given in Section 11, at $M_e = 9$, the sublayer thickness may be about 15% of the entire thickness of the boundary layer.

These features of the experimental velocity profiles for high supersonic velocities will, of course, be taken into consideration when constructing the semi-empirical theory of a turbulent boundary layer. The very possibility of formulating a semi-empirical theory of the turbulent boundary layer for high supersonic velocities is to an extent based on the existence of a sufficiently extended logarithmic section of the velocity profile in the turbulent core. The existence

of such a section permits us to use the semi-empirical formulas of Prandtl and Karman in the theory of the turbulent boundary layer for high Mach numbers, since these formulas, as shown in Section 10, always result in a logarithmic velocity profile, no matter what the density distribution in the boundary layer is.

The sharp transition from the laminar sublayer to the turbulent core (disintegration of the buffer zone) justifies the use of the Prandtl double-layer scheme (laminar sublayer-turbulent core) in a theory of the turbulent boundary layer for high supersonic velocities.

Finally, the latter feature of velocity profiles for high supersonic velocities (increase in the relative thickness of the laminar sublayer) indicates the increasing role of the laminar sublayer in the heat and mass transfer in the boundary layer. As a result, when calculating the heat and diffusive fluxes, one must take proper account of the thermal and diffusive properties of the sublayer (deviation of the Prandtl and Schmidt numbers from unity). As far as the computation of friction for large supersonic velocities is concerned, here it is apparently permissible to consider the flow in the laminar sublayer assuming that the Prandtl and Schmidt numbers are equal to unity.

<u>Equation of the turbulent boundary layer in a dissociating gas. Boundary conditions</u>. The general equations of the turbulent boundary layer in a multicomponent mixture of chemically reacting gases were obtained in Chapter II. In the present chapter, we shall confine our attention to stationary flows in boundary layer under the assumption that the turbulent Prandtl and Schmidt numbers are equal to unity.

The fundamental equations will be written in the following form: equation of continuity

$$\frac{\partial}{\partial x}(\rho u r_0) + \frac{\partial}{\partial y}(\rho v r_0) = 0. \tag{4.84}$$

momentum equation

$$\rho u \frac{\partial u}{\partial x} + \rho v \frac{\partial u}{\partial y} = -\frac{dp}{dx} + \frac{\partial}{\partial y}\left[(\mu + \varepsilon)\frac{\partial u}{\partial y}\right], \qquad (4.85)$$

energy equation

$$\rho u \frac{\partial H}{\partial x} + \rho v \frac{\partial H}{\partial y} = \frac{\partial}{\partial y}\left(\varepsilon \frac{\partial H}{\partial y}\right) +$$
$$+ \frac{\partial}{\partial y}\left\{\frac{\mu}{Pr}\left[\frac{\partial H}{\partial y} + \sum_i (Le_i - 1) h_i \frac{\partial c_i}{\partial y} + \right.\right. \qquad (4.86)$$
$$\left.\left. + (Pr - 1)\frac{\partial}{\partial y}\left(\frac{u^2}{2}\right)\right]\right\},$$

equation of the conservation of species i

$$\rho u \frac{\partial c_i}{\partial x} + \rho v \frac{\partial c_i}{\partial y} = \frac{\partial}{\partial y}\left(\varepsilon \frac{\partial c_i}{\partial y}\right) + \frac{\partial}{\partial y}\left(\frac{\mu}{Sc_i}\frac{\partial c_i}{\partial y}\right) + w_i, \qquad (4.87)$$

equation of state

$$p = \rho R T \sum_i \frac{c_i}{M_i}. \qquad (4.88)$$

Total enthalpy H is given by the expressions

$$H = h + \frac{u^2}{2}, \quad h = \sum_i c_i h_i, \quad h_i = \int_0^T c_{pi} dT + h_i^0. \qquad (4.89)$$

For a nonpermeable surface, the boundary conditions for the velocities have the usual form

$$\left.\begin{array}{l} u = v = 0 \quad \text{for } y = 0, \\ u \to U_e \quad \text{for } y \to \infty. \end{array}\right\} \qquad (4.90)$$

The boundary conditions for the total enthalpy can be easily obtained from Equation (4.89). At the wall, we have

$$H = h_w = \sum_i c_{iw} \int_0^{T_w} c_{pi} dT + \sum_i c_i h_i^0 \quad \text{for } y = 0, \qquad (4.91)$$

at the outer edge of the boundary layer

$$H \to H_e = h_e + \frac{v_e^2}{2} = \sum_i c_{ie} \int_0^{T_e} c_{pi} dT + \sum_i c_{ie} h_i^0 + \frac{v_e^2}{2}$$
$$\text{for } y \to \infty. \tag{4.92}$$

The boundary conditions for total enthalpy (4.91) and (4.92) contain concentrations of species i at the wall, c_{iw}, and at the outer boundary, c_{ie}. The concentration of species i at the outer boundary is usually known from the solution for the outer flow. Therefore, the boundary condition for concentrations at the outer boundary has the form

$$c_i \to c_{ie} \quad \text{for} \quad y \to \infty. \tag{4.93}$$

The concentration at the wall c_{iw} in the presence of surface catalytic reactions is generally unknown beforehand and must be determined when solving the problem with the aid of the boundary condition (4.36) [for air, at not too high wall temperatures, the condition simplifies to (4.65)]. The boundary conditions for concentration at the wall are known in two extreme cases: 1) surface is absolutely noncatalytic ($k_{wi} = 0$). In this case, in view of the condition (4.36)

$$\frac{\partial c_i}{\partial y} = 0 \quad \text{for } y = 0; \tag{4.94}$$

2) surface is absolutely catalytic ($k_{wi} \to \infty$). In this case, in view of the same condition (4.36), we have

$$c_i = c_i^{(e)} \quad \text{for } y = 0. \tag{4.95}$$

For air, and not too high surface temperature, $c_A^{(e)} = 0$ for $y = 0$. Therefore, condition (4.95) simplifies to

$$c_i = 0 \quad \text{for } y = 0. \tag{4.96}$$

In the theory of the turbulent boundary layer, it is useful in many cases to use the energy equation and the equation of conservation

of species i in terms of the Crocco variables (2.63), (2.64). Below
the flow in the turbulent boundary layer will be discussed within
the framework of the double-layer Prandtl scheme (laminar sublayer-
turbulent core). For this reason, it will be convenient to write
these equations separately for the sublayer and the core, making use
of the assumption, stated earlier in this chapter, that the turbulent
Prandtl and Schmidt numbers are equal to unity.

In the laminar sublayer, we have:
the energy equation

$$
\rho u \frac{\mu}{\tau} \frac{\partial H}{\partial \xi} + \left(\frac{\partial \pi}{\partial u} - \frac{dp}{d\xi} \frac{\mu}{\tau} \right) \frac{\partial H}{\partial u} =
$$
$$
= \frac{\partial}{\partial u} \left\{ \tau \left[\frac{1}{Pr} \frac{\partial H}{\partial u} + \frac{1}{Pr} \sum_i (Le_i - 1) h_i \frac{\partial c_i}{\partial u} + \left(1 - \frac{1}{Pr} \right) u \right] \right\}, \tag{4.97}
$$

the equation of conservation of species i

$$
\rho u \frac{\mu}{\tau} \frac{\partial c_i}{\partial \xi} + \left(\frac{\partial \pi}{\partial u} - \frac{dp}{d\xi} \frac{\mu}{\tau} \right) \frac{\partial c_i}{\partial u} = \frac{\mu}{\tau} w_i + \frac{\partial}{\partial u} \left(\frac{\tau}{Sc_i} \frac{\partial c_i}{\partial u} \right). \tag{4.98}
$$

In the turbulent core, the equations of energy and conservation
of species i in terms of the Crocco variables become

$$
\rho u \frac{\partial H}{\partial \xi} - \frac{dp}{d\xi} \frac{\partial K}{\partial u} = \frac{\tau^2}{\varepsilon} \frac{\partial^2 H}{\partial u^2}, \tag{4.99}
$$

$$
\rho u \frac{\partial c_i}{\partial \xi} - \frac{dp}{d\xi} \frac{\partial c_i}{\partial u} = w_i + \frac{\tau^2}{\varepsilon} \frac{\partial^2 c_i}{\partial u^2}. \tag{4.100}
$$

The boundary conditions for Equations (4.97) - (4.100) will be
written in the following form:

$$
\left.
\begin{aligned}
H &= h_w, \ c_i = c_{iw} && \text{for } u = 0; \\
H &\to H_\infty, \ c_i \to c_{i\infty} && \text{for } u \to U'_\infty
\end{aligned}
\right\} \tag{4.101}
$$

It should be noted that the comments made at the beginning of
the present section regarding the boundary conditions for concentra-
tions at the wall are valid also in this case.

<u>Damkohler's number. Equilibrium, frozen, and nonequilibrium flows.</u>
The flow in the boundary layer with chemical reactions occuring in the
outer flow and in the boundary layer itself depends on the relation
between the rates of the diffusive and chemical processes.

Consider the equation of conservation of an atomic species (4.87),
assuming for simplicity that the mixture is binary and consists of
atoms and molecules. The expression in (4.60) will be used to repre-
sent the mass rate of formation of the atomic species. Substituting
this expression in the equation of conservation, we have

$$\rho u \frac{\partial c_A}{\partial x} + \rho v \frac{\partial c_A}{\partial y} =$$
$$= \frac{\partial}{\partial y}\left[\left(\frac{\mu}{Sc} + \varepsilon\right)\frac{\partial c_i}{\partial y}\right] + \rho^2 M_A^2 k_r (1 + c_A)\frac{c_A^{(e)\prime} - c_A^*}{1 - c_A^{(e)\prime}} .$$

Let us pass in this equation to dimensionless quantities, introducing
as the unit of length the characteristic dimension of the body L; as
the unit of velocity, the velocity of the incident flow U_∞; as the
units of density and viscosity, the density and viscosity of the
incident flow ρ_∞ and μ_∞. Upon making this substitution and performing
simple algebra, we obtain

$$\bar{\rho}\bar{u}\frac{\partial c_A}{\partial x} + \bar{\rho}\bar{v}\frac{\partial c_A}{\partial y} - \frac{1}{Re_L}\frac{\partial}{\partial y}\left[\left(\frac{\bar{\mu}}{Sc} + \bar{\varepsilon}\right)\frac{\partial c_A}{\partial y}\right] =$$
$$= Da \cdot \bar{\rho}^2 (1 + c_A)\frac{c_A^{(e)\prime} - c_A^2}{1 - c_A^{(e)\prime}} .$$

Here

$$Re_L = \frac{\rho_\infty U_\infty L}{\mu_\infty}, \qquad Da = \frac{\dfrac{L}{U_\infty}}{\dfrac{1}{\rho_\infty^2 M_A^2 k_r}} .$$

The dimensionless parameter Da, appearing on the right-hand side
of the equation thus obtained, is called the Damkohler number. The
meaning of the Damkohler number is easy to see by considering separately
the numerator and the denominator of the last equation. In fact, it
is easily seen that quantity L/U_∞, in the numerator, characterizes the
time spent by a particle in the boundary layer, (T_{flow}). The quantity
in the denominator, $1/\rho_\infty^2 M_A^{-2} k_r = t_{chem}$, also has the dimension of time.

This quantity characterizes the lifetime of an atom and is the characteristic time giving the rate of a chemical process.

Thus, the Damkohler number is the ratio of two characteristic times: time spent by the particle in the flow (time of diffusion) and the duration of a chemical reaction, i.e.,

$$Da = \frac{t_{\text{потока}}}{t_{\text{хим}}} = \frac{\dfrac{L}{U_\infty}}{\dfrac{1}{\rho_\infty^2 M_A^{-3} k_r}}. \qquad (4.102)$$

If Da → 0, then the duration of a chemical reaction is much longer than the time spent by the particle in the flow ($t_{chem} \gg t_{flow}$), and consequently, the effect of chemical reactions in the gas phase on the flow in the boundary layer is insignificant. In this case, the gas mixture in the boundary layer may be considered chemically inert, and the boundary layer may be regarded as of chemically "frozen." The products of dissociation, atoms, in this case appear in the boundary layer only due to their diffusion from the outer flow. For a chemically frozen boundary layer, the equation of conservation of species i is simplified, since the term expressing the mass rate of formation of species i is equal to zero, ($w_i \equiv 0$).

If the Damkohler number is very large, Da → ∞, then the duration of a chemical reaction is much smaller than the time spent by a particle in the boundary layer ($t_{chem} \ll t_{flow}$). Consequently, there will be enough time for a local thermodynamic equilibrium to be established at each point of the boundary layer. The distribution of the concentrations of each species will not depend on transfer processes (convection and diffusion), but will only depend on the local values of the temperature and pressure. The similarity to the equation of conservation of species i will not occur in this case, and the distribution of concentrations will be determined from the condition $w_i = 0$ (the equality sign must not be confused with the identity sign in the case of a frozen flow). The boundary layer in which thermodynamic equilibrium is established is called an "equilibrium" layer.

When the Damkohler number has a finite value, the rates of the chemical process and the transfer processes turn out to be of the same order ($t_{flow}/t_{chem} \sim 1$). Therefore, the thermodynamic state of the boundary layer will differ from its equilibrium state. Such a boundary layer will be briefly called "nonequilibrium" layer. To determine the concentration distribution in this case, one must use the equation of conservation of the individual species in their general form.

§ 23. Velocity Profile, Integral Thicknesses, and Friction on a Flat Plate

Returning to Section 12, it is not hard to see that many of the results obtained there are also valid in the case of flow of a dissociating gas over a flat plate. In fact, the expression for the velocity profile in the turbulent core, (3.28), was obtained from the Karman formula without any assumptions about the density variation in the turbulent core. Therefore, it can also be used to calculate the velocity profile on a plate in the presence of dissociation. This expression, using the assumption (3.1) according to which friction τ is constant across the boundary layer and equals τ_w, becomes

$$\eta = \eta_1 + \frac{\zeta}{f} \int_{u_n}^{\bar{u}} \exp\left[\varkappa\zeta \int_{u_n}^{\bar{u}} \sqrt{\frac{\rho}{\rho_w}}\, d\bar{u}\right] d\bar{u}. \tag{4.103}$$

Using Equation (4.103), we find the derivative $d\eta/d\varphi$ in the turbulent core which will be found necessary below

$$\frac{d\eta}{d\varphi} = \frac{1}{f} \exp\left(\varkappa\zeta \int_{u_n}^{\bar{u}} \sqrt{\frac{\rho}{\rho_w}}\, d\bar{u}\right). \tag{4.104}$$

In the laminar sublayer, we shall use a linear relation for the velocity profile, similar to the one used in Section 12.

$$\varphi = \eta. \tag{4.105}$$

This relation was justified on the basis of experimental data in Sections 11 and 13.

The derivative $d\eta/d\phi$ in the laminar sublayer is obviously equal to

$$\frac{d\eta}{d\varphi} = 1. \tag{4.106}$$

To determine the Reynolds numbers, constructed from the momentum loss thickness and the displacement thickness, as well as the form parameter

$$H^* = \delta^*/\delta^{**}$$

one can use the expressions (3.42), (3.44), and (3.45), obtained in Section 12 for an arbitrary density distribution in the boundary layer.

For convenience, we list these expressions here

$$
\left.
\begin{aligned}
\mathrm{Re}^{**} &= \frac{e^{-\varkappa a}}{/\varkappa^2} \frac{\mu_w}{\mu_e} \exp\left[\varkappa\zeta \int_0^1 \left(\frac{\rho}{\rho_w}\right)^{\!\!1/s} d\bar{u}\right] \times \\
&\quad \times \left[1 - \frac{2 + \frac{1}{2}\frac{\rho'(1)}{\rho_e}}{\varkappa\zeta\left(\frac{\rho_e}{\rho_w}\right)^{\!\!1/s}}\right], \\[2mm]
\mathrm{Re}^{*} &= \frac{e^{-\varkappa a}}{/\varkappa} \frac{\mu_w}{\mu_e} \exp\left[\varkappa\zeta \int_0^1 \left(\frac{\rho}{\rho_w}\right)^{\!\!1/s} d\bar{u}\right] \times \\
&\quad \times \left[1 + \frac{\rho'(1)}{\rho_e} - \frac{1}{\varkappa\zeta}\left(\frac{\rho_w}{\rho_e}\right)^{\!\!1/s} \times \right. \\
&\quad \left. \times \left(\frac{1}{2}\frac{\rho'(1)}{\rho_e} + \frac{\rho''(1)}{\rho_e} - \frac{3}{2}\frac{\rho'(1)^2}{\rho_e^2}\right)\right], \\[2mm]
H^* &= \left[1 + \frac{\rho'(1)}{\rho_e} - \frac{1}{\varkappa\zeta}\left(\frac{\rho_w}{\rho_e}\right)^{\!\!1/s} \times \right. \\
&\quad \times \left(\frac{1}{2}\frac{\rho'(1)}{\rho_e} + \frac{\rho''(1)}{\rho_e} - \frac{3}{2}\frac{\rho'(1)^2}{\rho_e^2}\right) \times \\
&\quad \left. \times \left[1 - \frac{2 + \frac{1}{2}\frac{\rho'(1)}{\rho_e}}{\varkappa\zeta\left(\frac{\rho_e}{\rho_w}\right)^{\!\!1/s}}\right].
\end{aligned}
\right\} \tag{4.107}
$$

Here

$$\rho'(1) = \left(\frac{d\rho}{d\bar{u}}\right)_{\bar{u}=1}, \quad \rho''(1) = \left(\frac{d^2\rho}{d\bar{u}^2}\right)_{\bar{u}=1}$$

It is easy to see that to calculate friction one can use formulas obtained in Section 12. One must not try, however, to be specific about the functional dependence of the gas density in the boundary layer on the velocity in these formulas. This refers to the function K which, for an arbitrary density distribution in the boundary layer, should be written in the form

$$K = \int_0^1 \left(\frac{\rho}{\rho_e}\right)^{n_s} d\bar{u}. \tag{4.108}$$

The form of the functions F, G, and N which are necessary to calculate friction remains the same in this case of a flow of a dissociating gas. For convenience, we shall list all the relations necessary for calculating friction

$$\left.\begin{array}{l} \left(\dfrac{c_f}{c_{f_0}}\right) = \left(\dfrac{FK}{2N}\right)^2, \\[2mm] F = 0.242\, c_{f_0}^{-\frac{1}{2}}, \quad G = \lg\left(\dfrac{\mu_e}{\mu_e}\right), \\[2mm] N + \lg N = \lg \dfrac{FK}{2} + \dfrac{1}{2}(F + G). \end{array}\right\} \tag{4.109}$$

It will be recalled that the local friction coefficient c_{f_0} on a plate in an incompressible fluid can be calculated either using the Karman Formula (3.59) or Formulas (3.80). The dynamic viscosity coefficient can be determined using the power law (3.61). The function N can be easily calculated using the last of Equations (4.109) and a table of decimal logarithms.

In a similar fashion, all the formulas for the local and average friction, obtained in Section 12, may be extended to the case of a dissociating gas. The effect of the thermochemical state of flow in the boundary layer on the drag will, of course, be manifested through $\rho(u)$ and the viscosity μ. Thus, the problem of calculating the drag reduces to establishing a relationship between the temperature and density, and the velocity.

The next section of the present chapter will be devoted to the derivation of these relations for frozen, equilibrium, and nonequilibrium flows in the boundary layer.

§ 24. Longitudinal Flow Around a Flat Plate with
Prandtl and Schmidt Numbers Equal to Unity

Relationship between velocity profiles and total enthalpy. Let us consider the longitudinal flow of a gas around a flat plate ($dp/dx = 0$) at supersonic velocity (Figure 22). The Prandtl and Schmidt numbers (consequently, also the Lewis number) will be assumed to be equal to unity. In this case, the differential equations of momentum (4.85), energy (4.86), and conservation of species 1 (4.87) become

$$\rho u \frac{\partial u}{\partial x} + \rho v \frac{\partial u}{\partial y} = \frac{\partial}{\partial y}\left[(\mu + \varepsilon)\frac{\partial u}{\partial y}\right], \tag{4.110}$$

$$\rho u \frac{\partial H}{\partial x} + \rho v \frac{\partial H}{\partial y} = \frac{\partial}{\partial y}\left[(\mu + \varepsilon)\frac{\partial H}{\partial y}\right], \tag{4.111}$$

$$\rho u \frac{\partial c_i}{\partial x} + \rho v \frac{\partial c_i}{\partial y} = \frac{\partial}{\partial y}\left[(\mu + \varepsilon)\frac{\partial c_i}{\partial y}\right] + w_i. \tag{4.112}$$

Equations (4.110) and (4.111) and the boundary conditions (4.101) imply a similitude relation between the velocity field and the total enthalpy field

$$\frac{u}{U_e} = \frac{H - h_w}{H_e - h_w}. \tag{4.113}$$

Solving Equation (4.113) for H, we get

$$H = h_w + (H_e - h_w)\bar{u} \qquad \left(\bar{u} = \frac{u}{U_e}\right). \tag{4.114}$$

Equilibrium flow of an ideally dissociating gas. In the case of complete thermodynamic equilibrium, the concentration of the atomic species in the mixture is uniquely determined by the local values of pressure and temperature. This relation of concentration to pressure and temperature for an ideally dissociating gas is given by Equation (4.83). Since the pressure is constant across the boundary layer, the pressure p in this equation must be set equal to its value at the outer edge of the boundary layer p_e. As a result, we have

$$c_A = \left[1 + \frac{\rho_e}{\rho_d}\frac{T_d}{T}\exp\frac{T_d}{T}\right]^{\frac{1}{2}}. \tag{4.115}$$

Here p_d and T_d are the characteristic pressure and temperature (for oxygen and nitrogen, the values of these quantities are listed in Table 18).

The relation between the velocity profiles, temperatures, and concentrations can be easily obtained by substituting the expression for the enthalpy of an ideally dissociating gas, (4.74) into the left-hand side of Equation (4.114). The substitution followed by simple algebra yields the following relation:

$$\bar{\beta}\bar{u}^2 - (\bar{H}_e - \bar{h}_w)\bar{u} - \bar{h}_w + 4\bar{T} + c_A(1 + \bar{T}) = 0. \tag{4.116}$$

Here

$$\begin{aligned}
\bar{\beta} &= \frac{U_e^2}{2D}, \\
\bar{h}_w &= \frac{h_w}{D} = c_{Aw} + (4 + c_{Aw})\bar{T}_w, \\
\bar{H}_e &= \frac{H_e}{D} = c_{Ae} + (4 + c_{Ae})\bar{T}_e + \bar{\beta}, \\
\bar{T} &= \frac{T}{T_d}.
\end{aligned} \right\} \tag{4.117}$$

Equations (4.115) and (4.116) enable us to establish the relation between velocity and temperature and concentration. Placing Equation (4.115) in Equation (4.116), we obtain the following quadratic equation in terms of dimensionless velocity:

$$\bar{\beta}\bar{u}^2 - a\bar{u} + b = 0. \tag{4.118}$$

Here

$$\begin{aligned}
a &= \bar{H}_e - \bar{h}_w, \\
b &= 4\bar{T} + (1 + \bar{T})\left[1 + \bar{p}_e\bar{T}^{-1}\exp\left(\frac{1}{\bar{T}}\right)\right] - \bar{h}_w, \\
\bar{p}_e &= \frac{p_e}{p_d}.
\end{aligned} \right\} \tag{4.119}$$

Solving Equation (4.118) for $\bar{u}$, we get

$$\bar{u} = \frac{a \pm \sqrt{a^2 - 4\bar{\beta}b}}{2\bar{\beta}}. \tag{4.120}$$

The sign in front of the radical in Equation (4.120) is chosen to satisfy the condition $\bar{u} \leq 1$.

After a relationship between the velocity and temperature is established with the aid of Equation (4.120), one can use Equation (4.115) to establish a relation between the velocity and concentration.

The density distribution in the boundary layer can be easily determined for the known temperature and concentration by using the relation

$$\frac{\rho}{\rho_e} = \left(\frac{T}{T_e}\right)^{-1} \frac{1 + c_{A_e}}{1 + c_A}, \tag{4.121}$$

which can be obtained from the equation of state (4.88), assuming that the pressure is constant across the boundary layer.

Using the density distribution and Formulas (4.108) and (4.109), one can determine the local friction coefficient.

Frozen flow of an ideally dissociating gas over a catalytic plate. In a frozen flow, the rate of chemical reactions is negligibly small compared with the rate of diffusion ($w_A \equiv 0$). For this reason, the concentration distribution is completely determined by diffusion processes.

The equation for the conservation of the atomic species (4.112) in this case becomes

$$\rho u \frac{\partial c_A}{\partial x} + \rho v \frac{\partial c_A}{\partial y} = \frac{\partial}{\partial y}\left[(\mu + \epsilon) \frac{\partial c_A}{\partial y}\right]. \tag{4.122}$$

The conservation of molecular species, c_{A_2}, in this case is unnecessary, since for a binary mixture the concentration $c_{A_2} = 1 - c_A$.

Equations (4.110) and (4.122), as well as the boundary conditions (4.101), imply similitude between the velocity and concentration fields:

$$\frac{u}{U_e} = \frac{c_A - c_{Aw}}{c_{Ae} - c_{Aw}} . \tag{4.123}$$

In order to determine the atomic concentration at the wall, we use the boundary condition (4.65) which, assuming that the order of the catalytic reaction is equal to unity (which is true for air, for not too high wall temperature), after simple algebra can be written in the form

$$\tau_w \left(\frac{dc_A}{d\bar{u}} \right)_w = \rho_w k_w U_e c_{Aw}. \tag{4.124}$$

Evaluating the derivative $(dc_A/d\bar{u})_w$ from Equation (4.123), we obtain, according to Equation (4.124), the following expression for the concentration at the wall:

$$c_{Aw} = c_{Ae}(1 + A_w)^{-1}, \quad A_w = \frac{\rho_w k_w U_e}{\tau_w} . \tag{4.125}$$

For $k_w = 0$, which corresponds to the case of an absolutely noncatalytic wall, $c_{A_w} = c_{A_e}$, i.e., the atomic concentration in the boundary layer is constant over its cross-section and equal to the value at the outer boundary [this follows from Equation (4.123)].

For $k_w \to \infty$, which corresponds to the case of an absolutely catalytic wall, $c_{A_w} \to 0$, i.e., all atoms which diffuse toward the wall become recombined.

Solving Equation (4.123) for c_A, we obtain the dependence of the atomic concentration on the velocity

$$c_A = c_{Aw} + (c_{Ae} - c_{Aw})\bar{u}. \tag{4.126}$$

Substituting expression (4.126) into Equation (4.116) and solving the latter for temperature, we obtain

$$\bar{T} = \frac{T}{T_e} = \frac{[k_w + (H_e - \bar{h}_w)\bar{u} - (c_{Ae} - c_{Aw})\bar{u} - \frac{1}{2}\bar{u}^2 - c_{Aw}]}{[1 + c_{Aw} + (c_{Ae} - c_{Aw})\bar{u}]} . \tag{4.127}$$

Here $\bar{\beta}$, $\bar{h}_w$, $\bar{H}_e$ are given by Equations (4.117), and c_{A_w} is given by Equation (4.125).

The density and friction can be found using Equations (4.121) and (4.108), (4.109).

Nonequilibrium flow of an ideally dissociating gas [14]. In order to determine the dependence of density on velocity, one must establish a relation between the temperature and the velocity and concentration, and of concentration with velocity and temperature. The dependence of the temperature on velocity and concentration can be easily obtained from Equation (4.116), and is arrived at without any assumptions as to the thermochemical state of flow in the boundary layer, by solving it for the temperature

$$\bar{T} = [\bar{h}_w + (\bar{H}_e - \bar{h}_w)\bar{u} - \bar{\beta}\bar{u}^2 - c_A](4 + c_A)^{-1}. \tag{4.128}$$

In order to establish the dependence of concentration on velocity and temperature, we turn to the equation of conservation of the atomic species, written in terms of Crocco variables. It is not hard to obtain this equation from Equations (4.98) and (4.100), by setting $dp/d\xi = 0$, $Sc_i = 1$ in the latter. Combining Equations (4.98) and (4.100), thus simplified, into one equation, we have

$$\rho u \frac{\partial c_A}{\partial \xi} = \frac{\tau^2}{\rho + \epsilon} \frac{\partial^2 c_A}{\partial u^2} + w_A. \tag{4.129}$$

For simplicity, we shall assume that concentration is a function of only the velocity u and does not depend on the longitudinal coordinate ξ, i.e., $\partial c_A/\partial \xi = 0$ (implicit dependence on the physical coordinate x remains, since $c_A = c_A[u(x,y)]$. To justify this assumption, we note that it is strictly valid if the flow in the boundary layer is frozen or if it is in a state of equilibrium (see the preceding sections of the present chapter). Consequently, we are entitled to expect that the explicit dependence $c_A(\xi)$ is so weak that it may be neglected[6].

Footnote (6) appears on page 269.

With this assumption, Equation (4.129) becomes

$$\frac{d^2 c_A}{du^2} = -\frac{\mu + \epsilon}{\tau^2} w_A.$$

(4.130)

Integrating Equation (4.130) twice and determining the integration constants from the conditions at the wall, we obtain

$$c_A = c_{Aw} + \left(\frac{dc_A}{du}\right)_w - \int_0^u du \int_0^u \frac{\mu + \epsilon}{\tau^2} w_A \, du.$$

(4.131)

Making use of the boundary condition (4.124) and the condition at the outer boundary ($c_A = c_{A_e}$ for $u = U_e$), we find an equation for the concentration of atoms at the wall in the presence of surface catalytic reactions

$$c_{Aw} = \left(c_{A_e} + \int_0^{U_e} du \int_0^u \frac{\mu + \epsilon}{\tau^2} w_A \, du\right)(1 + A_w)^{-1},$$

(4.132)

where A_w is given by Equation (4.125)

For later use, it will be more convenient to write Equation (4.131) in the following form, which is easily obtained if one uses the conditions at the outer edge of the boundary layer:

$$c_A = c_{Aw} + [c_{A_e} - c_{Aw} + I(1)] \bar{u} - I(\bar{u}).$$

(4.133)

Here

$$I(\bar{u}) = U_e^2 \int_0^{\bar{u}} d\bar{u} \int_0^{\bar{u}} \frac{\mu + \epsilon}{\tau^2} w_A \, d\bar{u}.$$

(4.134)

Equation (4.133) implies that the influence of nonequilibrium dissociation on the distribution of atomic concentration in the boundary layer can be taken into account by calculating $I(\bar{u})$. In the particular case of a frozen flow, in the boundary layer ($w_A \equiv 0$) $I(\bar{u}) \equiv 0$, and the distribution of the atomic concentration is given by Equation (4.126).

In order to determine $I(\bar{u})$, we write it in the form

$$I(\bar{u}) = U_e^2 \int_0^{\bar{u}} d\bar{u} \int_0^{\bar{v}} \frac{w_A \, d\bar{u}}{\tau_L \left(\frac{\partial u}{\partial y}\right)}.$$

(4.135)

By transferring in the integral of Equation (4.135) to the universal coordinates (3.8) and substituting the expression for the mass rate of formation of the atomic species, w_A (4.60), we have

$$I(\bar{u}) = -\frac{\zeta^4}{Re_{xw}} \frac{\rho_w}{\rho_d} \int_0^{\bar{u}} d\bar{u} \int_0^{\bar{u}} C_r \left(\frac{\rho}{\rho_w}\right)^3 (1 + c_A) \frac{c_A^{(r)^2} - c_A^2}{1 - c_A^{(r)}} \frac{d\eta}{d\psi} d\bar{u}.$$

(4.136)

Here

$$C_r = \frac{\frac{x}{U_e^*}}{\frac{m_A^*}{k_r \rho_d \rho_w}}, \qquad Re_{xw} = \frac{U_e \rho_w x}{\mu_w}.$$

(4.137)

The quantity C_r, as can be easily seen, represents the Damkohler number (4.102). The physical interpretation of this number was discussed in detail in Section 22. In those cases when we do deal with dissociation reactions, C_r is sometimes called the recombination parameter. If the parameter is large, the flow will be steady; if it is small, it will be frozen.

The derivative $d\eta/d\psi$, in Equation (4.136), is given by Equation (4.104) in the case of the turbulent core, and by (4.106) in the laminar sublayer. The friction parameter ζ is given by Equation (3.8), and the equilibrium atom concentration $c_A^{(e)}$ is determined by Equation (4.68).

To calculate the concentration profile using Formula (4.133), one can use the method of successive approximations. First, the characteristics of the boundary layer $c_A(u)$, $T(u)$, $\rho(u)$, c_f, ζ are computed for frozen and steady flows (see the preceding sections of the present chapter). As the zero-order approximation for the atomic concentration, we can use either the atomic concentration in the frozen flow (parameters of the frozen flow will be denoted below with the subscript f), i.e., $c_A^{(0)} = c_A^{(f)}$, or the arithmetic mean of the concentrations

in the frozen and steady flows, i.e., $c_A^{(0)} = 1/2 (c_A^{(f)} + c_A^{(e)})$ (the subscript e will refer to equilibrium values). After using Formula (4.133) to find the dependence of concentration on velocity in the first approximation, $c_A^{(1)}$, we use formulas (4.128) and (4.121) to determine the temperature and density, $T^{(1)}$ and $\rho^{(1)}$. Having the density distribution, we use Formulas (4.109), (3.8), (4.104) and (4.106) to determine the values of $c_f^{(1)}$, $\zeta^{(1)}$, $(dn/d\phi)^{(1)}$, etc.

Figures 60 - 64 give the results of calculating flow in the boundary layer on a wedge with the semi-angle at the vertex equal to 30° immersed in a flow of oxygen at the velocity $U_\infty = 7$ km/sec with the pressure and temperature in the oncoming flow equal to $p_\infty = 2.85 \cdot 10^{-4}$ atm and $T = 220°K$[7]. The temperature of the wall was assumed to be 720°K. The values of the characteristic parameters and the rate of recombination for oxygen were assumed to be the same as those in Tables 10 and 14. In these figures, the letters (e), (f), (ne), refer to plots describing the equilibrium, frozen, and nonequilibrium flows, respectively, in the boundary layer.
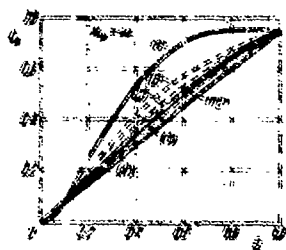
Figure 60

Figure 60 illustrates the dependence of the concentration of oxygen atoms on the velocity at a section of the boundary layer on a completely catalytic wall ($k_w = \infty$). To illustrate the convergence process for nonequilibrium flow calculation, the same diagram includes plots (dashed) obtained in various approximations (the numbers in the diagram indicate the order of the approximation). As can be seen in Figure 60, the convergence of the method is completely satisfactory.

For the same flow conditions ($k_w = \infty$), Figure 61 shows the dependence of the temperature on velocity in the boundary layer; Figure 62

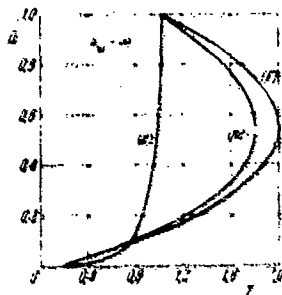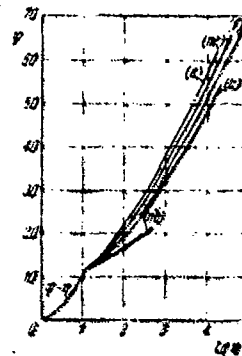Footnote (7) appears on page 270.

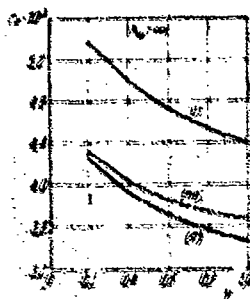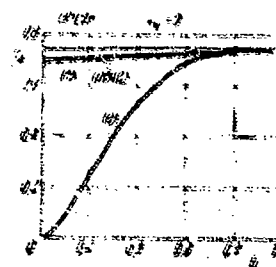Figure 61

Figure 62

Figure 63

Figure 64

shows the velocity profiles for equilibrium, frozen, and nonequilibrium flows in the boundary layer [see Formulas (4.103) and (4.105)]. In addition, Figure 62 shows the velocity profile for an incompressible fluid [see Formula (3.4); this profile is indicated by the symbol (no)] and the velocity profile, calculated, for the same external conditions and conditions at the surface of the wedge, as in the case of the plots (e), (f), and (ne), but without taking into account the dissociation in the boundary layer [see Formula (3.99); this profile is designated by the symbol (c)]. The plots in Figure 62 were obtained for $k_w = \infty$.

Figure 63 gives the plots of the local friction coefficient on the wedge ($k_w = \infty$) as functions of the longitudinal coordinate. It can be

seen from the diagram that in this case the friction in an equilibrium flow is much greater (approximately 1.3 times greater) than the fric- tion for a frozen flow. This indicates that, when calculating the drag, one must take proper account of the thermochemical processes in the boundary layer.

Figure 64 gives the dependence of the concentration of oxygen atoms on the velocity in the boundary layer at a completely noncataly- tic wall ($k_w = 0$). When calculating nonequilibrium flow for this case, the concentration distribution in frozen flow was used as the zero-order approximation. As can be seen in the diagram (the notation is the same as in Figure 60), the fact that we took into consideration the nonequilibrium character of dissociation resulted in a slight change of the concentration profile as compared with the frozen flow.

. The methods of calculating friction in an ideally dissociating gas presented in this section may, if necessary, be extended to the case of a partially excited dissociating gas whose properties were described in Section 21.

§ 25. Heat and Mass Transfer in the Boundary Layer on a Flat Plate for Prandtl and Schmidt Numbers Different From Unity

It was already noted above (Section 22) that, at hypersonic velocities, the relative thickness of the laminar sublayer increases, and as a result we observe an increasing role of the molecular heat conductivity and diffusion in the processes of heat and mass transfer in a turbulent boundary layer. This fact makes it necessary in certain cases to rigorously take into account the thermal and diffusive prop- erties of the laminar sublayer when determining the heat and mass transfer on the surface.

In the first approximation, this can be done by abandoning the assumption that the Prandtl and Schmidt numbers are equal to unity,

considering these numbers constant across the laminar sublayer and
equal to their values at the wall. However, if the laminar sublayer
occupies a significant portion of the entire turbulent boundary layer
(20 - 30% and more), such an approximation may be insufficient. The
problem is that the Prandtl and Schmidt numbers in dissociating air
depend on the degree of dissociation. The approximate estimations
made by Dorrance [15] for dissociating oxygen lead to the following
dependence of these criteria on the degree of dissociation:

$$Pr = Pr_0 \frac{(1 + 0.25\, c_0)(1 + c_0)}{1 + 1.62 c_0}, \quad Sc = Sc_0\,(1 + c_0). \qquad (4.138)$$

Here c_0 is the concentration of atomic oxygen. From these expressions,
it is easy to estimate the dependence of the Lewis number on the
degree of dissociation

$$Le = Le_0 \frac{1 + 0.25\, c_0}{1 + 1.62 c_0}. \qquad (4.139)$$
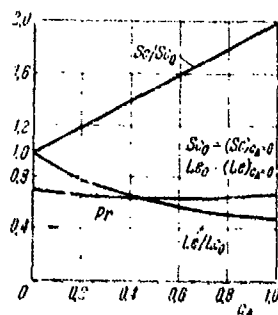
Figure 65

The results of the calcula-
tions based on the above formulas
are shown in Figure 65. The dia-
gram makes it clear that the
Prandtl number varies relatively
little with the degree of disso-
ciation. The same Prandtl number
may change by approximately a
factor of two. A subsequent com-
parison of these relationships
with the more accurate results
showed that the variation of the
Pr and Sc numbers, as described above, is similar also in the case of
the dissociating air. Thus, if the variation of the atomic concen-
tration is such that the Prandtl number undergoes a noticeable change
across the laminar sublayer, then it might be necessary to take this
change into account in the calculations.

The deviation of the Prandtl and Schmidt numbers from unity implies, within the framework of the double-layer turbulent boundary layer model, that the dynamic, thermal and diffusive thicknesses of the laminar sublayer are generally different. It is not hard to show, using the equations of motion, energy, and conservation of species i in the laminar sublayer that

$$\eta_{nr} = \frac{\eta_{n}}{\sqrt{Pr}}, \qquad \eta_{nn} = \frac{\eta_{n}}{\sqrt{Sc}}. \tag{4.140}$$

The subscripts "th" and "d" here stand for "thermal" and "diffusive", respectively.

Inspection of (4.140) indicates that if Pr < 1 and Sc < 1 (as is the case in dissociating air), then the thicknesses of the thermal and diffusive laminar sublayers are greater than the thickness of the dynamic sublayer. In this case, the thermal and diffusive sublayers occupy a portion of the turbulent core with a logarithmic velocity distribution (Figure 66). Taking this fact into account, it is easy to estimate the differences among the dimensionless velocities at the boundaries of the dynamic, thermal and diffusive sublayers. In fact, assuming approximately the logarithmic velocity profile in an incompressible fluid (3.100) for the turbulent core, in view of (4.140), we obtain

$$\varphi_{nr} = \varphi_{n} - 2.875 \lg Pr, \quad \varphi_{nn} = \varphi_{n} - 2.875 \lg Sc. \tag{4.141}$$

Figure 66

Setting Pr = 0.72, Sc = 0.5, ϕ_l = 11.5, we find

$$\frac{\varphi_{nr}}{\varphi_l} = 1.03, \qquad \frac{\varphi_{nn}}{\varphi_{n}} = 1.07.$$

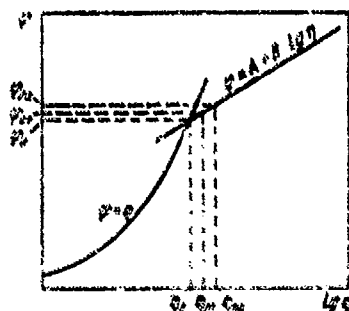This approximate analysis implies that for Pr < 1 and Sc < 1 (for air), it is not necessary to take into account the

discrepancies in the velocities at the boundaries of the dynamic, thermal, and diffusive laminar sublayers, and consequently these velocities may be determined from Equation (3.31).

The relationship of total enthalpy to velocity and concentration. Reynolds similitude. Recovery enthalpy. In order to establish an approximate relation among total enthalpy, velocity, and concentration, we turn to the equations of energy in the Crocco variables, (4.97) and (4.99).

For a flat plate ($dp/d\xi = 0$), these equations become

$$\rho u \frac{\mu}{\tau} \frac{\partial H}{\partial \xi} + \frac{\partial \tau}{\partial u} \frac{\partial H}{\partial u} =$$
$$= \frac{\partial}{\partial u} \left\{ \tau \left[\frac{1}{Pr} \frac{\partial H}{\partial u} + \frac{1}{Pr} \sum_i (Le_i - 1) h_i \frac{\partial c_i}{\partial u} + \left(1 - \frac{1}{Pr} \right) u \right] \right\} \qquad (4.142)$$

in the laminar sublayer, and

$$\rho u \frac{\partial H}{\partial \xi} = \frac{\tau^2}{\varepsilon} \frac{\partial^2 H}{\partial u^2} \qquad (4.143)$$

in the turbulent core.

Next we shall make a simplifying assumption: we assume that total enthalpy is a function of only the longitudinal velocity, i.e., $H = H(u)$. To justify this assumption, we note that it is strictly valid if the Prandtl and Schmidt numbers are equal to unity. In this case, as shown in the preceding section, there is an integral of the energy Equation (4.119), which is similar to the Crocco integral. Consequently, one can expect that for small deviations of the Prandtl and Schmidt numbers from unity, the dependence of total enthalpy on the longitudinal coordinate, $H(\xi)$, will be sufficiently weak.

In addition to the above assumption, we make as before the assumption that the friction stress is constant across the layer, i.e., $\tau = \text{const} = \tau_w$.

Using these assumptions, Equations (4.142) and (4.143) become, respectively,

$$\frac{d}{du}\left[\frac{dH}{du} + \sum_i (\text{Le}_i - 1) h_i \frac{\partial c_i}{\partial u} + (\text{Pr} - 1) u\right] = 0, \qquad (4.144)$$

$$\frac{d^2 H}{du^2} = 0. \qquad (4.145)$$

Integrating Equation (4.144) and determining the constant of integration from the condition at the wall (for u = 0 q = q_w), we find

$$\frac{dh}{du} + \sum_i (\text{Le}_i - 1) h_i \frac{\partial c_i}{\partial u} + (\text{Pr} - 1) u = \frac{\text{Pr} \, q_w}{\tau_w}. \qquad (4.146)$$

Here

$$q_w = \frac{\tau_w}{\text{Pr}}\left[\frac{dH}{du} + \sum_i (\text{Le}_i - 1) h_i \frac{\partial c_i}{\partial u}\right]_w \qquad (4.147)$$

is the thermal flux at the wall. Equation (4.147), as can be easily seen, follows from the definition of heat flux in a multicomponent mixture, (1.79) taking into account only the energy transfer due to heat conductivity and mass diffusion.

Performing integration from 0 to u in (4.146), and determining the integration constant from the condition H = H_w at v = 0, we obtain a relation between the total enthalpy and velocity and concentration in the laminar sublayer

$$H = h_w + \text{Pr}\frac{2c_h}{c_f}(H_r - H_w)\bar{u} - $$
$$- \sum_i (\text{Le}_i - 1)\int_0^{\bar{u}} h_i \frac{\partial c_i}{\partial u} d\bar{u} + \frac{1}{2}(1 - \text{Pr}) U_e^2\bar{u}^2. \qquad (4.148)$$

Here $\dfrac{2c_h}{c_f}$ is the Reynolds similitude parameter,

$$c_h = \frac{|q_w}{\rho_e U_e (H_r - h_w)}, \qquad (4.149)$$

c_h is the dimensionless heat transfer coefficient (Stanton number),

H_r is the equilibrium enthalpy of a thermally insulated wall or the recovery enthalpy (definition of H_r and $2c_h/c_f$ will be given below).

In the turbulent core, the relation of the total enthalpy to velocity and concentration will be found by integraing Equation (4.145) twice. The first constant of integration will be determined assuming that the heat flux is constant across the boundary layer and equal to its value at the wall, i.e., $q = const = q_w$. The second integration constant will be determined from the condition at the outer edge: for $u \to U_e$, $H \to H_e$. As a result, we obtain

$$H = H_e - \frac{2c_h}{c_f}(H_r - h_w)(1 - \bar{u}). \qquad (4.150)$$

Furthermore, let us consider the case when there is no heat transfer between the gas and the wall ($h_w = H_r$). We equate total enthalpies from Equations (4.148) and (4.150) at the boundary of the laminar sublayer and solve the resulting equation for H_r. This yields

$$H_r = h_e + Pr^{t_0}\frac{U_e^2}{2} + \sum_i (Le_i - 1)\int_0^{\bar{u}_\delta} h_i \frac{dc_i}{d\bar{u}} d\bar{u}. \qquad (4.151)$$

We note that in formulating (4.151), we made use of the approximate relation (3.150). The expression for the enthalpy of recovery, H_r, (4.151) is sufficiently general in the sense that it may be used for calculating the equilibrium, frozen, and nonequilibrium flows.

If we introduce the recovery factor r, just as for a homogeneous gas, i.e.,

$$H_r = h_e + r\frac{U_e^2}{2}, \qquad (4.152)$$

then by equating Equations (4.151) and (4.152), we obtain an expression for the recovery factor in a multicomponent mixture of gases

$$r = Pr^{t_0} + 2\sum_i (Le_i - 1)\int_0^{\bar{u}_\delta} \frac{h_i}{U_e^2} \frac{dc_i}{d\bar{u}} d\bar{u}. \qquad (4.153)$$

To determine the Reynolds similitude parameter, we equate the total enthalpies from Equations (4.148) and (4.150) at the boundary of the laminar sublayer and solve the resulting equation for the parameter in question. This yields

$$\frac{2c_h}{c_f} = Pr^{-\frac{2}{3}}(H_r - h_w)^{-1}\left[h_e + Pr^{\frac{2}{3}}\frac{U_e^2}{2} - h_w + \right.$$
$$\left. + \sum_i (Le_i - 1)\int_0^{\bar{u}_\pi} h_i \frac{\partial c_i}{\partial \bar{u}}\, d\bar{u}\right].$$

(4.154)

In deriving relation (4.154), we use the approximate expressions (3.150), (3.159).

Making use of Equations (4.149) and (4.154), we find an expression for the heat flux at the wall:

$$q_w = \frac{1}{2}c_f \rho_e U_e Pr^{-\frac{2}{3}}\left[h_e + Pr^{\frac{2}{3}}\frac{U_e^2}{2} - h_w + \right.$$
$$\left. + \sum_i (Le_i - 1)\int_0^{\bar{u}} h_i \frac{\partial c_i}{\partial \bar{u}}\, d\bar{u}\right].$$

(4.155)

The definition of total enthalpy (4.89), under the assumption that the specific heat capacities of the individual species do not depend on the temperature, yields an expression for the temperature

$$T = \left(H - \sum_i c_i h_i^0 - \frac{u^2}{2}\right)\left(\sum_i c_i c_{pi}\right)^{-1}.$$

(4.156)

The above expressions for the total enthalpy in the laminar sublayer and the turbulent core, recovery factors, Reynolds similitude parameter, heat flux, and temperature contain the concentrations of the individual species, which are as yet unknown. Thus, the problem reduces to establishing a relationship between the concentration and velocity in the laminar sublayer and the turbulent core. The form of this relationship will be different depending on thermochemical state of flow, i.e., on whether the flow will be steady, frozen or nonsteady.

Steady flow of an ideally dissociating gas [16]. We shall consider the steady flow of an ideally dissociating gas. For later use, we note that the difference between the enthalpies of the atomic and molecular species may be approximately considered to be equal to the dissociation energy. In fact, taking the fact into account that

$$h_A = \frac{10}{2}\left(\frac{R}{2M_A}\right)T + h_A^0, \quad h_M = \frac{8}{2}\left(\frac{R}{2M_A}\right)T + h_M^0.$$

we find

$$h_A - h_M = \left(\frac{R}{2M_A}\right)T + (h_A^0 - h_M^0) = \left(\frac{R}{2M_A}\right)T + D \approx D. \tag{4.157}$$

For such gases as oxygen and nitrogen, the approximation made in (4.157) does not result in any noticeable errors in calculations.

Making use of Equation (4.157), we obtain from the relation (4.148) the following expression for total enthalpy in the laminar sublayer

$$\begin{aligned}
B = \frac{H}{D} = \bar{h}_w + \Pr\frac{u_e}{r_f}(\bar{h}_r - \bar{h}_w)\bar{u} + \\
+ (1 - \Pr)\overline{lu}^2 - (Le - 1)(c_A - c_{Aw}) \tag{4.158}
\end{aligned}$$

The dimensionless quantities $\bar{h}_w$, $\bar{h}_r$ and $\bar{u}$ are given by Equations (4.117).

The Reynolds similitude parameter $2c_h/c_f$ and the recovery enthalpy H_r, generally given by Equations (4.154) and (4.151), become

$$\frac{2c_h}{c_f} = \Pr^{-\gamma_0}(\bar{h}_r - \bar{h}_w)^{-1}[\bar{h}_e + \beta \Pr^{\gamma_0} - \bar{h}_w + \\
+ (Le - 1)(c_{Ae} - c_{Aw})]. \tag{4.159}$$

$$H_r = \frac{H_r}{D} = \bar{h}_e + \beta \Pr^{-\gamma_0}[(Le - 1)(c_{Ae} - c_{Aw})]. \tag{4.160}$$

It will be recalled that in Equations (4.159) and (4.160) the subscript r refers to parameters calculated for the case when there is no heat transfer between the gas and the wall.

The expression for the heat flux (4.155) in an ideally disso-
ciating gas becomes

$$q_w = \frac{1}{2} c \rho_e U_e \mathrm{Pr}^{-\prime\prime} J) \times$$
$$\times [\bar{h}_e + \bar{\beta}\mathrm{Pr}^{\prime\prime} - \bar{h}_w + (\mathrm{Le} - 1)(c_{A_1} - c_{Aw})]. \quad (4.161)$$

The total enthalpy in the turbulent core (4.150), in view of
Equation (4.159), can be written in the form

$$\Pi = \frac{H}{D} = \Pi_e - \mathrm{Pr}^{-\prime\prime}[\bar{h}_e + \bar{\beta}\mathrm{Pr}^{\prime\prime} - \bar{h}_w +$$
$$+ (\mathrm{Le} - 1)(c_{A_1} - c_{A_L})](1 - \bar{u}). \quad (4.162)$$

A similar transformation of the expression for the total
enthalpy in the laminar sublayer, (4.158), yields

$$\Pi = \frac{H}{D} = \bar{h}_w + \mathrm{Pr}^{\prime\prime}[\bar{h}_e + \bar{\beta}\mathrm{Pr}^{\prime\prime} - \bar{h}_w +$$
$$+ (\mathrm{Le} - 1)(c_{A_1} - c_{Aw})]\bar{u} + (1 - \mathrm{Pr})\overline{u}^2 - (\mathrm{Le} - 1)(c_A - c_{Aw}). \quad (4.163)$$

For Pr = Le = 1 Equations (4.162) and (4.163) reduce to Equation
(4.114) of the preceding section.

The dependence of the atomic concentration on the pressure and
temperature is in this case given by Equation (4.115).

Equations (4.162), (4.163), (4.156) and (4.115) permit us in
principle to determine the dependence of enthalpy, temperature, and
concentration on the velocity in the boundary layer. However, for
convenience in calculations it is useful to make certain modifications.
Substituting the expression for the enthalpy h, (4.74), into the left-
hand side of Equation (4.163), after simple algebra we obtain the
following equation for the velocity $\bar{u}$, in view of (4.115):

$$\beta\bar{u}^2 - a\bar{u} - b = 0, \quad (4.164)$$

where

$$a = \mathrm{Pr}^{-\frac{1}{3}}[\bar{h}_e + \bar{\beta}\mathrm{Pr}^{\frac{1}{3}} - \bar{h}_w + (\mathrm{Le}-1)(c_{An} - c_{Aw})],$$

$$b = \mathrm{Pr}^{-1}\left\{\bar{h}_w + (\mathrm{Le}-1)c_{Aw} - \mathrm{Le}\left[1 + \frac{p_e}{p_d}\frac{1}{\bar{T}}\exp\left(\frac{1}{\bar{T}}\right)\right]^{-\frac{1}{3}}\right\},$$

$$\bar{T} = \frac{T}{T_d}.$$

$$(4.165)$$

Solving Equation (4.164), we find the dependence of velocity on temperature in the laminar sublayer

$$\bar{u} = \frac{a \pm \sqrt{a^2 + 4\bar{\beta}b}}{2\bar{\beta}}.$$

$$(4.166)$$

Similarly, substituting Equation (4.74) into the left-hand side of Equation (4.162), we obtain, in view of (4.115), an equation relating the temperature and velocity in the turbulent core

$$\bar{\beta}\bar{u}^2 - a\bar{u} - c = 0,$$

$$(4.167)$$

where a is given by the first of Equations (4.165), and c has the form

$$c = h_e - a - 4\bar{T} - \left[1 + \bar{p}_e\bar{T}^{-1}\exp\left(\frac{1}{\bar{T}}\right)\right]^{-\frac{1}{3}}, \quad \bar{p}_e = \frac{p_e}{p_d}.$$

$$(4.168)$$

Solving Equation (4.167) for $\bar{u}$, we find a relation between the temperature and velocity in the turbulent core

$$\bar{u} = \frac{a \pm \sqrt{a^2 + 4\bar{\beta}c}}{2\bar{\beta}}.$$

$$(4.169)$$

In Equations (4.166) and (4.169), the sign in front of the radical is chosen to satisfy the condition $\bar{u} \leq 1$.

The determination of the concentration and temperature for the flow around a thermally insulated wall is simpler than for a thermally

conducting wall, since the coefficient a in Equations (4.166) and
(4.169) becomes zero. The value of the temperature at the boundary
of the laminar sublayer can in this case be found from the condition

$$(\bar{\rho}\overline{u_n^2} = b)_r.$$ (4.170)

where the dimensionless velocity at the boundary of the laminar
sublayer, $(\bar{u}_l)$, is given by Equation (3.31).

If the above computational procedure is to be followed, we must
be given the values of the parameters at the outer edge of the boun-
dary layer,(U_e, T_e, p_e), and at the wall, (T_w). The atom concentra-
tion at the outer edge, c_{Ae}, must also be given. Assuming that the
outer flow is in a state of equilibrium, c_{Ae} can be determined from
T_e and p_e using Formula (4.115). The atom concentration at the wall
c_{Aw} can be similarly obtained from T_w and p_e. In the case of thermo-
chemical equilibrium, the occurrence of catalytic processes on the
wall, taking place at a finite rate, will obviously not influence the
distribution of concentration in the boundary layer.

The distribution of parameters in the boundary layer can be
found from the above relations by using the method of successive
approximations. As seen from Equations (4.165), the concentration at
the boundary of the laminar sublayer, c_{Al}, is the quantity which will
be approximated in the calculation. As the zero-order approximation
for c_{Al}, one can use the value obtained for Pr = Sc = 1 (see the pre-
ceding section). From the same calculation we adapt the value of the
friction parameter ζ, which is necessary from the very beginning, to
determine the dimensionless velocity at the boundary of the laminar
sublayer, $\bar{u}_l$ [Formula (3.31)]. In this connection, we note that it
is not necessary to obtain a better approximation for $\bar{u}_l$, since a
slight deviation of the Prandtl and Schmidt numbers from unity has
very little effect on the value of friction (ζ).

After $\bar{u}_l$ is determined, we use Equations (4.166) for $0 < \bar{u} < \bar{u}_l$ and (4.169) for $\bar{u}_l < \bar{u} < 1$ to establish a relationship between the temperature and velocity in the boundary layer in the first approximation. When calculating the flow over a plate at zero angle of attack, the values of the temperature Equations (4.165) and (4.168) must be given in the interval ranging from the temperature of the wall to the stagnation temperature. In calculating the flow over a plate at a nonzero angle of attack, when the temperature at the edge of the boundary layer may set equal to the temperature behind the front shock wave, the values of the temperature must be given in the interval ranging from the temperature of the wall to the temperature of the outer edge. (In this case, the temperature in the boundary layer usually varies monotonically).

Upon establishing a relationship between the velocity and the temperature with the aid of Formula (4.115), one can determine the dependence of concentration on velocity, etc.

Given the distribution of concentration and temperature, we can find the dependence of density on velocity [Equation (4.121)], and then also the local friction coefficient (4.109). Given the friction coefficient and the values of the parameters at the wall, boundary at the laminar sublayer, and the outer edge of the boundary layer, we can use Equation (4.161) to calculate the heat flux.

The Prandtl, Schmidt, and Lewis numbers can be found for a given atom concentration at the wall using the approximate formulas obtained by Durrance, (4.138) and (4.139), assuming $Pr_0 = 0.7$, $Sc_0 = 0.5$, $Le_0 = 1.4$.

Frozen flow of an ideally dissociating gas at a catalytic wall [17]. In the preceding subsection it was shown that, in the case of frozen flow in the boundary layer ($w_A \equiv 0$), and under the assumption that the Schmidt number is equal to unity, we have a particular integral of the equation of conservation of species 1

(4.126), according to which the concentration depends only on the velocity, i.e., $c_A = c_A(u)$. In the case of frozen flow along a flat plate with the Schmidt number different from unity, we shall assume approximately that the concentration as before depends only on the velocity, and does not depend on the longitudinal coordinate. One can expect that for small deviations of the Schmidt number from unity, the dependence of concentration on the longitudinal coordinate $c_A (\zeta)$ will be sufficiently weak. In addition, we also make the simplifying assumption (3.1) stating that the friction stress is constant across the boundary layer: $\tau = \text{const} = \tau_w$.

Using these assumptions, we obtain from Equations (4.98) and (4.100) the following relation for the concentration in the laminar sublayer and the turbulent core:

$$\frac{d^2 c_A}{du^2} = 0. \tag{4.171}$$

As the boundary condition on the concentration at the wall we use Expression (4.65), assuming that the order of the catalytic reaction, n, is unity. After simple algebra, we write the expression in the form

$$\tau_w \left(\frac{d c_A}{du} \right)_w = \rho_w k_w Sc\, U_{A w} \tag{4.172}$$

Integrating Equation (4.171) once, in view of Equation (4.172), we find

$$\frac{d c_A}{du} = Sc\, A_w c_{A w} \qquad A_w = \frac{\rho_w k_w u^*}{\tau_w}. \tag{4.173}$$

Integrating (4.173) and determining the integration constant from the condition at the wall stating that $c_A = c_{Aw}$ for $u = 0$, we determine the dependence of concentration on velocity in the laminar sublayer

$$c_A = c_{Aw}(1 + Sc\, A_w u) \tag{4.174}$$

The derivative of concentration with respect to the dimensionless velocity at the boundary of the laminar sublayer on the side of the turbulent core, $(dc_A/d\bar{u})_{\bar{u} = \bar{u}_l + 0}$, will be found from the condition that the diffusive flows of the atomic species in either direction from the boundary of the sublayer and the core be equal:

$$\left(\frac{dc_A}{d\bar{u}}\right)_{\bar{u}=\bar{u}_l+0} = \frac{1}{Sc}\left(\frac{dc_A}{d\bar{u}}\right)_{\bar{u}=\bar{u}_l-0}.$$

(4.175)

Using this relation and the condition at the outer edge: $c_A = c_{Ae}$ at $u = U_e$, we find the relationship between the concentration and velocity in the turbulent core

$$c_A = c_{Ae} - c_{Aw}A_w(1 - \bar{u}).$$

(4.176)

Equating the concentration values obtained from Equations (4.173) and (4.176) at the boundary of the laminar sublayer, we obtain an expression for the atom concentration at the wall as a function of the parameter of catalytic recombination, A_w:

$$c_{Aw} = c_{Ae}(1 + A_w Sc^{2/3})^{-1}.$$

(4.177)

In obtaining the relation (4.177), we made the approximation

$$1 - (1 - Sc)\bar{u}_l \approx Sc^{2/3}.$$

(4.178)

Assuming that $Sc = 0.5$, with the velocity $\bar{u}_l$ ranging from 0.6 to 0.86, the computational error when Formula (4.178) is used does not exceed ±10%.

Expressions (4.174) and (4.176) may be transformed to a form not containing the parameter of catalytic recombination A_w by eliminating

this parameter with the aid of Equation (4.177). After simple rearrangements, we obtain

$$\left.\begin{aligned}
c_A &= c_{Aw} + \mathrm{Sc}^{1/3}(c_{Ae} - c_{Aw})\bar{u}, \\
c_A &= c_{Ae} - \mathrm{Sc}^{-2/3}(c_{Ae} - c_{Aw})(1 - \bar{u}).
\end{aligned}\right\} \qquad (4.179)$$

The first of these equalities is valid in the laminar sublayer; the second — in the turbulent core. When the Schmidt number is equal to unity, the equalities reduce to the relation (4.126) which was obtained earlier.

Formulas (4.174), (4.176) and (4.177) imply that for $k_w = 0$ (this corresponds to flow around an absolutely noncatalytic wall) $c_{Aw} = c_{Ae}$, i.e., the atom concentration in the boundary layer is constant over the cross-section and equal to its value at the outer edge. For $k_w \rightarrow \infty$ (this corresponds to a flow around an absolutely catalytic wall) $c_{Aw} = 0$, i.e., all atoms that diffuse toward the wall become recombined.

Using Equations (4.174) and (4.177), as well as the relations (4.160), (4.159) and (4.161), which are valid in the case of a frozen flow, we obtain expressions for the recovery enthalpy, Reynolds similitude parameter, and heat flux in a frozen turbulent boundary layer on a flat plate with arbitrary catalytic properties of the surface:

$$\bar{H}_r = \bar{h}_e + \beta \mathrm{Pr}^{1/3} + [(\mathrm{Le}^{2/3} - 1)\mathrm{Sc}^{1/3}c_{Ae}\psi_w]_r,$$

$$\frac{2c_h}{c_f} = \mathrm{Pr}^{-2/3}(\bar{H}_r - \bar{h}_w)^{-1} \times \qquad (4.180)$$

$$\times [\bar{h}_e + \beta \mathrm{Pr}^{1/3} - \bar{h}_w + (\mathrm{Le}^{2/3} - 1)\mathrm{Sc}^{1/3}c_{Ae}\psi_w], \qquad (4.181)$$

$$q_w = \frac{1}{2}c_f \rho_e U_e \mathrm{Pr}^{-2/3}D \times$$

$$\times [\bar{h}_e + \beta \mathrm{Pr}^{1/3} - \bar{h}_w + (\mathrm{Le}^{2/3} - 1)\mathrm{Sc}^{1/3}c_{Ae}\psi_w]. \qquad (4.182)$$

In Equations (4.180) - (4.182) we use the approximation

$$1 + (\mathrm{Le} - 1)\bar{u}_n \approx \mathrm{Le}^{1/3}, \qquad (4.183)$$

and introduce the function

$$\psi_w = \left(1 + \frac{1}{A_w \mathrm{Sc}^{2/3}}\right)^{-1}.$$ (4.184)

It is easy to see that, for an absolutely catalytic wall ($k_w \to \infty$), the function $\psi_w \to 1$, and for an absolutely noncatalytic wall, ($k_w = 0$) $\psi_w \to 0$.

If the effect of the catalytic properties of the wall on friction (c_f) and the Prandtl and Lewis numbers is disregarded, then using relation (4.182), it is easy to obtain the expression for the ratio of the heat flux (for an arbitrary catalytic recombination rate) to the heat flux on an absolutely catalytic wall

$$\frac{q_w}{(q_w)_{k_w \to \infty}} =$$
$$= 1 - \frac{(\mathrm{Le}^{1/3} - 1)\,\mathrm{Sc}^{1/3} c_{Ae} D}{h_e + \mathrm{Pr}^{1/3} \dfrac{U_e^2}{2} + (\mathrm{Le}^{1/3} - 1)\,\mathrm{Sc}^{1/3} c_{Ae} D - h_w}(1 - \psi_w).$$ (4.185)

Formula (4.185) allows us to estimate the effect of the catalytic capacity of the wall on the local heat flux. Figure 67 illustrates the result of the calculation based on (4.185) for air flow over a flat plate. The computation was made for a pressure corresponding to an altitude of 45 km above sea level and the temperature of the wall, $T_w = 700°$ K. On the abscissa axis, we plotted the rate of catalytic recombination and indicated the range of k_w for a number of materials (for more details, see Figure 58). Figure 67 shows that the catalytic capacity of a wall has a very strong effect on the heat flux. This fact permits us to conclude that a suitable choice of the material used for spacecraft skin may significantly reduce the heat transfer to surface. The fact that the curve calculated for the flight velocity of 2.5 km/sec lies below the curve for 3 km/sec is explained by saying that nitrogen begins to dissociate after the entire oxygen in the outer flow had already dissociated[8].
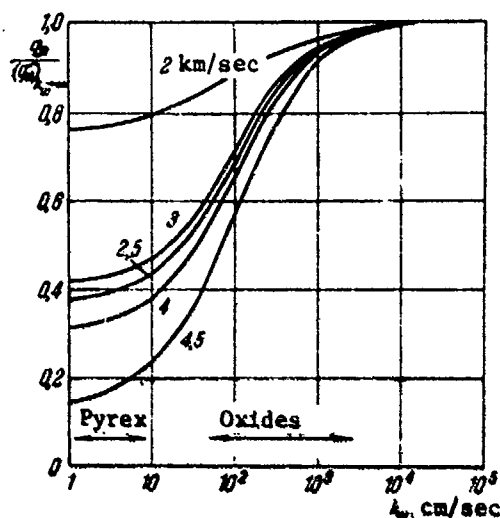

Footnote (8) appears on page 270.

Figure 67

Next we shall establish a relationship between the temperature and velocity. Substituting in the left-hand side of Equation (4.163) the expression for enthalpy of an ideally dissociating gas, (4.74), and solving the resulting equation for the temperature, we obtain an expression for the temperature as a function of velocity in the laminar sublayer:

$$T = (4 + c_A)^{-1} [\bar{h}_w + Pr^{*} \{\bar{h}_e + \tfrac{1}{2} Pr^{*} - \bar{h}_w + (Le^{*} - 1) Sc^{*} c_{Aw} \psi_w \} \bar{u} - Pr \tfrac{1}{2} \bar{u}^2 + (Le - 1) r_{Aw} - Le\, r_A]. \quad (4.186)$$

Here c_A and c_{Aw} are given by Equations (4.174) and (4.177).

Similarly, Equation (4.162) can be used to obtain the relation between the temperature and velocity in the turbulent core

$$T = (4 + c_A)^{-1} \{H_e - \tfrac{1}{2} \bar{u}^2 - c_A - Pr^{*} [\bar{h}_e + \tfrac{1}{2} Pr^{*} - \bar{h}_w + (Le^{*} - 1) Sc^{*} c_{Aw} \psi_w](1 - \bar{u})\}. \quad (4.187)$$

Here c_A and c_{Aw} are given by Equations (4.176) and (4.177).

The dimensionless quantities $\bar{h}_e$, $\bar{h}_w$, $\bar{\beta}$, $\bar{T}$ in Formulas (4.186) and (4.187) are given by Equations (4.117) and (4.162).

Given the dependence of the temperature on velocity and Equation (4.121), we can determine the dependence of the density on velocity, which in turn enables us to calculate the local friction coefficient from Formulas (4.109).

A convenient correlation formula for the friction coefficient of frozen flow in the boundary layer was obtained by Dorrance [18] who calculated friction for wide parameter ranges ($10^5 \leqslant \mathrm{Re} \leqslant 10^8$; $0 \leqslant M_e \leqslant 4$; $0{,}04 \leqslant T_w/T_e \leqslant 1$). The formula has the form

$$\frac{c_f}{c_{f0}} = 2\left(\frac{1 + c_{Ae}}{1 + c_{Aw}}\right)^{1/3} - 1. \tag{4.188}$$

Here c_{f0} is the friction coefficient calculated without considering dissociation (but considering the effect of the Mach number and the temperature factor). The difference between the results based on Formula (4.188) and the exact results does not exceed 4%. Formula (4.188) implies that dissociation changes the friction coefficient by no more than $\pm 22\%$ as compared with c_{f0}. In addition, inspection of Formula (4.188) shows that an increase in the catalytic capacity of the wall ($c_{Aw} \to 0$) leads to an increase in the friction coefficient.

Figures 68 - 72 give the results of calculating the boundary layer characteristics according to the method presented above for a flow of dissociating oxygen around a plate [19].

Figures 68 and 69 give the plots of the local coefficient versus the Reynolds number for two Mach numbers: $M_e = 4$ and $M_e = 10$. The following values were used in the calculation: $T_e = 3600°$ K, $p_e = 1$ atm, Pr = 0.72, Le = 1.4, $c_{Aw} = 0$. Skin friction was calculated without considering dissociation effects according to a method presented in Section 12. As seen in the plots, the friction coefficients for
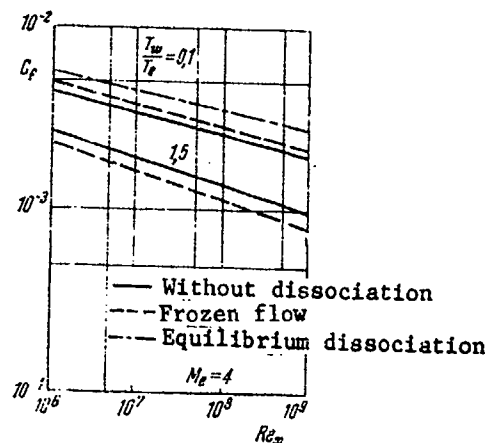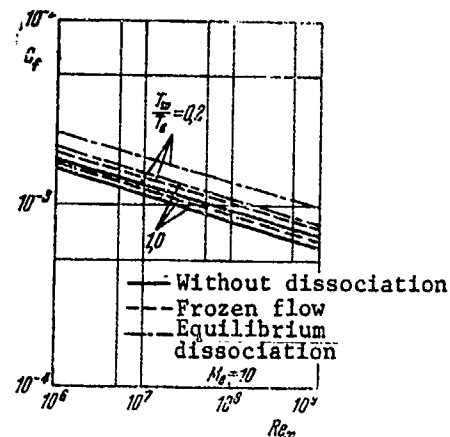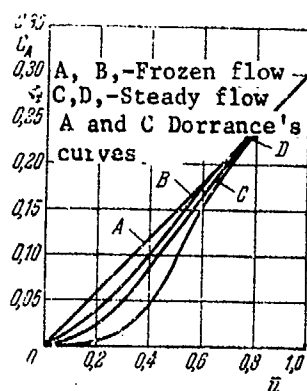
Figure 68
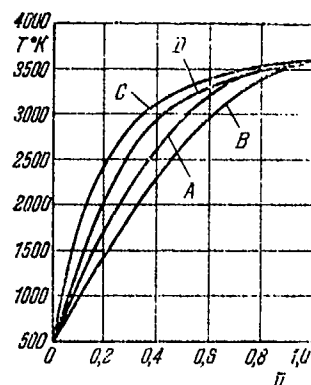

Figure 69

Figure 70

Figure 71

a frozen flow of a gas differ from the friction coefficients calculated for the same conditions, but in the absence of dissociation, by no more than 20%, which is in good agreement with the results obtained by Dorrance [Formula (4.188)]. In the case of equilibrium dissociation, the difference may amount to 40%.

Figures 70 and 71 are the plots of the concentration and temperature versus the velocity in a frozen (curves A, B) and equilibrium (curves C, D) boundary layer, calculated for the conditions:

$M_e = 2.2$, $T_e = 3600°$ K, $T_w = 500°$ K, $c_{Ae} = 0.3$, $c_{Aw} = 0$. Curves A and C, obtained by Dorrance [20], are also given in Figures 70 and 71 for comparison. The difference between curves B and D, calculated using the methods of the present section, and Dorrance's curves A and C, is due to the fact that Dorrance used the relation connecting total enthalpy, concentration, and velocity which is obtained for $Pr = Sc = 1$ [Equations (4.114) and (4.126)]. Therefore, Dorrance's method is very similar to the methods presented in Section 24. The deviation of the Prandtl and Schmidt numbers from unity was considered by Dorrance only in the expression for the Reynolds similitude parameter and through the introduction of the recovery factor. It should also be noted that in his paper Dorrance did not take into account the contribution of the vibrational degrees of freedom to the heat capacity of molecules.

By the method of § 25
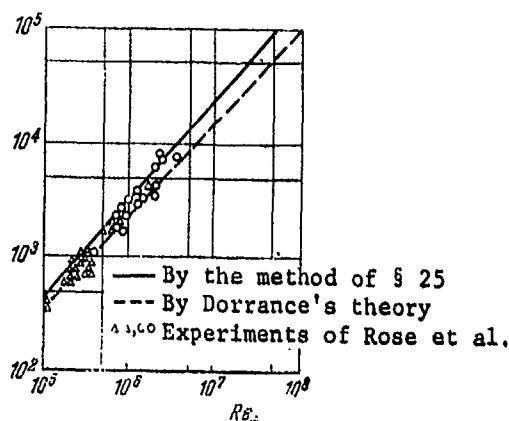By Dorrance's theory
Experiments of Rose et al.

Figure 72

Figure 72 is a plot of the heat transfer coefficient versus the Reynolds number obtained according to the method presented (frozen flow) for the conditions: $M_e = 2$, $T_w/T_e = 0.1$, $c_{Ae} = 0.31$ (c_h^{-1} is plotted on the axis of ordinates). For comparison, the same figure includes a plot obtained by Dorrance (dashed curve). The difference between the theoretical plots is due to both the reasons indicated in the discussion of Figures 70 and 71 and to the fact that, in calculating skin friction, Dorrance used a formula from the semi-empirical Prandtl theory, in contrast with Karman's formula used in the present method. Figure 72 also includes the experimental points obtained by measuring heat transfer on a cylinder with a spherical nose. The measurements were done by Rose et al. [21] in a region where the longitudinal pressure gradient was close to zero. The distribution of the experimental points is characterized by a large scatter. Nevertheless, the agreement between the theoretical results and the experimental data may be considered satisfactory.

Nonequilibrium flow of an ideally dissociating gas. The results
of calculating the equilibrium and frozen flows in the boundary layer,
given in the preceding subsections of the present section, showed con-
vincingly that the thermochemical state of a gas may have a substantial
effect on the drag. It is obvious that the flow in the boundary layer
assumes an even greater importance in heat transfer calculations. Of
course, it is possible to estimate the heat flux to the surface in
the two limiting cases considered in the preceding subsections —
namely, for steady and frozen flows. However, with the aid of the
methods presented in these subsections, it is impossible to analyze
the character of flow in the boundary layer. In many cases important
in practice, it may be necessary to estimate heat transfer with the
dissociation reaction proceeding at a finite rate comparable with the
rate of diffusion, which results in a nonequilibrium flow in the
boundary layer. The nonequilibrium flow of an ideally dissociating
gas under the assumption that the Prandtl and Schmidt numbers are
equal to unity was considered in the preceding section. In heat
transfer calculation, as was pointed out many times above (Chapter III),
it is necessary to consider the deviation of the Prandtl and Schmidt
numbers from unity.

The general expressions for the heat flux q_w, enthalpy of
recovery H_r, Reynolds similitude parameter $2c_h/c_f$, as well as the
relation of total enthalpy to concentration and velocity for arbitrary
Prandtl and Schmidt numbers, were established at the beginning of the
present section. To solve the problem in question, we must establish
a relation between concentration and velocity. It seems justified,
on the basis of considerations given in the discussion of nonequili-
brium flow for $Pr = Sc = 1$ (Section 24), and frozen flow for $Pr \neq$
$\neq Sc \neq 1$ (Section 25), to make the simplifying assumption that the
concentration depends only on velocity in the boundary layer, and does
not depend on the longitudinal coordinate, i.e., $c_A = c_A(u)$. In
addition, we shall make the usual assumption that the friction stress
is constant across the boundary layer, i.e., $\tau = const = \tau_w$. With
these assumptions, Equations (4.98) and (4.100) become, respectively

$$\frac{d^2c_A}{du^2} = -Sc\left(\frac{\mu}{\tau}\right)\frac{w_A}{\tau_w}, \qquad \frac{d^2c_A}{du^2} = -\left(\frac{\varepsilon}{\tau}\right)\frac{w_A}{\tau_w}. \tag{4.189}$$

The first of these equations is valid in the laminar sublayer; the second — in the turbulent core. Integrating the first of Equations (4.189) and using the boundary condition (4.124), we have

$$\frac{dc_A}{d\bar{u}} = Sc\,A_w c_{Aw} - Sc\,I_a(\bar{u}). \tag{4.190}$$

Here

$$I_a(\bar{u}) = U_*^2 \int_0^{\bar{u}} \left(\frac{\mu}{\tau}\right)\frac{w_A}{\tau_w}\,d\bar{u}, \tag{4.191}$$

and A_w is given by the second of Equations (4.125).

It should be noted that the concentration of the atomic species at the wall, (c_{Aw}), is as yet unknown, and will be determined later.

Integrating Equation (4.190) and determining the integration constant for conditions at the wall, $(c_A = c_{Aw}$ for $\bar{u} = 0)$, we find the distribution concentration in the laminar sublayer

$$c_A = c_{Aw}(1 + Sc\,A_w\bar{u}) - Sc\,I_a(\bar{u}), \tag{4.192}$$

where

$$I_a(\bar{u}) = U_*^2 \int_0^{\bar{u}} d\bar{u} \int_0^{\bar{u}} \left(\frac{\mu}{\tau}\right)\frac{w_A}{\tau_w}\,d\bar{u}.$$

Now we proceed to determine the concentration profile in the turbulent core. Integrating the second of Equations (4.189) once, we get

$$\frac{dc_A}{d\bar{u}} = \left(\frac{dc_A}{d\bar{u}}\right)_{\bar{u}=\bar{u}_{,1}+0} - I_\tau(\bar{u}),$$

$$I_\tau(\bar{u}) = U_c^2 \int_{\bar{u}_{,1}}^{\bar{u}} \left(\frac{c}{\tau}\right) \frac{w_A}{\tau_w} d\bar{u}.$$

(4.193)

Here $\bar{u}_l$ is the dimensionless veloci^ at the boundary of the laminar sublayer given by Equation (3.31).

The derivative of concentration with respect to the dimensionless velocity at the boundary of the laminar sublayer on the side of the turbulent core, $(dc_A/d\bar{u})_{\bar{u} = \bar{u}_l + 0}$, will be determined from the condition that the diffusive flows of the atomic species in both directions — from the boundary between the sublayer and the turbulent core — are equal, (4.175). Using this condition and Equation (4.190), we find

$$\left(\frac{dc_A}{d\bar{u}}\right)_{\bar{u}=\bar{u}_{,1}+0} = A_w c_{Aw} - I_{,1}(\bar{u}_n).$$

(4.194)

Substituting Expression (4.194) in Equation (4.193), and performing the resulting integration, after determining the integration constant from the condition at the outer boundary ($c_A = c_{Ae}$ for $\bar{u} = 1$), we shall obtain the distribution of concentration in the turbulent core

$$c_A = c_{A,} + I_\tau(1) - I_\tau(\bar{u}) - (1 - \bar{u})[A_w c_{Aw} - I_{,1}(\bar{u}_n)],$$

(4.195)

where

$$I_\tau(\bar{u}) = U_c^2 \int_{u_n}^{\bar{u}} d\bar{u} \int_{u_n}^{\bar{u}} \left(\frac{c}{\tau}\right) \frac{w_A}{\tau_w} du.$$

Equating the values of concentration from Equations (4.192) and (4.195) at the boundary between the sublayer and the turbulent core, and solving the resulting equation for concentration at the wall, we obtain the following expression for it

$$c_{Aw} = (1 + Sc^{1/3} A_w)^{-1} \times$$
$$\times [c_{Ae} + I_\tau(1) + Sc\, I_n(\bar{u}_n) + (1 - \bar{u}_n)\, I_n(\bar{u}_n)]. \tag{4.196}$$

In deriving (4.196), we used Equation (4.178).

The concentration distribution in the laminar sublayer, (4.192), and in the turbulent core (4.195), may in certain cases be conveniently used in the form that does not involve the parameter of catalytic recombination A_w. Eliminating A_w from Equations (4.192) and (4.195) with the aid of the Expression (4.196), we shall have in the laminar sublayer

$$c_A = c_{Aw} + Sc^{1/3}(c_{Ae} - c_{Aw})\bar{u} + Sc^{1/3}[I_\tau(1) + Sc\, I_n(\bar{u}_n) +$$
$$+ (1 - \bar{u}_n)\, I_n(\bar{u}_n)]\,\bar{u} - Sc\, I_n(\bar{u}), \quad (4. \tag{4.197}$$

and in the turbulent core

$$c_A = c_{Ae} - Sc^{1/3}(c_{Ae} - c_{Aw})(1 - \bar{u}) + I_\tau(1) - I_\tau(\bar{u}) -$$
$$- Sc^{1/3}[I_\tau(1) + Sc\, I_n(\bar{u}_n)](1 - \bar{u}) + Sc^{1/3}\bar{u}_n I_n(\bar{u}_n)(1 - \bar{u}). \tag{4.198}$$

In the frozen flow ($w_A \equiv 0$), the functions I_{th}, I_l and $\dot{I}_l$ become zero, and Equations (4.197) and (4.198) reduce to relation (4.179) of the present section.

The dimensionless integral quantities I_l and I_{th}[(4.192) and (4.195)], appearing in the concentration distributions, characterize the total "power" of the sources of formation of the atomic species, contained within a certain volume, whose extension in the y-direction is determined by the limits of integration, and the base area may be assumed to be equal to unity. The expressions for these quantities can be obtained similarly to the expression for the quantity $I(\bar{u})$ (4.136) in the preceding section. For this reason, leaving out simple algebra, we shall merely state the expressions for these quantities in their final form:

$$I_{\eta}(\bar{u}) = \frac{\zeta^4}{\mathrm{Re}_{xw}} \frac{\rho_w}{\rho_d} \int\limits_0^{\bar{v}} d\bar{u} \int\limits_0^{\bar{u}} C_r \left(\frac{\rho}{\rho_w}\right)^3 (1+c_A) \frac{c_A^{(r)^2} - c_A^2}{1 - c_A^{(r)^2}} \frac{d\eta}{d\varphi} d\bar{u}, \qquad (4.199)$$

$$I_{\tau}(\bar{u}) = \frac{\zeta^4}{\mathrm{Re}_{xw}} \frac{\rho_w}{\rho_d} \int\limits_{\bar{u}_n}^{\bar{u}} d\bar{u} \int\limits_{\bar{u}_n}^{\bar{u}} C_r \left(\frac{\rho}{\rho_w}\right)^3 (1+c_A) \frac{c_A^{(r)^2} - c_A^2}{1 - c_A^{(r)^2}} \frac{d\eta}{d\varphi} d\bar{u}. \qquad (4.200)$$

Here ζ is the friction parameter (3.8), C_r is the recombination parameter (4.137), Re_{xw} is the Reynolds number (4.137), $d\eta/d\phi$ is given by Equation (4.104) in the turbulent core and by (4.106) in the laminar sublayer. The equilibrium atom concentration $c_A^{(e)}$ is given by (4.68).

The quantity $\dot{I}_\zeta(\bar{u})$, which is also necessary to calculate the concentration distribution, is given by

$$I_{\eta}(\bar{u}) = \frac{dI_{\eta}(\bar{u})}{d\bar{u}}. \qquad (4.201)$$

The velocity at the boundary of the laminar sublayer, $\bar{u}_\ell$, can be determined from Equation (3.31).

The concentration profile can be calculated using the method of successive approximations applied to Formulas (4.197) and (4.198) or to (4.192) and (4.195). The order of calculation remains the same as in nonequilibrium flow calculations for $\mathrm{Pr} = \mathrm{Sc} = 1$ (see Section 24).

In Equations (4.197) and (4.198), the first two terms on the right-hand sides give the contribution of diffusion to the concentration distribution, and the remaining terms, containing I_η, $I_{\eta\eta}$, I_τ, give the contribution of the chemical reactions to this distribution. The mutual effect of diffusion and chemical reactions on each other is manifested through the concentration at the wall c_{Aw} (4.196), which depends on the rates of both processes. The flow in the boundary layer will be determined by the relative contributions of diffusion

and chemical reactions to the concentration distribution. If the recombination parameter is $C_r = \infty$, the contribution of the chemical processes will be infinitely large compared with the contribution of diffusion (the sum of the terms containing the integral quantities in Equations (4.197), (4.198) will be infinitely large compared with the diffusive terms). In this case, the flow will be steady and the concentration distribution can be determined from the condition $w_A = 0$. In the other extreme case, when the recombination parameter is equal to zero ($C_r = 0$), the diffusion process will be the dominant factor (frozen flow). Thus, the objective of the computation reduces to establishing the role of diffusion and chemical reactions in the transfer processes in the boundary layer.

Given the concentration distribution (4.197), (4.198), it is easy to obtain the expressions for the Reynolds similitude parameter, recovery enthalpy and heat flux for a nonsteady flow in the boundary layer. For this purpose, we use Equations (4.159) and (4.161), substituting in them $c_{A l}$ as given by (4.197).

As a result, we obtain

$$\frac{2\tau_h}{c_f} = Pr^{-\nu}(\bar{H}_e - \bar{h}_w)^{-1}(\bar{h}_e + \tilde{\beta}Pr^\nu - \bar{h}_w +$$
$$+ (Le^\nu - 1)Sc^\nu(c_{Ae} - c_{Aw}) + (Le^\nu - 1)Sc^\nu[I_1(1) +$$
$$+ Sc\,I_2(\bar{a}_a) + (1 - \bar{a}_a)\,I_2(\bar{a}_a)] - (Le - 1)Sc\,I_2(\bar{a}_a)]. \qquad (4.202)$$

$$\bar{H}_r = \bar{h}_w + \tilde{\beta}Pr^\nu + [(Le^\nu - 1)Sc^\nu(c_{Ae} - c_{Aw}) +$$
$$+ (Le^\nu - 1)Sc^\nu[I_1(1) + Sc\,I_2(\bar{a}_a) + (1 - \bar{a}_a)\,I_2(\bar{a}_a)] -$$
$$- (Le - 1)Sc\,I_2(\bar{a}_a)]_r. \qquad (4.203)$$

$$q_w = \frac{1}{2}c_f\rho_e U_e Pr^{-\nu}D(\bar{h}_e + \tilde{\beta}Pr^\nu - \bar{h}_w +$$
$$+ (Le^\nu - 1)Sc^\nu(c_{Ae} - c_{Aw}) + (Le^\nu - 1)Sc^\nu[I_1(1) +$$
$$+ Sc\,I_2(\bar{a}_a) + (1 - \bar{a}_a)\,I_2(\bar{a}_a)] - (Le - 1)Sc\,I_2(\bar{a}_a)]. \qquad (4.204)$$

The concentration at the wall in Equations (4.202) – (4.204) is given by Equation (4.196), and the integral quantities I_{th}, I_l, I_2 by Equations (4.199) – (4.201). The subscript r in the Expression (4.203) refers to conditions at a thermally insulated wall.

The distribution of enthalpy in the boundary layer is determined by Equations (4.163) in the laminar sublayer and (4.162) in the turbulent core upon a substitution of the concentrations as given by (4.197) and (4.198), respectively.

The temperature distribution can be obtained from the enthalpy distribution by solving Equation (4.74) for temperature. As a result, we obtain

$$T = (4 + c_A)^{-1}(H - \overline{u}^2 - c_A)$$ (4.205)

Furthermore, Equations (4.121) and (4.109) can be used to determine the density in the boundary layer and the local friction coefficient at the wall.
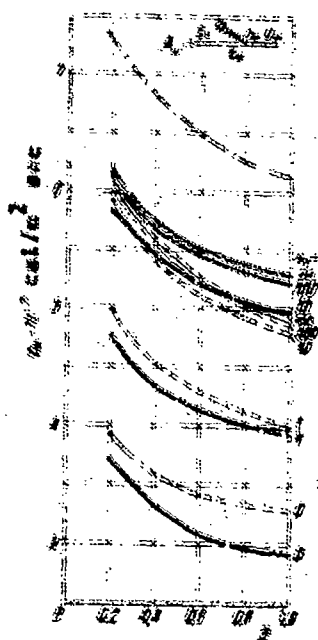
Figure 73 gives the results of calculating local heat fluxes on a wedge with the 30° half-angle at the vertex, immersed in a stream of oxygen moving at the velocity $U_\infty = 7$ km/sec, for the pressure and temperature in the oncoming flow $p_\infty = 2.85 \cdot 10^{-4}$ atm and $T = 220°$ K. The wall temperature is assumed to equal 720° K. A computation of heat fluxes for frozen (see Equation (4.182); dashed curves] and nonequilibrium [see Equation (4.204); solid curves] flows in the boundary layer was done for a number of values of the catalytic recombination parameter A_{w1} in the range from 0 to ∞ [this parameter

Figure 73

differs from the catalytic recombination parameter A_w used in the present section [see Formula (4.125)] in only an additional factor $(A_{wl} = Sc^{2/3} A_w)$].

It will be recalled that the value $A_{wl} = 0$ corresponds to flow over an absolutely noncatalytic surface, and the value $A_{wl} = \infty$ to flow over an absolutely catalytic surface. The value of the heat flux for a steady flow in the boundary layer (dot-dash curve) was determined using Formula (4.161).

It will be noted that the values of the local friction coefficient, which are necessary for calculating the heat flux from Formulas (4.161), (4.182) and (4.204), were calculated using a method presented in the preceding section (i.e., under the assumption that the Prandtl and Schmidt numbers are constant and equal to unity).

§ 26. Conclusion

The methods of calculating skin friction and heat transfer in the turbulent boundary layer of a dissociating gas, presented in this chapter, are easily seen to be an extension of the methods used in the theory of a homogeneous gas flow, presented in Chapter III (Sections 12 and 15). At the same time, one can point to a number of papers written by Soviet and foreign workers in which the approach to the problem of the turbulent boundary layer in a dissociating gas differs to a greater or lesser degree from the approach used in this chapter.

The case of equilibrium dissociation in a turbulent boundary layer on a flat plate was discussed by S. I. Kosterin and Yu. A. Koshmarov [22]. Their analysis was based on a model of an ideally dissociating gas and on the semi-empirical Prandtl theory. The Prandtl, Schmidt numbers and their turbulent analogs were assumed to be equal to unity. S. I. Kosterin and Yu. A. Koshmarov's method is largely similar to the method used in Section 24.

The effect of equilibrium dissociation on skin friction and heat transfer on a flat plate for the Prandtl and Schmidt numbers different from unity was discussed in the paper by I. P. Ginzburg [23]. The calculation of friction in that paper was based on the semi-empirical Prandtl theory.

The method of calculating skin friction and heat transfer on a flat plate in equilibrium and frozen flows was proposed by Dorrance. The basic features of this method and some of the results of the calculation were discussed in Section 25 (see the footnote on Dorrance's paper).

Heat transfer from a nonequilibrium turbulent boundary layer to a catalytic surface was calculated by Kulgein [24]. In this paper, the deviation of the dissociation process from equilibrium was taken into account only in the laminar sublayer, and in the turbulent core, the flow was assumed to be frozen. A computer-assisted calculation of heat transfer was made for various conditions of flow in the external stream and at the wall.

The methods of calculating friction and heat transfer in an ideally dissociating gas presented in Sections 24 and 25 (for a binary mixture of atoms and molecules) can be easily extended to the case of a flow of a multicomponent dissociating mixture. It is for that reason that Section 25, in particular, gives the expressions for total enthalpy, Reynolds similitude parameter, recovery enthalpy, and heat flux in a multicomponent mixture. The computation of the concentration fields for steady and frozen flows in a multicomponent mixture is in principle no different from the calculation of the same fields in a binary mixture. To calculate the nonequilibrium flows of a multicomponent mixture, data on the mass rates of formation of species, presented in Section 20 of Chapter IV, must be used.

The method can be easily extended to the flow of a partially excited dissociating gas whose properties were described in detail in Sections 20 and 21.

Finally, in the approximation used in Sections 17 and 18 making use of the formulas obtained in Sections 17, 18, and in Chapter IV, it is possible to calculate skin friction and heat transfer in the presence of a longitudinal pressure gradient. The necessary expressions for the integral thicknesses and the form parameter H^* are given in Section 23.

An almost complete lack of experimental data on the characteristics of the turbulent boundary layer in a dissociating gas prevents us from estimating the accuracy of the computational methods presented. Nevertheless, the good agreement between the theoretical and experimental data in the absence of dissociation (Chapter III) leads us to hope that the methods of Chapter IV, which are an extension of the methods of Chapter III, will also give satisfactory results.

FOOTNOTES

Footnote (1) on page 186.   For more details about thermodynamic
                             properties of gases at high tempera-
                             tures, see the monograph: Zel'dovich,
                             Ya. B., Rayzer, Yu. P., Fizika udarnykh
                             voln i vysokotemperaturnykh gidrodinami-
                             cheskikh yavleniy (Physics of Shock
                             Waves and High-Temperature Hydrodynamic
                             Phenomena), Fizmatgiz, Moscow, 1963.

Footnote (2) on page 189.   Figure 56, prepared by Hansen, has been
                             reprinted from the book: Dorrance, W.H.
                             Hypersonic Flow of a Viscous Gas, 1966.

Footnote (3) on page 199.   See the paper by M.S. Zakhar'yevskiy
                             which was already cited in this section.

Footnote (4) on page 200.   A presentation of the theory of the
                             absolute reaction rates goes beyond the
                             objective of the present book. Those
                             interested in the theory are advised to
                             consult the monograph by Glesston,
                             Leidler, and Eyring, which was already
                             cited in this section.

Footnote (5) on page 200.   Concerning this question, we recommend
                             the paper by Rosner which contains a
                             summary and an extensive bibliography:
                             Rosner, D. Convective Diffusion as an
                             Intruder in Kinetic Studies of Surface
                             Catalyzed Reactions, AIAA J. 2, No. 4
                             (1964); Russian translation: Raketn.
                             Tekhn. i Kosmonaut., Nov. 4, 1964.

Footnote (6) on page 234.   The principle, used here as the basis
                             for our analysis of a nonequilibrium
                             flow, might be called (by analogy with
                             the well-known principle, introduced by
                             L. Lees in the theory of the laminar
                             boundary layer) the principle of local
                             similitude for the turbulent boundary
                             layer. According to this principle,
                             the concentration and temperature
                             (enthalpy) profiles are similar to the
                             velocity profiles in each section.

Footnote (7) on page 237.   The calculations were done at the request of the author by O. K. Zakharova.

Footnote (8) on page 254.   A similar result was obtained for the laminar boundary layer near the front stagnation point, as reported in Goulard's paper quoted earlier in this chapter.

REFERENCES

1) Ступоченко Е. В., Стаханов И. П., Самуйлов Е. В., Плешанов А. С., Рождественский И. Б., Термодинамические свойства воздуха в интервале температур от 1000 до 12 000° К и интервале давлений от 0,001 до 1000 атм, в сб. «Физическая газодинамика», АН СССР, Москва, 1959.

2) Предводителев А. С. и др., Таблицы термодинамических функций воздуха (для температур от 200 до 6000° К и давлений от 0,00001 до 100 атм), АН СССР, Москва, 1962.

3) Penner S. S., Chemistry problems in jet propulsion, Aeronautical sciences and controlled flight, v. 1, Pergamon Press, London—New York — Paris — Los Angeles, 1957.

4) Lighthill M. J., Dynamics of the dissociating gas, Part I, Equilibrium Flow, Journ. Fluid Mech. 2, № 1, 1—32 (1957); русский перевод: Вопр. ракетн. техн., №№ 5, 6; ИЛ, 1957.

5) Годнев И. В., Вычисление термодинамических функций по молекулярным данным, Гостехиздат, Москва, 1956.
Глесстон С., Теоретическая химия, ИЛ, Москва, 1950.

6) Кондратьев В. Н., Кинетика химических газовых реакций, АН СССР, Москва, 1958.
Захарьевский М. С., Кинетика химических реакций, Изд-во Ленингр. гос. ун-та им. Жданова, 1959.

7) Глесстон С., Лейдлер К., Эйринг Г., Теория абсолютных скоростей реакций, ИЛ, Москва, 1948.

8) Gurney J. P., General formulation of surface catalytic reactions, AIAA Journ. 4, № 7 (1966); русский перевод: Ракетн. техн. и космонавт., № 7, 1966.

9) Рей К., Химическая кинетика воздуха при высокой температуре, в сб. «Исследование гиперзвуковых течений», «Мир», Москва, 1964.

10) Chung P. M., Chemical reacting nonequilibrium boundary layer, Advances in Heat Transfer, Ed. Hartnett J. P., Irvine T. F., 2, Acad. Press, New York—London, 1965.

11) Hanson F., Aproximation for the thermodynamic and transport properties of high temperature air, NASA TR, № 50 (1959).

12) Glass I. I., Takano A., Nonequilibrium expansion of dissociated oxygen and ionized argon around a corner, Progress Aero. Sci. 6, Pergamon Press, Oxford—London—Edinburgh—New York — Paris, 1965.

13) Ступоченко Е. В., Лосев С. А., Осипов А. И., Релаксационные процессы в ударных волнах, «Наука», Москва, 1965.

14) Лапин Ю. В., Турбулентный пограничный слой на каталитической поверхности в неравновесно диссоциирующем газе, МЖГ, № 3 (1967).

15) Дорренс У. Х., Гиперзвуковые течения вязкого газа, «Мир», Москва, 1966.

16) Лапин Ю. В., Турбулентный пограничный слой в диссоциирующем газе, Журн. техн. физ., т. XXXII, вып. 4, 473—479 (1962).

17) Лапин Ю. В., Влияние каталитической рекомбинации на теплопередачу в замороженном турбулентном пограничном слое, Тр. Ленингр. политехн. ин-та им. М. И. Калинина, № 248, «Машиностроение», Москва — Ленинград (1965).

18) Дорренс У. Х., Гиперзвуковые течения вязкого газа, «Мир», Москва, 1966.

19) Л а п и н Ю. В., С е р г е е в Г. П., Влияние диссоциации на трение и теплообмен в турбулентном пограничном слое, Тр. Ленингр. политехн. ин-та им. М. И. Калинина, № 230, «Машиностроение», Москва — Ленинград (1964).

20) D o r r e n s W. H., Dissociation effects upon compressible turbulent boundary layer skin friction and heat transfer, ARS Journ. 31, № 1 (1961); русский перевод: Вопр. ракетн. техн., № 12, ИЛ, 1961.

21) R o s e P. H., P r o b s t e i n R. F., A'd a m s Mc. C., Turbulent heat transfer through a highly cooled, partially dissociated boundary layer, Journ. Aero-Space Sci. 25, № 12, 751—760 (1958); русский перевод: Механика, № 4 (56), ИЛ, 1959.

22) K o s t e r i n S. I., K o s h m a r o v Yu. A., Turbulent boundary layer on a flat plate in a stream of dissociating gas, Internat. Journ. Heat Mass Transfer 6, 46—49, Pergamon Press (1960).

23) Г и н з б у р г И. П., Турбулентный пограничный слой в сжимаемой жидкости (смеси газов), Вестн. Ленингр. ун-та, § 1, 75—88 (1961).

24) K u l g e i n N. G., Heat transfer from a nonequilibrium turbulent boundary layer to catalytic surface, AIAA Journ 3, № 2 (1965); русский перевод: Ракетн. техн. и космонавт., № 2, 1965.

CHAPTER V

TURBULENT BOUNDARY LAYER WITH MASS TRANSFER BETWEEN THE GAS AND THE SOLID SURFACE

§ 27. Introduction

In Chapter III and Chapter IV we discussed the properties of the
turbulent boundary layers which are formed on bodies of various
shapes, in the absence of mass transfer between the gas and the solid
wall. When bodies move at very large supersonic velocities through
the dense layers of the atmosphere, the processes of mass transfer
between the gas and surface begin to play an important role. Strong
heating may lead to a change of the state of a solid body: to its
melting, vaporization, and the subsequent removal of the surface
material by the gas flow. The first data on mass transfer for bodies
moving at very large supersonic velocities were obtained more than
forty years ago as a result of studies done on the motion of meteors.
In recent decades, interest in the problem has grown even more due
to the advances in rocket and space technology. The phenomena which
occur when moving bodies are heated to very high temperatures became
the subject of extensive experimental and theoretical studies. One
of the most important results of those studies was the conclusion

that it is possible to use special ablating coverings in order to thermally insulate the front portions of rockets and spacecraft. At the present time, it has apparently been accepted that the heat protection of hypersonic vehicles by means of ablating coverings is the most effective method from a weight and design standpoint. Mass transfer plays an important role in cooling the walls of combustion chambers, supersonic air scoops, nozzles, rocket engines, etc.

Heat protection coverings are widely made of construction synthetics, synthesized on the base of thermoreactive phenol-formaldehyde and epoxy resins [1]. With respect to resin-reinforcing fillers, use is made of textolite, glass-textolite, asbestos, chromium, high-melting oxides of magnesium, aluminum, nylon, Terylene, and other materials.

Materials that decompose at relatively low temperatures (up to 1000° K) are of great interest today: teflon kapron, polyethylene, organic glass. When heat protection coverings made of these materials undergo decomposition, the boundary layer becomes filled with gases of various molecular weights, which in many cases leads to a strong "blowing effect" that reduces the heat flux to the surface. By now a great number of various heat proof materials have been investigated and applied. However, regardless of the diversity of these materials, it was noted that heat protection coverings decompose basically due to the following physical-chemical processes: surface pyrolysis of the binding depolymerization, vaporization, sublimation, combustion, melting, erosion. In a majority of cases, the rate of combustion of the coke residue of the binding resin is used as the defining rate of decomposition, of a synthetic covering. Removal processes in the liquid phase may play an important role if a covering has a large percentage of quartz and glass fillers. An example of such a heat protection covering is an asbestos-textolite covering in which the following processes are observed upon heating: coking, dehydration of asbestos, chemical interaction of coke residue with oxygen and nitrogen, sublimation of coke residue, flow of melted silica fiber (SiO_2), vaporization of melted SiO_2. The result of all these

processes is that the composition of the gas mixture in the boundary layer becomes very complicated [2]. Depending on the conditions, the mixture may contain the following components: O_2, O, N_2, N, C, C_2, C_3, CO, CO_2, CN, HCN, H_2, H, Si, SiO, SiO_2, ScC, SiC_2, Si_2C and others.

The process of surface decomposition through the mechanisms indicated, all at the same time or some of them, has come to be called mass removal. One of the possible mechanisms resonable for mass removal is illustrated in Figure 74, a.
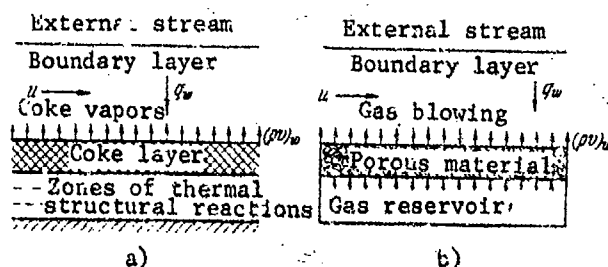
Figure 74

In certain cases, a surface may be cooled by forced injection of a substance into the boundary layer through the porous wall (Figure 74, b). One may use air, water vapor, light gases (hydrogen, helium), and other gases and vapors [3] as the cooling material in porous cooling.

The presence of lateral mass flow in the boundary layer, caused by the injection of mass through the porous wall, sublimation of a solid surface, or vaporization of a liquid film, has an effect on the structure of the boundary layer, (velocity, temperature profiles, etc.) which is proportional to the intensity of the flow. Along with the change of the local characteristics of the boundary layer, its integral characteristics are modified. In particular, the injection usually leads to a reduction of friction and heat flux on the wall. Exceptions may occur only in those cases when the mass injected into the boundary layer reacts chemically with the components of the fundamental flow, and the heat thus released may in the final analysis

result in an increase of heat flux on the wall. The phenomenon in
which friction and heat flux are reduced upon the injection of mass
into the boundary layer is sometimes called the "blocking effect".

The present chapter will be devoted to a description of some of
the phenomena mentioned above and to a presentation of the methods
of calculating friction and heat transfer for the case of mass
injection into the boundary layer. We shall discuss flows near a
porous (or sublimating) plate immersed in a supersonic gas stream,
with no chemical interaction between the mass injected and the gas of
the fundamental flow.

In conclusion, we note that a solution of this problem, either
of an experimental or theoretical nature, is still far from realiza-
tion. In fact, only the first few results have been obtained. Many
theoretical and experimental aspects of the problem remain unclear.
In view of this fact, it seems advisable to give a brief survey of
the basic approaches used in this area of the theory of the
turbulent boundary layer.

§ 28. Basic Trends in the Study of the Turbulent
Boundary Layer with Mass Transfer
Between the Gas and the Surface

This area of investigations has developed primarily during the
past ten to fifteen years. An acquaintance with papers related to
this area proves that the development has followed the same paths
as the development of the theory of the turbulent boundary layer in
a compressible gas in the absence of mass transfer between the gas
and the surface (some results of these investigations) were discussed
in Chapter III). Similarly as before, there are three principal
trends: (1) semi-empirical, based on a generalization of the Prandtl
and Karman Formulas, (2.68) and (2.69), to the flow of a compressible
gas with mass transfer between the gas and the wall (this approach
may also be characterized as one using the logarithmic velocity
profile; (2) semi-empirical, based on power-law velocity profiles;

(3) empirical, based on direct use of experimental data.

Thus far, the first approach has been followed the most. In a majority of papers following this approach, the following expression for the friction stress in the boundary layer is used

$$\tau = \tau_w + (\rho v)_w u. \tag{5.1}$$

Here $(\rho v)_w$ is the mass flux at the surface of a body.

Equation (5.1) can be easily obtained using the following simple considerations. We expand $(\tau - \rho_w v_w u)$ into a Taylor series

$$\tau(\xi, y) - \rho_w v_w u(\xi, y) = \tau(\xi, 0) + \left[\frac{\partial}{\partial y}(\tau - \rho_w v_w u)\right]_{\substack{y=0 \\ \xi=0}} y + \ldots$$

Noting that the equation of motion (2.52) for a flat plate and the second of the boundary conditions (2.73) imply that

$$\left[\frac{\partial}{\partial y}(\tau - \rho_w v_w u)\right]_{y=0} = 0,$$

we arrive at Equation (5.1). The fact that expression (5.1) is used for the friction stress means essentially that we assume the mass flux in the boundary layer to be constant

$$\rho v = \text{const} = (\rho v)_w.$$

Equation (5.1), as can be easily seen, leads to invalid results at the outer edge of the boundary layer, where we must satisfy the condition $\tau = 0$ for $u = U_e$.

The actual character of the friction stress distribution in the boundary layer with mass addition may be seen in Figure 75 [4], which shows the results of the friction measurements for various values of the injection parameter B, defined by

$$B = \frac{2 \rho_w v_w}{c_f \rho_e U_e} = \frac{2 \rho_w v_w U_e}{\tau_w}. \tag{5.2}$$

Figure 75

The distribution of the tangential stresses was given in Figure 75 as a function of the dimensionless distance from the wall y/δ, where δ is the thickness of the boundary layer. It can be seen from the diagram that in the absence of mass addition (B = 0), the maximum of the friction stress τ will occur at the wall. With an increase of the injection parameter, the friction stress at the wall decreases noticeably, and in the boundary layer it noticeably increases, attaining a maximum in a region adjacent to the wall. The same results, given in the form of the relation $\tau/\tau_w = f(\bar{u})$, are shown in Figure 76. We can see that in the region $\bar{u} \leq 0.5$ the distribution of the friction stresses is described well by Equation (5.1) (dotted straight line) written in the form

$$\tau = \tau_w (1 + B\bar{u}). \tag{5.3}$$

Disregarding the fact that Equation (5.3) poorly describes the distribution of tangential stresses in the outer region of the boundary layer, it turns out to be fully applicable in the calculation of the integral characteristics of the boundary layer (friction, displacement and momentum loss thicknesses, etc). This can be explained using the same considerations as those presented in Section 10 because of Equation (3.1).

Using Equation (5.3), the Prandtl and Karman Formulas, (2.68) and (2.69), may be used to obtain the following expressions for the velocity profiles in the turbulent core of the boundary layer:

$$u = \frac{1}{c_1} \exp \left[\varkappa \int \left(\frac{\tau}{\tau_w B_0} \right) d\bar{u} \right]. \tag{5.4}$$

$$\eta \cdot C_4 + C_6 \zeta \int \text{oxp}\left[\varkappa \zeta \int \left(\frac{\frac{\nu}{\rho_w}}{1 + B\nu} \right)^{\cdot} d\bar{u} \right] d\bar{u}. \qquad (5.5)$$

Here C_4, C_5, C_6 are the constants of integration, and η and ζ are given by Equations (3.8).
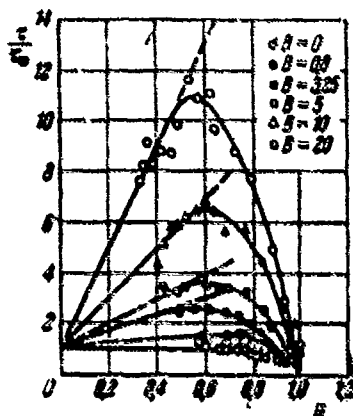
Figure 76

It is not hard to see that, when there is no injection ($B = 0$), Equations (5.4) and (5.5) reduce to Equations (3.6) and (3.7), respectively, which gives the velocity profile in the turbulent core on a nonpermeable wall.

Equations (5.4) and (5.5) lead, respectively, to the following expressions for the momentum loss thickness (2.76):

$$\delta^{**} \leftarrow \frac{\varkappa^2 \mu_w}{s_r \nu_r C_r} \int \left(\frac{s}{s_w} \right)^{\prime\prime} \frac{a(1 - a)\varkappa}{(1 + B\nu)^{\cdot}} \exp\left[\varkappa^2 \int \left(\frac{\frac{\nu}{s_w}}{1 + B\bar{u}} \right)^{\cdot} d\bar{u} \right] d\bar{u}. \qquad (5.6)$$

$$\delta^{**} = \frac{\zeta \mu_w C_r}{s_r \nu_r} \int \left(\frac{s}{r_w} \right) a(1 - a) \text{oxp} \left[\varkappa^2 \int \left(\frac{\frac{s}{s_w}}{1 + B\bar{u}} \right)^{\cdot} d\bar{u} \right] d\bar{u} \qquad (5.7)$$

In the absence of injection ($B = 0$) Equations (5.6) and (5.7) reduce to Equations (3.9) and (3.10) respectively[1].

The differences among the papers written by various workers are usually related to the determination of the constants of integration C_9, S_6, and to the methods of evaluating the integrals in Equations (5.6) and (5.7)[2]. One of the first papers containing an analysis of the turbulent boundary layer on a porous plate with addition of mass of the same physical-chemical properties as those of the gas in the oncoming flow, was written by Dorrance and Dore [5]. The velocity profile in that paper was determined on the basis of the

Footnotes (1) and (2) appear on page 171.

Prandtl formula [see (5.4)] under the assumption that the distribution of tangential stresses in the boundary layer is described by Equation (5.3). The friction coefficient was found using the usual method with the aid of the integral momentum relation (2.80), which in the case of a flow over a flat plate becomes

$$\frac{d\delta^{**}}{dx} = \frac{c_f}{2}(1 + B). \qquad (5.8)$$

The Dorrance and Dore method was extended to the case where a substance with properties different from those of the oncoming flow was added to the boundary layer, by V. P. Motulevich [6]. Later V. P. Motulevich extended this method to the case of the sublimation of the plate surface, at the time improving his computational procedures [7].

L. Ye. Kalikhman [8] investigated the turbulent boundary layer in an incompressible fluid with the addition of a substance with the same physical properties as those of the gas flowing over the surface. He obtained a solution on the basis of the semi-empirical Prandtl theory (2.68) using the boundary condition at the wall, similar to the condition in the boundary layer of a free streamline, which is equivalent to assuming that there is no laminar sublayer near the wall.

The question of the effect of the Prandtl and Lewis numbers on skin friction of a flat plate with injection through the porous wall of a substance inert relative to the gas in the fundamental flow was studied in the paper by I. P. Ginzburg, G. V. Kocheryzhenkov, and N. I. Mordvinova [9].

An analysis of the problem in question on the basis of the limiting friction and heat transfer laws can be found in the papers by S. S. Kutateladze and A. I. Leont'yev et al. [10].

The semi-empirical theory of the turbulent boundary layer on a chemically active ablating surface was developed by Denison [11] and applied to ablating graphite surfaces.

The second approach, based on power-law expressions for velocity profiles, has not been pursued to a great extent. Among the papers using the second approach, we shall mention one written by V. D. Sovershennyi [12] in which — in addition to a flow near a porous plate — he discussed flow on a permeable surface with a small longitudinal pressure gradient.

The empirical theory of friction and heat transfer on a porous plate with injection of air into air was proposed by V. P. Mugalev [13]. The method is based on the similarity, established by the author experimentally, between the flow with a longitudinal positive pressure gradient and the flow on a porous plate with injection. The similarity is seen in the velocity profiles in the boundary layer for the flows indicated above. Introducing the form parameter $f_w = (\rho_w v_w/\rho_e U_e)\, \mathrm{Re}^{**0.25}$, V. P. Mugalev brings the integral momentum relation to a form allowing its linearization, similarly as it was done in the well-known L. G. Loytsyanskiy method [14]. The rest of the computation proceeds in the same way as in the case of a boundary layer with a longitudinal pressure gradient.

The empirical theory of heat and mass transfer on a flat plate in the presence or absence of chemical reactions in the boundary layer was developed by Spalding, Auslander, and Sandarom (see their paper, already quoted in this section). Their method is to an extent similar to Spalding and Chi's method of calculating friction on a nonpermeable plate, discussed in Section 14. Just as in the latter case, in the paper in question some of the determining functions are chosen on the basis of an analysis of the semi-empirical methods of computation, and others on the basis of experimental data.

As an aid in the computation of the drag, heat transfer, and consumption of the cooling substance, tables and graphs were constructed for Mach numbers ranging from 0 to 12, and the temperature factor (T_w/T_∞) ranging from 0.05 to 20. The cases considered involved injection of air, helium, and hydrogen into the air. For

hydrogen, two groups of tables are given: one in which combustion was considered, and the other in which it was not.

It will be noted that Spalding, Auslander, and Sandarom's paper also contains a detailed analysis of many semi-empirical methods as well as an extensive bibliography.

§ 29. Experimental Investigations of the Turbulent Boundary Layer with Mass Transfer

At the present time we have at our disposal a fairly large amount of experimental data on the effect of injection of various gases on the characteristics of a turbulent boundary layer (velocity and temperature profiles, friction, heat transfer, etc.). A majority of the experimental data were obtained for flows without longitudinal pressure gradients (plate, cone)[3]. Unfortunately, great technical difficulties in conducting such experiments have in many cases resulted in significant errors (up to 100%), which is indicated by the large discrepancies in the experimental points obtained by various workers for the same conditions. The basic experimental method of determining local friction had for a long time involved measurements of the velocity and temperature profiles. More accurate direct methods of measuring local forces of friction with the aid of a "floating" element, used extensively in the investigation of flows on nonpermeable surfaces (see Section 11), are still very imperfect. In a number of papers, the accuracy with which various characteristics are measured is insufficient. These circumstances resulted in a situation in which the effect of individual parameters on friction and heat transfer still is unknown, and in certain cases, the experimental data obtained by various authors are contradictory.

In the present section, we shall mainly discuss the results of the experimental studies of the boundary layer characteristics, with

---

Footnote (3) appears on page 321.

FTD-HC-23-723-71

injection at supersonic velocities. The experimental data for subsonic flows will usually be given in summary diagrams.

V. P. Mugalev's experiments[4]. V. P. Mugalev obtained extensive data on the flow structure in a turbulent boundary layer with injection, and on the effect of the individual parameters (M_e, Re_x numbers, properties of the injected gas, etc.) on heat transfer. The experiments included measurements of the velocity, temperature, concentration, and density profiles in the boundary layer, and of heat transfer on a flat porous plate, for a wide range of flow parameters and injection intensity.

Figure 77 gives the velocity profiles for conditions involving addition of air to an air stream moving at a subsonic velocity (U_e = 51 m/sec). We can see that, as the injection increases, the velocity profiles become deformed and less solid. For a large intensity of injection ($v_w/U_e > 0.02$), the profiles undergo an inflection, and the derivative $(\partial u/\partial y)_w$ tends to zero. From this variation of the velocity profiles, V. P. Mugalev concluded that for moderate injection intensities (up to an appearance of an inflection point), the effect of injection is similar to the effect of a longitudinal positive pressure gradient, and for larger injection intensities, the velocity profile becomes similar to a jet profile.
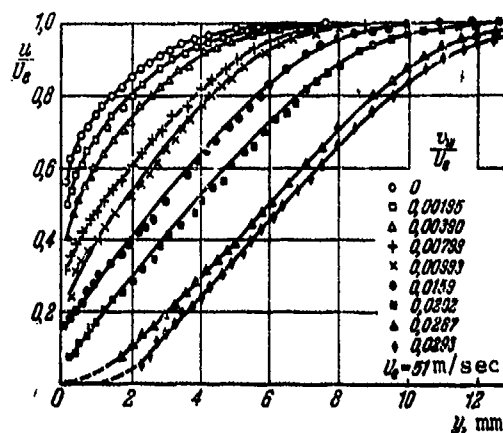
Figure 77

Footnote (4) appears on page 321.

Figure 78 shows the velocity and temperature profiles, obtained under identical conditions (M_e = 0.08) with air injection. On the axis of ordinates in this diagram we plot Y/Y_e and $Y/Y_{e\,t}$, where $Y = \int_0^y \frac{v}{v_e(\tau)}\, dy$, and Y_e and $Y_{e\,t}$ are the coordinates of the boundaries of the dynamic and thermal boundary layers. The injection parameter B** is given by

$$B^{**} = \frac{\rho_w v_w}{\rho_e U_e} \mathrm{Re}^{**0.25} \cdot \frac{T_w}{T_e}.$$

A comparison for the velocity profiles and the stagnation temperature gradients shows their approximate similarity. At the same time, for large values of the injection parameter, heat transfer is somewhat greater than momentum transfer.
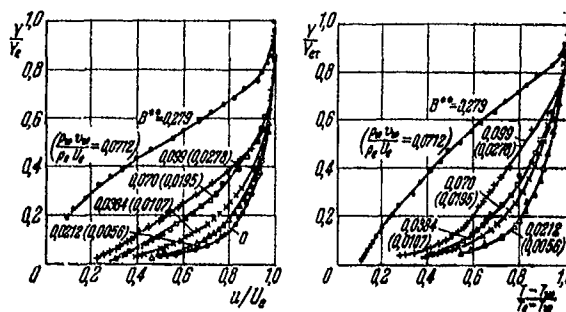
Figure 78

In Figure 79 a similar comparison was made for the velocity and relative concentration profiles in the boundary layer for injection of carbon dioxide into the air stream, also obtained under identical conditions (M_e = 2.5; T_w/T_{r0} = 1.1). We can see that the velocity and concentration profiles are approximately similar.

Thus, in this case, we may conclude that injection of gases into a boundary layer has a similar effect on the velocity, temperature, and concentration profiles. At the same time, the author notes that there does not exist any similarity between the profiles indicated in the case of injection.
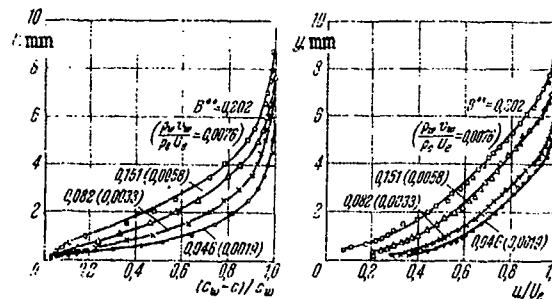
Figure 79

Measurements of heat transfer were made in the wind tunnels with injection of cold gases (helium, air, carbon dioxide, argon and krypon) into the boundary layer. The Mach and Reynolds numbers varied within the intervals $0 \leq M_e \leq 3.7$; $10^5 < Re_x \leq 10^7$. The temperature factor T_w/T_{r0} varied for 0.5 to 1. The heat transfer coefficients for transfer to porous surface were determined on the basis of the heat balance equation from the measured values of the temperatures of the injected gas at the wall, flow rate of the injected gas, and the external flow parameters.

The results of the experiments in which the effect of injection on heat transfer was measured with addition of various gases and for various Mach numbers of the external flow, are given in Figure 80 [1 - helium (M_e = 2.5); 2 - carbon dioxide (M_e = 2.5); 3 - argon (M_e = 2.5); 4 - krypton (M_e = 2.5); 5 - air ($M_e \approx 0$); 6 - air (M_e = 2.5); 7 - air (M_e = 3.7)]. According to the author's estimate, the maximum possible experimental error did not exceed 10 - 40% for $(M_1/M_2)^b B_{h0} \approx 0.5 - 5$.

On the basis of the data given in Figure 80, we conclude that the variation of the parameters M_e, Re_x, and T_w/T_{r0} in the range investigated does not have any effect on the criterion relations

$$q_w/(q_w)_{B_h=0} = f_1(B_h) \quad \text{and} \quad q_w/(q_w)_{B_h=0} = f_2(B_{h0}).$$

Figure 80

[Here $B_h = (\rho_w v_w)/\rho_e U_e c_h$;

$B_{h0} = (\rho_w v_w)/\rho_e U_e (c_h)_{B_h = 0}$;

q_w, $(q_w)_{B_h = 0}$ are the heat

fluxes to the wall in the presence
and absence of injection, and

T_w = idem].

On the basis of an analysis
of the experimental data on the
effect of injection on heat
transfer, V. P. Mugalev proposed
a simple approximate formula
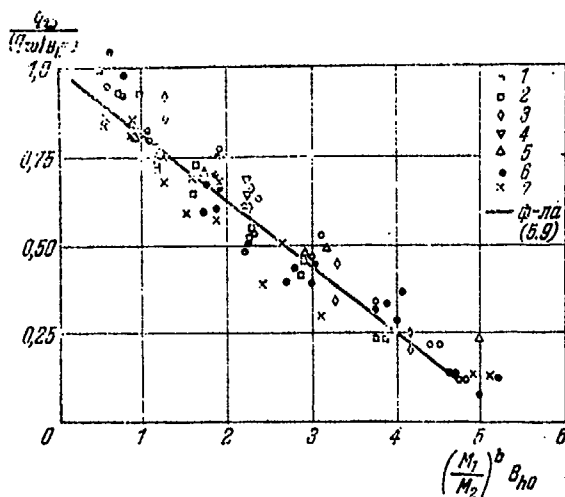
for heat fluxes

$$\frac{q_w}{(q_w)_{B_h=0}} = 1 - 0.19\left(\frac{M_1}{M_2}\right)^b B_{h0}. \qquad (5.9)$$

Here M_1 and M_2 are the molecular weights of the gas at the outer
edge of the boundary layer and of the injected gas; $b = 0.35$ for
$0.2 < (M_1/M_2) < 1$; $b = 0.7$ for $1 < (M_1/M_2) < 8$; $b = 1$ for $(M_1/M_2 = 14.5$. The approximate Formula (5.9) is applicable for $q_w/(q_w)_{B_h=0} \geqslant 0.1$.

Pappas' and Okuno's experiments [15]. These authors investigated
the dependence of the mean friction heat transfer coefficients, as
well as of the recovery coefficient and the Reynolds similitude
parameter on the injection of air, helium, and freon-12 through
a porous wall of a cone with a 12° angle at the vertex for the Mach
numbers of the air stream (on a cone) 0.7; 3.67; 4.35 and the
Reynolds numbers on the order $9.5 \cdot 10^6$.

The results of the measurements made by Pappas and Okuno are
given in Figures 81 - 89. The following notation is used in these
figures: c_F is the mean friction coefficient; c_H is the mean heat
transfer coefficient; $B_{F0} = 2\rho_w v_w/\rho_e U_e(c_F)_{B=0}$ is the injection parameter for

a supersonic flow; $B_{F_0} = 2\rho_w v_w / \rho_\infty U_\infty (c_F)_{B=0}$ is the injection parameter for a subsonic flow; U_e, ρ_e is the velocity and density at the edge of a boundary layer; M_e is the Mach number at the outer edge of the boundary layer (in the case of a subsonic flow $M_e = M_\infty$); $r = (T_r - T_w)/T_e^* - T_w)$ is the recovery factor; T_r is the recovery temperature; T_e^* is the stagnation temperature in the outer flow; $Re_x = U_e \rho_e x /_e \mu$ is a Reynolds number for a supersonic flow, $Re_x = U_\infty \rho_\infty x / \mu_\infty$ is the Reynolds number for a subsonic flow; x is the distance measured along the cone. The subscript "zero" refers to the parameter values in the case of no injection.

Figures 81 and 82 are plots of $c_F/(c_F)_{B=0}$ on a thermally insulated surface versus the Mach number for various values of the injection parameter B_{F0}.

In addition, Figure 82 also includes the experimental point obtained by Mickley and Davis [16], obtained by measuring local friction on the basis of the velocity profiles on a plate in incompressible fluid. Inspection of Figures 81 and 82 enables us to conclude that the Mach number at the outer edge of the boundary layer has a substantial effect on the ratio $c_F/(c_F)_{B=0}$. This effect increases with an increase of the injection parameter B_{F0}.

Figures 83 and 84 show the results of the measurements of the heat transfer coefficients for various injection intensities of helium, air, and freon-12, and for $M_e = 3.67$ and 4.35. The same data for helium and air, supplemented by data for $M_e = 0.7$, are shown in different coordinates in Figures 85 and 86. Figures 85 and 86 make it clear that for M_e ranging from 0.7 to 3.67, the effect of the Mach number on the ratio $c_H/(c_H)_{B=0}$ is small, which agrees with the data obtained by V. P. Mugalev considered above. For M_e in the range from 3.67 to 4.35, the character of this dependence changes sharply, which is in disagreement with other results available, as well as with the results obtained by the same authors in the interval $0.7 \leq M_e \leq 3.67$. Figure 87 is a plot of the
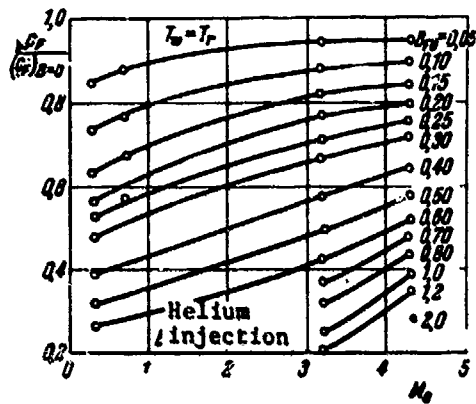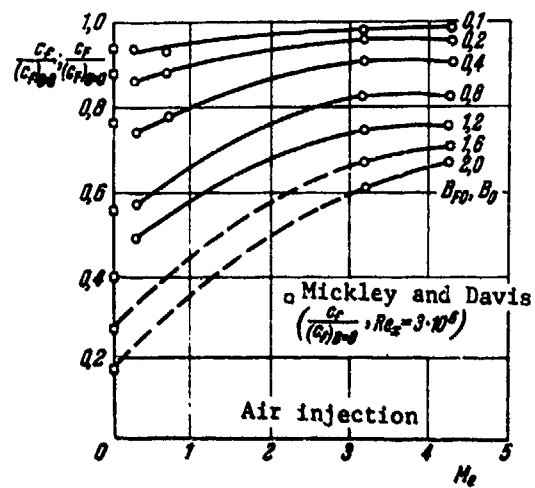
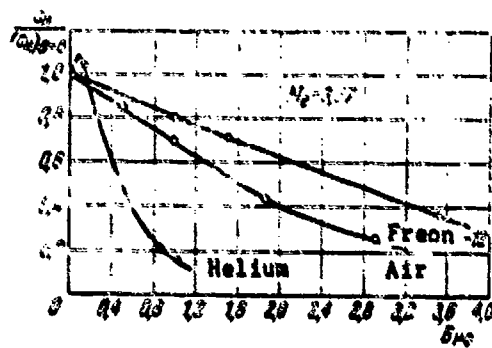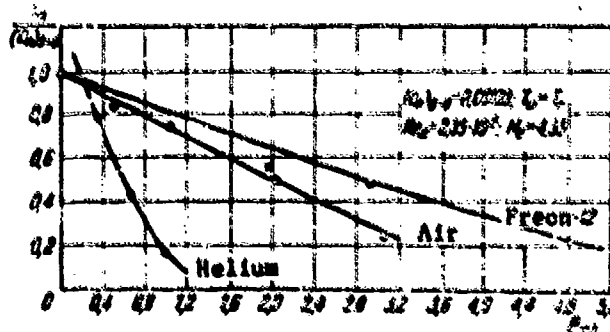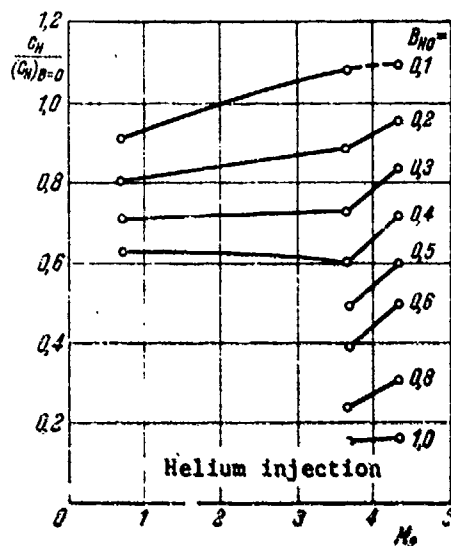Figure 81

Figure 82

Figure 83
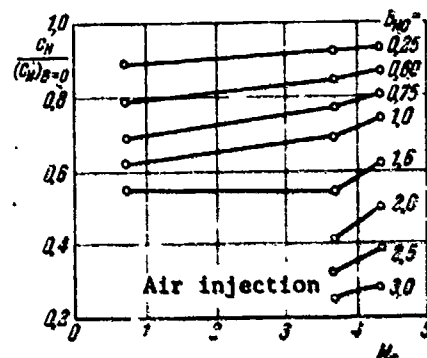

Figure 84

Figure 85

Figure 86

recovery factor r versus the injection parameter for the Mach numbers 0.7 and 4.35. As can be seen from the diagram, for the Mach number 0.7, the recovery factor for air and freon injection decreases with an increase in the injection intensity. For helium injection, it first increases up to 1.25, and then falls off. For M_e = 4.35, the recovery factor first decreases for all injected gases, and then becomes larger. The fact that the values of the recovery factor exceed unity is particularly striking.

Figures 88 and 89 represent plots of the Reynolds similitude parameter $2c_H/c_p$ versus the injection intensity of air and helium for various Mach numbers. We note the character of the variation of the Reynolds similitude parameter for helium injection (Figure 89) at supersonic velocities. First the parameter increases, attaining a maximum equal to 1.35, and then decreases noticeably.

An analysis of the experimental data obtain by Pappas and Okuno shows that an injection of a substance into the boundary layer leads to a significant change in the characteristics of the boundary layer. Moreover, the character of the variation of such quantities as the recovery factor and the Reynolds similitude parameter differs significantly from the behavior of these quantities when tere is no injection.
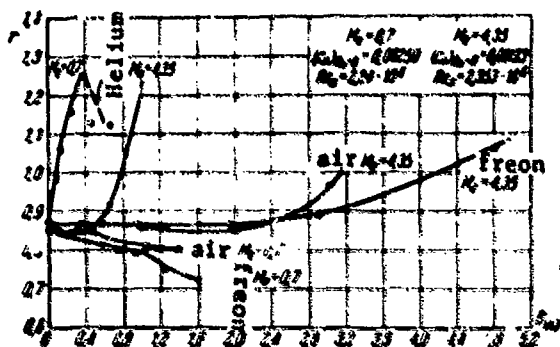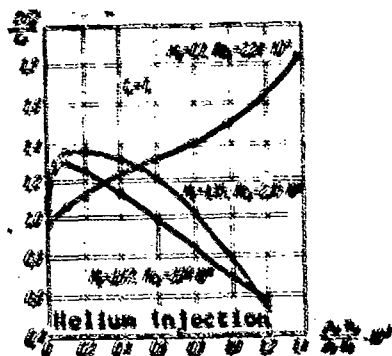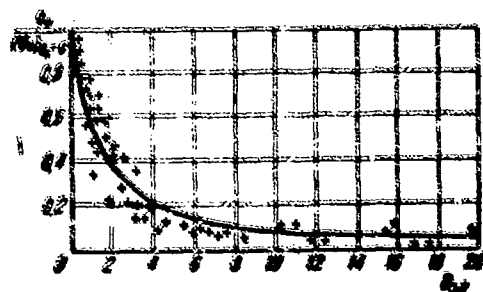
Figure 87
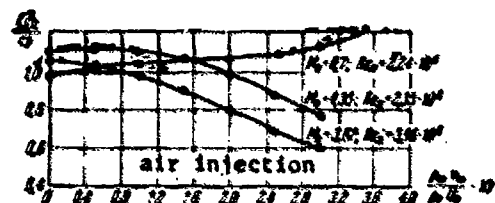

Figure 89

Figure 90

Figure 88

Fogaroli and Saydah's experiments [17]. The paper by Fogaroli and Saydah contains the results of a hypersonic wind tunnel investigation of the effect of air injection on friction and heat transfer in a turbulent boundary layer on a porous cone at Mach numbers equal to 5.3 and 8.1 on the cone, and for a variation of the injection parameter $B_w = \frac{\rho_w v_w}{\rho_e v_e (c_f)_{x,o}}$ from 0 to 20. The half-angle at the vertex of the cone was 7.5°.

Figure 90 is a plot of the ratio of heat flux with injection to heat flux without injection versus the injection parameter for various values of the Mach number at the edge of the boundary layer. Figure 90 also contains the data of other workers (points in the diagram have no names). The scatter of the experimental points is fairly large, and thus it is difficult to estimate the influence of the Mach number on heat flux.

To a first approximation, we can apparently assume that the Mach number does not have an effect on heat flux. The curve given in the figure was calculated using the following approximate formula:

$$\frac{q_w}{(q_w)_{B_{h_0}=0}} = \left[\left(\frac{1}{2}B_{h_0}\right)^2 + 1\right]^{\frac{1}{2}} - \frac{1}{2}B_{h_0}. \tag{5.10}$$

Experimental data obtained by other authors. Figure 91, adapted from Nash's paper[5], is a summary plot of the experimental data obtained by various authors who measured skin friction with injection (v_* is the dynamic velocity). The same figure includes a curve calculated using the formula

$$\frac{\tau_w}{(\tau_w)_{l_w=0}} = \exp\left[-0.9\left(\frac{v_w \rho_w}{v_* \rho_w}\right)\right]\sqrt{\frac{\tau_w}{\tau_w}\frac{2}{(\tau_w)_{l_w=0}}} \cdot \left[1 - \sqrt{\frac{(\tau_w)_w}{\tau_w}} \cdot \right]. \tag{5.11}$$

Equation (5.11) was obtained by Nash as a generalization of the Turcotte formula [18] introduced for an incompressible fluid.

Examination of the above experimental results of injection of various substances into a turbulent boundary layer enables us to draw the following conclusions.

Injection of a substance into a boundary layer lowers the skin friction and heat transfer on the surface. An injection of light gases has the greatest effect.

The velocity profiles in the boundary layer undergo distortion upon injection, becoming less solid as the intensity of injection increases. For intense injection, an inflection point appears on the velocity profile, and the profiles themselves resemble jet profiles.

Injection of various gases into the boundary layer may have a great effect on the recovery factor and the Reynolds similitude parameter.
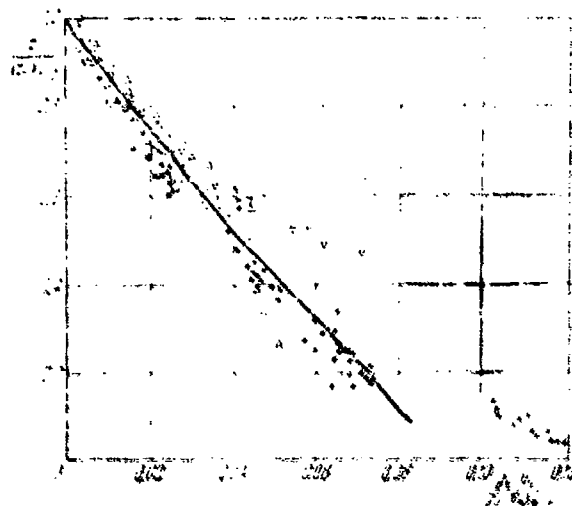

Footnote (5) appears on page 322.

Figure 91

The Mach number at the outer edge of the boundary layer has a noticeable effect on friction $[c_p/(c_p)_{B=0}]$. The effect is greater, the greater the intensity.

A majority of the experimental data indicates that the Mach number has no effect (or a weak one) on heat transfer $[c_H/(c_H)_{B=0} = c_f/(c_f)_{B=0}]$.

In conclusion, we note that all the data considered above were obtained in experiments involving nonreacting gas mixtures.

The number of studies of the turbulent boundary layer with an injection of chemically active gases is at the present time very limited [19].

§ 10. Boundary Conditions at the Wall and at the Outer Edge of the Boundary Layer in the Presence of Mass Transfer Between the Surface and the Gas. Heat Flux at the Wall

The formal boundary conditions for the longitudinal velocity component, concentration, and total enthalpy in the presence of mass

transfer between the surface and the gas can be written in the usual form

$$u = 0, \quad c_i = c_{iw}, \quad H = h_w \quad \text{for} \quad y = 0; \atop u = U_e, \quad c_i = c_{ie}, \quad H = H_e \quad \text{for} \quad y \to \infty. \Bigg\} \quad (5.12)$$

The boundary condition for the normal velocity component at a permeable wall has the form

$$v = v_w \quad \text{at} \quad y = 0 \qquad (5.13)$$

in contrast with the condition $v = 0$ at $y = 0$ at a nonpermeable wall. The surface of a plate is usually assumed to be semipermeable, i.e., permeable for the injected substance and nonpermeable for the gas flowing around the surface.

The expressions for the enthalpy at the wall and at the outer edge of the boundary layer have the form

$$h_w = \sum_i c_{iw} h_{iw}, \qquad h_{iw} = \int_0^{T_w} c_{pi} dT + h_i^0. \qquad (5.14)$$

$$H_e = h_e + \frac{u^2}{2}, \qquad h_e = \sum_i c_{ie} h_{ie}, \qquad h_{ie} = \int_0^{T_e} c_{pi} dT + h_i^0. \qquad (5.15)$$

The species concentrations at the outer edge of the boundary layer, c_{ie}, are usually assumed to be known from the solution for the external flow. In a majority of cases, it is assumed that the external flow is in a state of thermochemical equilibrium, i.e., $c_{ie} = c_{ie}^{(0)}$. Thus, the boundary conditions at the outer edge of the boundary layer are usually completely defined. The conditions at the wall for the concentrations c_{iw} and velocities v_w are interdependent, as will be seen later. The value of v_w may, in principle, be specified if we deal with injection through a porous surface. The values of concentration at the wall, c_{iw}, in this case must be determined from auxiliary conditions in the course of solving the problem.

In the case of a flow over a sublimating surface, the normal velocity component v_w cannot be arbitrarily specified and must, just as the concentration at the surface c_{iw}, be determined from auxiliary conditions in the course of solving the problem (in the case of equilibrium sublimation, one of these auxiliary conditions is given by the Clausius-Clapeyron equation, which relates the concentration of the sublimate to the temperature and pressure at the wall).

In order to derive the auxiliary relations connecting the flux of a substance injected into the boundary layer through a porous surface (or forming due to sublimation) to the concentrations of the species at the wall, we shall establish the condition of conservation of species i at the gas-solid interface (Figure 92). The
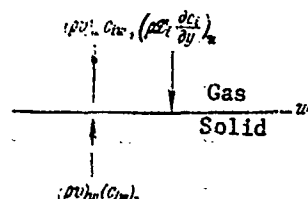
figure shows that species i travels from the gas to the wall by diffusion. The mass flux of species i migrating in this way is obviously equal to $\left(\rho \mathscr{D}_i \frac{\partial c_i}{\partial y}\right)_w$ [$\mathscr{D}_i$ is the effective diffusion coefficient (1.58); here we consider mass diffusion]. At the same time, species i travels from the surface into the boundary layer with the flow of the substance, $(\rho v)_w$, injected through the wall. The amount of species i, carried in this fashion, is obviously equal to $(\rho v)_w c_{iw}$. In addition, if species i becomes a component of the mixture, injected into the boundary layer through the porous surface (or sublimating) and the concentration of the species inside the surface is (c_{iw}), then the amount of species i entering the boundary layer through injection will be equal to $(\rho v)_w (c_{iw})$. If a chemical reaction occurs at the wall, as a result of which an amount g_{iw} of species i is added (or subtracted) (g_{iw} is the mass rate of formation of species i per unit area), then the condition for the conservation of species i at the wall, taking into account all the transfer processes indicated above, can obviously be written in the form

$$g_{iw} = -\rho_w \mathscr{D}_i \left(\frac{\partial c_i}{\partial y}\right)_w + \rho_w v_w [c_{iw} - (c_{iw})].$$ (5.16)

Figure 92

Substituting the expression g_{iw} (4.35) into the left-hand side of Equation (5.16), we get

$$\rho_u \mathscr{D}_{iw}\left(\frac{\partial c_i}{\partial y}\right)_w - \rho_u v_w [c_{iw} - (c_{iw})_-] =$$
$$= k_{wi}[(\rho c_i)_w^{n_i} - K_w(\rho c_j)_w^{n_j}]. \tag{5.17}$$

For species that are not contained in the mixture injected into the boundary layer, the value of (c_{iw}) may be set equal to zero. When only one species is injected, $(c_{iw})_- = 1$. It is obvious that for an injected mixture inside the wall, we always have $\sum_i (c_{iw})_- = 1$.

If there are no chemical reactions on the surface $(g_{iw} = 0)$, condition (5.16) becomes

$$\rho_w v_w [c_{iw} - (c_{iw})_-] - \rho_w \mathscr{T}_{iw}\left(\frac{\partial c_i}{\partial y}\right)_w = 0. \tag{5.18}$$

When one species is injected through the wall $[(c_{iw})_- = 1]$, Equation (5.18) can be written in the form

$$\rho_w v_w = \rho_w v_w c_{iw} - \rho_w \mathscr{D}_{iw}\left(\frac{\partial c_i}{\partial y}\right)_w. \tag{5.19}$$

Now we proceed to consider the heat balance at the gas-solid interface (Figure 93). The heat is supplied to the surface of the body through heat conductivity and mass diffusion

$$q_w = \lambda_w\left(\frac{\partial T}{\partial y}\right)_w + \sum_i \rho_w \mathscr{D}_{iw} h_{iw}\left(\frac{\partial c_i}{\partial y}\right)_w$$
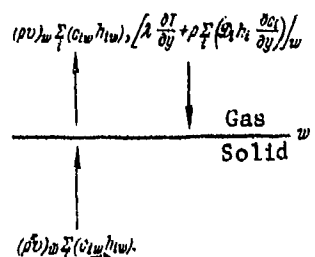

Figure 93

The heat is carried from the surface to the boundary layer by the flux of the substance injected into the boundary layer: $(\rho_u v_u)\sum_i c_{iu} h_{i..}$; the following heat flux flows in the direction from the solid body toward the interface: $\rho_w v_w \sum_i (c_{iv} h_{iv})_-$ (temperature gradient in the body is assumed to be zero). Thus, the heat flux contributing to the heating

295

of the wall (inside the wall), turns out to equal

$$q_{s} = \lambda_{w} \left(\frac{\partial T}{\partial y}\right)_{w} + \sum_{i} \rho_{w} \mathcal{D}_{iw} h_{iw} \left(\frac{\partial c_{i}}{\partial y}\right)_{w} - \\ - \rho_{w} v_{w} \sum_{i} [c_{iw} h_{iw} - (c_{iw} h_{iw})_{-}]. \quad (5.20)$$

Taking into account the expression for the heat flux from the gas to the wall, (4.147), we bring Equation (5.20) to the form

$$q_{s} = \frac{\mu_{w}}{Pr} \left[\left(\frac{\partial h}{\partial y}\right)_{w} + \sum_{i} (Le_{i} - 1) h_{iw} \left(\frac{\partial c_{i}}{\partial y}\right)_{w}\right] - \\ - \rho_{w} v_{w} \sum_{i} [c_{iw} h_{iw} - (c_{iw} h_{iw})_{-}]. \quad (5.21)$$

For sublimating species we can write

$$(h_{iw})_{-} = h_{iw} - h_{iL}, \quad (5.22)$$

where h_{iL} is the heat of sublimation of species i. Substituting Equation (5.22) into the expression (5.20), we get

$$q_{s} = \lambda_{w} \left(\frac{\partial T}{\partial y}\right)_{w} + \sum_{i} \rho_{w} \mathcal{D}_{iw} h_{iw} \left(\frac{\partial c_{i}}{\partial y}\right)_{w} - \\ - \rho_{w} v_{w} \sum_{i} h_{iw} [c_{iw} - (c_{iw})_{-}] - \rho_{w} v_{w} h_{L}, \quad (5.23)$$

where

$$h_{L} = \sum_{i} (c_{iw})_{-} h_{iL} \quad (5.24)$$

is the total heat of sublimation.

By expressing the diffusive flow of species i $\rho_{w} \mathcal{D}_{iw} \left(\frac{\partial c_{i}}{\partial y}\right)_{w}$ with the aid of Equation (5.18), we obtain from Equation (5.23) the following expression for heat flux which is useful in practical calculations:

$$q_{s} = \lambda_{w} \left(\frac{\partial T}{\partial y}\right)_{w} - \sum_{i} g_{iw} h_{iw} - (\rho_{w} v_{w}) h_{L}. \quad (5.25)$$

In conclusion, we note that the analysis done here for a sublimating surface can be easily extended to the case of vaporization with a gas-liquid interface. One must only replace the heat of sublimation

h_L with the heat of vaporization h_v.

The conditions (5.16) - (5.19) obtained in the present section relate the flux of the substance injected into the boundary layer (or produced due to sublimation) to the concentrations of the species at the wall. Thus, all the boundary conditions at the wall are now fully determined.

§ 31. Velocity Profile and Friction on a Flat Plate with Mass Addition to the Boundary Layer

The expression for the velocity profile in the turbulent core, based on the Karman formula (2.69) and on the distribution of the stresses of friction in the boundary layer (5.3), in general has the form (5.5). In order to determine the constant of integration C_6 in Equation (5.5), we make the same assumption as in Section 12: we assume that the derivative $dn/d\phi$ at the boundary of the laminar sublayer on the side of the turbulent core has the same value as in an incompressible fluid in the absence of injection, i.e., $(dn/d\phi)_{n_\zeta+0} = 1/f = \kappa\alpha$. In other words, it is assumed that $(dn/d\phi)_{n_\zeta+0}$ does not depend on compressibility, heat transfer or mass injection. The turbulence constants κ and α will be assumed to be equal to their values in an incompressible fluid ($\kappa = 0.4$, $\alpha = 12$). This assumption about the value of the derivative at the boundary of the sublayer and the turbulent core, as indicated by the slope of the velocity profiles in the case of injection (Figures 77 and 78), will not result in any noticeable errors in the computation.

Using the above assumption, one obtains the following expression for the velocity profile in the turbulent core:

$$ \eta = \eta_\circ + \frac{1}{f} \int_{n_\zeta}^{n} \exp\left[\kappa \int_{n_\zeta}^{n} \left(\frac{\frac{\tau}{\tau_w}}{1 + \beta\bar{u}} \right)^{1/2} d\bar{u} \right] d\bar{u}. \tag{5.26} $$

The slope of the velocity profile in the turbulent core is obviously given by

$$\frac{d\eta}{d\varphi} = \frac{1}{f} \exp\left[\varkappa \zeta \int_{\bar{u}_n}^{\bar{u}} \left(\frac{\frac{\rho}{\rho_w}}{1 + B\bar{u}} \right)^{\frac{1}{2}} d\bar{u} \right].$$

(5.27)

Here $\bar{u}_l$ is the dimensionless velocity at the boundary of the laminar sublayer (the question of the determination of $\bar{u}_l$ will be considered below).

In the case of a flow of constant density over a plate and injection into the boundary layer of a substance of the same composition as that of an oncoming flow ($\rho = \text{const} = \rho_e$), the expression for the velocity profile (5.26) after evaluation of the integrals will become

$$\eta = \eta_a - \alpha \sqrt{1 + B_* \varphi_a} +$$
$$+ \alpha \sqrt{1 + B_* \varphi} \exp\left[\frac{2\varkappa}{B_*} (\sqrt{1 + B_* \varphi} - \sqrt{1 + B_* \varphi_a}) \right].$$

(5.28)

Here

$$B_* = \frac{B}{\zeta} = \frac{r_w}{r_*}, \qquad \varphi_a = \frac{\varkappa_a}{v_*} = \bar{u}_a \zeta.$$

(5.29)

In order to determine the velocity profile in the laminar sublayer, we use Equation (3.106), first simplifying it by assuming that viscosity is constant in the sublayer ($\upsilon = \text{const} = \upsilon_w$). Next, substituting the relation (5.3) in Equation (3.106) and performing the integration, we obtain the following expression for the velocity profile in the laminar sublayer:

$$\varphi = \frac{1}{B_*} (\exp(B_* \eta) - 1).$$

(5.30)

For small injection intensities, expanding the exponent in a series and retaining only the first two terms of the series we find

$$\varphi = \eta \left(1 + \frac{1}{2} B_* \eta \right).$$

(5.31)

When there is no injection, the expressions (5.30) and (5.31) reduce to the expressions for the linear velocity profile, (3.30) which were obtained earlier.
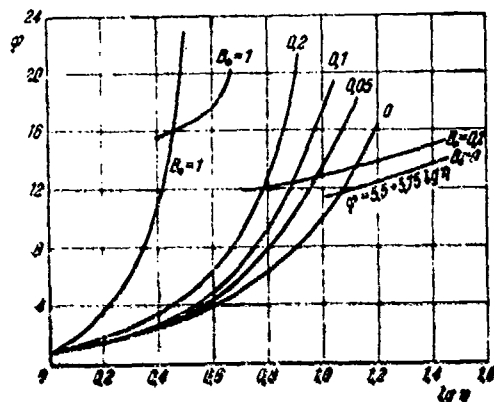
298

Figure 94

The velocity profiles in the laminar sublayer, calculated using Formula (5.30), are given in Figure 94. The diagram also includes the logarithmic velocity profile for an incompressible fluid for no injection. At first sight, the character of the variation of velocity in the laminar sublayer in Figure 94 seems to be paradoxical since the velocity profile here becomes more solid with an increase in the injection parameter, which contradicts the experimental data given above (Figures 77 and 78). However, this paradox is only apparent since Figures 77 and 78 deal with the actual velocities u/U_e, and Figure 94 with the velocity profiles expressed in terms of the universal coordinates $\phi = u/v_*$.

The problem of the thickness of the laminar sublayer and the velocity at its boundary in the turbulent core in the presence of injection is the least understood today. The scarce experimental data available to us enable us to conclude that the relative thickness of the laminar sublayer decreases with an increase in the injection intensity. Unfortunately, there are no numerical data available that would be based on reliable experimental results.

The expression for the velocity profile in the laminar sublayer (5.30), based on the law (5.3) for the distribution of tangential stresses, which is in good agreement in the laminar sublayer with the existing experimental data (Figure 76), can apparently be considered sufficiently reliable. Thus, if the thickness of the laminar sublayer η_l is calculated on the basis of certain considerations, then from (5.30) we can find ϕ_l and consequently,

$$\dot{u}_* = \phi_*/\zeta.$$

Van Driest [20] in determining the thickness of the laminar sublayer, used the condition similar to the condition (3.102), with the exception that the friction stress at the boundary of the sublayer, and not at the wall as in Equation (3.102), was the determining factor. In analogy with condition (3.102), this can be stated in the form

$$\delta_a = \alpha \frac{v_w}{\sqrt{\frac{\tau}{\rho_w}}} .$$ (5.32)

The simultaneous use of Equations (5.32), (5.3), and (5.30) leads to the following expression for the thickness of the laminar sublayer:

$$\eta_a \exp\left(\frac{1}{2} B_* \eta_a\right) = \alpha.$$ (5.33)

If there is no injection ($B_* = 0$), Equation (5.33) reduces to the condition $\eta_l = \alpha$, which was assumed below (Chapter III and IV).

The results of a computation of η_l and ϕ_l using Equations (5.33) and (5.30) are given in Figure 95.
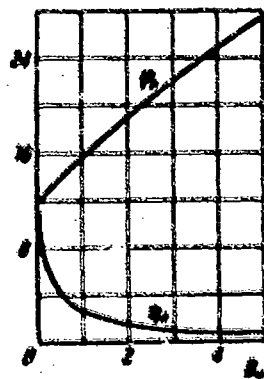

In addition to the velocity profiles in the laminar sublayer calculated using Formula (5.30), Figure 94 contains the velocity profiles in the turbulent core calculated using Formula (5.28) for three values of the injection parameter $B_* = 0$; 0.2 and 1. The boundary of the laminar sublayer was here determined from Equation (5.33).

Figure 95

Now let us proceed to consider the problem of calculating the friction on a flat plate with injection. It is not hard to see that with the assumption ($C_6 = 1/f$), made in the present chapter, the expression for the momentum loss thickness, (5.7), becomes

$$\delta^{**} = \frac{\zeta^2\mu_w}{\rho_e U_e l}\int_0^1\frac{\rho}{\rho_w}\bar{u}(1-\bar{u})\exp\left[\varkappa\zeta\int_0^{\bar{u}}\left(\frac{\frac{\rho}{\rho_w}}{1+B\bar{u}}\right)^{1/2}d\bar{u}\right]d\bar{u}. \tag{5.34}$$

Here, as earlier in Section 12 of Chapter III, in calculating δ^{**}, we assume approximately that the derivative η in the entire boundary layer is given by Equation (5.27), which was obtained for the turbulent core. Here we skip, as it were, over the laminar sublayer. The lower boundary of the turbulent core is accordingly shifted to the wall ($\bar{u}_l \to 0$). Such an assumption, as was shown in Chapter III, is applicable to a flow near a nonpermeable surface, and it is even more applicable with injection, since injection lowers the relative thickness of the laminar sublayer. The integral on the right-hand side of Equation (5.34) can be evaluated using the asymptotic expansion (3.39). After some calculations we find the first approximation

$$\delta^{**} = \frac{\mu_w(1+B)}{\jmath\varkappa^2\rho_e U_e}\exp\left[\varkappa\zeta\int_0^1\left(\frac{\frac{\rho}{\rho_w}}{1+B\bar{u}}\right)^{1/2}d\bar{u}\right]. \tag{5.35}$$

Furthermore, substituting the expression (5.35) in the integral momentum relation (5.8), and following the procedure indicated in Section 12, we obtain the following system of equations which enables us to determine the local friction coefficient on a flat plate:

$$\left.\begin{array}{ll}\dfrac{c_f}{c_{f0}} = \left(\dfrac{FK}{2N}\right)^2, & K = \displaystyle\int_0^1\left(\dfrac{\frac{\rho}{\rho_e}}{1+B\bar{u}}\right)^{1/2}d\bar{u}, \\[3mm] F = 0.242c_{f0}^{1/2}, & G = \lg\left(\dfrac{\mu_e}{\mu_w}\right), \\[3mm] N + \lg N = \lg\dfrac{FK}{2} + \dfrac{1}{2}(F+G). \end{array}\right\} \tag{5.36}$$

Here c_{f0} is the friction coefficient on a plate in an incompressible fluid with no injection, given either by the Karman Formula (3.59) or by Formula (3.80). The viscosity of a gas mixture at the wall can be calculated using the relations given in Chapter I. Chapter I also contains a description of techniques that can be used to calculate the viscosity of gas mixtures. The function N is easily computed

using a table of decimal logarithms and the last of Equation (5.36), in which the right-hand side is known. In order to determine the function K (see the second of Equation (5.36), it is necessary to establish a relationship between the intensity of the gas (gas mixture) in the boundary layer and its velocity. The form of this relation will be determined by the flow conditions in the boundary layer (presence or absence of chemical reactions) and the assumptions made in establishing the relation between the velocity, concentrations, and temperature (for example, assumptions about the magnitude of Prandtl and Schmidt numbers).

Letting the Reynolds numbers in the first of Equation (5.36) go to infinity ($Re_x \rightarrow \infty$), we obtain [similarly, as was the case in the analysis of the flow around a nonpermeable plate (Section 12)], the following limiting formula for the ratio c_f/c_{f0}:

$$\frac{c_f}{c_{f0}} = K^2.$$

(5.37)

Equation (5.37) makes it possible to determine the limiting value of the flow rate coefficient $c_m = \rho_w v_w/\rho_e U_e$, at which the friction at the wall becomes zero. Recalling that by definition $B = 2c_m/c_f$, we can write Equation (5.37) with the aid of the second of Equation (5.36) in the form

$$1 = \left[\int_0^1 \sqrt{\frac{\frac{\rho}{\rho_e}}{\frac{c_f}{c_{f0}} + \frac{2c_m}{c_{f0}}\bar{u}}}\, d\bar{u} \right]^2.$$

(5.38)

Setting on the right-hand side of Equation (5.38) $c_f/c_{f0} = 0$, we obtain an expression for the limiting value of the flow rate coefficient

$$(c_m)_{lim} = \frac{c_{f0}}{2} \left[\int_0^1 \sqrt{\frac{\frac{\rho}{\rho_e}}{\bar{u}}}\, d\bar{u} \right]^2.$$

(5.39)

For injection into the boundary layer of a gas of the same density as that of the gas in the oncoming flow ($\rho = const = \rho_e$), Formula (5.39) yields $(c_m)_{lim}$.

Now we shall consider certain particular cases of the flow near a flat plate with injection of mass into the boundary layer.

§ 32.   Boundary Layer on a Flat Plate with Injection and the Prandtl and Schmidt Numbers Equal to Unity [12]

Let us consider a flow of a gas of homogeneous composition over a flat plate. The gas injected through a porous surface into the boundary layer will also be assumed homogeneous, but its physical-chemical properties will be assumed different from the gas in the main flow. In addition, we shall assume that the substance injected is inert relative to the gas in the main flow, i.e., there are no chemical reactions, and the mixture in the boundary layer may be considered binary. We shall also assume that the specific heat capacities of both species are constant, i.e., they do not depend on the temperature. The Prandtl and Schmidt numbers and their turbulent analogs are assumed to be equal to unity.

With those assumptions the equations of the boundary (4.85) – (4.87) become

$$
\begin{aligned}
\rho u \frac{\partial u}{\partial x} + \rho v \frac{\partial u}{\partial y} &= \frac{\partial}{\partial y}\left[(\mu + \varepsilon)\frac{\partial u}{\partial y}\right], \\
\rho u \frac{\partial H}{\partial x} + \rho v \frac{\partial H}{\partial y} &= \frac{\partial}{\partial y}\left[(\mu + \varepsilon)\frac{\partial H}{\partial y}\right], \\
\rho u \frac{\partial c_2}{\partial x} + \rho v \frac{\partial c_2}{\partial y} &= \frac{\partial}{\partial y}\left[(\mu + \varepsilon)\frac{\partial c_2}{\partial y}\right].
\end{aligned}
\tag{5.40}
$$

The boundary conditions for the system (5.40) will be written in the form

$$
\begin{aligned}
u &= 0, & v &= v_w, & H &= H_w, & c_2 = c_{2w} \ \text{ for } y = 0; \\
u &= U_w, & H &= H_w, & c_2 &= 0 & \text{ for } y \to \infty.
\end{aligned}
\tag{5.41}
$$

The subscript 2 will refer here and below to the parameters of the injected substance, and the subscript 1 to the parameters of the oncoming flow.

Since the mixture in the boundary layer is binary, the convenience of conserving species 1 is no longer present ($c_1 = 1 - c_2$). The condition for the concentration c_2 at the outer boundary indicates that there is no injected substance in the external flow.

The equation of state (1.86) for a mixture of two gases becomes

$$p = \rho \frac{R}{M} T,$$

(5.42)

where

$$M = \frac{M_1 M_2}{M_1 c_2 + M_2 (1 - c_2)}$$

(5.43)

is the molecular weight of the binary mixture.

The system (5.40) and the boundary conditions (5.41) imply similitude of velocity, total enthalpy, and concentration fields

$$\frac{u}{U_e} = \frac{H - H_w}{H_e - H_w} = \frac{c_{2w} - c_2}{c_{2w}}.$$

(5.44)

From Equation (5.44) we can derive the obvious relations

$$H = H_w + (H_e - H_w)\, \bar{u},$$

(5.45)

$$c_2 = c_{2w} (1 - \bar{u})$$

(5.46)

According to the definition of total enthalpy, we have

$$H = c_p T + \frac{u^2}{2};$$
$$c_p = c_2 c_{p2} + (1 - c_2) c_{p1} = c_{p1} + (c_{p2} - c_{p1}) c_2.$$

(5.47)

Since

$$H_w = c_{pw} T_w = [c_{2w} c_{p2} + (1 - c_{2w}) c_{p1}] T_w$$

(5.48)

$$H_e = c_{pe} T_e + \frac{U_e^2}{2} = c_{p1} T_e + \frac{U_e^2}{2}.$$

(5.49)

from Formula (5.45), in view of Equations (5.47) – (5.49), we obtain the following equality giving the relation between the temperature and velocity

$$\frac{T}{T_w} = [1 - \omega\bar{u} - \beta\bar{u}^2 - \theta(1 - \bar{u})][1 - \theta(1 - \bar{u})]^{-1}. \qquad (5.50)$$

Here

$$\omega = 1 - \left(1 + \frac{\gamma-1}{2}M_e^2\right)\frac{T_e}{T_w}; \qquad M_e^2 = \frac{U_e^2}{(\gamma-1)c_{p1}T_e};$$

$$\beta = \frac{\gamma-1}{2}M_e^2\frac{T_e}{T_w}; \qquad \theta = c_{2w}\left(1 - \frac{c_{p2}}{c_{p1}}\right). \qquad (5.51)$$

If there is no mass injection into the boundary layer ($c_{2w} = 0$) or if there is injection of a gas with the same specific heat capacity as that of the oncoming flow ($c_{p2} = c_{p1}$), Equation (5.50) reduces to the Crocco integral (3.47).

Furthermore, using the equation of state (5.42), Equations (5.43) and (5.50), we obtain an expression for the density in the boundary layer

$$\frac{\rho}{\rho_w} = \frac{[1 - \delta][1 - \theta(1 - \bar{u})]}{[1 - \delta(1 - \bar{u})][1 - \omega\bar{u} - \beta\bar{u}^2 - \theta(1 - \bar{u})]}, \qquad (5.52)$$

where

$$\delta = c_{2w}\left(1 - \frac{M_1}{M_2}\right). \qquad (5.53)$$

Expression (5.52) implies that, in addition to the Mach number at the outer edge of the boundary layer, M_e, and the temperature factor T_w/T_e, the third important parameter which determines the distribution of the density in the boundary layer is the concentration of the injected substance at the wall, c_{2w}.

In order to obtain a solution in a closed form, one must find a relation between the injection parameter b, defined by Equation (5.2), and the concentration c_{2w}. This relation can be obtained from Equation (5.19), which expresses the conservation condition for the

injected substance at the wall. Taking into account the assumption
that the Schmidt number $(Sc = \mu_w/\rho_w \mathcal{D}_{uw})$ is equal to unity, we put (5.19)
in the form

$$\rho_w v_w = \rho_w v_w c_{2w} - \tau_w \left(\frac{\mathstrut dc_2}{du}\right)_w.$$ (5.54)

Using Equation (5.45), we find from the expression (5.54) the
desired relation between the injection parameter B and the concen-
tration of the injected substance at the wall

$$c_{2w} = \frac{B}{1+B}.$$ (5.55)

$$B = \frac{c_{2w}}{1 - c_{2w}}.$$ (5.56)

Equation (5.55) implies that the concentration of the injected
substance at the wall for a finite value of the parameter B is always
less than unity, and in the limit assumes the following values:
$c_{2w} \to 0$ for $B \to 0$, $c_{2w} \to 1$ for $B \to \infty$.

Making use of Equation (5.55), we replace c_{2w} in Formula (5.52)
by B. Then after simple algebra we obtain

$$\frac{\rho}{\rho_e} = (1 - \omega - \beta)\left\{1 + B\left[1 - \left(1 - \frac{M_2}{M_1}\right)(1 - a)\right]\right\} \times$$
$$\times \left\{1 + B\left[1 - \left(1 - \frac{M_2}{M_1}\right)(1 - a)\right]\right\}^{-1} \times$$ (5.57)
$$\times \left\{1 - \omega a - \beta a^2 - \frac{B}{1+B}\left(1 - \frac{M_2}{M_1}\right)(1 - a)\right\}^{-1}.$$

If the gas has a low velocity ($\beta = 0$) and if there is no heat
transfer between the gas and the wall ($\omega = 0$), Equation (5.57)
becomes

$$\frac{\rho}{\rho_e} = \frac{1+B}{1 + B\left[1 - \left(1 - \frac{M_2}{M_1}\right)(1 - a)\right]}.$$ (5.58)

The function K, which determines friction, is generally given by the
second of Equations (5.36), and in the case of $\omega = \beta = 0$ it becomes

$$K = \frac{2}{B} \sqrt{\frac{1+B}{\frac{M_1}{M_2}-1}} \left[\text{arctg} \sqrt{\frac{M_1}{M_2}-1} - \text{arctg} \sqrt{\frac{\frac{M_1}{M_2}-1}{B\frac{M_1}{M_2}+1}} \right] \qquad (5.59)$$

for $M_1 > M_2$

and

$$K = \frac{2}{B} \sqrt{\frac{1+B}{1-\frac{M_1}{M_2}}} \left[\text{arth} \sqrt{1-\frac{M_1}{M_2}} - \text{arth} \sqrt{\frac{1-\frac{M_1}{M_2}}{1+B\frac{M_1}{M_2}}} \right] \qquad (5.60)$$

for $M_1 < M_2$.

When the injected gas has the same molecular weight as the gas in the main flow, ($M_1 = M_2$), assuming that $\omega = \beta = 0$, the expression for K becomes

$$K = \frac{2}{B}(\sqrt{1+B}-1). \qquad (5.61)$$

In the general case, when the density is given by Equation (5.57), the integral in the expression for K (5.36) can be evaluated numerically or graphically.

When calculating the friction coefficient, we assume that the injection parameter B is given. After we determine the friction coefficient c_f with the aid of the system (5.36) using

$$\frac{\rho_w v_w}{\rho_0 U_e} = \frac{1}{2} B c_f \qquad (5.62)$$

we can determine the relative flow rate of injected gas. Thus, a computation for various values of the injection parameter B enables one to establish a relation between the friction and the flow rate of the injected substance, i.e., to determine the relation $c_f = c_f \left(\frac{\rho_w v_w}{\rho_e U_e} \right)$ for given flow conditions.

Figure 96 gives the plots of the friction coefficient versus the injection parameter for injection of various gases (freon-12, air,
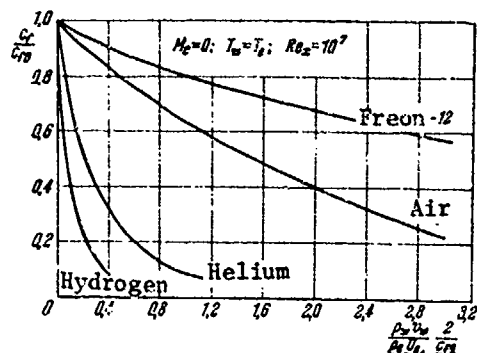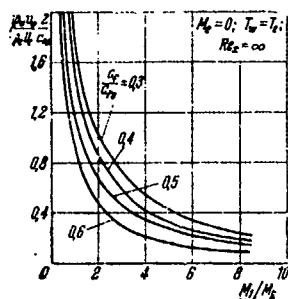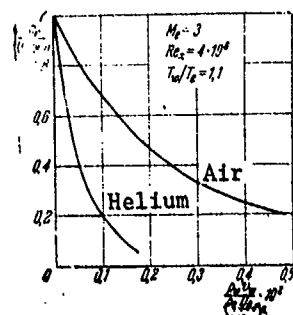
Figure 96

Figure 97

Figure 98

helium, and hydrogen) into an air boundary layer. The calculation was made for the conditions: $M_e = 0$, $T_w/T_e = 1$, $Re_x = 10^7$.

Figure 97 describes the effect of the ratio of molecular weights on the injection parameter for a fixed value of the friction coefficient. The figure shows that a change from injection of heavy gases to injection of light gases permits one to significantly reduce the value of the injection parameter.

Figure 98 illustrates the dependence of friction on the relative flow rate of the injected gas for the conditions $M_e = 3$, $Re_x = 4 \cdot 10^6$, $T_w/T_e = 1.1$. The upper curve was obtained for the injection of air into air, the lower one for injection of helium into air.

This method of calculating friction on a porous plate can be relatively easily extended to the case of sublimation of a surface immersed in a stream of high-temperature gas [22]. We know that if the surface temperature is lower than the temperature at the triple point in the phase diagram, then in a flow of a mixture of gases over a solid body, with the partial pressure of the vapors emanating from the solid in the oncoming flow lower than the pressure of the saturated vapors at the

surface temperature, the body will be vaporized (will sublimate) by
skipping the liquid phase. The mechanism of the transfer of various
quantities (momentum, heat and mass) in the boundary layer with
addition of mass through a porous surface and sublimation is identical.
Only the boundary conditions will be different. If, for a porous
addition the concentration of the injected substance at the wall may
change in an arbitrary way, then, for sublimation, the concentration
of the substance forming at the wall depends on the heat of subli-
mation and the surface temperature.

The concentration of the sublimating substance at the wall, c_{2w},
is given in terms of the partial vapor pressure p_2 by

$$c_{2w} = \frac{M_2}{M_w} \frac{p_2}{p_e},$$ (5.63)

where M_w is the molecular weight of the mixture at the wall [see
Equation (5.43)]. For equilibrium sublimation, the partial pressure
of the sublimate at the wall, p_2, is equal to the partial pressure
of the saturated vapors, p_2^*, at the temperature T_w, given by the
Clausius-Clapeyron law [23]:

$$\ln p_2^* = b - \frac{h_L M_2}{R T_w},$$ (5.64)

where b is an experimental constant, h_L is the latent heat of subli-
mation. Substituting in Equation (5.63)-for the molecular weight M_w—
its value from Formula (5.43) and keeping in mind Equation (5.64), we
obtain an expression for the concentration of the sublimate at the
wall given in terms of the wall temperature and the boiling temperature
$T_K(p_e)$:

$$c_{2w} = \left\{ 1 + \frac{M_1}{M_2}\left[\exp \frac{h_L M_2}{R}\left(\frac{1}{T_w} - \frac{1}{T_K}\right) - 1 \right] \right\}^{-1}.$$ (5.65)

If the temperature of the wall is equal to the boiling temperature,
$(T_w = T_K)$, the concentration of the sublimating substance at the
wall will become equal to unity, which corresponds to a type of

boiling in which the vapor flow rate and the concentration are no longer related by a boundary diffusion condition.

Given the sublimate concentration at the wall, (c_{2w}), it is easy to determine the value of the injection parameter B, related to c_{2w} by Equation (5.56). Making use of this equation, we obtain the following expression for the injection parameter for the case of sublimation of the surface material

$$B = \frac{M_e}{M_1}\left\{\exp\frac{h_L M_2}{R}\left(\frac{1}{T_w} - \frac{1}{T_K}\right) - 1\right\}^{-1}. \qquad (5.66)$$

Thus, this method of computing friction on a porous plate can be used in its entirety to calculate the equilibrium sublimation, the only difference being that the parameter B may not be specified arbitrarily but instead it must satisfy the condition (5.66).

§ 33. Heat and Mass Transfer in a Boundary Layer on a Flat Plate with Injection and the Prandtl and Schmidt Numbers Different from Unity

In this section, in contrast with the preceding one, we shall discuss a flow in the turbulent boundary layer on a flat plate with injection and the Prandtl and Schmidt numbers different from unity. The necessity of this type of analysis is due to the fact that for injection into the boundary layer of gases which differ in their physical-chemical properties from the gas in the oncoming flow, and in particular, for injection of light gases such as helium and hydrogen, the Prandtl and Schmidt numbers may differ significantly from unity. For example, the Schmidt number for the gas mixture hydrogen-air, calculated for the conditions: $T = 273°$ K and $p = 1$ atm, ranges from 0.2 to 1.7 depending on the species concentration. The Schmidt number for the mixture helium-air can also range from 0.2 to 1.7, and the Prandtl number for the same mixture varies from 0.5 to 1.1 depending on the species concentration (see Figure 99, mass concentration of helium is plotted on the abscissa axis).
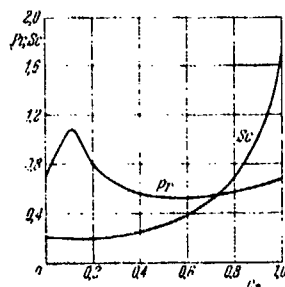
Figure 99

As was noted many times in the preceding chapters, the deviation of the Prandtl and Schmidt numbers from unity in the laminar sublayer is usually of no great significance when computing friction, but it may have a substantial influence on the heat and mass transfer between the gas and the wall.

To simplify the analysis, we shall assume that the Prandtl and Schmidt numbers are constant over the cross-section of the laminar sublayer and equal to their values at the wall. Otherwise, the analysis will be similar to the analysis done in the preceding section (chemical reactions are absent, specific heat capacities of the species are constant, the mixture is binary).

In order to establish an approximate relation between the velocity, total enthalpy, and concentration profiles, we shall use the equations for a turbulent boundary layer expressed in terms of the Crocco variables, (4.97) - (4.100), at the same time simplifying them by means of the assumption of local similitude, $\left(\frac{\partial H}{\partial \xi} = \frac{\partial c_i}{\partial \xi} = 0 \right)$, which was often used in the preceding chapters. In this case, the conservation equation for the injected species and the energy equation in the laminar sublayer, (4.98) and (4.97), become

$$\tau \frac{d^2 c_1}{du^2} = (Sc - 1) \frac{\partial \tau}{\partial u} \frac{dc_i}{du},$$ (5.67)

$$\frac{\partial \tau}{\partial u} \frac{dH}{du} = \frac{\partial q}{\partial u}.$$ (5.68)

Here

$$q = \frac{\tau}{Pr} \left[\frac{dH}{du} + (Pr - 1) u + (Le - 1)(c_{p2} - c_{p1}) T \frac{dc_2}{du} \right].$$ (5.69)

The quantity q may be called a generalized heat flux.

In the turbulent core the same equations can be written in the form

FTD-HC-23-723-71

311

$$\frac{d^2H}{du^2} = 0,\qquad(5.70)$$

$$\frac{d^2c_2}{du^2} = 0.\qquad(5.71)$$

The boundary conditions for Equations (5.67) - (5.70) have the form

$$\text{for } u = 0 \quad H = H_w, \quad c_2 = c_{2w}; \\ \text{for } u = U_e, \quad H = H_e, \quad c_2 = 0.\ \Big\}\qquad(5.72)$$

The problem of determining heat transfer reduces in this case, as usual, to a determination of the friction coefficient and of the relation between friction and heat transfer.

<u>The relation between the concentration and total enthalpy profiles, and the velocity profile in the laminar sublayer.</u> Assuming that the distribution of the friction stresses in the boundary layer is given by Equation (5.3), we put Equation (5.67) in the form

$$\frac{c_2''}{c_2'} = \frac{(Sc - 1)\,B}{1 + B\bar{u}}.\qquad(5.73)$$

Here primes signify differentiation with respect to the dimensionless velocity $\bar{u} = u/U_e$.

Integrating Equation (5.73) once and determining the constant of integration from the condition (5.19), which in this case, (Sc $\neq$ 1), becomes

$$\left(\frac{dc_2}{d\bar{u}}\right)_w = - B\,Sc\,(1 - c_{2w}),\qquad(5.74)$$

we obtain

$$c_2' = - BSc\,(1 - c_{2w})\,(1 + B\bar{u})^{Sc-1}.\qquad(5.75)$$

Integration of Equation (5.75), using the second of the boundary conditions (5.72), leads to the following relation which relates the concentration and velocity profiles in the laminar sublayer:

$$c_2 = 1 - (1 - c_{2w})(1 + B\bar{u})^{sc}. \tag{5.76}$$

It should be noted that Equation (5.76) cannot be used in this form, since we have not established the relation between the injection parameter B and the concentration at the wall, c_{2w}.

Now we turn to the energy Equation (5.68). Introducing the dimensionless quantities

$$\overline{H} = \frac{H}{h_e}; \quad \bar{\tau} = \frac{\tau}{\tau_w}; \quad \bar{q} = \frac{qU_e}{h_e\tau_w}; \quad \bar{u} = \frac{u}{U_e}, \tag{5.77}$$

we bring the equation to the form

$$\frac{d\bar{\tau}}{d\bar{u}} \frac{d\overline{H}}{d\bar{u}} = \frac{d\bar{q}}{d\bar{u}}, \tag{5.78}$$

where

$$\bar{q} = \frac{\bar{\tau}}{Pr}\left[\frac{d\overline{H}}{d\bar{u}} + (Pr - 1)\frac{U_e^2}{h_e}\bar{u} + \right. \\
\left. + (Le - 1)(c_{i,a} - c_{p1}) c_p^{-1}\left(\overline{H} - \frac{U_e^2}{2h_e}\bar{u}^2\right)\frac{dc_2}{d\bar{u}} \right]. \tag{5.79}$$

In Equation (5.79), in contrast with (5.69), temperature T is given in terms of total enthalpy and velocity by

$$T = \left(H - \frac{u^2}{2}\right) c_p^{-1}. \tag{5.80}$$

Making use of the expression (5.3), we integrate Equation (5.78) and determine the constant of integration from the condition at the wall. As a result we get

$$\bar{q} = \bar{q}_w + B(\overline{H} - \overline{h}_w). \tag{5.81}$$

Here

$$\left. \begin{array}{l} \bar{q}_w = \frac{q_w U_e}{h_e\tau_w} = \frac{2c_h}{c_f}(\overline{H}_r - \overline{h}_w), \\[2mm] c_h = \frac{q_w}{\rho_e U_e(H_r - h_w)}, \quad c_f = \frac{2\tau_w}{\rho_e U_e^2}, \end{array} \right\} \tag{5.82}$$

q_w is the heat flux from the gas to the wall, given by Equation (4.147), H_r is the equilibrium enthalpy of a thermally insulated wall, or the enthalpy of recovery (a definition of the last quantity will be given below).

We substitute the expression for q given in Equation (5.79) into Equation (5.81), and after simple algebra we obtain

$$\frac{d\bar{H}}{d\bar{u}} + (Pr - 1)\frac{U_e^2}{h_e}\bar{u} +$$
$$+ (Le - 1)(c_{i_1} - c_{p_1})c_p^{-1}\left(\bar{H} - \frac{U_e^2}{2h_e}\bar{u}^2\right)\frac{dc_1}{d\bar{u}} - \frac{B\,Pr}{1 + B\bar{u}}\bar{H} = \qquad (5.83)$$
$$= \frac{Pr}{1 + B\bar{u}}(\bar{q}_w - B\bar{h}_w). \qquad (5.83)$$

Equation (5.83) is a linear equation of first order with variable coefficients which can be integrated by quadratures. However, in order to obtain the final result in a simpler form, we shall limit ourselves to an approximate determination of the distribution of total enthalpy in the laminar sublayer. Thus we shall assume that $\bar{H}$ can be expanded in a series involving powers of the longitudinal velocity $\bar{u}$. Since $\bar{u} < 1$, we retain only three terms of the series. In this case we get

$$\bar{H} = \frac{H}{h_e} = a_0 + a_1\bar{u} + a_2\bar{u}^2. \qquad (5.84)$$

Using the condition at the wall $H = h_w$ at $u = 0$, we find that $a_0 = h_w/h_e = \bar{h}_w$. Then differentiating the expression (5.84) with respect to $\bar{u}$ and setting $\bar{u} = 0$, we obtain

$$a_1 = \left(\frac{d\bar{H}}{d\bar{u}}\right)_w, \quad a_2 = \frac{1}{2}\left(\frac{d^2H}{d\bar{u}^2}\right)_w. \qquad (5.85)$$

The coefficient a_1 will be found from Equation (5.83) for $\bar{u} = 0$:

$$a_1 = \left(\frac{d\bar{H}}{d\bar{u}}\right)_w = Pr\,\bar{q}_w + B\Lambda\bar{h}_w. \qquad (5.86)$$

Here

$$\Lambda = \frac{(c_{p_2} - c_{p_1})(1 - c_{2w})\,Sc\,(Le - 1)}{c_{p_1} + (c_{p_2} - c_{p_1})c_{2w}}. \qquad (5.87)$$

An expression for the coefficient a_2 will be obtained by differentiating Equation (5.83) with respect to $\bar{u}$, and then setting $\bar{u} = 0$. The result will be

$$\left(\frac{d^2\bar{H}}{d\bar{u}^2}\right)_w = Pr(\Lambda + Pr - 1)B\bar{q}_w + (1 - Pr)(\gamma - 1)M_\delta^2 +$$
$$+ B^2\bar{h}_w\Lambda[\Lambda + \Lambda(Le - 1)^{-1} + Sc - 1 + Pr]; \tag{5.88}$$
$$(\gamma - 1)M_\delta^2 = \frac{U_\delta^2}{h_\delta}.$$

Substituting the values of the coefficients a_0, a_1 and a_2 in (5.84), we obtain a relation connecting the velocity profile and the total enthalpy profile in the laminar sublayer:

$$\bar{H} = \frac{H}{h_\delta} = \bar{h}_w + (Pr\,\bar{q}_w + B\Lambda\bar{h}_w)\bar{u} +$$
$$+ \{Pr(\Lambda + Pr - 1)B\bar{q}_w + (1 - Pr)(\gamma - 1)M_\delta^2 + \tag{5.89}$$
$$+ B^2\bar{h}_w\Lambda[\Lambda + \Lambda(Le - 1)^{-1} + Sc - 1 + Pr]\}\frac{\bar{u}^2}{2}.$$

<u>A relation between the concentration and total enthalpy profiles, and the velocity profile in the turbulent core.</u> In order to establish a relation between the concentration and velocity profiles, we integrate Equation (5.71) once

$$\frac{dc_2}{d\bar{u}} = C. \tag{5.90}$$

The constant of integration C will be determined from the condition of continuity for the diffusive flows of the injected species at the boundary of the laminar sublayer

$$\frac{1}{Sc}\left(\frac{dc_2}{d\bar{u}}\right)_{\bar{u}_n - 0} = \left(\frac{dc_2}{d\bar{u}}\right)_{\bar{u}_n + 0}. \tag{5.91}$$

Using Equations (5.91) and (5.75), and integrating (5.90), we find a relation between the concentration and velocity in the turbulent core

$$c_2 = B(1 - c_{2w})(1 + B\bar{u}_n)^{Sc-1}(1 - \bar{u}). \tag{5.92}$$

Equating the concentrations obtained from Formulas (5.92) and (5.76) at the boundary of the laminar sublayer, we obtain a relation between

the injection parameter B and the concentration at the wall, c_{2w}:

$$c_{2w} = 1 - (1 + B)^{-1}(1 + B\bar{u}_n)^{1-Sc}. \qquad (5.93)$$

It should be noted that, if the Schmidt number is equal to unity, Equation (5.93) will reduce to Equation (5.55) of the preceding section. Using Equation (5.93), we bring Equation (5.92) to the form

$$c_2 = \frac{B}{1+B}(1 - \bar{u}). \qquad (5.94)$$

Now we establish a relation between the total enthalpy and the velocity in the turbulent core. Integrating Equation (5.70) once, we obtain

$$\frac{d\bar{H}}{d\bar{u}} = \text{const} = \frac{\bar{q}}{\bar{\tau}}. \qquad (5.95)$$

The constant of integration in the expression (5.95) will be determined from the condition that the generalized heat fluxes are equal at the boundary of the laminar sublayer. Using this condition and Equation (5.8), we find

$$\frac{d\bar{H}}{d\bar{u}} = \frac{1}{1+B\bar{u}_n}\left[\bar{H}_w + B\left(\bar{H}_n - \bar{h}_w\right)\right]. \qquad (5.96)$$

Integrating Equation (5.96), and determining the constant of integration from the condition at the outer edge, we obtain a relation between total enthalpy and velocity in the turbulent core

$$\bar{H} = \bar{H}_e - [1 + B\bar{u}_n]^{-1}\left[\bar{H}_w + B\left(\bar{H}_n - \bar{h}_w\right)\right](1 - \bar{u}). \qquad (5.97)$$

It is not hard to see that if there is no injection ($B = 0$), Equation (5.97) will reduce to Equation (4.150) of the preceding chapter.

Determination of the enthalpy of recovery H_r and the Reynolds similitude parameter $2c_h/c_f$. Letting $\bar{u} = \bar{u}_l$ in the expression (5.97), we obtain,

$$\bar{H}_{.1} = (1 + B\bar{u}_a)(1 + B)^{-1}\bar{H}_e - (1 - \bar{u}_a)(1 + B)^{-1}(\bar{q}_w - B\bar{h}_w). \qquad (5.98)$$

Equating the values of $\bar{H}_l$, determined from Formulas (5.98) and (5.89), at the boundary of the laminar sublayer, we obtain

$$\bar{h}_w[1 + B\Lambda\bar{u}_a - B(1 - \bar{u}_a)(1 + B)^{-1} +$$
$$+ B^2\Lambda[\Lambda + \Lambda(Le - 1)^{-1} + Sc + Pr - 1]\frac{\bar{u}_a^2}{2}] +$$
$$+ \bar{q}_w\left[Pr\,\bar{u}_a + (1 - \bar{u}_a)(1 + B)^{-1} + Pr(\Lambda + Pr - 1)B\frac{\bar{u}_a^2}{2}\right] = \qquad (5.99)$$
$$= (1 + B\bar{u}_a)(1 + B)^{-1}\bar{H}_e - (1 - Pr)\frac{\gamma - 1}{2}M_e^2\bar{u}_a^2.$$

If there is no heat transfer between the gas and the wall ($\bar{q}_w = 0$, $\bar{h}_w = \bar{H}_r$), Equation (5.99) easily implies the following expression for the enthalpy of recovery:

$$H_r = [h_e\left(1 + Pr^{\Lambda}\frac{\gamma - 1}{2}M_e^2\right) - H_e(1 + B)^{-1}(1 - \bar{u}_a)B] \times$$
$$\times \left\{1 + B\Lambda\bar{u}_a - B(1 - \bar{u}_a)(1 + B)^{-1} + \right.$$
$$\left. + B^2\Lambda[\Lambda + \Lambda(Le - 1)^{-1} + Sc + Pr - 1]\frac{\bar{u}_a^2}{2}\right\}^{-1}. \qquad (5.100)$$

Here we used the approximate relation (3.150).

Substituting the relation (5.82) in Equation (5.99) and solving the resulting equation for the Reynolds similitude parameter, we get

$$\frac{2c_h}{c_f} = [1 + Pr^{\Lambda}\frac{\gamma - 1}{2}M_e^2 - H_e B\frac{1 - \bar{u}_a}{1 + B} -$$
$$- h_w\left[1 + B\Lambda\bar{u}_a - B\frac{1 - \bar{u}_a}{1 + B} + B^2\Lambda[\Lambda + \Lambda(Le - 1)^{-1} + \right.$$
$$\left. + Sc + Pr - 1]\frac{\bar{u}_a^2}{2}\right\}\left\{(H_e - h_w)\left[Pr^{\Lambda} - \right.\right. \qquad (5.101)$$
$$\left.\left. - \frac{1 - \bar{u}_a}{1 + B}B + Pr(\Lambda + Pr - 1)B\frac{\bar{u}_a^2}{2}\right]\right\}^{-1}.$$

Here we used the approximate relation (3.159).

In the absence of injection, ($B = 0$), the expressions (5.100) and (5.101) reduce to their analogs obtained in Chapter III.

If the Prandtl and Schmidt numbers are equal to unity, we have independently of injection $H_r = H_e$ and $2c_h/c_f = 1$, as we can easily infer from Equations (5.100) and (5.101).

The temperature and density distribution in the boundary layer. Given the distribution of total enthalpy $\bar{H}$ and concentration, as well as Equations (5.80) and (5.47), we can find the temperature distribution in the boundary layer

$$\frac{T}{T_e} = \frac{11}{1+\left(\frac{21}{c_{M}}-1\right)c_i}\left(\bar{H} - \frac{\gamma-1}{2}M_e^2 u^2\right). \tag{5.102}$$

In the laminar sublayer $\bar{H}$ and c_2 are given by Equations (5.89) and (5.76); in the turbulent core-by Equations (5.97) and (5.94).

Using the condition of constant pressure across the boundary layer, the equation of state (5.42), and Equations (5.43) and (5.102), we obtain the density distribution in the boundary layer

$$\frac{\rho}{\rho_e} = \frac{1+\left(\frac{c_m}{c_n}-1\right)c_i}{1+\left(\frac{M_i}{M_i}-1\right)c_i}\left(\bar{H} - \frac{\gamma-1}{2}M_e^2 u^2\right)^{-1}. \tag{5.103}$$

The friction can be calculated from the relation between the density and velocity using Equation (5.36). It will be recalled that the concentration of the injected species at the wall, c_{2w}, can be determined from the injection parameter B in accordance with Equation (5.93).

Computational procedure. As the initial data we must be given: the Mach number at the outer edge of the boundary layer M_e, Reynolds number $Re_x = U_e x/\nu_e$, temperature of the wall, T_w, temperature at the outer edge of the boundary layer, T_e. We must also be given the molecular weights and specific heat capacities of the injected gas and the gas flowing over the surface of a plate.

Given the values of the injection parameter B, we can use the method presented in Section 32, i.e., assuming that the Prandtl

and Schmidt numbers are equal to unity, to determine the local friction coefficient with injection, c_f, and the friction parameter ζ, which is related to c_f by Equation (3.8). Then, given the values of B and ζ we determine the parameter B_* [see Formula (5.20 (5.29)]. Formulas (5.33) and (5.30) can be used to calculate the thickness of the laminar sublayer n_l and the velocity at the boundary of the laminar sublayer n_l. Then, using the Schmidt number as a parameter, from Equation (5.93) we find c_{2w} as a function of B (Figure 100,a). Given the composition of the mixture at the wall, (c_{w2}), and the conditions at the wall (T_w, p), we can determine the actual Schmidt number at the wall (Sc_w)[6] (Figure 100,b). Using the data of Figures 100,a and 100,b (see the key in the diagram), we can find Sc_w as a function of the injection parameter (Figure 100,c). After the relation between B and Sc_w is established, Formula (5.93) can be used to determine the actual concentration of the injected species at the wall, c_{2w}. Similarly, we can determine the value of the Prandtl number Pr_w. However, in many cases this is not necessary

Figure 100

since the dependence of the Prandtl number on the composition is much weaker as compared with the Schmidt number, and the number may be assumed constant. Given the values of the Schmidt and Prandtl numbers, we can calculate the Lewis number ($Le_w = Pr_w/Sc_w$). Then we determine the following in this order: function A [using Equation (5.87)], recovery enthalpy H_r [using Equation (5.100)], Reynolds similitude parameter [using Equation (5.101)], heat flux $\tilde{q}_w$ [using Equation (5.82)], enthalpy and concentration in the laminar sublayer [using Equations (5.89) and (5.76)], and in the turbulent core [using Equations (5.97) and (5.94)], temperature and density in the boundary layer [using Equations (5.102) and (5.103)], friction [using Equation (5.36)].

The heat flux from the gas to the wall can be calculated from

---

Footnote (6) appears on page 322.

$$q_w = \frac{\bar{q}_w \lambda_e \tau_w}{U_e}.$$

<div align="right">(5.104)</div>

As can be seen from Equation (5.21), the heat flux which contributes to the heating of the body (inside the body) is, in this case, equal to

$$q_e = \frac{v_w - U\tau_w [h_w - (h_e)_e]}{U_e}.$$

<div align="right">(5.105)</div>

Figure 101 is a plot of the ratio $c_f/(c_f)_{B=0}$ versus the flow rate of the injected gas (hydrogen), obtained for $Pr = Sc = 1$ (solid line) and for $Pr = 0.7$, $Sa = Sc_w$ (dashed line). A comparison of these curves shows that the deviation of the Prandtl and Schmidt
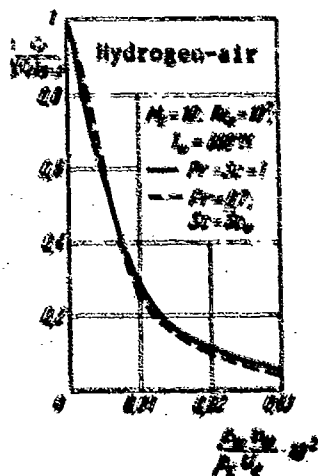

Figure 101

numbers from unity has only a slight effect on the value of the friction coefficient. For this reason, it is not necessary to use higher-order approximations (for c_f, H_r, $2c_h/c_f$) in the computation. This fact permits us to expect that, with an accuracy sufficient in practical calculations, the friction coefficient with injection may in many cases be calculated using a method based on the assumption that the Prandtl and Schmidt numbers are equal to unity (Section 32).

When calculating the parameters characterizing the heat transfer between the gas and the wall ($2c_h/c_f$, H_r), the fact that the Prandtl and Schmidt numbers are different from unity must be taken into consideration.

FOOTNOTES

Footnote (1) on page 279. It should be noted that the expressions (5.6), (5.7), just as (3.9), (3.10) are approximate, since they are obtained if one neglects the laminar sublayer, simultaneously extending the turbulent core up to the wall, which is valid in the case when the laminar sublayer is relatively thin.

Footnote (2) on page 279. A detailed analysis of these discrepancies may be found in: Spalding, D. B., D. M. Auslander and T. R. Sundarom, The Calculation of Heat and Mass Transfer through the Turbulent Boundary Layer on a Flat Plate at High Mach numbers, with and without Chemical Reaction, "Supersonic Flow, Cnemical Processes and Radiative Transfer", Oxford-London-New York-Paris-Frankfurt, pp. 211-276, 1964.

Footnote (3) on page 282. It should be noted that in experiments involving injection at high supersonic velocities it is not always possible to obtain gradient-free flows over a plate or a cone. This is due to the effect of an extended boundary layer on the external flow. We note incidentally that a theory of the interaction between the turbulent boundary layer and the hypersonic external flow is at the present time in its infancy. See, for example, Barnes, J. W. and H. H. Tang. Strong and Weak Interaction Parameters for Turbulent Flow, AIAA Journ., Vol. 4, No. 10 (1966); Russian translation: Raketn. Tekh. i Kosmonavt., No. 10, 1966.

Footnote (4) on page 283. Mugalev, V. P., Experimental Investigation of the Turbulent Boundary Layer on a Plate with Injection of Air and Carbon Dioxide at Supersonic Velocities. Trudy Moskovskogo fizicheski-tekhnicheskogo instituta, Oborongiz, No. 4, 1959. Mugalev, V. P., Experimental Investigation of the Subsonic Turbulent Boundary Layer on a Plate with Injection. Izvestiya vysshikh uchebnykh zavedeniy,

Series of Aeronautics Technology, No. 3, 1959. Mugalev, V. P., An Investigation of Heat Transfer and Turbulent Boundary Layer Characteristics on a Porous Surface. Teplo- i massoperenos (Heat and Mass Transfer), Vol. I, "Energiya" Publishing House, Moscow, 1968.

Footnote (5) on page 291.   Figure 91 and Formula (5.11) are given in survey article: Squire, L. C. Some Notes on Turbulent Boundary Layers with Fluid Injection at High Supersonic Speeds, ARC CP, No. 740, 1964.

Footnote (6) on page 319.   The methods of calculating the diffusion and viscosity coefficients for a gas mixture were discussed in Chapter I. Handbooks and aids that might help in the computation are also indicated there (see, for example, the monograph by Bretshnayder, [5] on page 39a.

REFERENCES

1) Пластмассы--наиболее стойкий материел при очень высоких температурах (обзор), Вопр. ракетн. техн., № 4, ИЛ, (1960).
Пластмассы в ракетной технике (обзор), Вопр. ракетн. техн. №№ 7, 8, ИЛ, 1961.

2) Тирский Г. А., Анализ состава ламинарного пограничного слоя на поверхности горящих пластиков, Космические исследования 2, вып. 4 (1964).

3) Подробное описание различных методов охлаждения поверхностей, подвергающихся воздействию высоких температур, можно найти в книге: Авдуевский В. С., Данилов Ю. И. и др., Основы теплопередачи в авиационной и ракетной технике, Оборонгиз, Москва, 1960.

4) Wooldridge C. E., Muzzy R. J., Boundary layer turbulence measurements with mass addition and combustion, AIAA Journ. 4, № 11 (1966); русский перевод: Ракетн. техн. и космонавт., № 11, 1966.

5) Dorrance W. H., Dore F. J., The effect of mass transfer on the compressible turbulent boundary layer skin friction and heat transfer, Journ. Aero. Sci. 21, № 6, 404—410 (1954).
Dorrance W. H., The effect of mass transfer on the compressible turbulent boundary layer skin friction and heat transfer — an addendum, Journ. Aero. Sci. 23, № 3, 283—284 (1956).

6) Мотулевич В. П., Теплообмен и трение пластины в потоке газа при образовании турбулентного пограничного слоя с пористой подачей инородного вещества, Инж.-физ. журн. 3, № 8 (1960).

7) Мотулевич В. П., Сублимация пластины в потоке газа при образовании турбулентного пограничного слоя, сб. «Физическая газодинамика, теплообмен и термодинамика газов высоких температур», АН СССР, Москва, 1962.
Мотулевич В. П., Турбулентный тепло- и массообмен на пластине при пористом отсосе и подаче различных газов, Инж.-физ. журн. 6, № 4 (1963).

8) Калихман Л. Е., Турбулентный пограничный слой несжимаемой жидкости на пористой стенке, Журн. техн. физ., т. XXV, вып. 11 (1955).

9) Гинзбург И. П., Кочерыженков Г. В., Мордвинова Н. И., Турбулентный пограничный слой на проницаемой пластине, Вестн. Ленингр. гос. ун-та 13, сер. матем., мех. и астрон., вып. 3 (1964).

10) Кутателадзе С. С., Леонтьев А. И., Турбулентный пограничный слой сжимаемого газа, СО АН СССР, 1962.
Тепло, массообмен и трение в турбулентном пограничном слое, Сб. под ред. С. С. Кутателадзе, СО АН СССР, 1964.

11) Denison R. M., The turbulent boundary layer on chemically aktive ablating surface, Journ. Aero. Sci. 28, № 6. (1961); русский перевод: Вопр. ракетн. техн., № 1, ИЛ, 1962.

12) Совершенный В. Д., Турбулентный пограничный слой на проницаемой поверхности, Мех. жидк. и газа № 3 (1966).

13) Мугалев В. П., Приближенный метод расчета трения и теплоотдачи при вдувании воздуха в турбулентный пограничный слой, Тр. Моск. физ.-техн. ин-та, № 5 (1960).

14) Лойцянский Л. Г., Механика жидкости и газа, Гостехиздат, Москва, 1957.

15) P a p p a s C. C., O k u n o A. F., The relation between skin friction and heat transfer for the compressible turbulent boundary layer with gas injection, NASA TN, D-2857 (1965).

16) M i c k l e y H. S., D a v i s R. C. Momentum transfer for low over a flat plate with blowing, NACA TN, № 4017 (1957).

17) F o g a r o l i R. P., S a y d a h A. R., Turbulent heat transfer and skin friction measurements on a porous cone with air injection at high Mach number, AIAA Journ. 4, № 6 (1966); русский перевод: Ракетная техн. и космонавт., № 6, 1966.

18) T u r c o t t e D. L., A sublayer theory for fluid injection into the compressible turbulent boundary layer, Journ. Aero-Space Sci. 27, № 9 (1960).

19) K u l g e i n N. G., Transport process in a combustive turbulent boundary layer, Journ. of Fluid Mech. 12, part 3 (1962).
  См. также уже цитированную в этой главе работу Вулдриджа и Мущи.

20) V a n D r i e s t E. R., On the aerodynamic heating of blunt bodies, Zeitschr. angew. Math. und Phys. Bd. IX, 5/6 (1958).

21) Л а п и н Ю. В., Трение и теплообмен в сжимаемом турбулентном пограничном слое на пластине при наличии ввода вещества. Журн. техн. физ., т. XXX, вып. 8 (1960).

22) Л а п и н Ю. В. Турбулентный тепломассообмен на пластине при наличии сублимации и пористом подводе различных газов, Журн. техн. физ., т. XXXIV, вып. 5 (1964).

23) К а р а п е т ь я н ц М. X. Химическая термодинамика, Госхимиздат, Москва, 1953.

NOTATION

Roman Letters

A   — see Equation (3.173);

A_k — chemical symbols of reactants, Equation (4.1);

A   — speed of sound;

$$B = \frac{\rho_w v_w}{\rho_e U_e} \frac{2}{c_f}, \qquad B_0 = \frac{\rho_w v_w}{\rho_e U_e} \frac{2}{(c_f)_{B=0}},$$

$$B_F = \frac{\rho_w v_w}{\rho_e U_e} \frac{2}{c_F}, \qquad B_{F0} = \frac{\rho_w v_w}{\rho_e U_e} \frac{2}{(c_F)_{B=0}},$$

$$B_h = \frac{\rho_w v_w}{\rho_e U_e} \frac{1}{c_h}, \qquad B_{h0} = \frac{\rho_w v_w}{\rho_e U_e} \frac{1}{(c_h)_{B_h=0}},$$

$$B_H = \frac{\rho_w v_w}{\rho_e U_e} \frac{1}{c_H}, \qquad B_{H0} = \frac{\rho_w v_w}{\rho_e U_e} \frac{1}{(c_H)_{B_H=0}},$$

$$B_\bullet = \frac{B}{\zeta} = \frac{v_w}{v_\bullet}$$

                            injection parameters;

b   — impact parameter, Equation (1.16);

c_F — average friction coefficient, Equation (3.62);

c_H — average heat transfer coefficient;

c_f — local friction coefficient, Equation (2.85);

c_h — local heat transfer coefficient, Equation (2.91);

c_i — mass concentration of species i, Equation (1.29);

c_m — flow rate coefficient for the injected substance, Equation (2.86);

C_r — recombination parameter, Equation (4.137);

c_v — specific heat capacity at constant volume, Equation (1.43);

c_p — specific heat capacity at constant pressure;

c_{pi} — specific heat capacity of species i at constant pressure;

c_{vi} — specific heat capacity of species i at constant volume;

D   — energy of dissociation per unit molecular mass, Equation (4.46);

D_{ij} — diffusion coefficient for a multicomponent mixture, Equation (1.53);

$\mathcal{D}_{ij}$ — diffusion coefficient for a binary mixture, Equation (1.59);

$\mathcal{D}_i$ — effective diffusion coefficient, Equation (1.58);

$\mathcal{D}_i^T$ — thermodiffusion coefficient;

$\mathcal{D}_\tau$ — turbulent diffusion coefficient, Equation (2.31);

Da — Damkohler number, Equation (4.102);

d — diameter of a sphere;

E — internal energy of a gas, Equation (1.38);

E_0 — energy of a gas at zero absolute temperature;

E_a — activation energy;

ΔE_0 — dissociation energy per unit mole of starting substance, Equation (4.22);

E_{aw} — activation energy for a surface reaction;

e_i — energy of the internal degrees of freedom of a molecule of species i;

f_i — distribution function;

F — function defined by Equations (3.77) and (3.92);

G — function defined by Equation (3.78);

g_{ij} — see Equation (1.16);

g_{iw} — mass rate of formation of species i per unit area;

g_i — statistical weight;

H — total enthalpy of a mixture, Equation (1.94);

H^* = δ^*/δ^{**}, form parameter;

h — enthalpy of a mixture, Equation (1.100);

h_i — enthalpy of species i;

h_i^0 — heat of formation of species i under standard conditions;

H_r — enthalpy of recovery;

h — Planck constant;

h_{iL} — heat of sublimation of species i;

J_i — mass flux density vector of species i, Equation (1.10);

k — Boltzmann constant;

k_T — thermodiffusive ratio, Equation (1.61);

K_i — numerical rate of formation of the molecules of species i per unit volume, Equation (1.27);

K_n — see Equation (4.7),

K_p — see Equation (4.12),

K_x — see Equation (4.15),   equilibrium constants;

K_c — see Equation (4.16)

k_{wi}, k_{wj} — rates of forward and reverse surface reactions;

k', k'' — rates of reverse reactions in the gas phase;

K_w — equilibrium constant for the surface reaction;

k_d — rate of dissociation;

k_2 — rate of recombination;

I_{ij} — collision integral;

$I(\bar{u})$ — see Equation (3.36);

L — characteristic length;

Le_i — effective Lewis number, Equation (1.103);

Le — Lewis number for a binary mixture, Equation (1.105);

Le_t — turbulent Lewis number, Equation (2.34);

l — turbulent path of mixing;

M_i — molecular weight of species i;

M — molecular weight of a mixture;

M_e — Mach number at the outer edge of the boundary layer;

m_i — mass of a particle of species i;

n_i — numerical density of particles of species i, Equation (1.1);

n — number of particles per unit volume, Equation (1.7);

$[n_i] = n_i/N_A$ — number of moles of species i per unit volume;

n_i, n_j — order of forward and reverse surface reactions;

N_A — Avogadro number;

N — see Equation (3.82);

p — pressure of a mixture, Equation (1.8);

p_i — partial pressure of species i, Equation (1.8);

p_d — characteristic pressure of an ideally dissociating gas;

P — pressure tensor, Equations (1.12) and (1.64);

P_i — pressure tensor of species i, Equation (1.11);

Pr — Prandtl number;

Pr_t — turbulent Prandtl number, Equation (2.33);

Q_p — partition function for a gas of unit pressure;

Q — total partition function; see also Equation (3.181);

Q_c — partition function for a gas of unit concentration;

Q_i — kinetic energy flux density vector of species i, Equation (1.13);

q — heat flux density vector, Equations (1.14) and (1.76);

q_w — heat flux from the gas to the wall, Equation (2.88);

q_s — heat flux inside the body, Equation (5.20);

R — universal gas constants;

Re* — Reynolds number constructed from the displacement thickness, Equation (3.43);

Re** — Reynolds number, constructed from the momentum loss thickness, Equation (3.17);

Re_x — Reynolds number constructed from the parameters at the outer edge of the boundary layer, Equation (3.18);

r — radius vectors with components x, y, z;

r_w — radius of lateral curvature of a body of revolution;

Sc_t — turbulent Schmidt number, Equation (2.36);

Sc — Schmidt number for a binary mixture, Equation (1.105);

Sc_i — effective Schmidt number, Equation (1.103);

$\dot{S}$ — strain rate tensor, Equation (1.67);

T — gas temperature, Equation (1.8);

T_d — characteristic dissociation temperature;

T_r — characteristic rotational temperature and temperature of recovery;

T_v — characteristic vibrational temperature;

t — time;

v_i — velocity of a particle of species i (components v_x, v_y, v_z);

v — center-of-mass velocity, Equation (1.4);

$\bar{v}_i$ — mean velocity of particles of species i, Equation (1.3);

V_i — thermal velocity of particle of species i, Equation (1.5);

$\vec{V}_i$ — rate of diffusion of species i, Equations (1.6) and (1.53);

v_* — dynamic velocity, Equation (3.8);

u — longitudinal velocity component;

w_i — mass rate of formation of species i, Equation (1.30);

W — active portion of a catalytic surface;

x — x-component of vector r;

x_i — molar concentration;

X — catalytic molecule.

Greek Letters

α — universal turbulence constant, Equation (3.102);

β — see Equations (3.48) and (3.49);

$\bar{\beta}$ — see Equation (4.117);

γ $= c_p/c_v$;

γ_w — catalytic capacity of the wall, Equation (4.61);

δ^* — displacement thickness, Equation (2.77);

δ^{**} — momentum loss thickness, Equation (2.76);

δ — boundary layer thickness, Equation (5.53);

δ_n^{**} — energy loss thickness, Equation (2.89);

ε — turbulent viscosity coefficient, Equation (2.30);

$\dot{\varepsilon}$ — unit tensor, Equation (1.66);

ζ — friction parameter, Equation (3.8);

η — universal coordinate, Equation (3.8);

η_i — coordinate of the boundary of the laminar sublayer;

κ — universal turbulence constant ($\kappa = 0.4$), Equation (2.69);

λ — molecular heat conductivity coefficient;

λ_t — turbulent heat conductivity coefficient, Equation (2.32);

λ_{eff} — effective heat conductivity coefficient, Equation (1.82);

λ_R — coefficient of heat conductivity due to mass transfer, Equation (1.81);

μ — dynamic viscosity coefficient;

ν — kinematic viscosity coefficient;

ν_k', ν_k'' — stoichiometric reaction coefficients, Equation (4.1);

ξ — Crocco variable, Equation (2.59);

ρ_1 — partial density of species 1, Equation (1.8);

ρ — gas density, Equation (1.8);

ρ_d — characteristic density of a partially excited dissociating gas, Equation (4.50);

ρ_{dL} — characteristic density of an ideally dissociating gas, Equation (4.51);

σ — see Equation (4.20);

τ — stress of friction;

ϕ — universal coordinate, Equation (3.8);

$\phi(\bar{u})$ — see Equation (3.34);

Ψ — flux density vector, Equation (1.9);

ψ_i — summation invariants, Equation (1.21);

Ψ — see Equation (3.25);

ω — see Equations (3.48) and (3.49);

Ω — see Equation (3.196).

Subscripts

e — parameters at the outer edge of the boundary layer;

w — parameters at the wall;

s — parameters at the stagnation point;

∞ — parameters at infinity in the oncoming flow;

0 — parameters in an incompressible fluid, as well as parameters for no injection;

r — parameters in the absence of heat transfer between the gas and the wall;

l — parameters at the boundary of the laminar sublayer;

t — parameters in the turbulent core;

t — parameters at the point of transition of laminar flow into turbulent flow.

Superscripts

(e) — equilibrium flow;

(f) — frozen flow;

(ne)— nonequilibrium flow;

line above signifies: in Chapter I — statistical averaging over velocities, Equation (1.2); in Chapter II — time averaging, Equation (2.2); in Chapter III - V — dimensionless quantities.

SYMBOL LIST

Russian	Typed	Meaning
Эфф	eff	effective
Т	t	turbulent
Н	n	not defined
ОПР	def	defining
ЭКСП	exp	experiment
ВОЗД	air	air
Л	l	laminar
СР	av	average
ТеОР	theory	theory
ПЛ	pl	plane
ПОТОК	flow	of flow
ХИМ	chem	chemical
ЛТ	lth	laminar-thermal
ЛД	ld	laminar-diffusive
ПРеД	lim	limiting
Т	th	thermal
Д	d	diffusive
К	K	boiling